



Department of Petroleum Engineering

Fluid Flow Projects

Seventy Third Semi-Annual Advisory
Board Meeting Brochure and Presentation
Slide Copy

September 30, 2009

**Tulsa University Fluid Flow Projects
Seventy Third Semi-Annual Advisory Board Meeting Agenda
Wednesday, September 30, 2009**

*Tuesday,
September 29, 2009*

*Tulsa University High-Viscosity Oil Projects
Advisory Board Meeting
University of Tulsa – Allen Chapman Activity Center (ACAC) - Gallery
440 South Gary
Tulsa, Oklahoma
8:15 – 11:30 a.m.*

*Tulsa University High-Viscosity Oil Projects, Tulsa University Hydrate Flow Performance
JIP and Tulsa University Fluid Flow Projects Workshop Luncheon
University of Tulsa – Allen Chapman Activity Center – (ACAC) – Atrium
440 South Gary
Tulsa, Oklahoma
12:00 – 1:00 p.m.*

*Tulsa University Fluid Flow Projects Workshop
University of Tulsa – Allen Chapman Activity Center (ACAC) - Gallery
440 South Gary
Tulsa, Oklahoma
1:00 – 3:00 p.m.*

*Tulsa University High-Viscosity Oil Projects, Tulsa University Hydrate Flow Performance
JIP, Tulsa University Fluid Flow Projects and Tulsa University Paraffin Deposition Projects
Tour of Test Facilities
University of Tulsa North Campus
2450 East Marshall
Tulsa, Oklahoma
3:30 – 5:30 p.m.*

*Tulsa University High-Viscosity Oil Projects, Tulsa University Hydrate Flow
Performance JIP and Tulsa University Fluid Flow Projects
Reception
Oklahoma Aquarium
300 Aquarium Drive
Jenks, Oklahoma
6:00 – 9:00 p.m.*

*Wednesday,
September 30, 2009*

*Tulsa University Fluid Flow Projects
Advisory Board Meeting
University of Tulsa – Allen Chapman Activity Center (ACAC) - Gallery
440 South Gary
Tulsa, Oklahoma
8:00 a.m. – 5:00 p.m.*

*Tulsa University Paraffin Deposition Projects
Dinner
University of Tulsa – Allen Chapman Activity Center – Alcove
440 South Gary
Tulsa, Oklahoma
5:30 – 9:00 p.m.*

*Thursday,
October 1, 2009*

*Tulsa University Paraffin Deposition Projects
Advisory Board Meeting
University of Tulsa – Allen Chapman Activity Center (ACAC) - Gallery
440 South Gary
Tulsa, Oklahoma
8:00 a.m. – 1:00 p.m.*

Tulsa University Fluid Flow Projects

Seventy Third Semi-Annual Advisory Board Meeting Agenda

Wednesday, September 30, 2009

8:00 a.m.	Breakfast – Allen Chapman Activity Center - Gallery	
8:30	Introductory Remarks	Cem Sarica
8:45	TUFFP Special Presentation Uncertainty and Risk Analysis in Multiphase Flow	Selen Cremaschi
9:00	TUFFP Progress Reports Liquid Entrainment in Annular Two-Phase Flow in Inclined Pipes Modeling of Gas-Liquid Flow in an Upward Vertical Annulus	Kyle Magrini Tingting Yu
10:30	Coffee Break	
10:45	TUFFP Progress Reports Modeling of Hydrodynamics and Dispersions in Oil-Water Pipe Flow Slug Flow Evolution in Gas-Oil-Water Flow in Hilly-Terrain Pipelines	Anoop Sharma Gizem Ersoy-Gokcal
12:15 p.m.	Lunch – Allen Chapman Activity Center – Chouteau C	
1:15 p.m.	TUFFP Progress Reports Effects of High Oil Viscosity on Slug Liquid Holdup in Horizontal Pipes Investigation of Slug Length for High Viscosity Oil-Gas Flow Effect of Pipe Diameter on Drift Velocity for High Viscosity Liquids	Ceyda Kora Eissa Alsafran Anoop Sharma
2:45	Coffee Break	
3:00	TUFFP Project Reports Low Liquid Loading Three-Phase Flow High Pressure – Large Diameter Multiphase Flow Loop Unified Model Improvements	Kiran Gawas Cem Sarica Holden Zhang
4:00	TUFFP Questionnaire	Holden Zhang
4:15	TUFFP Business Report	Cem Sarica
4:30	Open Discussion	Cem Sarica
5:00	Adjourn	
6:00	TUPDP Dinner – Allen Chapman Activity Center - Alcove	

Table of Contents

Executive Summary	1
Introductory Presentation	5
TUFFP Progress Reports	
Executive Summary	13
Liquid Entrainment in Annular Gas-Liquid Flow in Inclined Pipes – Kyle Magrini	
Presentation	15
Report.....	55
Executive Summary	77
Upward Multiphase Flow in a Vertical Annulus – Tingting Yu	
Presentation	97
Executive Summary	131
Modeling of Hydrodynamics and Dispersions in Oil-Water Pipe Flow – Anoop Kumar Sharma	
Presentation	133
Report.....	157
Executive Summary	179
Slug Flow Evolution of Gas-Oil-Water Flow in Hilly-Terrain Pipelines – Gizem Ersoy Gokcal	
Presentation	183
Report.....	207
Executive Summary	225
Effects of High Oil Viscosity on Slug Liquid Holdup in Horizontal Pipes – Ceyda Kora	
Presentation	229
Report.....	247
Investigation of High Viscosity Oil Two-Phase Slug Length in Horizontal Pipes – Eissa Alsafran	
Presentation	257
Report.....	267
Investigation of Diameter Effect on Drift Velocity – Anoop Kumar Sharma	
Presentation	279
Report.....	293
Executive Summary	303
Low Liquid Loading Gas-Oil-Water Flow – Kiran Gawas	
Presentation	307
Report.....	325
Executive Summary	337
High Pressure – Large Diameter Multiphase Flow Loop – Polat Abduvayt, Scott Graham, Cem Sarica	
Presentation	341
Executive Summary	357
Unified Model Updates – Holden Zhang	
Presentation	359

Transient Modeling	
Executive Summary	363
2009 Questionnaire – Holden Zhang	
Presentation	365
TUFFP Business Report	
Presentation	367
Introduction	375
Personnel	377
Membership	379
Equipment and Facilities	381
Financial Status	383
Miscellaneous Information	389
Appendices	
Appendix A – Fluid Flow Projects Deliverables	393
Appendix B – Fluid Flow Projects Advisory Board Representatives	399
Appendix C – History of Fluid Flow Projects Membership	405
Appendix D – Contact Information	411

Executive Summary

Progress on each research project is given later in this Advisory Board Brochure. A brief summary of the activities is given below.

- “*Investigation of Gas-Oil-Water Flow*”. Three-phase gas-oil-water flow is a common occurrence in the petroleum industry. The ultimate objective of TUFFP for gas-oil-water studies is to develop a unified model based on theoretical and experimental analyses. A three-phase model has already been developed. There are several projects underway addressing the three-phase flow.
- “*Oil-Water Flow in Pipes*”. Our three-phase model requires knowledge on oil/water interaction. Moreover, oil-water flow is of interest for many applications ranging from horizontal well flow to separator design. The objectives of this study are to assess performance of current models by checking them against experimental data and improve the existing models through better closure relationships or develop new models if necessary.

After the completion of several experimental oil-water flow studies, efforts are concentrated on improvement of the modeling. A new model based on energy minimization is developed. The comparisons with the experimental data and other oil-water flow models prove that the newly developed model performs the best.

- “*High Viscosity Oil Two-phase Flow Behavior*”. Oils with viscosities as high as 10,000 cp are produced from many fields around the world. Current multiphase flow models are largely based on experimental data with low viscosity fluids. The gap between lab and field data may be three orders of magnitude or more. Therefore, current mechanistic models need to be verified with higher liquid viscosity experimental results. Modifications or new developments are necessary.

An earlier TUFFP study conducted by Gokcal showed that the performances of existing models are not sufficiently accurate for high viscosity oils with a viscosity range of 200 – 1000 cp. It was found that increasing oil viscosity had a significant effect on flow behavior. Mostly, intermittent flow (slug and elongated bubble) was observed in his study. Based on his results, this study focuses on the slug flow.

Gokcal (2008) developed a translational velocity closure relationship for all inclination angles. Moreover, he developed a slug frequency

correlation. Our efforts in this project continue at multiple fronts:

1. Translational velocity study: Diameter effect on the drift velocity is being investigated experimentally. The tests with 3 in. ID pipe have been completed. No significant change between 2 in. and 3 in. pipes is observed. The tests will be continued with a 6 in. ID pipe.
2. Slug length study: Gokcal (2008) reported that slug lengths followed a log-normal distribution, and the average slug length decreases as the liquid viscosity increases. Currently, a new study to further investigate the slug length is underway. Dr. Eissa Al-Safran of Kuwait University is working on this project as part of his sabbatical assignment with TUFFP.
3. Slug liquid holdup study: One of the important closure relationships of the slug flow is the slug liquid holdup. Current experimental study focuses on the investigation of the slug liquid holdup. During this period, the newly developed holdup measurement technique has been tested and implemented. A limited number of tests are conducted. Early results indicate that the liquid holdup is significantly higher compared to low viscosity oils.

- “*Droplet Homo-phase Interaction Study*”. There are many cases in multiphase flow where droplets are entrained from or coalesced into a continuous homophase. For example, in annular mist flow, the liquid droplets are in dynamic equilibrium with the film on the walls, experiencing both entrainment and coalescence. Very few mechanistic models exist for entrainment rate and coalescence rate. Understanding the basic physics of these phenomena is essential to model situations of practical interest to the industry. Droplet homo-phase covers a broad range of possibilities.

A past sensitivity study of multiphase flow predictive models showed that, in stratified and annular flow, the variation of droplet entrainment fraction can significantly affect the predicted pressure gradient. Although better entrainment fraction correlations were proposed, a need was identified to experimentally investigate entrainment fraction for inclined pipes. In the current study entrainment fraction for various inclination angles has been investigated using the 3-in. ID Severe Slugging facility. Entrainment fraction is measured using both a newly developed film extraction device and an iso-kinetic probe. 140 tests covering the inclination angle range of 0° - 90° have been conducted. The

data acquired includes entrainment fraction, average film thickness and wave characteristics such as wave height and celerity. The results show the dependency of entrainment fraction to the inclination angle of the pipe.

- “*Simplified Transient Flow Studies*”. TUFFP’s simplified transient flow studies project proposal ranked #5 in our recent questionnaire. Therefore, it is launched as a separate project. Dr. Michelle Li, a research associate, was assigned to the project. She was on maternity leave since the last Advisory Board meeting. Therefore, no progress is made in this project during this period.
- “*Low Liquid Loading Gas-Oil-Water Flow in Horizontal and Near Horizontal Pipes*”. Low liquid loading exists widely in wet gas pipelines. These pipelines often contain water and hydrocarbon condensates. Small amounts of liquids can lead to a significant increase in pressure loss along a pipeline. Moreover, existence of water can significantly contribute to the problem of corrosion and hydrate formation problems. Therefore, understanding of flow characteristics of low liquid loading gas-oil-water flow is of great importance in transportation of wet gas.

In a previous study, large amount of data were collected on various flow parameters such as flow patterns, phase distribution, onset of droplet entrainment, entrainment fraction, and film velocity. The results revealed a new flow phenomenon.

Mr. Kiran Gawas, a Ph.D. student has been assigned to continue this study. Kiran has focused on re-commissioning of the facility and conducting repeat experiments during this summer. His test results confirmed the observations made by Dong (2007).

- “*Multiphase Flow in Hilly Terrain Pipelines*”. Three-phase flow in hilly terrain pipelines is a common occurrence. The existence of a water phase in the system poses many potential flow assurance and processing problems. Most of the problems are directly related to the flow characteristics. Although the characteristics of two-phase gas-liquid flow have been investigated extensively, there are very few studies addressing multiphase gas-oil-water flow in hilly terrain pipelines. The general objectives of this project are to thoroughly investigate and compare existing models, and develop closure relationships and predictive models for three-

phase flow of gas-oil-water in hilly-terrain pipelines.

Since the Spring AB meeting, the data analysis has been continued. The data analysis showed variation of in-situ water cut along the hilly terrain section. Moreover, the effect of water cut on slug characteristics has been observed. A detailed progress is reported in this Advisory Board meeting.

- “*Up-scaling Studies*”. One of the most important issues that we face in multiphase flow technology development is scaling up of small diameter and low pressure results to large diameter and high pressure conditions. Studies with a large diameter facility would significantly improve our understanding of flow characteristics in actual field conditions. Therefore, our main objective in this study is to investigate the effect of pipe diameter and pressures on flow behavior using a larger diameter flow loop.

This project is one of the main activities of TUFFP, and a significant portion of the TUFFP budget is being allocated to the construction of this facility. The facility construction efforts are currently underway. Concrete work has been completed. Steel structures have been fabricated and expected to be mounted on the concrete structure during the months of September and October. As reported before The Sundyne Gas compressor is on location as well as the 500KVA diesel generator that will be providing the electricity for the compressor and liquid pumps. The separator has been received. The other equipment such as liquid pumps, liquid tanks, the surge tank for gas, flow-Meters, and instrumentation have been ordered and expected to be received this fall. Process equipment assembly is expected to be completed this fall. Due to budgetary limitations, we will defer some of the expenses to 2010.

- “*Gas-Liquid Flow in an Upward Vertical Annulus*.” TUFFP has not conducted any study on this topic since Caetano’s pioneering work in 1985. This project is initiated to improve our predictions for multiphase flow. A new mechanistic model has been developed. The new model is an extension of the TUFFP Unified Model to annulus flow. The new model performs better than the original Caetano and the current TUFFP Unified model. A final report has already been posted at the TUFFP website and a final presentation will be made at this Advisory Board meeting.
- “*Unified Mechanistic Model*”. TUFFP maintains, and continuously improves upon the TUFFP unified model. Collaborative efforts with Schlumberger Information Systems are underway to improve the speed and the performance of the software.

Current TUFFP membership stands at 16 (15 industrial companies and MMS). Efforts continue to further increase the TUFFP membership level. A detailed financial report is provided in this report. We thank our members for their continued support.

Several related projects are underway. The related projects involve sharing of facilities and personnel with TUFFP. The Paraffin Deposition consortium,

TUPDP, is into its third phase with 11 members. Phase IV of TUPDP is currently being formulated. It is expected to start April 1, 2010. The Center of Research Excellence (TUCoRE) initiated by Chevron at The University of Tulsa funds several research projects. TUCoRE activities in the area of Heavy Oil Multiphase Flow have resulted in a new Joint Industry Project (JIP) to investigate Heavy Oil Multiphase Flow in more detail. The JIP currently has three members.



Fluid Flow Projects

73nd Fluid Flow Projects Advisory Board Meeting

Welcome

Advisory Board Meeting, September 30, 2009

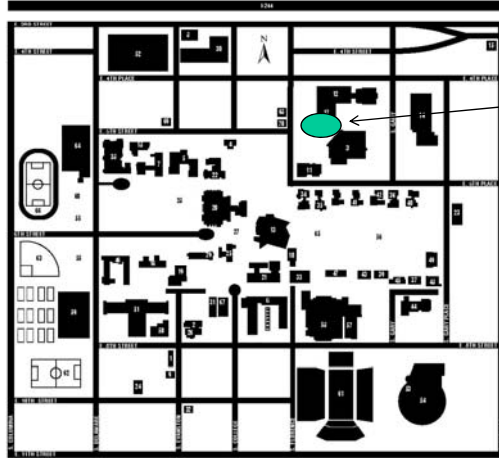
Safety Moment

- ◆ Emergency Exits
- ◆ Assembly Point – Grassy Area to Northwest
- ◆ Tornado Shelter
 - Room 115, Southeast Emergency Stairwell
 - Lower Level Restrooms
- ◆ Campus Emergency
 - Call 9-911
 - Campus Security, ext. 5555 or 918-631-5555
- ◆ Rest Rooms

Fluid Flow Projects



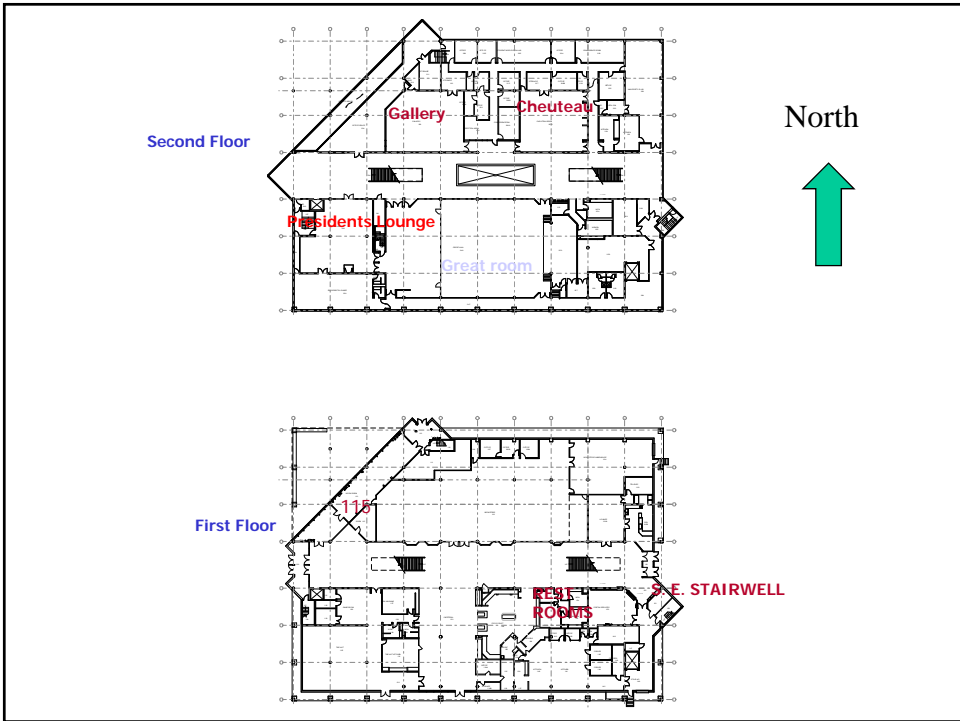
The University of Tulsa Campus Map



Assembly Area

 Fluid Flow Projects

Advisory Board Meeting, September 30, 2009



Introductory Remarks

- ◆ **73rd Semi-Annual Advisory Board Meeting**
- ◆ **Handout**
 - **Combined Brochure and Slide Copy**
- ◆ **Sign-Up List**
 - **Please Leave Business Card at Registration Table**

Team

- ◆ **Research Associates**
 - **Cem Sarica (Director)**
 - **Holden Zhang (Associate Director)**
 - **Polat Abduvayt**
 - **Mingxiu (Michelle) Li**
 - **Eissa Alsafran, (On Sabbatical Leave)**

Team ...

- ◆ **Project Coordinator**
 - Linda Jones
- ◆ **Project Engineer**
 - Scott Graham
- ◆ **Research Technicians**
 - Craig Waldron
 - Brandon Kelsey
- ◆ **Web Master**
 - Lori Watts

Team ...

- ◆ **TUFFP Research Assistants**
 - Gizem Ersoy (Ph.D.) – Turkey
 - Kiran Gawas (Ph.D.) – India
 - Benin (Ben) Chelinsky Jeyachandra (MS) – India
 - Ceyda Kora (MS) – Turkey
 - Kyle Magrini (MS) – USA (Graduated)
 - Anoop Sharma (MS) – India (Graduated)
 - Tingting Yu (MS) – PRC (Graduated)
 - Ge Yuan (MS) – PRC

Guests

◆ Colin Smith, BG

Agenda

- ◆ 8:30 **Introductory Remarks**
- ◆ 8:45 **Special Presentation**
 - **Uncertainty and Risk Analysis in Multiphase Flow**
- ◆ 9:00 **Progress Reports**
 - **Liquid Entrainment in Annular Two-Phase Flow in Inclined Pipes**
 - **Modeling of Gas-Liquid Flow in an Upward Vertical Annulus**
- ◆ 10:30 **Coffee Break**

Agenda ...

- ◆ **10:45 Progress Reports**
 - **Modeling of Hydrodynamics and Dispersions in Oil-Water Pipe Flow**
 - **Slug Flow Evolution in Gas-Oil-Water Flow in Hilly-Terrain Pipelines**
- ◆ **12:15 Lunch – Chouteau-C**
- ◆ **1:15 Progress Reports**
 - **Effects of High Oil Viscosity on Slug Liquid Holdup in Horizontal Pipes**
 - **Investigation of Slug Length for High Viscosity Oil-Gas Flow**
 - **Effect of Pipe Diameter on Drift Velocity for High Viscosity Liquids**

Agenda ...

- ◆ **2:45 Coffee Break**
- ◆ **3:00 Progress Reports**
 - **Low Liquid Loading Three-Phase Flow**
 - **High Pressure – Large Diameter Multiphase Flow Loop**
 - **Unified Model Improvements**
- ◆ **4:00 TUFFP Questionnaire**

Agenda ...

- ◆ 4:15 TUFFP Business Report
- ◆ 4:30 Open Discussion
- ◆ 5:00 Adjourn
- ◆ 6:00 TUPDP Dinner (Allen Chapman Activity Center - Alcove)

Other Activities

- ◆ September 29, 2009
 - TUHOP Meeting
 - TUFFP Workshop
 - ▲ Excellent Presentations
 - ▲ Beneficial for Everybody
 - Facility Tour
- ◆ October 1, 2009
 - TUPDP Meeting



Fluid Flow Projects

Executive Summary of Research Activities

Cem Sarica

Advisory Board Meeting, September 30, 2009

Droplet Homo-phase Studies

- ◆ **Significance**
 - Better Predictive Tools Lead to Better Design and Practices
- ◆ **General Objective**
 - Development of Closure Relationships
- ◆ **Past Study**
 - Earlier TUFFP Study Showed
 - ▲ Entrainment Fraction (FE) is Most Sensitive Closure Parameter in Annular Flow
 - ▲ Developed New FE Correlation
 - ✦ Utilizing In-situ Flow Parameters
 - ✦ Limited Data, Especially for Inclined Flow Conditions

Droplet Homo-phase Studies ...

◆ Current Study

- Liquid Entrainment in Annular Two-Phase Flow in Inclined Pipes
- Objectives
 - ▲ Acquire Data for Various Inclination Angles for 3-in. ID Pipe Using Severe Slugging Facility
 - ✦ Existing Data are for 1 and 1 ½ in.
 - ▲ Develop a New Closure Relationship

Droplet Homo-phase Studies ...

◆ Status

- New Dimensionless Groups are Proposed to Correlate Entrainment Fraction
- Experimental Study is Completed
 - ▲ Entrainment Fraction is Found to Vary with Inclination Angle
 - ▲ Performance Analysis of the Existing Correlations is Completed



Fluid Flow Projects

Liquid Entrainment in Annular Gas-Liquid Flow in Inclined Pipes

Kyle Magrini

Advisory Board Meeting, September 30, 2009

Outline

- ◆ Objectives
- ◆ Introduction
- ◆ Literature Review Summary
- ◆ Experimental Facility
- ◆ Measurement Techniques
- ◆ Experimental Results
- ◆ Model and Correlation Evaluation
- ◆ Conclusions

Objectives

- ◆ Acquire Experimental Data of Entrainment Fraction in Two-Phase Gas-Liquid Annular Flow for Inclination angles of 0° , 10° , 20° , 45° , 60° , 75° , and 90° from Horizontal
- ◆ Compare Data with Current Correlation and Model Predictions
- ◆ If Possible, Improve Existing Models with New Correlation

Introduction

- ◆ Multiphase Flow Mechanistic Models Are Tools in Multiphase Design and Applications
 - Pressure Gradient
 - Liquid Holdup
 - Temperature Gradient
 - Etc.

Introduction



- ◆ **These Mechanistic Models (e.g. TUFFP Unified Model) Require Closure Relationships**

- Interfacial Friction Factor
- Droplet Entrainment Fraction
- Slug Translational Velocity
- Etc.

Introduction

- 
- ◆ **Chen (2005a) Sensitivity Study Showed that for Annular Flow the TUFFP Unified Model and Xiao Model are Most Sensitive to Droplet Entrainment Fraction Compared to Other Closure Relationships**

Literature Review Summary

- ◆ Most Research and Methods are for Vertical Annular Flow
- ◆ In Most Methods, Empirical Constants are Implemented Based on Experimental Data
- ◆ Few Entrainment Fraction Experimental Data Points for Inclined Flow
- ◆ Conflicting Results for Pipe Inclination Effect on Entrainment Fraction

Experimental Facility

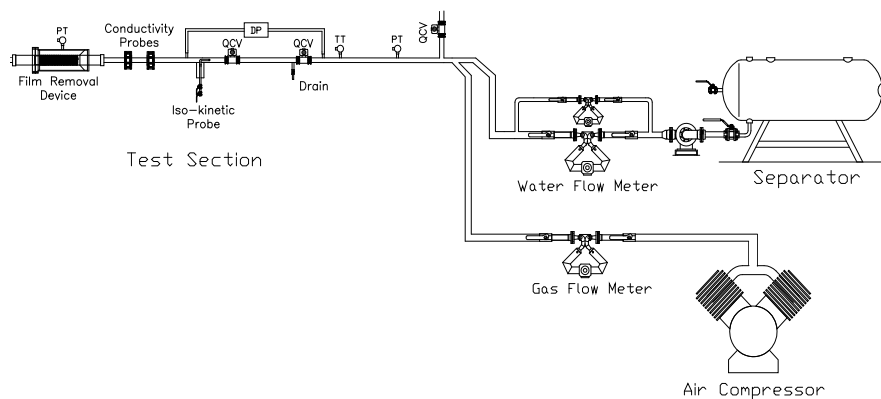
- ◆ 3 inch Severe Slugging Flow Loop



Experimental Facility ...

- ◆ Test Section 180 Diameters from Inlet to Ensure Fully Developed Flow
- ◆ Installation of Quick Closing Valves to Measure Local Liquid Holdup
- ◆ Installation of Conductivity Probes to Measure Wave Characteristics
- ◆ Measurement of Entrainment Fraction using Two Techniques

Experimental Facility ...



Testing Range

- **Superficial Water Velocity**
 - ▲ 0.0035, 0.01, 0.02, and 0.04 m/s
- **Superficial Air Velocity**
 - ▲ 40, 50, 60, 70, and 80 m/s
- **Inclination Angle**
 - ▲ 0°, 10°, 20°, 45°, 60°, 75°, and 90° from Horizontal

Measurement Techniques

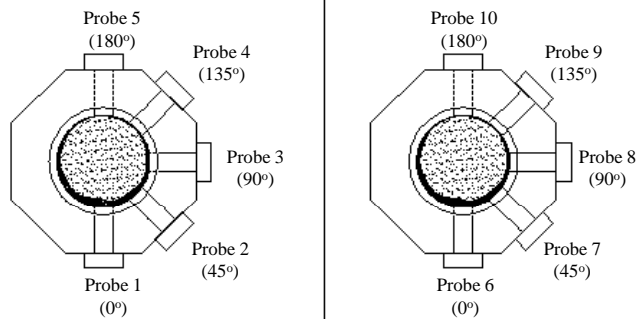
- ◆ **Conductivity Probe**
- ◆ **Film Removal Device**
- ◆ **Iso-kinetic Probe**

Conductivity Probe

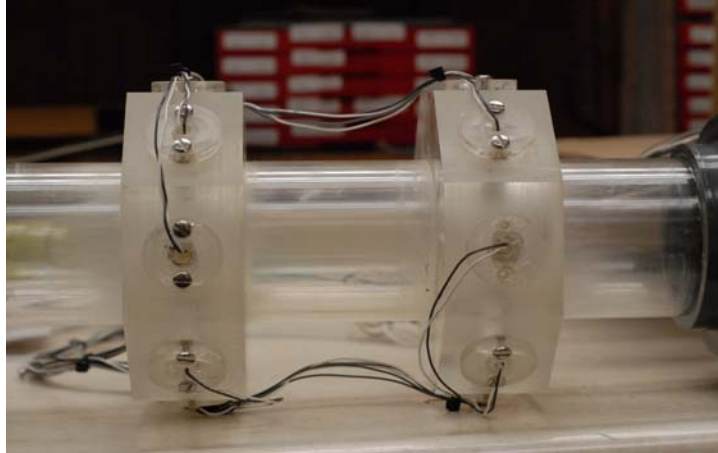


Conductivity Probe ...

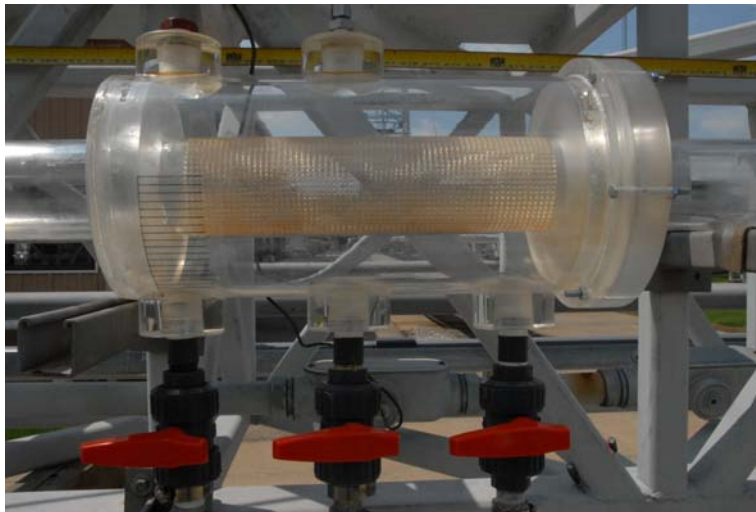
◆ Assembly Configuration



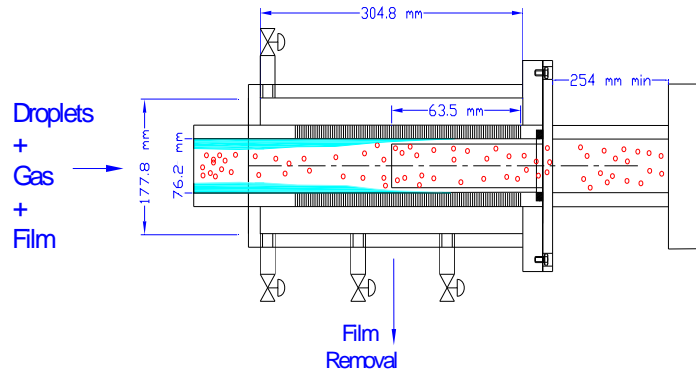
Conductivity Probe ...



Film Removal Device



Film Removal Device ...



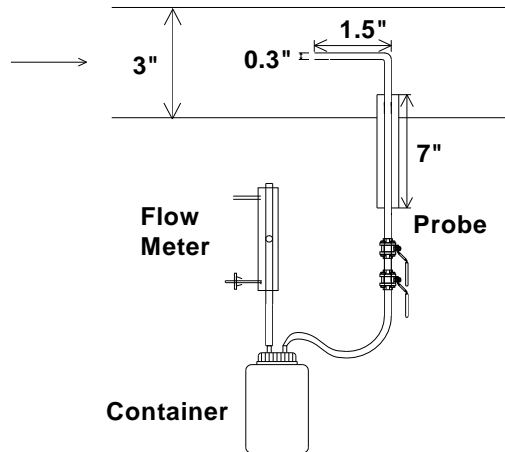
Film Removal Device ...

◆ Film Removal Device

- Measurement of Entrainment Fraction
- Liquid Film is Stripped Through Porous Section
- Film Flow Rate is Obtained
- Entrainment Fraction is Calculated:

$$F_E = 1 - \frac{W_{Film}}{W_{Liquid}}$$

Iso-kinetic Sampling Probe



Iso-kinetic Sampling Probe ...



Iso-kinetic Sampling Probe ...

◆ Iso-kinetic Sampling Probe

- Entrained Droplets are Sampled Over a Given Length of Time at Five Radial Distances
- Entrainment Flux Profile is Created
- Entrainment Fraction is Calculated by Integrating Flux Profile
- Most Accurate Under Low Liquid Flow Rates
- Iso-kinetic Conditions Only Reached at Low Gas Flow Rates

Experimental Results

- ◆ Entrainment Fraction
 - Film Removal Technique
 - Iso-kinetic Sampling
- ◆ Liquid Holdup
- ◆ Average Film Thickness
- ◆ Wave Characteristics
 - Celerity
 - Frequency
 - Amplitude
 - Wavelength

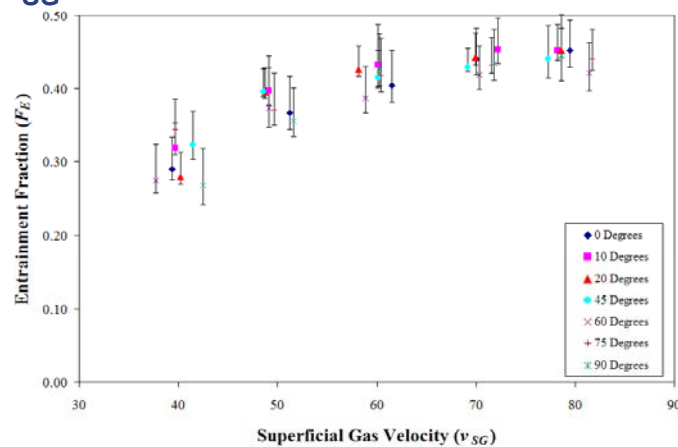
Entrainment Fraction

💧 Film Removal Technique

- 140 Data Points
- Each Test Repeated Three Times
- Clear Inclination Effect Observed
 - ⤴ Most Significant at Low v_{SG}
 - ⤴ Increases with Increasing v_{SL}

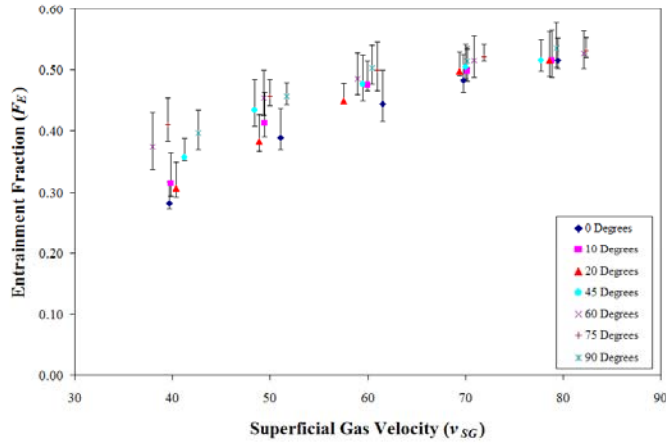
Film Removal Technique

💧 $v_{SG} = 0.0035 \text{ m/s}$



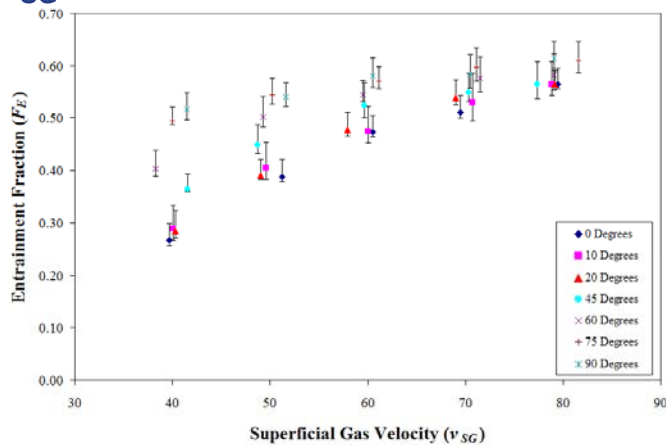
Film Removal Technique ...

• $v_{SG} = 0.01$ m/s



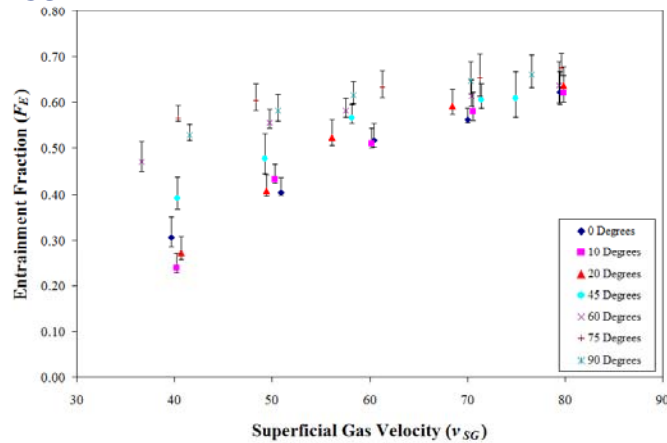
Film Removal Technique ...

• $v_{SG} = 0.02$ m/s



Film Removal Technique ...

💧 $v_{SG} = 0.04 \text{ m/s}$



Entrainment Fraction

💧 Iso-kinetic Sampling

➤ 48 Data Points

▲ $v_{SL} = 0.0035$ and 0.01 m/s

▲ $v_{SG} = 40$ and 50 m/s

➤ Each Test Repeated Twice

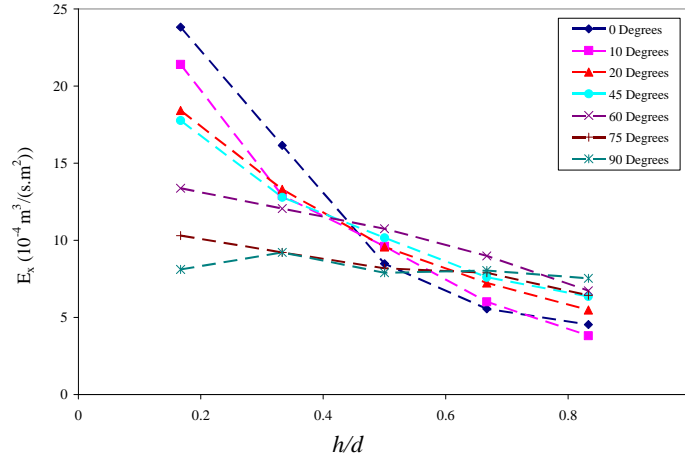
➤ Entrainment Flux Increases for Increasing v_{SL} & v_{SG}

➤ Inclination Angle Effect on Droplet Concentration Observed

▲ Increasing Inclination Angle Promotes Even Entrained Droplet Concentration

Iso-kinetic Sampling

• $v_{SL} = 0.0035 \text{ m/s}$, $v_{SG} = 40 \text{ m/s}$

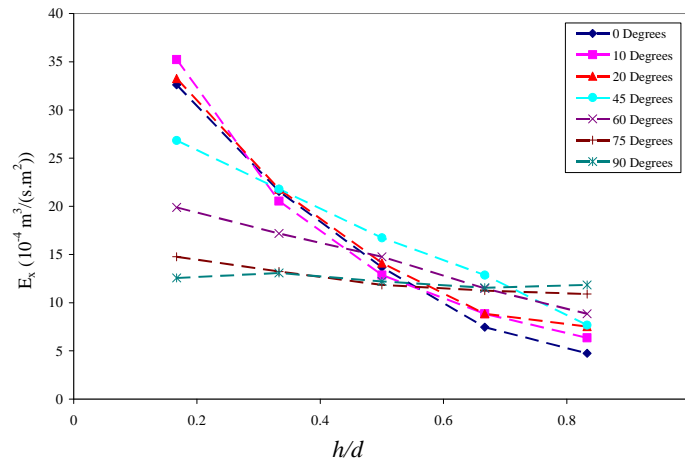


Fluid Flow Projects

Advisory Board Meeting, September 30, 2009

Iso-kinetic Sampling ...

• $v_{SL} = 0.0035 \text{ m/s}$, $v_{SG} = 50 \text{ m/s}$

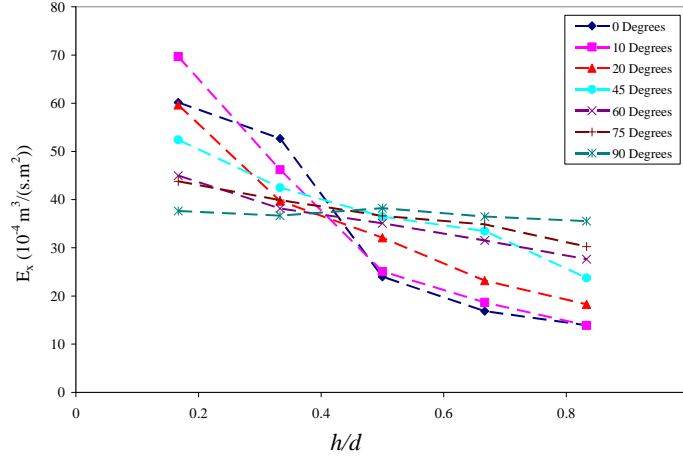


Fluid Flow Projects

Advisory Board Meeting, September 30, 2009

Iso-kinetic Sampling ...

• $v_{SL} = 0.01$ m/s, $v_{SG} = 40$ m/s

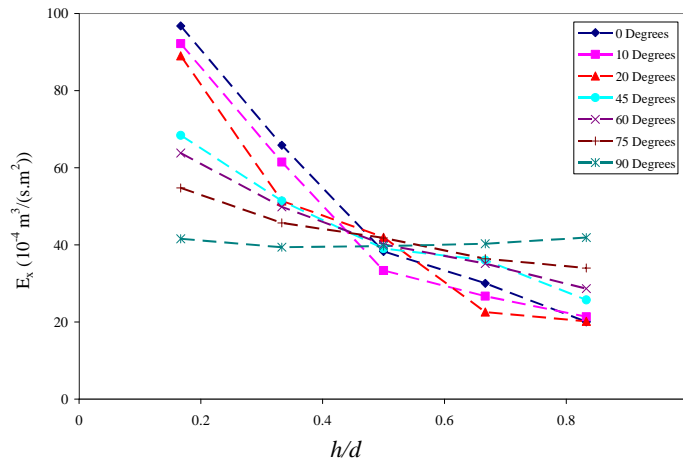


Fluid Flow Projects

Advisory Board Meeting, September 30, 2009

Iso-kinetic Sampling ...

• $v_{SL} = 0.01$ m/s, $v_{SG} = 50$ m/s

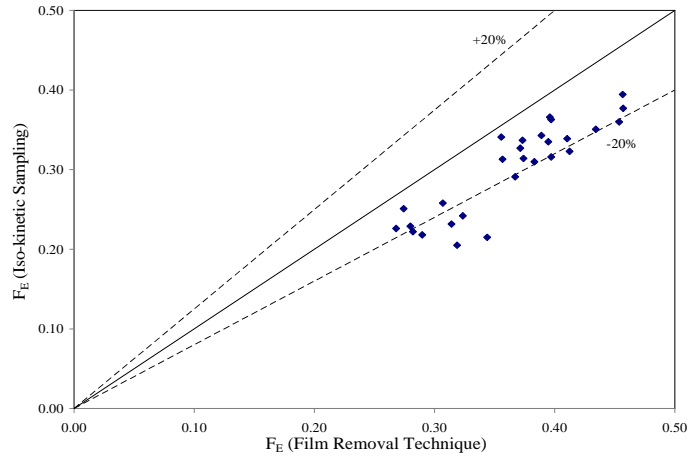


Fluid Flow Projects

Advisory Board Meeting, September 30, 2009

Entrainment Fraction

Entrainment Measurement Comparison

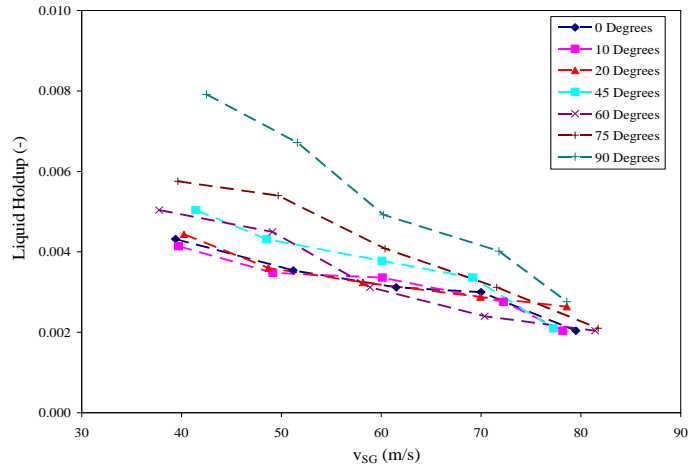


Liquid Holdup

- Holdup Decreases for Increasing v_{SG}
- Holdup Increases for Increasing v_{SL}
- At low v_{SL} and v_{SG} , Holdup Increases for Increasing Inclination Angle

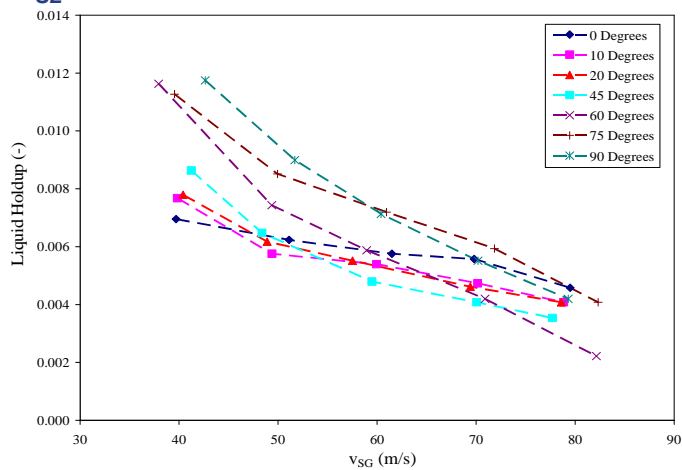
Liquid Holdup ...

• $v_{SL} = 0.0035 \text{ m/s}$



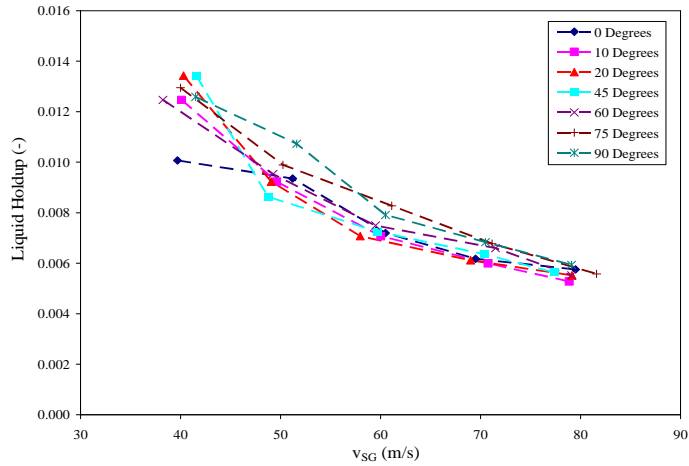
Liquid Holdup ...

• $v_{SL} = 0.01 \text{ m/s}$



Liquid Holdup ...

• $v_{SL} = 0.02 \text{ m/s}$

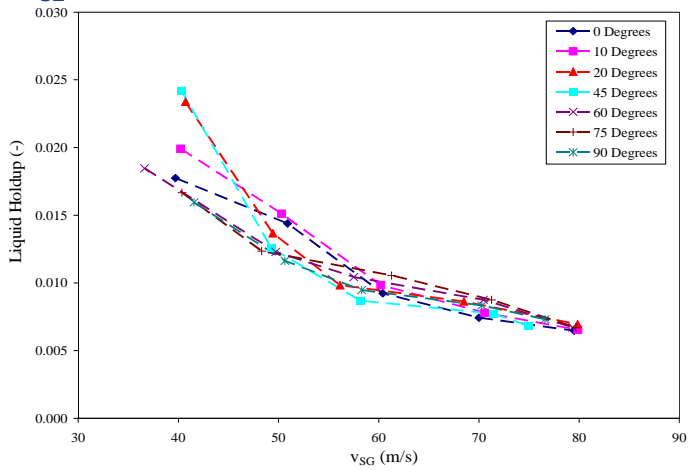


Fluid Flow Projects

Advisory Board Meeting, September 30, 2009

Liquid Holdup ...

• $v_{SL} = 0.04 \text{ m/s}$



Fluid Flow Projects

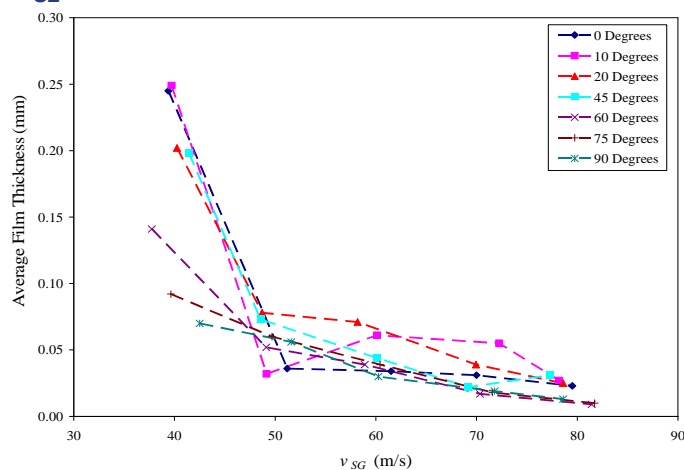
Advisory Board Meeting, September 30, 2009

Film Thickness

- ◆ Calculated by Averaging Film Height Time Trace
- ◆ Thickness Decreases for Increasing v_{SG} and Inclination Angle
- ◆ Thickness Increases for Increasing v_{SL}
- ◆ Inclination and v_{SG} Effect on Film Symmetry Observed

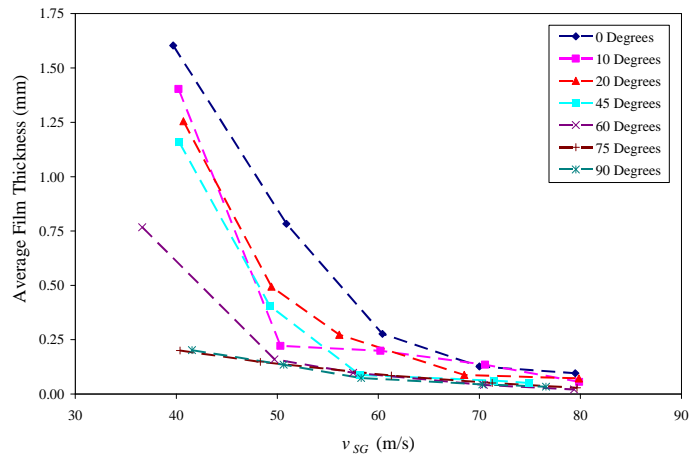
Film Thickness ...

◆ $v_{SL} = 0.0035$ m/s



Film Thickness ...

• $v_{SL} = 0.04$ m/s

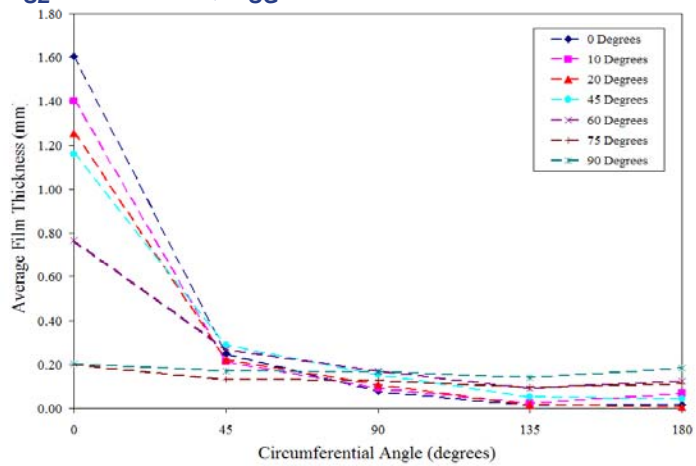


Fluid Flow Projects

Advisory Board Meeting, September 30, 2009

Film Thickness ...

• $v_{SL} = 0.04$ m/s, $v_{SG} = 40$ m/s

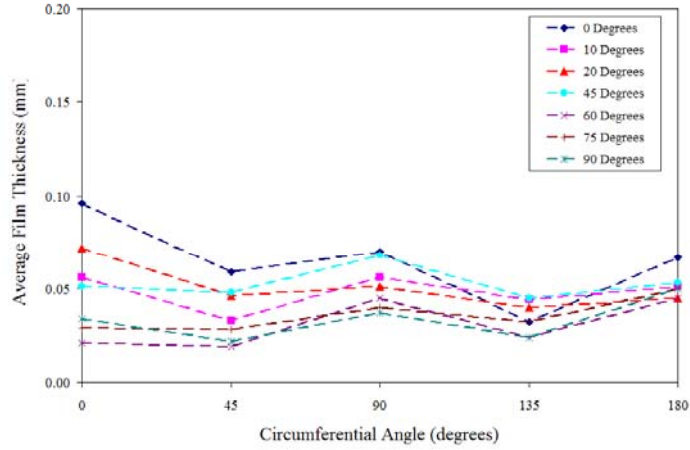


Fluid Flow Projects

Advisory Board Meeting, September 30, 2009

Film Thickness ...

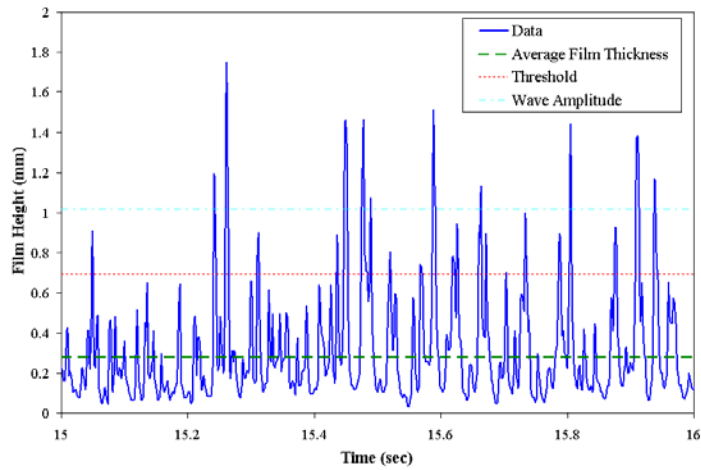
• $v_{SL} = 0.04 \text{ m/s}$, $v_{SG} = 80 \text{ m/s}$



Fluid Flow Projects

Advisory Board Meeting, September 30, 2009

Wave Characteristics



Fluid Flow Projects

Advisory Board Meeting, September 30, 2009

Wave Celerity

◆ Cross-Correlation Calculation

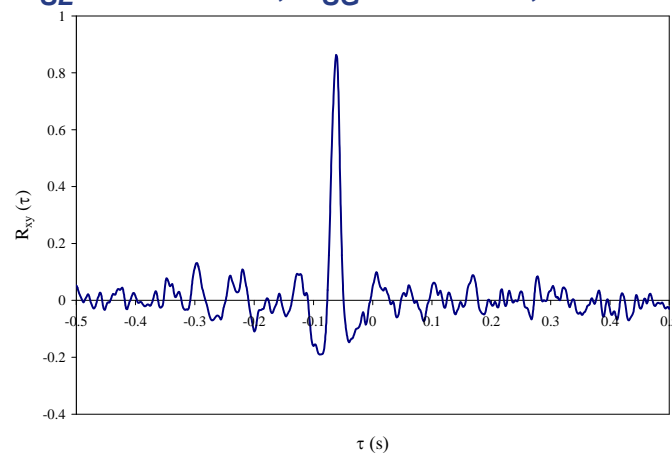
- MATLAB
- VBA Program

◆ Celerity Increases for Increasing v_{SG}

◆ Significant Effect at 10° and 20° from Horizontal

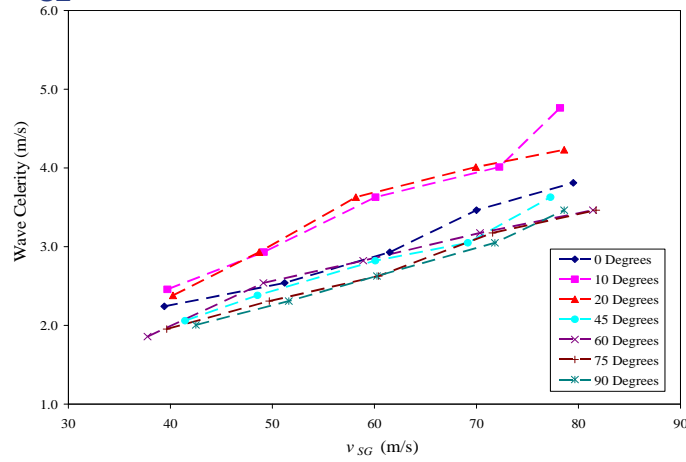
Wave Celerity ...

◆ $v_{SL} = 0.04$ m/s, $v_{SG} = 40$ m/s, $\theta = 0^\circ$



Wave Celerity ...

• $v_{SL} = 0.0035$ m/s

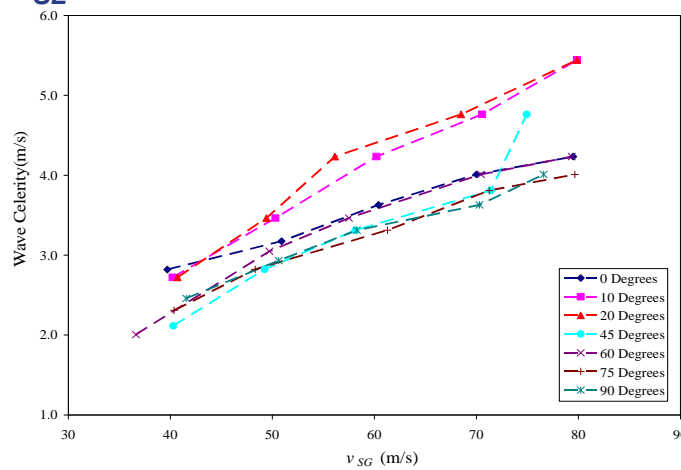


Fluid Flow Projects

Advisory Board Meeting, September 30, 2009

Wave Celerity ...

• $v_{SL} = 0.04$ m/s



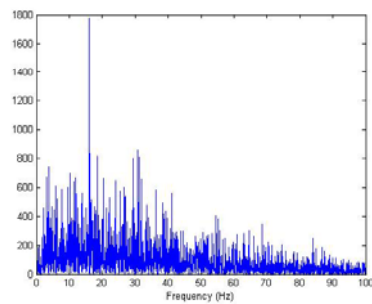
Fluid Flow Projects

Advisory Board Meeting, September 30, 2009

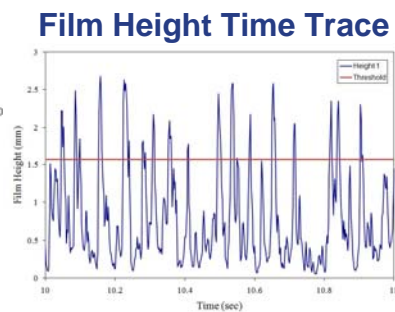
Frequency

- ◆ Calculation Methods
 - MATLAB Power Spectrum
 - Excel VBA Program
 - Manual Counting
- ◆ Frequency Increases with Increasing V_{SG}
- ◆ No Clear Inclination Effect Observed

Frequency ...

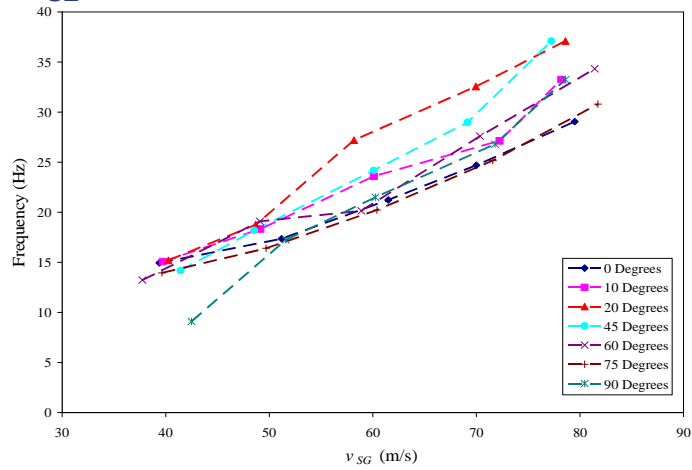


MATLAB Power Spectrum



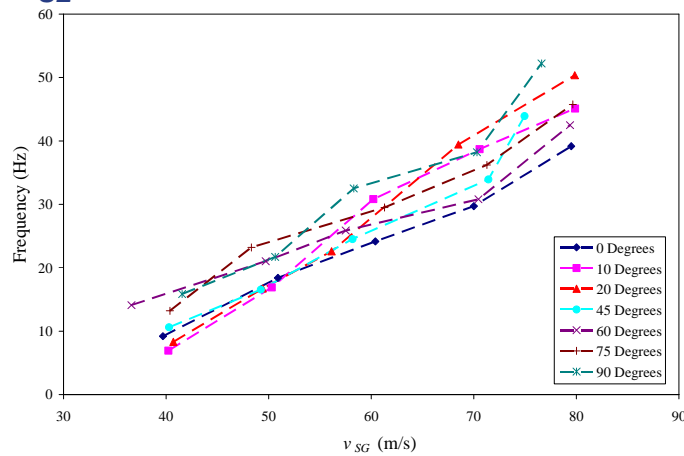
Frequency ...

🔹 $v_{SL} = 0.0035 \text{ m/s}$



Frequency ...

🔹 $v_{SL} = 0.04 \text{ m/s}$

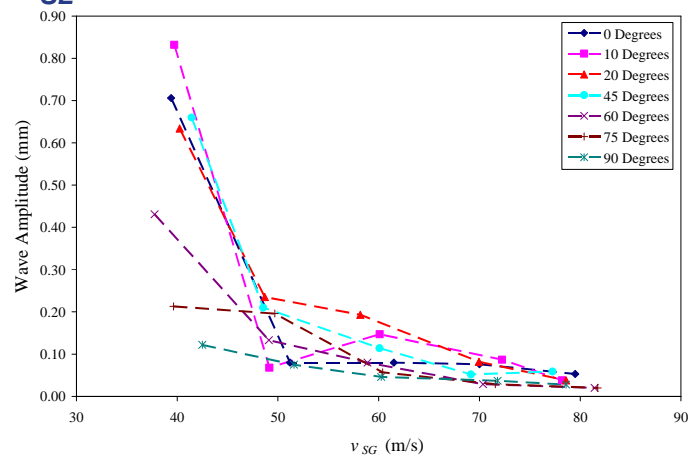


Wave Amplitude

- ◆ Calculated by Averaging Wave Crests
- ◆ Amplitude Decreases for Increasing v_{SG} and Inclination Angle
- ◆ Amplitude Increases for Increasing v_{SL}

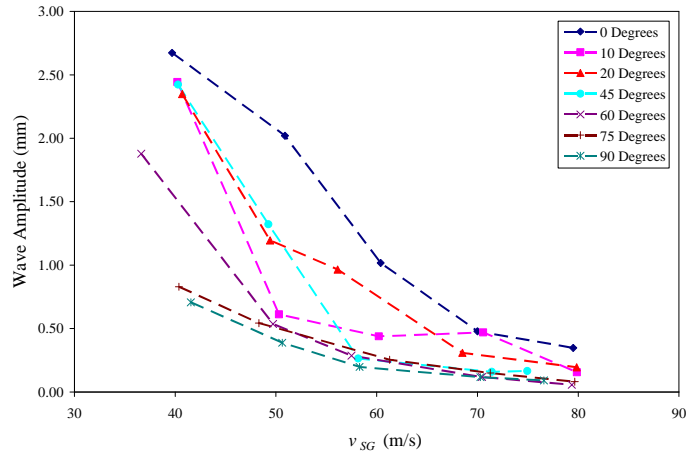
Wave Amplitude ...

◆ $v_{SL} = 0.0035$ m/s



Wave Amplitude ...

◆ $v_{SL} = 0.04$ m/s



Wavelength

◆ Calculated based on Celerity (v) & Frequency (ω):

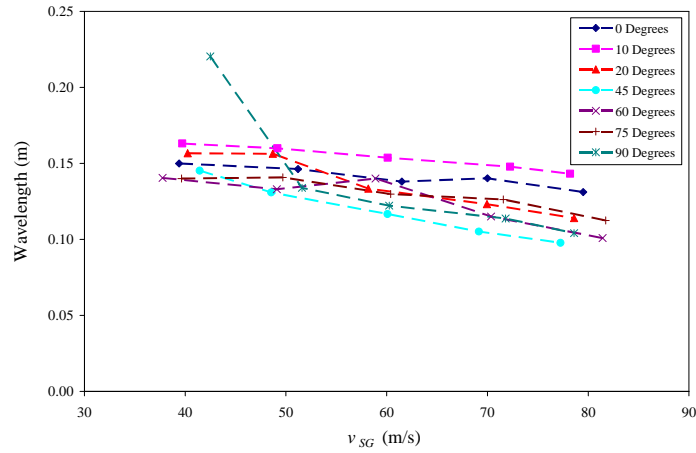
$$\lambda = \frac{v}{\omega}$$

◆ Wavelength Decreases for Increasing v_{SG}

◆ Inclination Effect for $v_{SL} = 0.04$ m/s

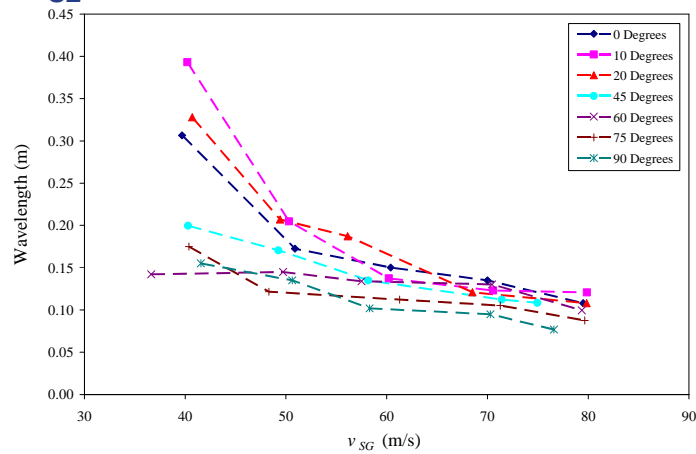
Wavelength ...

💧 $v_{SL} = 0.0035 \text{ m/s}$



Wavelength ...

💧 $v_{SL} = 0.04 \text{ m/s}$

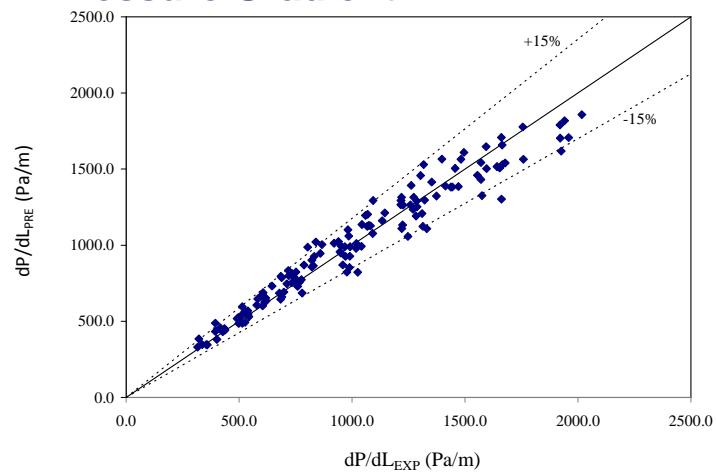


Model and Correlation Evaluation

- ◆ TUFFP Unified Model
 - Pressure Gradient Data
 - Liquid Holdup Data
- ◆ Present Study Entrainment Evaluation
- ◆ Entrainment Databank Evaluation

TUFFP Unified Model

◆ Pressure Gradient



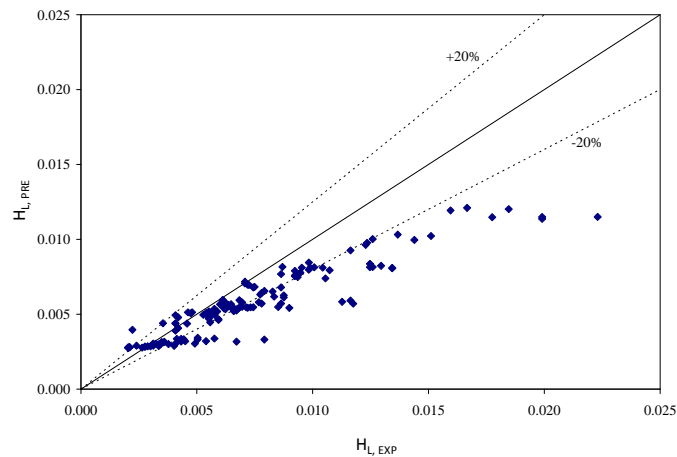
TUFFP Unified Model ...

Pressure Gradient

Data	Statistical Parameters					
	ε_1 (%)	ε_2 (%)	ε_3 (%)	ε_4 (Pa/m)	ε_5 (Pa/m)	ε_6 (Pa/m)
0°	0.6	8.8	13.5	-28.1	96.0	134.0
10°	-2.3	6.0	11.6	-38.8	69.4	95.6
20°	-3.7	6.3	12.6	-53.4	74.0	97.3
45°	7.1	10.7	11.3	40.4	89.8	98.6
60°	4.0	7.6	9.1	27.0	73.8	89.0
75°	2.2	6.0	4.5	22.5	62.1	77.3
90°	3.2	6.3	7.7	21.2	66.7	79.9
All Data	1.6	7.4	10.8	-1.3	76.0	101.6

TUFFP Unified Model ...

Liquid Holdup



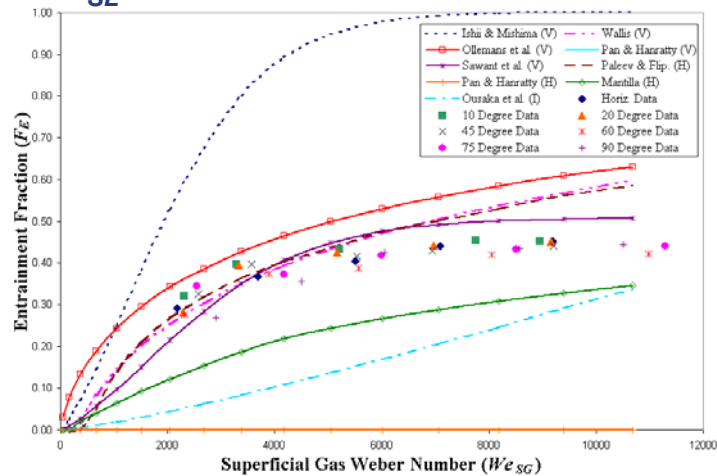
TUFFP Unified Model ...

💧 Liquid Holdup

Data	Statistical Parameters					
	ϵ_1 (%)	ϵ_2 (%)	ϵ_3 (%)	ϵ_4 (-)	ϵ_5 (-)	ϵ_6 (-)
0°	-11.4	14.9	30.4	-0.0012	0.0012	0.0016
10°	-10.8	16.1	32.6	-0.0013	0.0015	0.0022
20°	-13.0	15.5	32.7	-0.0014	0.0015	0.0022
45°	-12.2	20.7	39.8	-0.0015	0.0017	0.0026
60°	-11.1	26.1	48.1	-0.0016	0.0019	0.0021
75°	-23.1	26.4	53.6	-0.0021	0.0022	0.0016
90°	-27.0	27.3	57.8	-0.0023	0.0023	0.0016
All Data	-15.5	21.0	41.6	-0.0016	0.0018	0.0020

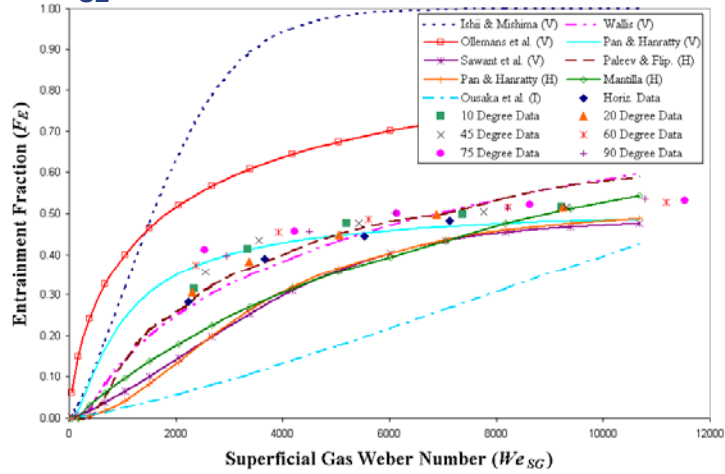
Present Study Entrainment Evaluation

💧 $Re_{SL} = 267$



Present Study Entrainment Evaluation ...

💧 $Re_{SL} = 760$

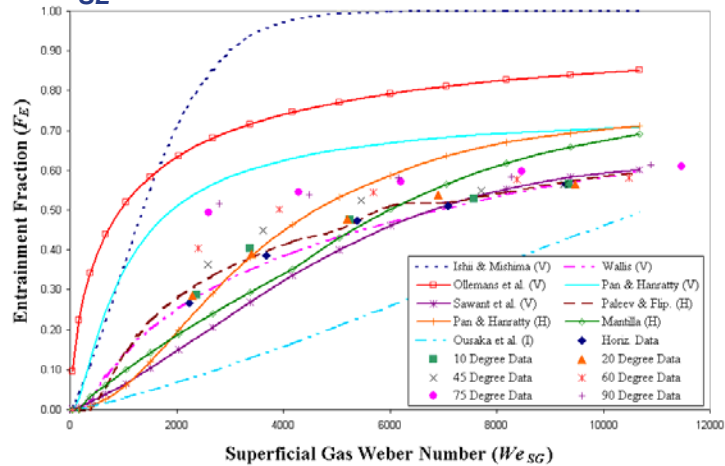


Fluid Flow Projects

Advisory Board Meeting, September 30, 2009

Present Study Entrainment Evaluation ...

💧 $Re_{SL} = 1520$

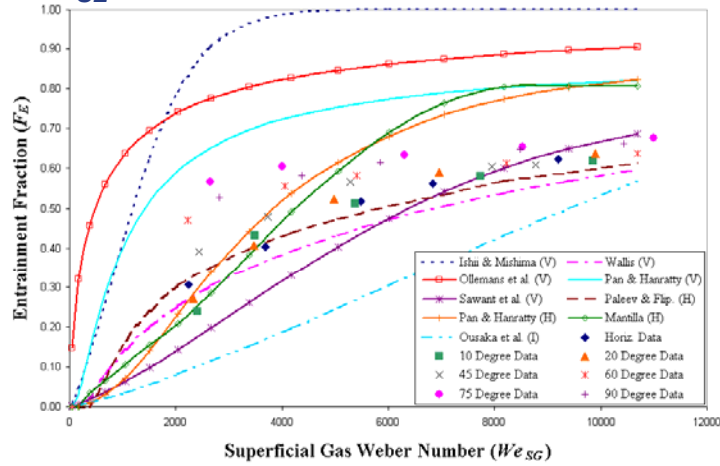


Fluid Flow Projects

Advisory Board Meeting, September 30, 2009

Present Study Entrainment Evaluation ...

● $Re_{SL} = 3040$



Present Study Entrainment Evaluation ...

Model/ Correlation	ϵ_1 (%)	ϵ_2 (%)	ϵ_3 (%)	ϵ_4 (-)	ϵ_5 (-)	ϵ_6 (-)
Ishii and Mishima (1987) Vert.	105.76	105.76	35.42	0.47	0.47	0.08
Wallis (1969) Vert.	-14.72	18.25	15.84	-0.07	0.09	0.08
Ollmans et al. (1986) Vert.	50.65	50.65	30.26	0.23	0.23	0.09
Pan and Hanratty (2002a) Vert.	-4.80	46.74	61.24	-0.01	0.20	0.24
Sawant et al. (2008) Vert.	-15.14	20.59	21.40	-0.07	0.09	0.10
Paleev and Flippov. (1966) Horiz.	-1.23	11.26	14.73	-0.01	0.05	0.07
Pan and Hanratty (2002b) Horiz.	-26.78	39.96	47.00	-0.10	0.17	0.20
Mantilla (2008) Horiz.	-15.34	25.29	25.10	-0.05	0.11	0.12
Ousaka et al. (1992) Inclined	73.87	97.44	75.10	0.34	0.44	0.31
Chen (2005) Inclined	70.21	70.21	23.03	0.31	0.31	0.06

Entrainment Databank Evaluation

◆ Data from 14 Sources

- 7 Horizontal
- 5 Vertical
- 2 Inclined

◆ Parameter Range

- Diameter: 0.006 – 0.1 m
- v_{SL} : 0.0035 – 5.11 m/s
- v_{SG} : 4 – 166 m/s
- Angle: 0 – 90°
- σ : 0.012 – 0.074 dyne/cm
- ρ_G : 1.23 – 55.5 kg/m³
- ρ_L : 820 – 1300 kg/m³

Entrainment Databank Evaluation

◆ All Data w/o HARWELL Databank (724)

Model/Correlation	ϵ_1 (%)	ϵ_2 (%)	ϵ_3 (%)	ϵ_4 (-)	ϵ_5 (-)	ϵ_6 (-)
Ishii and Mishima (1987) Vert.	95.4	106.9	217.0	0.24	0.27	0.23
Wallis (1969) Vert.	64.5	109.9	563.2	-0.05	0.16	0.23
Oliemans et al. (1986) Vert.	160.2	162.0	553.0	0.18	0.19	0.19
Pan and Hanratty (2002a) Vert.	21.4	56.0	117.0	0.00	0.12	0.17
Sawant et al. (2008) Vert.	25.8	119.9	882.2	-0.10	0.31	1.17
Paleev and Flippov. (1966) Horiz.	70.8	93.0	322.7	0.05	0.13	0.20
Pan and Hanratty (2002b) Horiz.	-20.1	37.0	45.9	-0.06	0.12	0.16
Mantilla (2008) Horiz.	18.2	44.4	78.7	0.02	0.12	0.15
Ousaka et al. (1992) Inclined	1.6	81.5	90.2	0.00	0.35	0.41

Entrainment Databank Evaluation ...

♦ All Data w/ HARWELL Databank (1449)

Model/Correlation	ϵ_1 (%)	ϵ_2 (%)	ϵ_3 (%)	ϵ_4 (-)	ϵ_5 (-)	ϵ_6 (-)
Ishii and Mishima (1987) Vert.	47.6	74.8	170.9	0.12	0.22	0.25
Wallis (1969) Vert.	52.8	92.8	407.4	0.00	0.19	0.24
Oliemans et al. (1986) Vert.	86.2	97.8	400.8	0.08	0.13	0.18
Pan and Hanratty (2002a) Vert.	-6.9	48.0	91.2	-0.08	0.15	0.18
Sawant et al. (2008) Vert.	-24.0	98.2	625.8	-0.22	0.33	0.85
Paleev and Flippov. (1966) Horiz.	58.2	102.0	264.6	0.00	0.21	0.28
Pan and Hanratty (2002b) Horiz.	-14.0	47.4	61.0	-0.06	0.17	0.20
Mantilla (2008) Horiz.	61.8	81.9	158.1	0.11	0.18	0.22
Ousaka et al. (1992) Inclined	59.6	103.0	151.8	0.16	0.34	0.36

Entrainment Databank Evaluation ...

♦ Vertical Data w/o HARWELL Databank (213)

Model/Correlation	ϵ_1 (%)	ϵ_2 (%)	ϵ_3 (%)	ϵ_4 (-)	ϵ_5 (-)	ϵ_6 (-)
Ishii and Mishima (1987) Vert.	22.3	42.0	55.3	0.14	0.19	0.25
Wallis (1969) Vert.	-28.0	33.7	40.2	-0.14	0.16	0.20
Oliemans et al. (1986) Vert.	16.8	22.3	29.4	0.06	0.09	0.11
Pan and Hanratty (2002a) Vert.	-15.6	21.8	31.8	-0.06	0.09	0.13
Sawant et al. (2008) Vert.	82.4	84.1	101.1	0.36	0.36	0.39
Paleev and Flippov. (1966) Horiz.	-7.7	24.7	34.6	-0.05	0.10	0.12
Pan and Hanratty (2002b) Horiz.	-28.9	37.4	48.8	-0.06	0.09	0.13
Mantilla (2008) Horiz.	-62.9	63.7	68.8	-0.31	0.32	0.36
Ousaka et al. (1992) Inclined	-0.9	23.3	38.1	-0.01	0.11	0.18

Entrainment Databank Evaluation ...

♦ Vertical Data w/ HARWELL Databank (938)

Model/Correlation	ϵ_1 (%)	ϵ_2 (%)	ϵ_3 (%)	ϵ_4 (-)	ϵ_5 (-)	ϵ_6 (-)
Ishii and Mishima (1987) Vert.	4.8	42.4	77.2	0.03	0.17	0.22
Wallis (1969) Vert.	25.3	66.1	115.0	0.00	0.20	0.24
Oliemans et al. (1986) Vert.	13.2	31.0	64.4	0.00	0.08	0.10
Pan and Hanratty (2002a) Vert.	-30.6	35.8	47.2	-0.13	0.15	0.21
Sawant et al. (2008) Vert.	100.0	111.4	204.4	0.23	0.28	0.34
Paleev and Flippov. (1966) Horiz.	33.3	91.4	171.6	-0.05	0.24	0.30
Pan and Hanratty (2002b) Horiz.	-12.6	53.1	68.2	-0.07	0.18	0.23
Mantilla (2008) Horiz.	67.0	106.7	201.4	0.08	0.27	0.33
Ousaka et al. (1992) Inclined	109.5	115.5	192.9	0.33	0.34	0.38

Entrainment Databank Evaluation ...

♦ Horizontal Data (318)

Model/Correlation	ϵ_1 (%)	ϵ_2 (%)	ϵ_3 (%)	ϵ_4 (-)	ϵ_5 (-)	ϵ_6 (-)
Ishii and Mishima (1987) Vert.	152.8	155.1	288.8	0.28	0.28	0.22
Wallis (1969) Vert.	156.4	187.4	784.7	0.01	0.19	0.29
Oliemans et al. (1986) Vert.	281.8	282.0	759.9	0.25	0.25	0.22
Pan and Hanratty (2002a) Vert.	58.5	80.5	151.1	0.05	0.12	0.17
Sawant et al. (2008) Vert.	104.8	184.5	1241.3	0.03	0.39	1.64
Paleev and Flippov. (1966) Horiz.	148.8	161.3	441.0	0.13	0.18	0.23
Pan and Hanratty (2002b) Horiz.	-7.1	32.1	45.7	-0.01	0.09	0.14
Mantilla (2008) Horiz.	40.8	59.3	99.7	0.05	0.12	0.16
Ousaka et al. (1992) Inclined	-74.1	80.6	36.4	-0.35	0.35	0.24

Entrainment Databank Evaluation ...

◆ Inclined Data (148)

Model/ Correlation	ϵ_1 (%)	ϵ_2 (%)	ϵ_3 (%)	ϵ_4 (-)	ϵ_5 (-)	ϵ_6 (-)
Ishii and Mishima (1987) Vert.	60.9	82.7	94.8	0.30	0.34	0.39
Wallis (1969) Vert.	-27.3	30.0	39.8	-0.08	0.09	0.11
Oliemans et al. (1986) Vert.	69.0	69.4	105.7	0.19	0.20	0.22
Pan and Hanratty (2002a) Vert.	-16.9	45.9	59.3	-0.03	0.16	0.21
Sawant et al. (2008) Vert.	-39.5	43.0	55.8	-0.11	0.13	0.17
Paleev and Flippov. (1966) Horiz.	-6.3	23.9	39.9	-0.01	0.06	0.07
Pan and Hanratty (2002b) Horiz.	-39.9	49.0	61.0	-0.11	0.16	0.20
Mantilla (2008) Horiz.	-10.0	30.5	36.9	-0.02	0.11	0.13
Ousaka et al. (1992) Inclined	73.3	80.3	92.5	0.34	0.34	0.40

Conclusions

- ◆ Clear Inclination Effect on Entrainment Observed
- ◆ No Significant Inclination Effect Observed for Frequency, Wavelength, and Celerity
- ◆ Inclination Effect Caused by Gravitational Force on Liquid Film and Entrained Droplets

Conclusions ...

- ◆ **Inability of Single Correlation or Model to Predict Entrainment at All Angles**
- ◆ **Entrainment Statistical Analysis Results:**
 - All Data – Pan & Hanratty (2002b)
 - Vertical Data – Oliemans et al. (1986)
 - Horizontal Data – Pan & Hanratty (2002b)
 - Inclined Data – Paleev & Flipp. (1966)
- ◆ **More Inclined Entrainment Data is Needed**
- ◆ **Entrainment Prediction Improvement is Needed**

Questions/Comments



Liquid Entrainment in Annular Gas-Liquid Flow in Inclined Pipes

Kyle Magrini

PROJECTED COMPLETION DATES:

Literature Review	Completed
Facility Modifications	Completed
Preliminary Correlation Development	Completed
Testing.....	Completed
Model and Correlation Validation.....	Completed
Final Report.....	Completed

Objectives

The objectives of this study are:

- to acquire liquid entrainment data in two-phase gas-water annular flow through pipes from horizontal to near vertical,
- to validate current methods with experimental results, and
- to improve current methods, if necessary, or develop a new method.

Introduction

Annular flow usually occurs at high gas velocities and low to medium liquid velocities. The liquid flows as a film along the wall of the pipe and as droplets entrained in the gas core. The interface between the gas core and liquid film is usually very wavy, causing atomization and deposition of liquid droplets. Under equilibrium conditions, the rate at which the droplets atomize and deposit becomes equal, resulting in a steady fraction of the liquid being entrained as droplets, F_E . This critical parameter is crucial to understand and model the behavior of annular flow.

Most multiphase flow prediction models (including the TUFFP unified mechanistic models) are based on a simplified (one-dimensional) two-fluid model in which empirical closure relationships (i.e. interfacial friction factor, interfacial area, droplet entrainment fraction, etc.) are needed. The performance of the multiphase flow model is determined by the accuracy and physical completeness of these closure relationships. The literature reveals that sufficient

physics of multiphase flow may not be contained in these empirical closure relationships. Therefore, further refinements of these closure relationships can significantly improve the performance of multiphase mechanistic models.

Chen (2005) conducted a sensitivity study to investigate the influence of individual closure relationships on the predictions of a multiphase mechanistic model. The study showed that in annular flow the variation in droplet entrainment fraction can substantially affect the predicted pressure gradient and liquid hold-up. Thus, the use of an accurate predictive model for entrainment fraction is imperative.

Experimental Study

TUFFP's 76.2-mm (3-in.) diameter severe slugging facility (shown in Fig. 1) is modified for this experimental study. The facility is capable of being inclined from horizontal to vertical. Pressure and temperature transducers are placed near the test section to obtain fluid properties and flowing characteristics that are used in the entrainment fraction correlations.

There were four major components in the test section: a quick-closing valve section, iso-kinetic sampling section, film removal section, and conductivity probe section.

Compressed air and Tulsa city tap water are used in this study. The surface tension of the tap water is measured frequently to ensure accurate results.

Testing Range

In this study, a large number of data points were collected at various conditions in terms of both fluid velocities and inclination angles. Superficial water velocities range from 0.0035 to 0.04 m/sec. Superficial gas velocities range from 40 to 80 m/sec. Experiments were conducted at inclination angles 0°, 10°, 20°, 45°, 60°, 75°, and 90° from horizontal.

Quick-Closing Valve Section

The quick-closing valve section is located 9.65 m ($L/d = 127$) from the inlet. It is 1.83 m long and consists of two 76.2-mm (3-in.) ball type quick-closing valves. A third quick-closing is installed in the bypass section at the inlet of the system. The three quick-closing valves are automated to trap the flowing liquid in the section and obtain the average liquid holdup. A small port is installed for the insertion of a syringe to obtain the volume of water collected.

Iso-kinetic Sampling Section

An iso-kinetic sampling system is utilized to determine the liquid entrainment in the gas stream. This section is located 11.6 m ($L/d = 152$) downstream of the inlet. The schematic and photograph of the system are shown in Figs. 2 and 3, respectively. The system consists of an iso-kinetic probe, a small container, and a gas flow meter. To ensure iso-kinetic conditions, two ball valves control the sampling rate to ensure the gas velocity in the probe is approximately the same as the gas velocity in the pipe. During each experiment, the iso-kinetic sampling probe traverses the pipe to obtain samples at different locations. The liquid droplets collected by the probe settle in the container while the gas sampled is vented to the atmosphere through the flow meter. This liquid volume and the sampling time are used to determine the entrainment flux for each location. The iso-kinetic sampling probe works best under low liquid flow rates where a more distinct division between the gas core and liquid film exists. The results of the iso-kinetic sampling probe are used in validating the results obtained from the film removal device.

Film Removal Section

The film removal section is located 13 m ($L/d = 172$) downstream of the inlet. The section consists of a film removal device and film volume tank. The film removal device is used to measure the entrainment fraction. To measure the entrainment, the device

utilizes a long porous section and inserted sleeve to separate the liquid film from the entrained droplets. Figures 4 and 5 display a schematic and picture of the film removal device. The flow passes through the porous section and the liquid film, traveling at a lower velocity than the gas core, is pushed through the porous section. The high inertia of the entrained droplets, flowing close to the gas velocity, prevents them from being removed through the porous section. To ensure no droplets will escape, a long sleeve was inserted close to where the liquid film dissipates. This sleeve is able to move in and out in the pipe to make sure the liquid film passes under the sleeve and only the gas core with droplets passes through the test section.

Conductivity Section

The conductivity section is utilized to obtain average thickness and wave characteristics of the liquid film. Located 12.5 m ($L/d = 164$) from the inlet, the conductance section consists of two octagonal shaped probe assemblies spaced 0.15 m apart. Figure 6 displays the conductance section with the assemblies. Each assembly contains five flush mounted probes installed from the bottom to the top of the pipe, spaced 45° apart. The orientation of the probes in each assemble can be found in Fig. 7.

Flush mounted conductance probes were chosen for this study due to the thin liquid films encountered at the studied flow conditions. Liquid films with thicknesses from 4 mm down to 0.03 mm can be measured with these probes. The flush mounted probes consist of two parallel plates, 1.59 mm wide and 10 mm long, spaced 1.5 mm apart. Brass is used in the construction of the probes due to its high conductivity and corrosion resistance. The flush mounted conductance probes are calibrated dynamically. The mean value of the voltage reading is paired with the mean film thickness to construct the calibration curve for that probe. An equation can then be found to correlate the film thickness (h_L) to the output voltage (V) for each probe. These equations are then used to determine the average film thickness and wave characteristics of the flowing film.

Uncertainty Analysis

The purpose of measurements is to numerically portray the performance of a process, Dieck (2002). There is an inherent error associated with each measurement. The definition of error is the difference between the measured and true values. Since the true value is rarely known, the error

associated with that value is unknown as well. Uncertainty Analysis is a method to estimate the limits of this unknown error and describe the quality of the experimental data.

There are two types of errors, random error and systematic error. Random errors affect the experimental data in a random fashion. Random uncertainty refers to the limits of these random errors and is based on the standard deviation of the data. Systematic errors are the difference between the average measured value and true value. These errors remain constant throughout the experimental process. Systematic uncertainty refers to the limit of the systematic errors.

When the data are not measured directly, i.e. entrainment fraction, the propagation of uncertainties should be calculated to determine the uncertainty of these parameters. Random uncertainty, systematic uncertainty, and the propagation of uncertainty will be discussed in more detail below. The uncertainty analysis of the experimental results for this study will also be reported.

Random Uncertainty

To obtain the random error, a sample of N samples of a population are used to calculate the standard deviation as

$$S_x = \left[\frac{\sum (X_i - \bar{X})^2}{N-1} \right]^{1/2}. \quad (1)$$

The standard deviation of the population average is calculated as

$$S_x^- = \frac{S_x}{\sqrt{N}}. \quad (2)$$

S_x^- is the random uncertainty with a 68% confidence level. To obtain the necessary 95% confidence level, the Student's t distribution is used. The random uncertainty can be stated as $\bar{X} - t_{95} S_x^- \leq X \leq \bar{X} + t_{95} S_x^-$.

Systematic Uncertainty

Systematic errors affect every measurement in the same way. Therefore, experimental data cannot be used to estimate the systematic uncertainty. Systematic errors are usually due to flaws in equipment, biased judgment, or an additional physical affect. In this study, the main source for systematic error is the calibration of the equipment.

Calibration errors were used to calculate the systematic uncertainties for the absolute pressure, differential pressure, and temperature transmitters and conductance probes. Systematic uncertainty calculation for the iso-kinetic, liquid holdup, and film removal device measurements are more complicated. These uncertainties are based on the experience of the researcher.

Each systematic uncertainty source, b_i , is combined to obtain the systematic uncertainty, B_R , using the following equation:

$$B_R = \left[\sum_{i=1}^N (b_i^2) \right]^{1/2}. \quad (3)$$

Combined Uncertainty

Measured uncertainty is the combination of the systematic and random elements of uncertainty. The combined uncertainty can be calculated by

$$U_{95} = \pm t_{95} \left[\left(\frac{B}{2} \right)^2 + (S_x^-)^2 \right]^{1/2} \quad (4)$$

The combined uncertainty is stated at the 95% confidence level. The test data can be expressed as $\bar{X} - U_{95} \leq X \leq \bar{X} + U_{95}$. In other words, the value X will be in the range $\bar{X} \pm U_{95}$, 95% of the time.

Uncertainty Propagation

When a parameter is a function of two or more directly measured parameters, the uncertainty in the derived parameter must be calculated based on the uncertainties of the parameters from which it was calculated. This process is the propagation of uncertainty. In this study, uncertainty propagation analysis was performed for the entrainment fraction from the film removal device, the gas superficial velocity, liquid superficial velocity, and average film thickness.

If y is a function of a, b, c, \dots , the uncertainty of y will be described as a function of independent uncertainties of a, b, c, \dots , and expressed as follows:

$$U_y = \sqrt{\left[\left(\frac{\partial y}{\partial a} \right)^2 (U_a)^2 + \left(\frac{\partial y}{\partial b} \right)^2 (U_b)^2 + \left(\frac{\partial y}{\partial c} \right)^2 (U_c)^2 + \dots \right]}. \quad (5)$$

The uncertainty analysis for the parameters in this study can be found in Table 1.

Experimental Results

140 tests were conducted at inclination angles of 0°, 10°, 20°, 45°, 60°, 75°, and 90° from horizontal. Measurements were obtained for liquid entrainment fraction, liquid holdup, pressure drop, average film thickness and wave characteristics of the liquid film.

Liquid Entrainment Fraction

Liquid entrainment fraction was obtained using two proven techniques, film removal and iso-kinetic sampling. Both methods have been used extensively by past researchers to obtain entrainment fraction. Liquid entrainment data measured using both techniques are presented. The results from both methods are also compared.

Film Removal Entrainment Results

Figures 8-11 display the results of entrainment fraction measurements using the film removal technique. Each figure is at constant superficial liquid velocity and includes the uncertainty associated with each entrainment measurement.

These figures show a clear effect of pipe inclination on entrainment. As pipe inclination from horizontal increases, entrainment fraction increases. Entrainment fraction reaches a maximum value at an angle of 90 degrees from horizontal. The figures also display the range of this inclination effect. Pipe inclination significantly affects entrainment at lower superficial gas velocities and higher superficial liquid velocities. At lower superficial gas velocities, the symmetry of the liquid film has a more significant effect on entrainment fraction. For horizontal flow, a thick liquid film is present at the bottom of the pipe. As the inclination angle from horizontal is increased, the film becomes more symmetrical. The transition of the liquid film distribution from a thick film at the bottom of the pipe to a symmetrical film promotes a larger surface area from which droplets are removed and entrained. As a result, entrainment fraction increases as the inclination angle increases. At high gas velocities, a symmetric liquid film is present at all inclination angles. This is evident in Figs. 8-11 where a common maximum entrainment value is approached for all inclination angles.

The inclination angle effect is also dependent on superficial liquid velocity. At low superficial liquid velocities, there is less inclination effect on entrainment fraction. This can be seen in Fig. 8. As the superficial liquid velocity is increased, the effect

of inclination is magnified at lower superficial gas velocities. This can be seen in Figs. 8-11.

In summary, the inclination angle of the pipe has a significant effect on entrainment fraction. This effect is more substantial at low superficial gas velocities and high superficial liquid velocities.

Iso-kinetic Sampling Entrainment Results

Tests were conducted at each inclination angle for superficial gas velocities of 40 and 50 m/s and low superficial liquid velocities of 0.0035 and 0.01 m/s. The entrainment flux profiles for these flow conditions are shown in Figs. 12-15. The figures exhibit the effect pipe inclination has on entrainment flux and droplet concentration profiles. Due to gravity and the asymmetry of the liquid film at horizontal flow, a large droplet concentration exists at the bottom of the pipe. As the pipe is inclined, the droplet concentration and entrainment flux profile become more symmetrical. Even droplet concentration and entrainment flux profiles exist for vertical flow due to the symmetry of the liquid film and vanishing of gravity effect across the pipe section. This clearly shows that for horizontal flow all the droplet atomization and deposition occurs at the bottom of the pipe. Once the inclination angle is increased, the film becomes more symmetrical, leading to atomizing and depositing of droplets across the entire inner circumference of the pipe. The increase in surface area for gas-water interaction leads to a uniform droplet concentration and even entrainment flux profile across the pipe. This also gives insight into how increasing in pipe inclination angle increases entrainment fraction.

Entrainment Measurement Methods Comparison

The film removal technique and iso-kinetic sampling have been the predominant methods used by researchers to measure entrainment fraction. However, the two methods use different techniques, and their results have never been compared. Figure 16 displays the results for the comparison of the entrainment measurements from the iso-kinetic and film removal techniques.

The absolute average actual relative difference between the two methods is 17.7%. The iso-kinetic sampling results are systematically lower than the film removal results. This comparison will not identify which technique is more accurate. Nevertheless, the comparison gives some insight when comparing entrainment results from the two measurement techniques.

Both techniques have many positive and negative characteristics. Iso-kinetic sampling is a direct measurement of the entrainment fraction and is simple in its design. However, calculation of entrainment fraction is quite complex. Integration of the entrainment flux profile in only one axial direction is a concern. Sampling of the disturbance waves at the interface may also cause large errors in the results. The film removal technique is an indirect measurement of entrainment fraction and is more difficult to construct. It is difficult to prevent drainage of re-deposited droplets and continuation of tall waves through the porous section. However, removal of the liquid film can be accurately controlled by regulating the pressure drop across the porous section. It is also much easier to visually determine the efficiency of the instrument.

Liquid Holdup

Figures 17-20 display the liquid holdup results for different inclination angles and varying superficial gas and liquid velocities. A decrease in liquid holdup with increasing superficial gas velocity is exhibited at all superficial liquid velocities and inclination angles. At the lowest superficial liquid velocities (0.0035 m/s), the liquid holdup increases for an increase in inclination angle. No significant inclination effect on liquid holdup could be found to explain the increase of liquid entrainment with inclination angle.

Film Thickness

The film thickness is measured using flush mounted conductivity probes installed from the bottom to the top of the pipe, spaced 45° apart. The average film thickness is determined by averaging a 40-second time trace for each probe. The average film thickness measured at the bottom of the pipe is shown in Figures 21-24 for different inclination angles and varying superficial velocities. The average film thickness increases with increasing superficial liquid velocity. As the superficial gas velocity increases, the average film thickness decreases as the film evenly distributes around the pipe. The same effect happens as the inclination increases. The increase in inclination angle promotes the symmetry of the film, decreasing the average film thickness at the bottom of the pipe.

Figure 25 displays the liquid film distribution around the pipe circumference at flow conditions of $v_{SL} = 0.04$ m/s and $v_{SG} = 40$ m/s. This clearly shows the inclination effect on the film distribution around the pipe. At horizontal, an asymmetrical film is present. As the pipe is inclined, the film slowly becomes more

even. At an inclination angle of 75° from horizontal, the film becomes symmetrical. Similar results occurred for other superficial liquid velocities and low superficial gas velocities. As the gas velocity increases, an even film distribution is approached at all inclination angles. This is shown in Fig. 26 for flow conditions of $v_{SL} = 0.04$ m/s and $v_{SG} = 80$ m/s.

Wave Characteristics

Wave Celerity

The wave celerity or velocity is calculated using cross-correlation between two conductivity probes spaced a known distance apart. The time delay between signals is determined using MATLAB and was confirmed with a hand written VBA program in Microsoft Excel. An example of the cross-correlation calculation can be found in Fig. 27 for flow conditions of $v_{SL} = 0.04$ m/s and $v_{SG} = 80$ m/s at horizontal. In Fig. 27, R_{xy} is a measure of the extent to which two signals correlate with each other as a function of the time displacement (τ). If the signals are equal, the cross correlation will be one, and if they are completely different, the cross correlation will be zero. Figures 28-31 display the wave celerity results for different inclination angles and varying superficial velocities. As seen in the figures, the wave celerity increases linearly with the increasing in the superficial gas velocity. The celerity is also dependent on the superficial liquid velocity. As the superficial liquid velocity is increased, the wave celerity also increases. The inclination angle effect on the wave celerity is more ambiguous. From horizontal, the wave celerity increases as the pipe is inclined. The wave celerity reaches a maximum point around the 10° to 20° inclination. After this maximum, the wave celerity will decrease until it reaches the minimum value near vertical. A correlation/relationship between inclination effects on wave celerity and entrainment fraction could not be determined from the test data.

Wave Frequency

Wave frequency is a measure of the number of waves per second (Hz) that travel on the film interface. The wave frequency is determined using a combination of the power spectrum method in MATLAB and manual counting of the waves. The power spectrum gives the predominant frequency or range of frequencies. The waves are then manually counted and compared to the power spectrum value. To determine if a film structure is counted as a wave, a wave threshold is determined based on the average film thickness. For this study the threshold was set at 2 times the average film thickness. For the case of $v_{SL} = 0.04$ m/s and v_{SG}

= 50 m/s at horizontal, the corresponding power spectrum can be found in Fig. 32. The time trace of the film height for the same flowing conditions is shown in Fig. 33. As can be seen in Fig. 32, the predominant frequency is 18 Hz, which matches the number of waves in the time trace.

Figures 34-37 display the wave frequency results for different inclination angles and superficial velocities. As seen in the figures, the wave frequency increases with increasing superficial gas velocity. The frequency is also dependent on the liquid superficial velocity. As the superficial gas velocity is increased, the increase in the superficial liquid velocity results in an increase in the wave frequency. There seems to be little inclination effect on the wave frequency.

Wave Amplitude

Wave amplitude is determined by averaging the wave heights of a film height time trace that are larger than the average film thickness plus 2 standard deviations. Figures 38-41 display the wave amplitude results for the varying inclination angles and superficial velocities. The wave amplitude demonstrates similar effects as the average film thickness (Figs. 21-24) with regard to superficial gas and liquid velocities and inclination angle. As seen in the figures, the wave amplitude decreases with increasing superficial gas velocity. An increase in superficial liquid velocity increases the wave amplitude. Inclination angle also affects the wave amplitude. As the inclination angle is increased, the wave amplitude decreases drastically, especially at higher inclination angles. The maximum wave amplitude is reached at horizontal where a thicker asymmetrical film is present. There seems to be a significant effect on the wave amplitude at 45° above which a large drop in wave amplitude occurs for all superficial liquid velocities. A connection between inclination effects on wave amplitude and entrainment fraction could not be determined from the test data.

Wavelength

The distance between waves or wavelength is determined based on the wave celerity and frequency. The wavelength is determined based on the following equation:

$$\lambda = \frac{c}{\omega}, \quad (6)$$

where c is the wave celerity and ω is the frequency. Figures 42-45 exhibit the wavelength results for the varying inclination angles and superficial velocities. In the figures, there is no consistent effect for

increasing the liquid superficial velocity and inclination angle. However, the increase superficial gas velocity decreases the wavelength. At $v_{SL} = 0.04$ m/s, an increase in superficial gas velocity from 40 to 50 m/s causes a large decrease in the wavelength for inclination angles below 45° from horizontal. However, as the superficial gas velocity continues to increase, the effect is minimal. Likewise, the inclination angle only affects the wavelength at this superficial liquid velocity. The wavelength decreases as the pipe is inclined from horizontal. This can be attributed to the decrease in the liquid film thickness due to the evening out of the film, resulting in smaller, faster waves. A relationship between inclination effects on wavelength and entrainment fraction could not be determined from the test data.

Method Evaluation

Experimental data for pressure gradient, liquid holdup and entrainment fraction are compared with available methods. Experimental results for pressure gradient and liquid holdup are compared to predictions by the TUFFP unified model (2003). Entrainment fraction data are compared with several methods developed for horizontal, vertical and inclined annular flows. Horizontal methods used in the comparison are Paleev and Flippovich (1966), Pan and Hanratty (2005b) and Mantilla (2008). Vertical flow methods analyzed include Wallis (1969), Oliemans (1986), Ishii and Mishima (1989), Pan and Hanratty (2002a) and Sawant (2008). The Ousaka *et al.* (1996) correlation and Chen (2005) model, developed for all inclinations, are also used in the evaluation.

Statistical Parameters

Statistical parameters are used to compare the performance of the models and correlations. The parameters are calculated using two error types, relative and actual. The relative and actual errors are expressed in Eqs. 7 and 8, respectively.

$$e_{ri} = \left(\frac{q_{i,Cal} - q_{i,Mea}}{q_{i,Mea}} \right) \times 100. \quad (7)$$

$$e_i = q_{i,Cal} - q_{i,Mea}. \quad (8)$$

In these two equations, the subscripts *Cal* and *Mea* refer to the calculated and measured values. Based on the relative and actual errors, the following six statistical parameters are defined:

Average relative error:

$$\varepsilon_1 = \frac{1}{N} \sum_{i=1}^N (e_{ri}). \quad (9)$$

Absolute average relative error:

$$\varepsilon_2 = \frac{1}{N} \sum_{i=1}^N |e_{ri}|. \quad (10)$$

Standard deviation about average relative error:

$$\varepsilon_3 = \sqrt{\frac{\sum_{i=1}^N (e_{ri} - \varepsilon_1)^2}{N-1}}. \quad (11)$$

Average actual error:

$$\varepsilon_4 = \frac{1}{N} \sum_{i=1}^N (e_i). \quad (12)$$

Absolute average actual error:

$$\varepsilon_5 = \frac{1}{N} \sum_{i=1}^N |e_i|. \quad (13)$$

Standard deviation about average actual error:

$$\varepsilon_6 = \sqrt{\frac{\sum_{i=1}^N (e_i - \varepsilon_4)^2}{N-1}}. \quad (14)$$

In the above equations, N is the number of data points.

The average relative error, ε_1 , and average actual error, ε_4 , are an indication of the agreement between the predicted and measured parameters. Positive values for these average errors indicate overestimation of the parameter. Negative values indicate underestimation of the parameter. The true performance can be masked by these parameters due to the cancellation of the negative and positive values. Therefore, the absolute average relative error, ε_2 , and the absolute average actual error, ε_5 , better reflect the agreement of the predicted and measured parameters. These parameters denote how large the errors are on the average. The standard deviations, ε_3 and ε_6 , indicate the degree of scattering around the corresponding average errors, ε_1 and ε_4 .

Pressure Gradient

The evaluation for pressure gradient can be found in Table 2 for the TUFFFP unified model. Table 2 displays the statistical parameters for all data, separated by pipe inclination angle. The TUFFFP unified model shows good agreement with the test data. The absolute average relative and actual errors for all data are 7.4% and 76 Pa/m, respectively. Figure 46 shows the comparisons with the predicted and measured pressure gradients for all angles.

Liquid Holdup

The TUFFFP unified model evaluation for liquid holdup can be found in Table 3. Table 3 displays the statistical parameters for the agreement of predicted and measured values at each pipe inclination and for all the data, cumulatively. Based on parameters ε_1 and ε_4 , the TUFFFP unified model underestimates the liquid holdup. This underestimation may be attributed to the model's use of the Oliemans *et al.* correlation for the prediction of entrainment. This correlation overestimates the entrainment fraction, resulting in an underestimation of the liquid holdup. The comparison of the entire liquid holdup data set shows absolute average actual and relative errors of 21% and 0.0018, respectively. The statistical analysis also shows that as the pipe inclination is increased, the TUFFFP unified model's performance worsens for liquid holdup prediction. Figure 47 displays the comparison of the measured liquid holdup values and the TUFFFP unified model predictions.

Entrainment Fraction

Data from the present study and the entire entrainment data bank are compared with available entrainment fraction methods to evaluate their performance.

Present Study Entrainment Evaluation

The 140 entrainment tests from this study are compared with the available methods developed for varying pipe inclinations. Table 4 displays the results of these comparisons. Based on the statistical parameters ε_2 and ε_5 , the correlation derived by Paleev and Flippovich (1966) performed the best. However, as Wallis (1968) discussed, the Paleev and Flippovich correlation does not properly take into account liquid viscosity effect and will perform poorly when fluids other than water are used. Wallis

(1969) later properly took this viscosity effect into account in his correlation. His correlation performed satisfactorily with ε_2 and ε_5 values of 18.25% and 0.09. Sawant *et al.* (2008) correlation performed well due to its accurate prediction of the maximum entrainment value. However, due to its hyperbolic tangent functionality, the correlation has a tendency to over predict entrainment. The mechanistic model developed by Mantilla (2008) performed reasonably well. This model, although more complex in nature, takes into account the effect of wave characteristics on entrainment fraction. Based on the experimental results from this study, the correlation by Wallis (1969) best predicts the entrainment fraction. This equation is simple and takes into account the predominant fluid properties and forces governing the entrainment fraction.

Entrainment Databank Evaluation

An extensive statistical analysis was conducted using the present study and other available entrainment data to evaluate the previously mentioned methods. Table 5 contains all available entrainment data, including the working fluids, pipe orientation and flow conditions of each study. Tables 6 and 7 display the statistical parameters for each method against all the entrainment data. In Table 6, the Harwell databank is omitted to avoid a biased evaluation toward vertical flow methods. Tables 8 and 9 contain the statistical parameters for the methods against all available vertical entrainment data. Once again, the Harwell databank is omitted from Table 8 to avoid a biased evaluation toward the Oliemans *et al.* correlation which is developed based on the Harwell databank. The Harwell databank is included in the vertical entrainment evaluation shown in Table 9. Tables 10 and 11 present the evaluations of the methods for available horizontal and inclined data.

Based on the parameters ε_2 and ε_5 in Tables 5, the correlation by Pan and Hanratty (2002b) for horizontal flow and the mechanistic model developed by Mantilla (2008) most accurately predict entrainment fraction at all pipe inclinations. The correlation by Pan and Hanratty systematically underpredicts entrainment fraction while the Mantilla model overpredicts the values. Although these methods perform the best, an approximately 40% ε_2 value is associated with their prediction of entrainment. This error demonstrates the inability of one model or correlation to be utilized for all pipe inclinations for the prediction of entrainment fraction. With addition of the Harwell databank in Table 7, the Pan and Hanratty vertical flow correlation emerges due to the biased evaluation toward vertical flow

correlations. However, the Pan and Hanratty horizontal flow correlation still most accurately predicts the entrainment fraction for all pipe inclination angles.

Based on the unbiased evaluation in Table 8, the Oliemans *et al.* (1986) correlation and vertical correlation by Pan and Hanratty (2002a) most accurately predict entrainment fraction. Both correlations had ε_2 and ε_5 values of approximately 22% and 0.09, respectively. The Oliemans *et al.* correlation systematically overpredicts the data while the correlation by Pan and Hanratty underpredicts the entrainment. With the addition of the Harwell databank in Table 9, the Oliemans *et al.* correlation most accurately predicts the entrainment fraction, as expected.

The Pan and Hanratty (2002b) horizontal correlation most accurately predicts entrainment fraction for available horizontal entrainment data. As shown in Table 10, this correlation has ε_2 and ε_5 values of 32.1% and 0.09, respectively. Based on ε_1 and ε_4 values, the correlation has a tendency to underpredict the entrainment fraction.

In the evaluation shown in Table 11, over two-thirds of the data are from the present study. Therefore, the statistical analysis is biased toward the analysis presented in the previous section. This effect demonstrates the need for more inclined entrainment data to prevent the dominance of one study on the analysis. Based on the evaluation in Table 11, the correlation by Paleev and Flippovich (1966) most accurately predicts entrainment fraction. However, as discussed earlier, this correlation is unable to account for entrainment variation due to change of fluids. Therefore, the correlation developed by Wallis (1969) and the model by Mantilla (2008) are better choices for the prediction of entrainment in inclined pipes. Both have similar errors associated with their predictions and systematically underestimate entrainment fraction.

In summary, the statistical analysis conducted in this study demonstrates the inability of one correlation or model to accurately predict entrainment fraction for all inclination angles. Furthermore, by utilizing a specific model or correlation based on the pipe inclination angle, more accurate entrainment predictions can be achieved. Based on the statistical analysis for vertical annular flow, the Oliemans *et al.* correlation most accurately predicts entrainment fraction. This correlation is based on the Harwell databank which encompasses a large range of fluid properties and flow conditions. For horizontal

annular flow entrainment prediction, the Pan and Hanratty horizontal correlation most accurately predicts the entrainment. This correlation takes into account the effects of gravity and droplet size on entrainment fraction and explicitly incorporates a critical flow rate to calculate maximum entrainment. Based on the statistical analysis for inclined annular flow, the Mantilla mechanistic model and Wallis correlation have shown similar prediction abilities. The Wallis correlation can be better utilized due to its simplistic form. However, the Mantilla model encompasses wave characteristics, which many believe are the key to understanding the entrainment process. Although the most accurate correlations have been determined for each pipe orientation, ε_2 values of 20 to 50% are associated with these models and correlations. Overall, the statistical analysis has shown the need for improvement for entrainment prediction.

Conclusions

In this study, 140 tests were conducted for two-phase inclined annular flow in a 76.2-mm ID pipe. Liquid entrainment, film thickness, liquid holdup, and wave characteristics were measured in the experiments.

A clear inclination effect on entrainment fraction was observed. This effect occurred at low superficial gas velocities and was more prominent in higher superficial liquid velocities. A relationship between inclination effects on liquid holdup and wave characteristics and entrainment fraction could not be determined from the test data. Further analysis is needed.

Several entrainment fraction prediction methods were evaluated with the available entrainment data. Based in all available data, the Pan and Hanratty (2002b) correlation performed the best at all pipe orientations. For vertical annular flow, the Oliemans *et al.* (1986) correlation predicted the entrainment fraction most accurately. The Pan and Hanratty (2002a) correlation was most accurate in predicting the entrainment fraction for horizontal flow. The Wallis (1969) correlation and the mechanistic model developed by

Mantilla (2008) most accurately predicted entrainment for inclined annular flow.

Although the most accurate entrainment prediction methods were determined for each pipe orientation, absolute average relative errors of 20 and 50% were associated with these methods. Overall, the statistical analysis proved the need for improvement in entrainment prediction.

Nomenclature

b_i	= Elemental systematic uncertainty
B_R	= Combined systematic uncertainty
c	= Celerity [m/s]
d	= Pipe diameter [m]
e_{ri}	= Relative error
e_i	= Actual error
E_X	= Liquid entrainment fraction [$\text{m}^3/(\text{s}\cdot\text{m}^2)$]
F_E	= Entrainment fraction
h_L	= Liquid film thickness [mm]
H_L	= Liquid holdup
ID	= Inner pipe diameter
L	= Length [m]
N	= Sample size
S_X	= Standard deviation of a population
S_x	= Standard deviation of a population average
t_{95}	= Student's t
U_{95}	= Combined uncertainty with 95% confidence
v	= velocity [m/s]
X_i	= i th element in a population
\bar{X}	= Population average
$\varepsilon_1 - \varepsilon_6$	= Statistical parameters
θ	= Inclination angle [degree]
λ	= Wavelength [m]
ω	= Frequency [Hz]
τ	= Time displacement [s]

Subscripts

Cal	= Calculated
E	= Entrained
Mea	= Measured
SG	= Superficial gas
SL	= Superficial liquid

References

- Chen, X.: "Droplet-Homophase Interaction Study," TUFFP Spring 2005 ABM Brochure, pp. 135-186. (2005).
- Dallman, J.C.: "Investigation of Separated Flow Model in Annular Gas-Liquid Two-Phase Flow," PhD Dissertation, University of Illinois at Urbana, Champaign (1978).
- Deryabina, O.N., Semenenko, V.F., and Medvedev, A.E.: "Distribution of the Liquid Phase in Dispersed-Annular Flow," *Thermal Engr.*, 36(12), pp. 207-235 (1989).
- Dieck, R. H.: Measurement Uncertainty: Methods and Application, Third Edition, ISA (2002).
- Fore, L.B. and Dukler, A.E.: "The Distribution of Drop Size and Velocity in Gas-Liquid Annular Flow," *Int. J. Multiphase Flow*, 21(2), pp. 137-149 (1995).
- Geraci, G., Azzopardi, B.J., and van Maanen, H.R.E.: "Inclination Effects on Circumferential Film Distribution in Annular Gas/Liquid Flows," *AIChE J.*, 53(5), pp. 1144-1150 (2007).
- Ishii, M., and Mishima, K.: "Droplet Entrainment Correlation in Annular Two-Phase Flow," *Int. J. of Heat and Mass Transfer*, 32(10), pp. 1835-1846 (1989).
- Laurinat, J.E.: "Studies on the Effects of Pipe Size on Horizontal Annular Two-Phase Flows," PhD Dissertation, University of Illinois at Urbana, Champaign (1982).
- Mantilla, I.: "Mechanistic Modeling of Liquid Entrainment in Gas in Horizontal Pipes," PhD Dissertation, University of Tulsa (2008).
- Oliemans, R.V., Pots, B.F.M., and Trompe, N.: "Modeling of Annular Dispersed Two-Phase Flow in Vertical Pipes," *Int. J. Multiphase Flow*, 12(5), pp. 711-732 (1986).
- Ousaka, A., and Kariyasaki, A.: "Distribution of Entrainment Flow Rate for Air-Water Annular Two-Phase Flow in a Horizontal Tube," *JSME Int. J.*, 35(2), pp. 354-360 (1992).
- Ousaka, A., Nagashima, T., and Kariyasaki, A.: "Effect of Inclination on Distribution of Entrainment Flow Rate in an Inclined Upward Annular Flow," *Trans. the Japan Soc. of Mech. Eng., Part B*, v 62, n 600, pp. 2950-2956 (1996).
- Owen, D.G., Hewitt, G.F., and Bott, T.R.: "Equilibrium Annular Flows at High Mass Fluxes: Data and Interpretation," *PCH PhysioChemical Hydrodynamics*, 6(1/2), pp. 115-131 (1985).
- Paleev, I.I., and Filipovich, B.S.: "Phenomena of Liquid Transfer in Two-Phase Dispersed Annular Flow," *Int. J. Mass Transfer*, 9, pp. 1089-1093 (1966).
- Pan, L., and Hanratty, T.J.: "Correlation of Entrainment for Annular Flow in Vertical Pipes," *Int. J. Multiphase Flow*, 28(3), pp. 363-384 (2002a).
- Pan, L., and Hanratty, T.J.: "Correlation of Entrainment for Annular Flow in Horizontal Pipes," *Int. J. Multiphase Flow*, 28(3), pp. 385-408 (2002b).
- Paras, S.V., and Karabelas, A.J.: "Droplet Entrainment and Deposition in Horizontal Annular Flow," *Int. J. Multiphase Flow*, 17(4), pp. 455-468 (1991b).
- Sawant, P., Ishii, M., and Mori, M.: "Droplet Entrainment Correlation in Vertical Upward Co-Current Annular Two-Phase Flow," *Nuclear Engineering and Design*, 238, pp. 1342-1352 (2008).
- Schadel, S.A.: "Atomization and Deposition Rates in Vertical Annular Flow," PhD Dissertation, University of Illinois at Urbana, Champaign (1988).
- Tayebi, D., Nuland, S., and Fuchs, O.: "Droplet Transport in Oil/Gas and Water/Gas Flow in High Gas Densities," *Int. J. Multiphase Flow*, 26, pp. 741-761 (2000).
- Wallis, G.B.: "Phenomena of Liquid Transfer in Two-Phase Dispersed Annular Flow," *Int. J. Heat and Mass Transfer*, 11(3), pp. 783-785 (1968).
- Wallis, G.B.: One Dimensional Two-Phase Flow, McGraw-Hill (1969).

Wicks, M. and Dukler, A.E.: "Entrainment and Pressure Drop in Concurrent Gas-Liquid Flow: I. Air-Water in Horizontal Flow," *AIChE J.*, 6(3), pp. 463-468 (1960).

Williams, L.R.: "Effect of Pipe Diameter on Horizontal Annular Two-Phase Flow," PhD Dissertation, University of Illinois at Urbana, Champaign (1990).

Zhang, H.Q., Wang, Q., Sarica, C., and Brill, J.P.: "Unified Model of Gas-Liquid Pipe Flow via Slug Dynamics. Part I. Model Development," *ASME J. of Energy Res. Tech.*, 125(4), pp. 266-273 (2003).

Table 1: Uncertainty Analysis Results

Parameter	Instrument	Random Uncertainty	Systematic Uncertainty	Combined Uncertainty
Liquid Flow Rate	Micro Motion flow meter	0.23%	0.05%	0.46%
Gas Flow Rate	Micro Motion flow meter	0.37%	0.04%	0.74%
Pressure	Rosemount pressure transmitter	0.41%	1.10%	1.37%
Pressure Drop	Rosemount differential pressure transmitter	0.22%	1.00%	1.10%
Temperature	Rosemount temperature transmitter	0.06 °C	0.5 °C	0.52 °C
Liquid Holdup	Quick-closing valve section	1.68%	5.60%	6.53%
Liquid Entrainment	Isokinetic sampling system	3.84%	5.8%	9.58%
Liquid Film Height	Flush mounted conductance probe	0.015 mm	0.025 mm	0.039 mm
Diameter	(-)	0.01%	0.07%	0.07%
Gas Velocity	(-)	0.62%	1.83%	2.21%
Liquid Velocity	(-)	0.34%	0.76%	1.02%

Table 2: TUFFP Unified Model Pressure Gradient Evaluation

Data	Statistical Parameters					
	ε_1 (%)	ε_2 (%)	ε_3 (%)	ε_4 (Pa/m)	ε_5 (Pa/m)	ε_6 (Pa/m)
0°	0.6	8.8	13.5	-28.1	96.0	134.0
10°	-2.3	6.0	11.6	-38.8	69.4	95.6
20°	-3.7	6.3	12.6	-53.4	74.0	97.3
45°	7.1	10.7	11.3	40.4	89.8	98.6
60°	4.0	7.6	9.1	27.0	73.8	89.0
75°	2.2	6.0	4.5	22.5	62.1	77.3
90°	3.2	6.3	7.7	21.2	66.7	79.9
All Data	1.6	7.4	10.8	-1.3	76.0	101.6

Table 3: TUFFP Unified Model Liquid Holdup Evaluation

Data	Statistical Parameters					
	ε_1 (%)	ε_2 (%)	ε_3 (%)	ε_4 (-)	ε_5 (-)	ε_6 (-)
0°	-11.4	14.9	30.4	-0.0012	0.0012	0.0016
10°	-10.8	16.1	32.6	-0.0013	0.0015	0.0022
20°	-13.0	15.5	32.7	-0.0014	0.0015	0.0022
45°	-12.2	20.7	39.8	-0.0015	0.0017	0.0026
60°	-11.1	26.1	48.1	-0.0016	0.0019	0.0021
75°	-23.1	26.4	53.6	-0.0021	0.0022	0.0016
90°	-27.0	27.3	57.8	-0.0023	0.0023	0.0016
All Data	-15.5	21.0	41.6	-0.0016	0.0018	0.0020

Table 4: Evaluation of Published Correlations and Models against Entrainment Fraction Measurements of Present Study

Model/ Correlation	ε_1 (%)	ε_2 (%)	ε_3 (%)	ε_4 (-)	ε_5 (-)	ε_6 (-)
Ishii and Mishima (1987) Vertical	105.76	105.76	35.42	0.47	0.47	0.08
Wallis (1969) Vertical	-14.72	18.25	15.84	-0.07	0.09	0.08
Oliemans <i>et al.</i> (1986) Vertical	50.65	50.65	30.26	0.23	0.23	0.09
Pan and Hanratty (2002a) Vertical	-4.80	46.74	61.24	-0.01	0.20	0.24
Sawant <i>et al.</i> (2008) Vertical	-15.14	20.59	21.40	-0.07	0.09	0.10
Paleev and Flippovich (1966) Horizontal	-1.23	11.26	14.73	-0.01	0.05	0.07
Pan and Hanratty (2002b) Horizontal	-26.78	39.96	47.00	-0.10	0.17	0.20
Mantilla (2008) Horizontal	-15.34	25.29	25.10	-0.05	0.11	0.12
Ousaka <i>et al.</i> (1992) Inclined	73.87	97.44	75.10	0.34	0.44	0.31
Chen (2005) Inclined	70.21	70.21	23.03	0.31	0.31	0.06

Table 5: Available Experimental Entrainment Data Conditions

Source	Tests	Angle (degrees)	Fluids	D (m/s)	v_{SG} (m/s)	v_{SL} (m/s)	ρ_G (kg/m ³)	ρ_L (kg/m ³)	σ (mN/m)
Dallman (1979)	137	0	Air-Water	0.0231	15-88	0.0072-0.9	1.6-2.75	1000	73
Laurinat (1982)	72	0	Air-Water	0.0508	11-131	0.0161-0.6	1.3-2.5	1000	73
Williams (1990)	30	0	Air-Water	0.0953	26-88	0.03-0.12	1.3-1.85	1000	73
Paras and Karabelas (1991b)	17	0	Air-Water	0.0508	30-65	0.03-0.2	1.2-2.3	1000	73
Ousaka and Kariyasaki (1992)	12	0	Air-Water	0.026	15-40	0.06-0.2	1.2-1.4	1000	73
Tayebi et al. (2000)	21	0	Oil -SF6 Water-SF6	0.1	4-7	0.25	22-46.5	820-1000	22-73
Mantilla (2008)	42	0	Air-Water Air-Water	0.0508	20-80	0.0035-0.1	2.5	988-1128	35-73
Owen (1985)	49	90	Air-Water	0.0318	17-75	0.0495-0.3993	2.93	1000	73
Schadel (1989)	58	90	Air-Water	0.0254, 0.042	19-116	0.0152-0.1036	1.38-1.69	1000	73
Deryabina (1989)	66	90	Air-Water	0.013 - 0.052	10-80	0.0177-0.505	3.58	1000	73
Fore (1995)	20	90	Air-Water	0.0508	24-36	0.0148-0.0591	1.24-1.37	1000	73
Harwell	725	90	Various	0.006-0.0318	2.7-166	0.0048-5.11	1.23-55.5	40-1300	12-73.9
Ousaka et al. (1996)	60	0, 30, 45, 60, 75	Air-Water	0.026	15-40	0.06-0.2	1.3-2.2	1000	73

Table 6: Evaluation of Models and Correlations against All Entrainment Data Excluding the Harwell Databank (724 Data Points)

Model/Correlation	ϵ_1 (%)	ϵ_2 (%)	ϵ_3 (%)	ϵ_4 (-)	ϵ_5 (-)	ϵ_6 (-)
Ishii and Mishima (1987) Vertical	95.4	106.9	217.0	0.24	0.27	0.23
Wallis (1969) Vertical	64.5	109.9	563.2	-0.05	0.16	0.23
Oliemans <i>et al.</i> (1986) Vertical	160.2	162.0	553.0	0.18	0.19	0.19
Pan and Hanratty (2002a) Vertical	21.4	56.0	117.0	0.00	0.12	0.17
Sawant <i>et al.</i> (2008) Vertical	25.8	119.9	882.2	-0.10	0.31	1.17
Paleev and Flippovich (1966) Horizontal	70.8	93.0	322.7	0.05	0.13	0.20
Pan and Hanratty (2002b) Horizontal	-20.1	37.0	45.9	-0.06	0.12	0.16
Mantilla (2008) Horizontal	18.2	44.4	78.7	0.02	0.12	0.15
Ousaka <i>et al.</i> (1992) Inclined	1.6	81.5	90.2	0.00	0.35	0.41

Table 7: Evaluation of Models and Correlations against All Entrainment Data Including the Harwell Databank (1449 Data Points)

Wallis (1969) Vertical	52.8	92.8	407.4	0.00	0.19	0.24
Oliemans <i>et al.</i> (1986) Vertical	86.2	97.8	400.8	0.08	0.13	0.18
Pan and Hanratty (2002a) Vertical	-6.9	48.0	91.2	-0.08	0.15	0.18
Sawant <i>et al.</i> (2008) Vertical	-24.0	98.2	625.8	-0.22	0.33	0.85
Paleev and Flippovich (1966) Horizontal	58.2	102.0	264.6	0.00	0.21	0.28
Pan and Hanratty (2002b) Horizontal	-14.0	47.4	61.0	-0.06	0.17	0.20
Mantilla (2008) Horizontal	61.8	81.9	158.1	0.11	0.18	0.22
Ousaka <i>et al.</i> (1992) Inclined	59.6	103.0	151.8	0.16	0.34	0.36

Table 8: Evaluation of Models and Correlations against Vertical Entrainment Data Excluding the Harwell Databank (213 Data Points)

Wallis (1969) Vertical	-28.0	33.7	40.2	-0.14	0.16	0.20
Oliemans <i>et al.</i> (1986) Vertical	16.8	22.3	29.4	0.06	0.09	0.11
Pan and Hanratty (2002a) Vertical	-15.6	21.8	31.8	-0.06	0.09	0.13
Sawant <i>et al.</i> (2008) Vertical	82.4	84.1	101.1	0.36	0.36	0.39
Paleev and Flippovich (1966) Horizontal	-7.7	24.7	34.6	-0.05	0.10	0.12
Pan and Hanratty (2002b) Horizontal	-28.9	37.4	48.8	-0.06	0.09	0.13
Mantilla (2008) Horizontal	-62.9	63.7	68.8	-0.31	0.32	0.36
Ousaka <i>et al.</i> (1992) Inclined	-0.9	23.3	38.1	-0.01	0.11	0.18

Table 9: Evaluation of Models and Correlations against Vertical Entrainment Data Including the Harwell Databank (938 Data Points)

Wallis (1969) Vertical	25.3	66.1	115.0	0.00	0.20	0.24
Oliemans <i>et al.</i> (1986) Vertical	13.2	31.0	64.4	0.00	0.08	0.10
Pan and Hanratty (2002a) Vertical	-30.6	35.8	47.2	-0.13	0.15	0.21
Sawant <i>et al.</i> (2008) Vertical	100.0	111.4	204.4	0.23	0.28	0.34
Paleev and Flippovich (1966) Horizontal	33.3	91.4	171.6	-0.05	0.24	0.30
Pan and Hanratty (2002b) Horizontal	-12.6	53.1	68.2	-0.07	0.18	0.23
Mantilla (2008) Horizontal	67.0	106.7	201.4	0.08	0.27	0.33
Ousaka <i>et al.</i> (1992) Inclined	109.5	115.5	192.9	0.33	0.34	0.38

Table 10: Evaluation of Models and Correlations against Horizontal Entrainment Data (318 Data Points)

Pan and Hanratty (2002a) Vertical	58.5	80.5	151.1	0.05	0.12	0.17
Sawant <i>et al.</i> (2008) Vertical	104.8	184.5	1241.3	0.03	0.39	1.64
Paleev and Flippovich (1966) Horizontal	148.8	161.3	441.0	0.13	0.18	0.23
Pan and Hanratty (2002b) Horizontal	-7.1	32.1	45.7	-0.01	0.09	0.14
Mantilla (2008) Horizontal	40.8	59.3	99.7	0.05	0.12	0.16
Ousaka <i>et al.</i> (1992) Inclined	-74.1	80.6	36.4	-0.35	0.35	0.24

Table 11: Evaluation of Models and Correlations against Inclined Entrainment Data (148 Data Points)

Model/ Correlation	ϵ_1 (%)	ϵ_2 (%)	ϵ_3 (%)	ϵ_4 (-)	ϵ_5 (-)	ϵ_6 (-)
Ishii and Mishima (1987) Vertical	60.9	82.7	94.8	0.30	0.34	0.39
Wallis (1969) Vertical	-27.3	30.0	39.8	-0.08	0.09	0.11
Oliemans <i>et al.</i> (1986) Vertical	69.0	69.4	105.7	0.19	0.20	0.22
Pan and Hanratty (2002a) Vertical	-16.9	45.9	59.3	-0.03	0.16	0.21
Sawant <i>et al.</i> (2008) Vertical	-39.5	43.0	55.8	-0.11	0.13	0.17
Paleev and Flippovich (1966) Horizontal	-6.3	23.9	39.9	-0.01	0.06	0.07
Pan and Hanratty (2002b) Horizontal	-39.9	49.0	61.0	-0.11	0.16	0.20
Mantilla (2008) Horizontal	-10.0	30.5	36.9	-0.02	0.11	0.13
Ousaka <i>et al.</i> (1992) Inclined	73.3	80.3	92.5	0.34	0.34	0.40

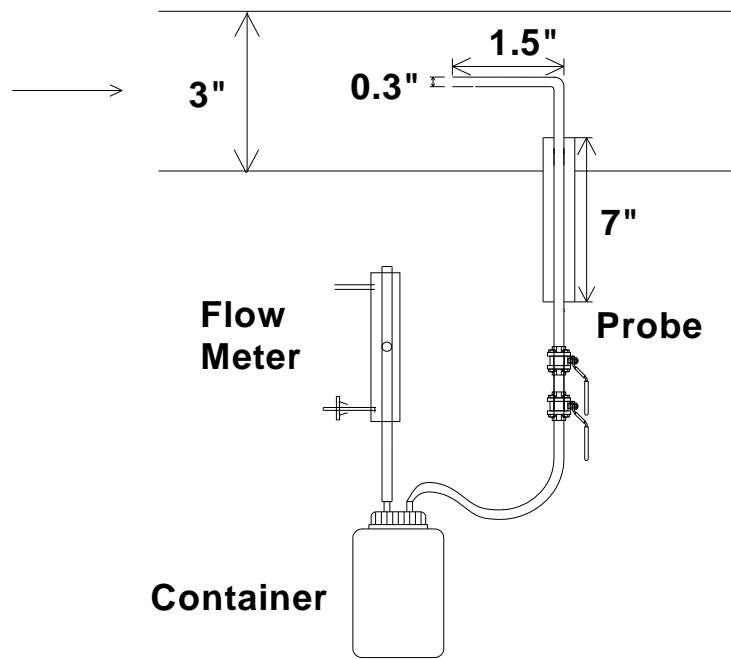


Figure 2: Iso-kinetic Sampling System Schematic



Figure 3: Iso-kinetic Sampling Probe

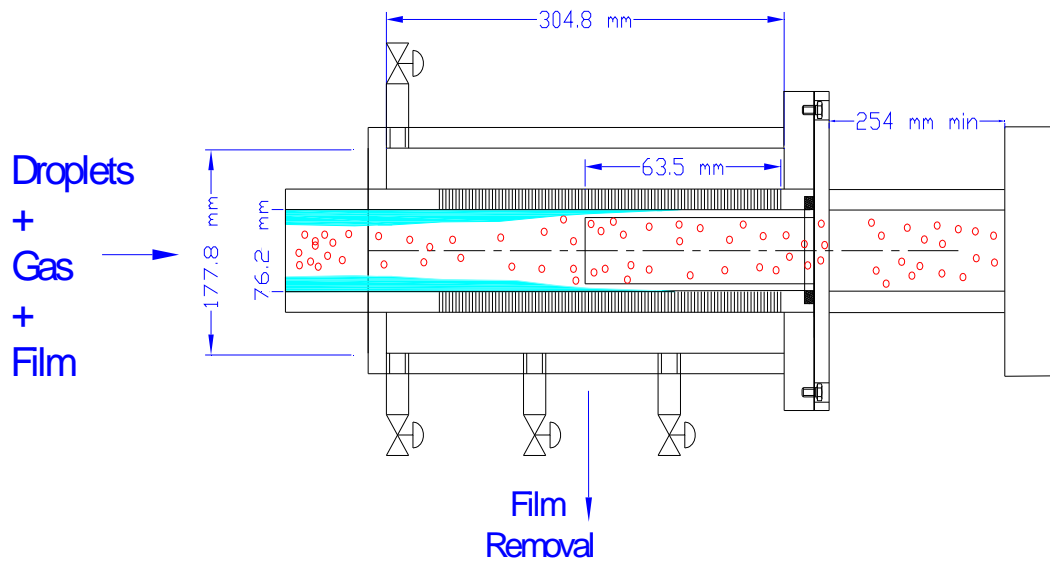


Figure 4: Film Removal Device Schematic

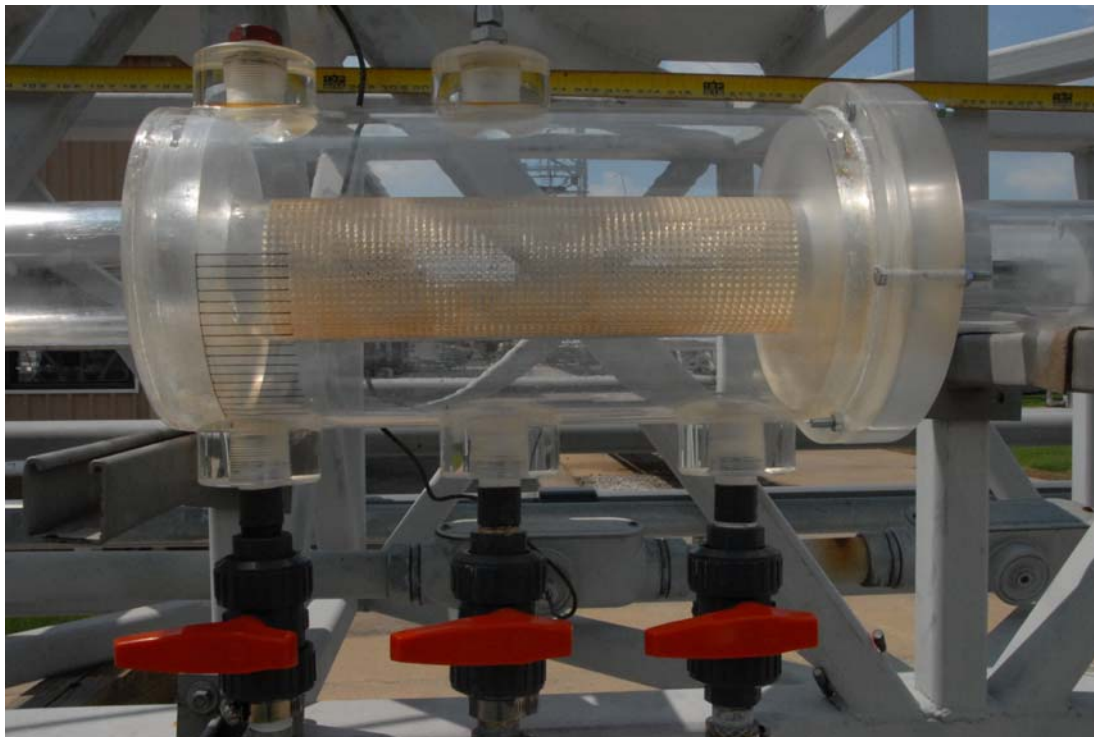


Figure 5: Film Removal Device

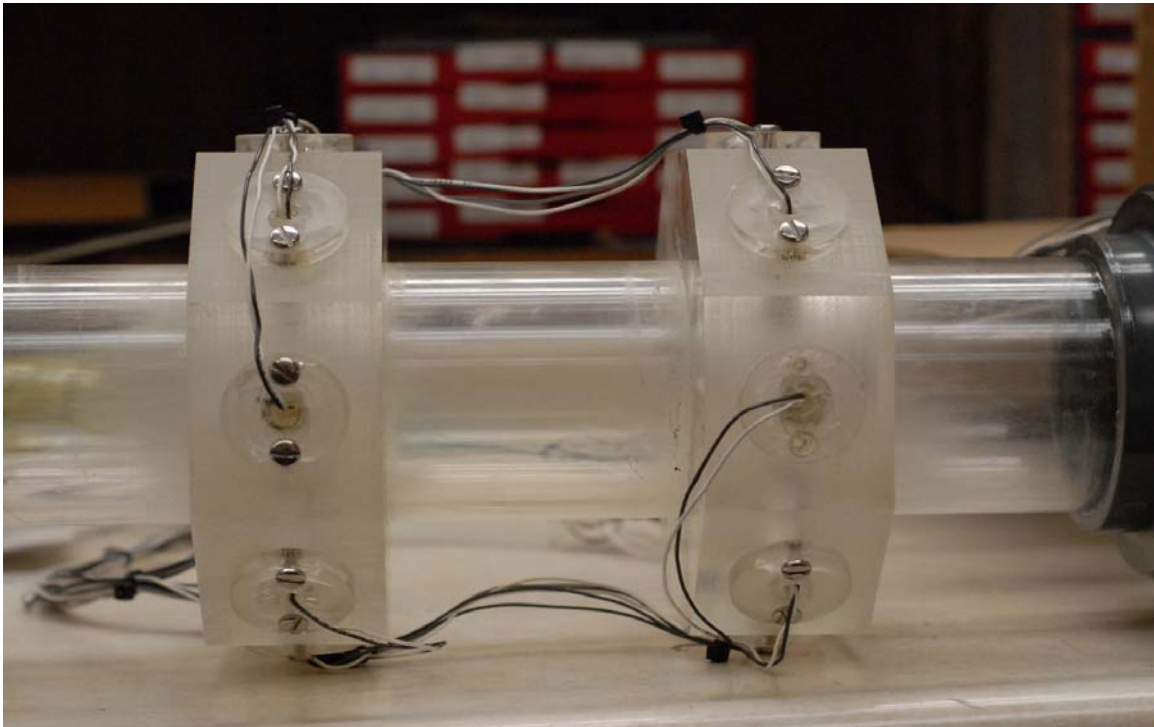


Figure 6: Conductivity Assembly

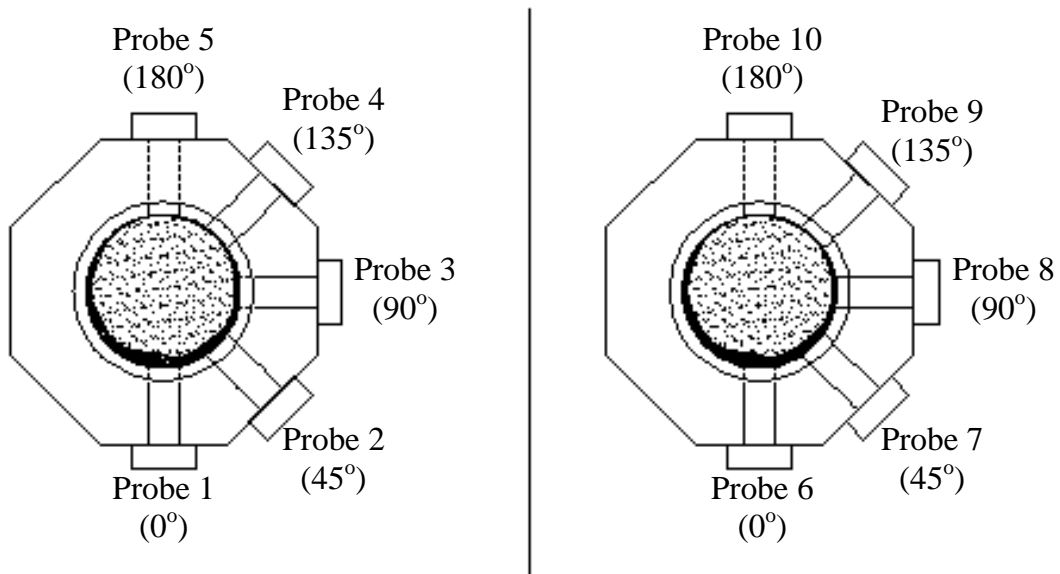


Figure 7: Conductivity Probe Orientation

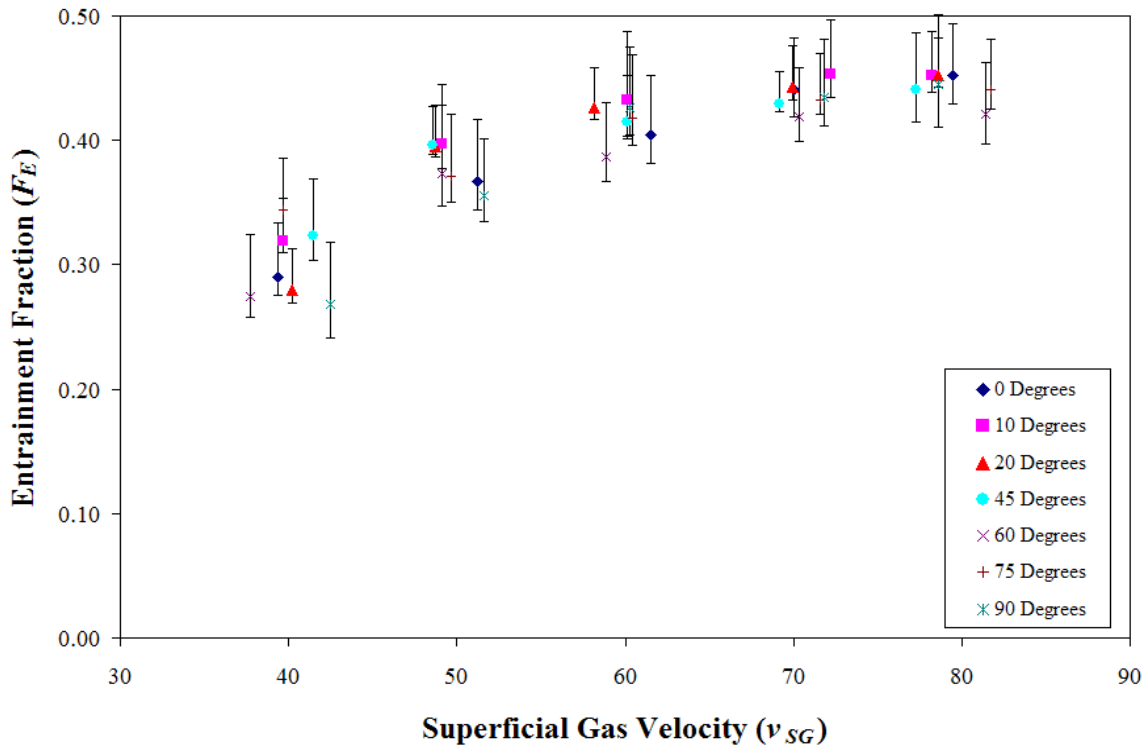


Figure 8: Film Removal Entrainment Results ($v_{SL} = 0.0035$ m/s)

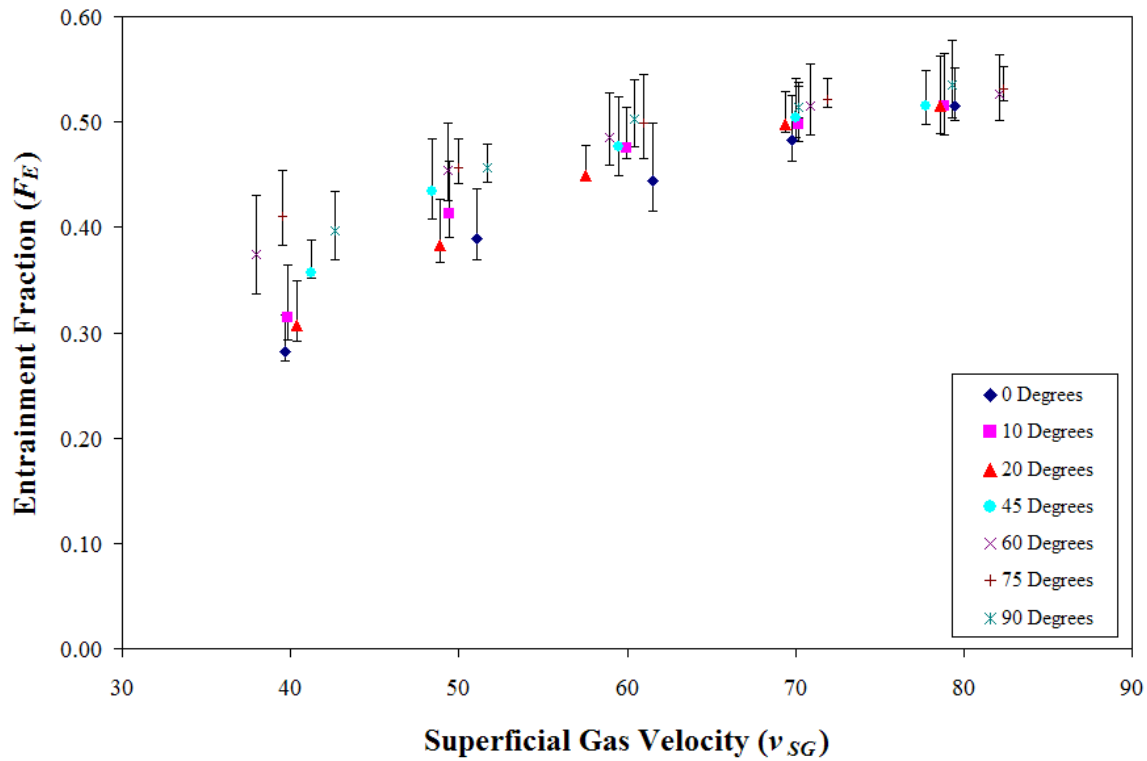


Figure 9: Film Removal Entrainment Results ($v_{SL} = 0.01$ m/s)

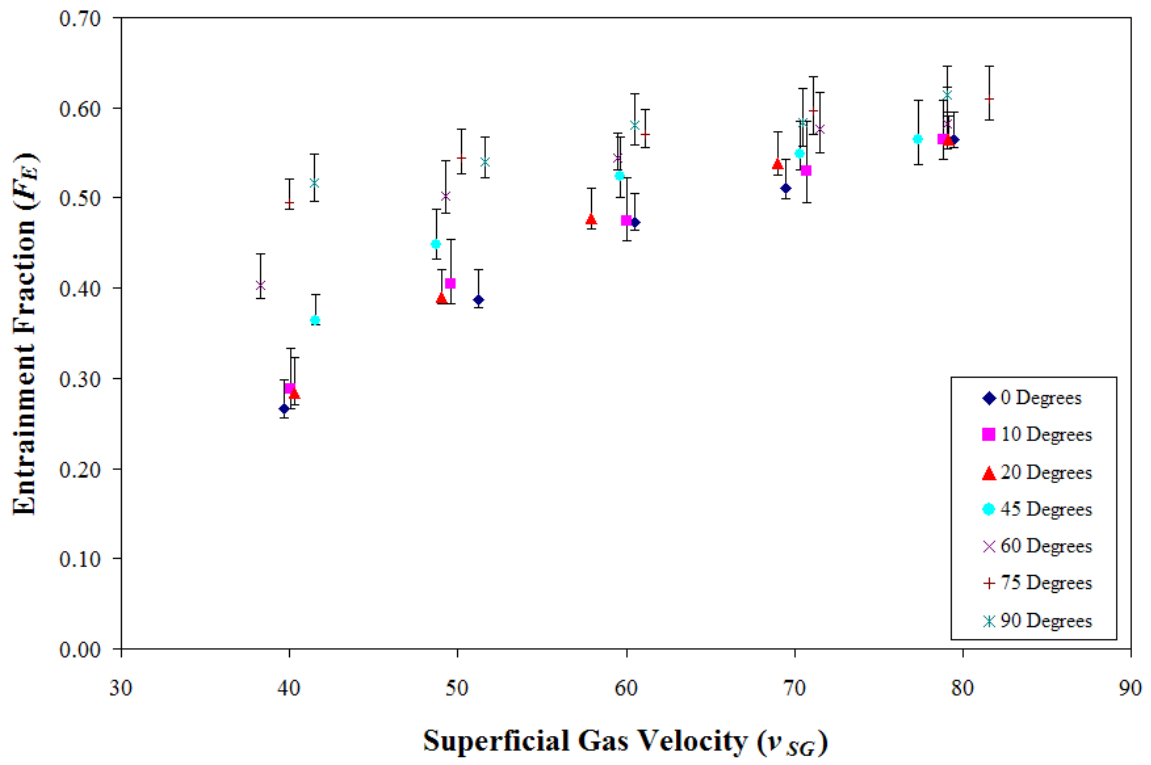


Figure 10: Film Removal Entrainment Results ($v_{SL} = 0.02$ m/s)

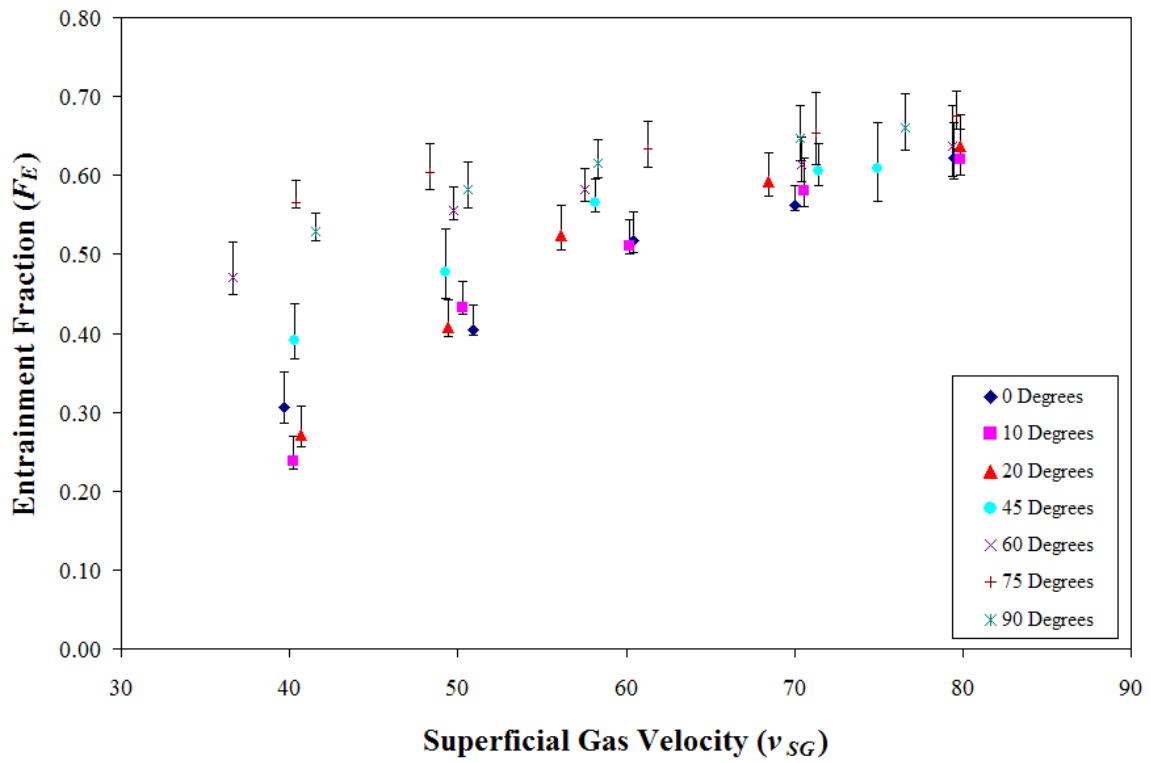


Figure 11: Film Removal Entrainment Results ($v_{SL} = 0.04$ m/s)

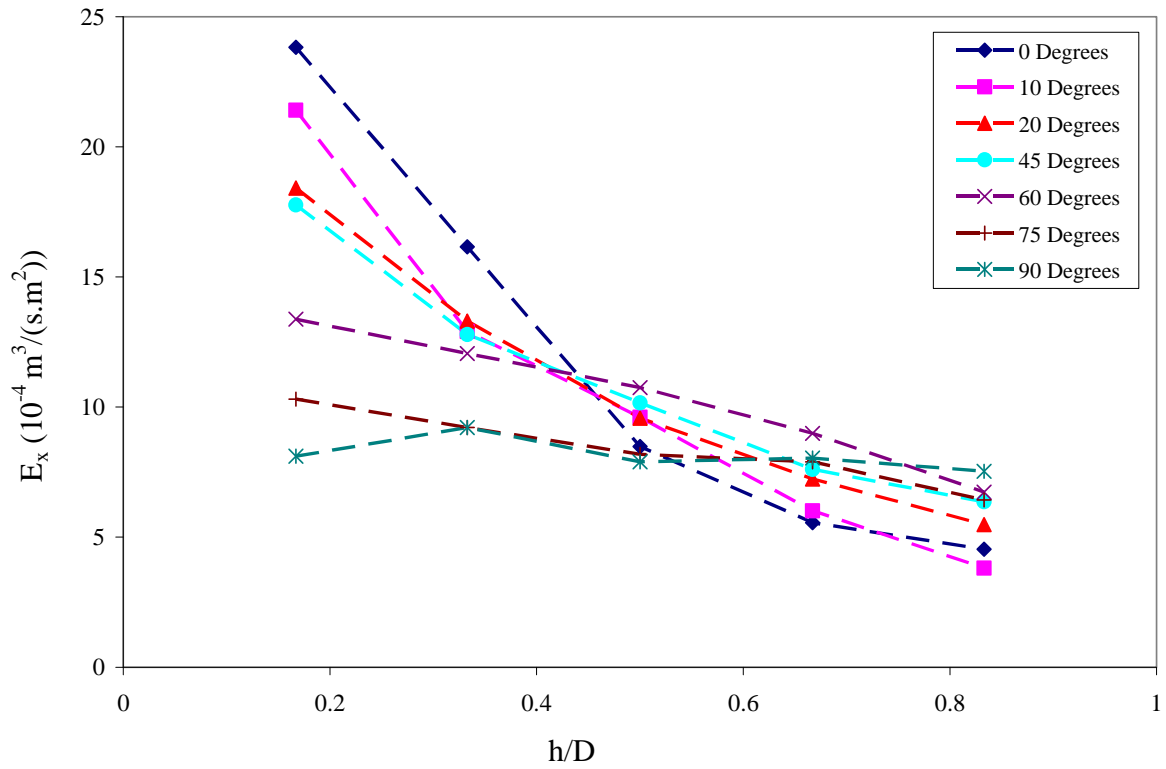


Figure 12: Entrainment Flux Profile ($v_{SL} = 0.0035$ m/s, $v_{SG} = 40$ m/s)

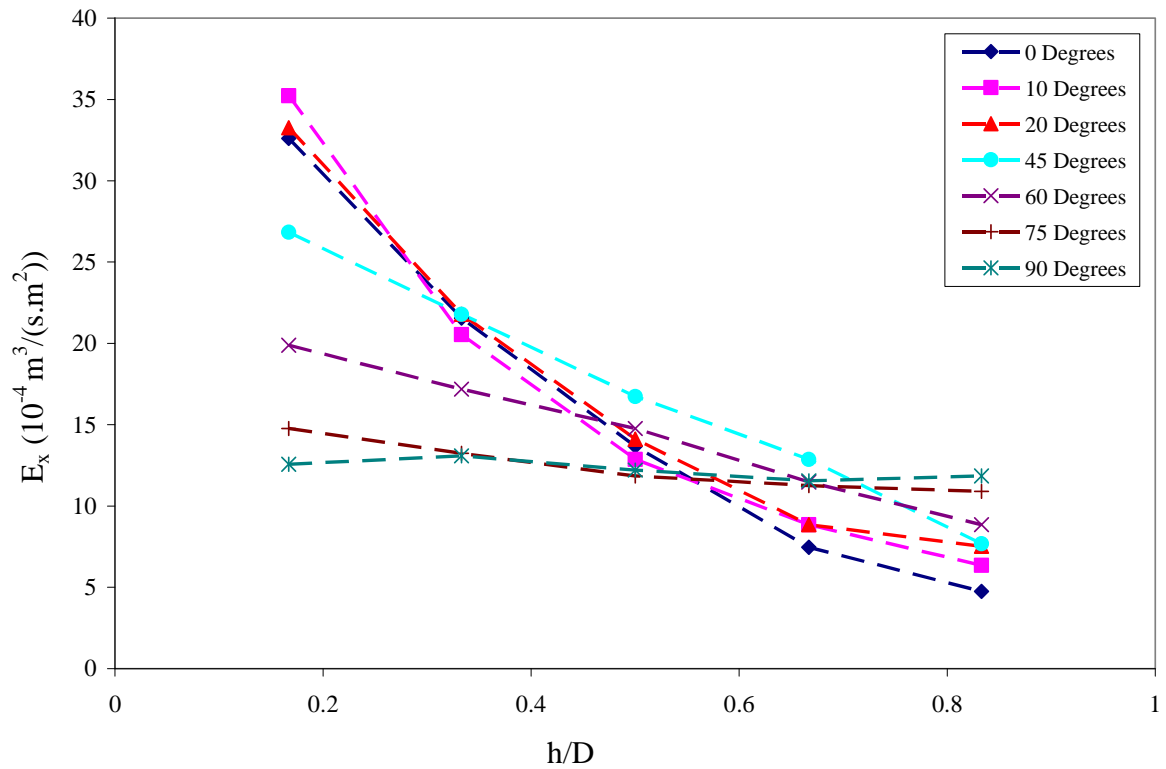


Figure 13: Entrainment Flux Profile ($v_{SL} = 0.0035$ m/s, $v_{SG} = 50$ m/s)

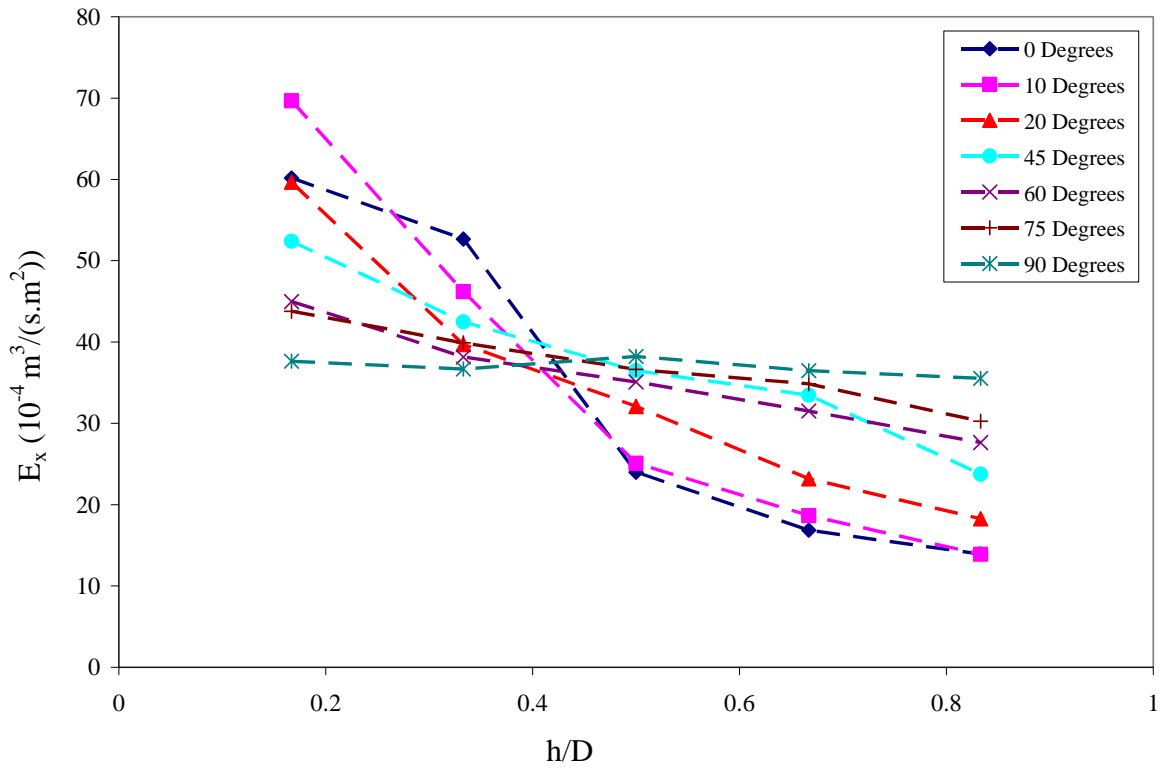


Figure 14: Entrainment Flux Profile ($v_{SL} = 0.01$ m/s, $v_{SG} = 40$ m/s)

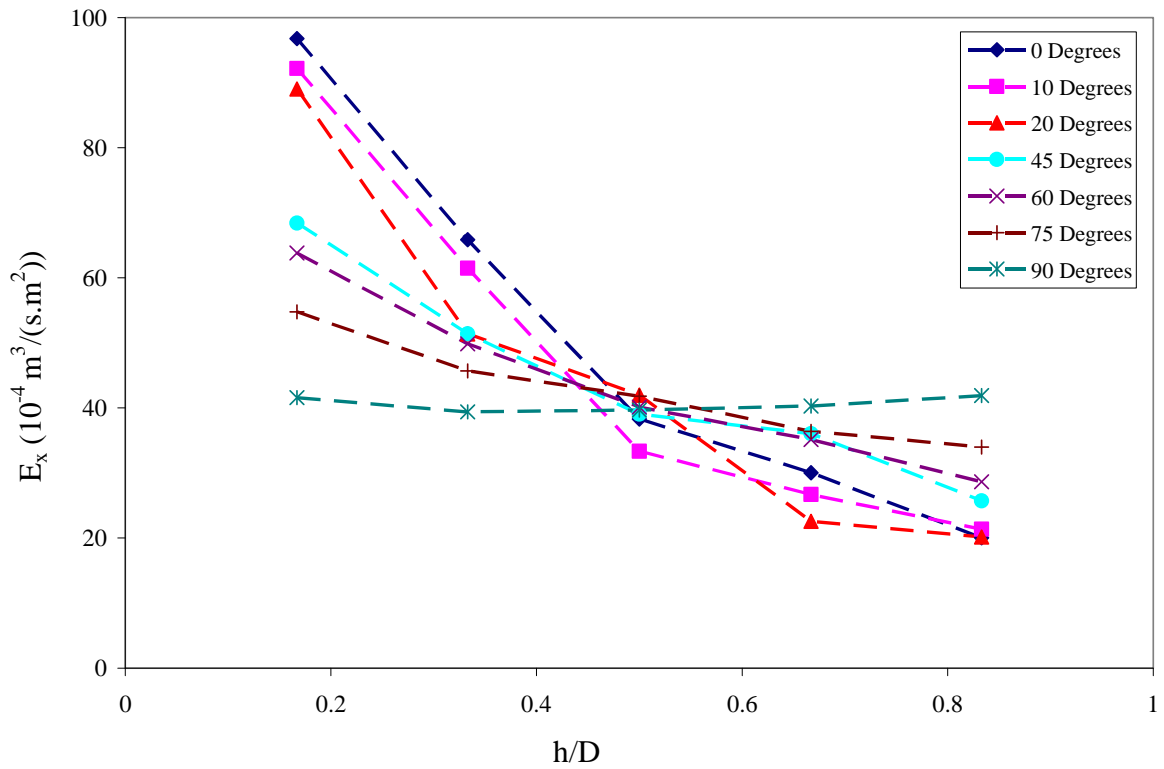


Figure 15: Entrainment Flux Profile ($v_{SL} = 0.01$ m/s, $v_{SG} = 50$ m/s)

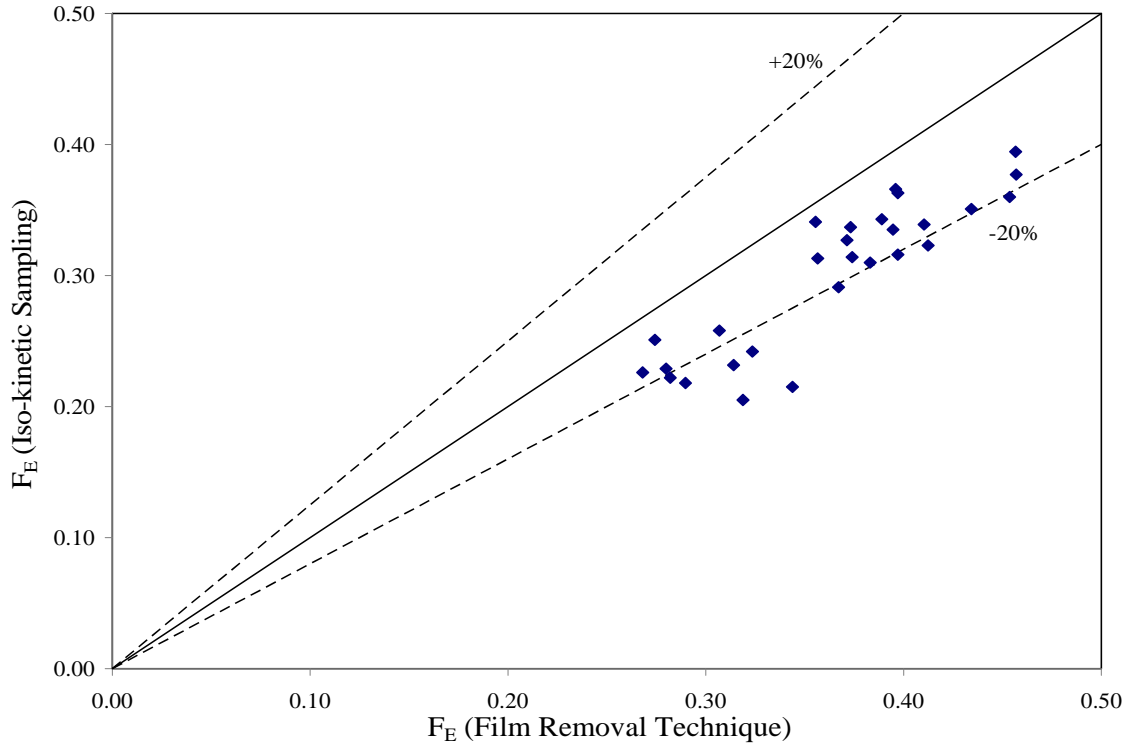


Figure 16: Comparison of Film Removal and Iso-kinetic Sampling Techniques

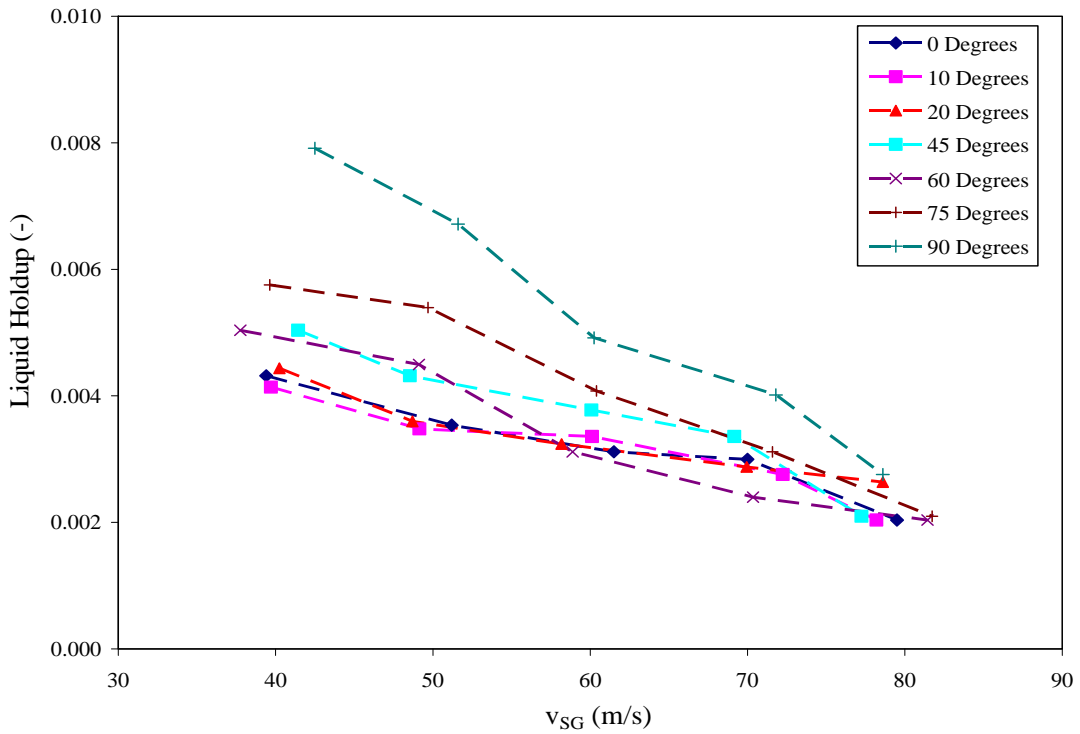


Figure 17: Liquid Holdups for $v_{SL} = 0.0035$ m/s

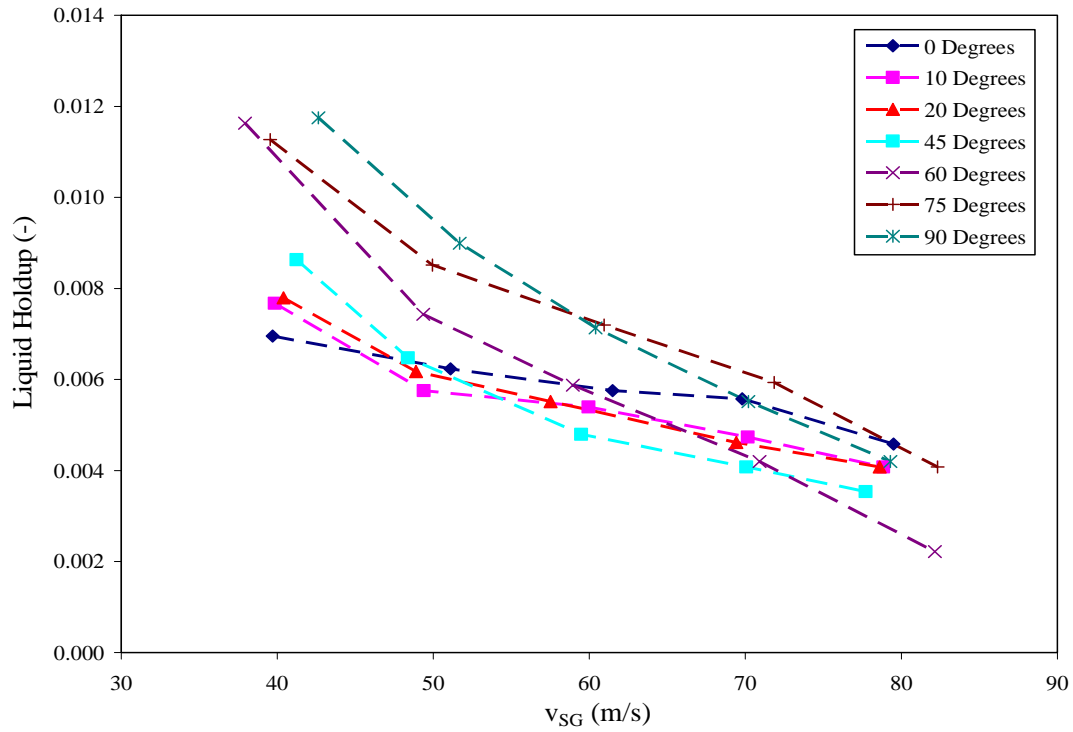


Figure 18: Liquid Holdups for $v_{SL} = 0.01$ m/s

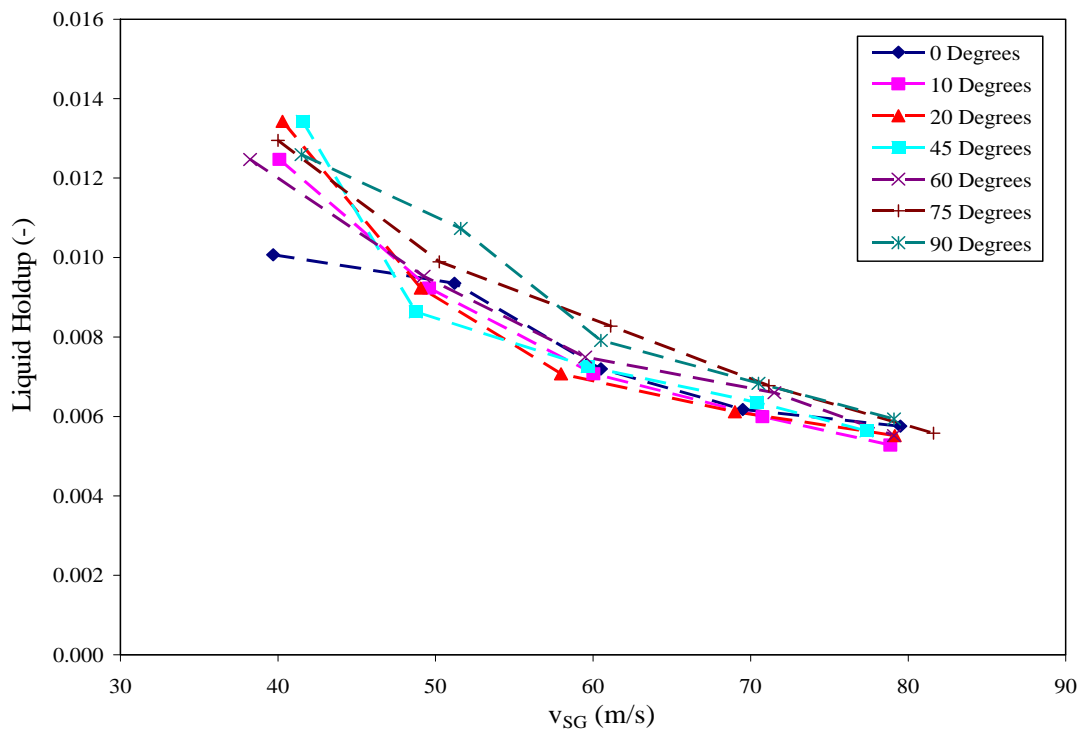


Figure 19: Liquid Holdups for $v_{SL} = 0.02$ m/s

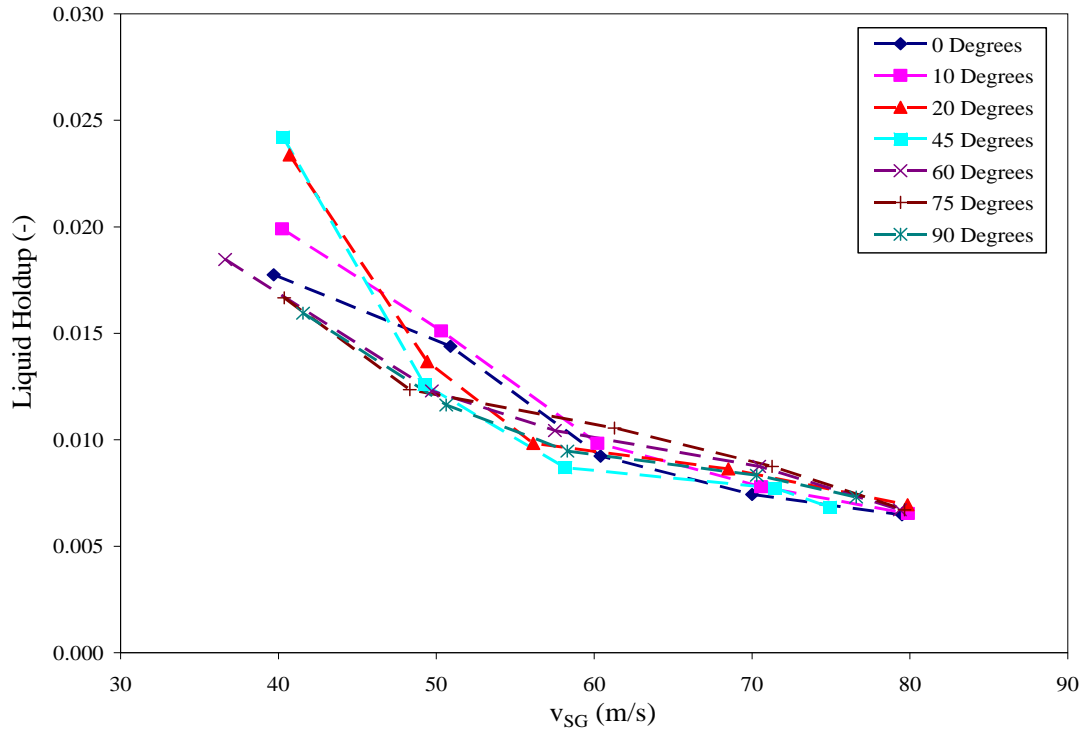


Figure 20: Liquid Holdups for $v_{SL} = 0.04$ m/s

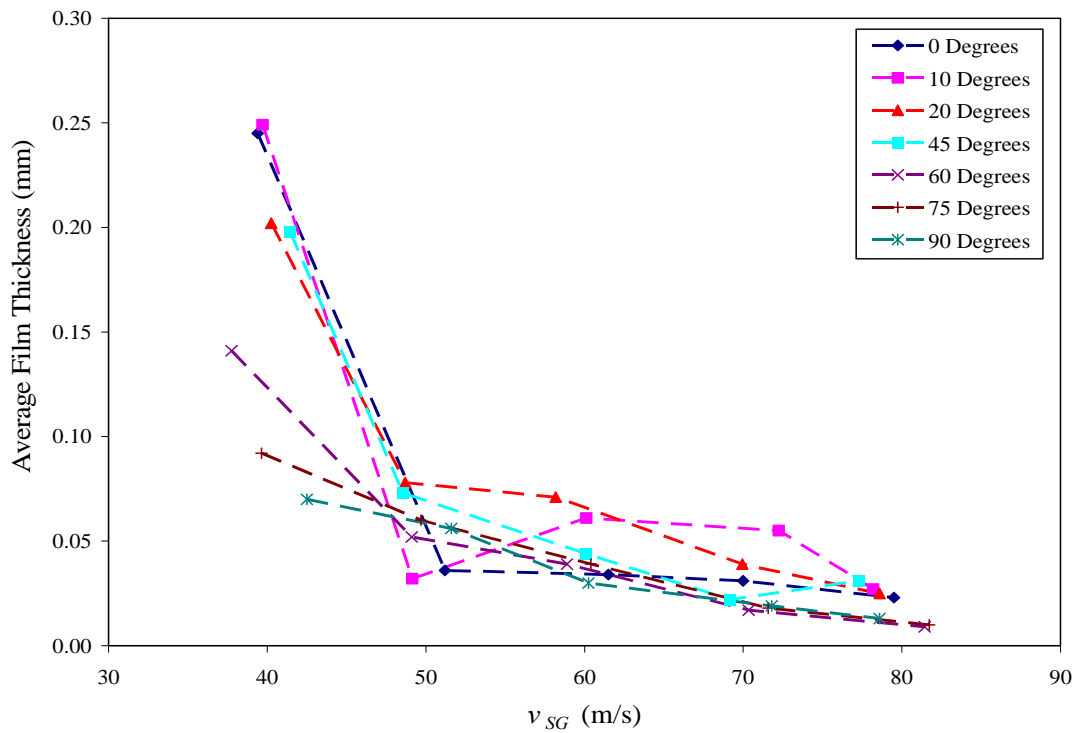


Figure 21: Average Bottom Film Thickness for $v_{SL} = 0.0035$ m/s

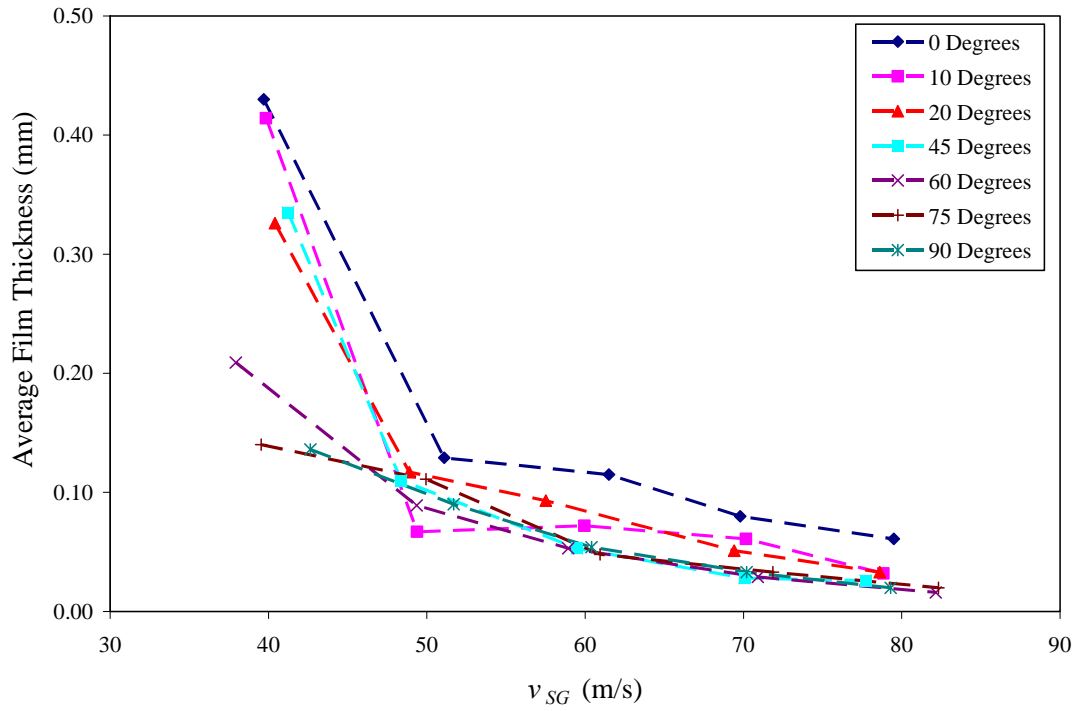


Figure 22: Average Bottom Film Thickness for $v_{SL} = 0.01$ m/s

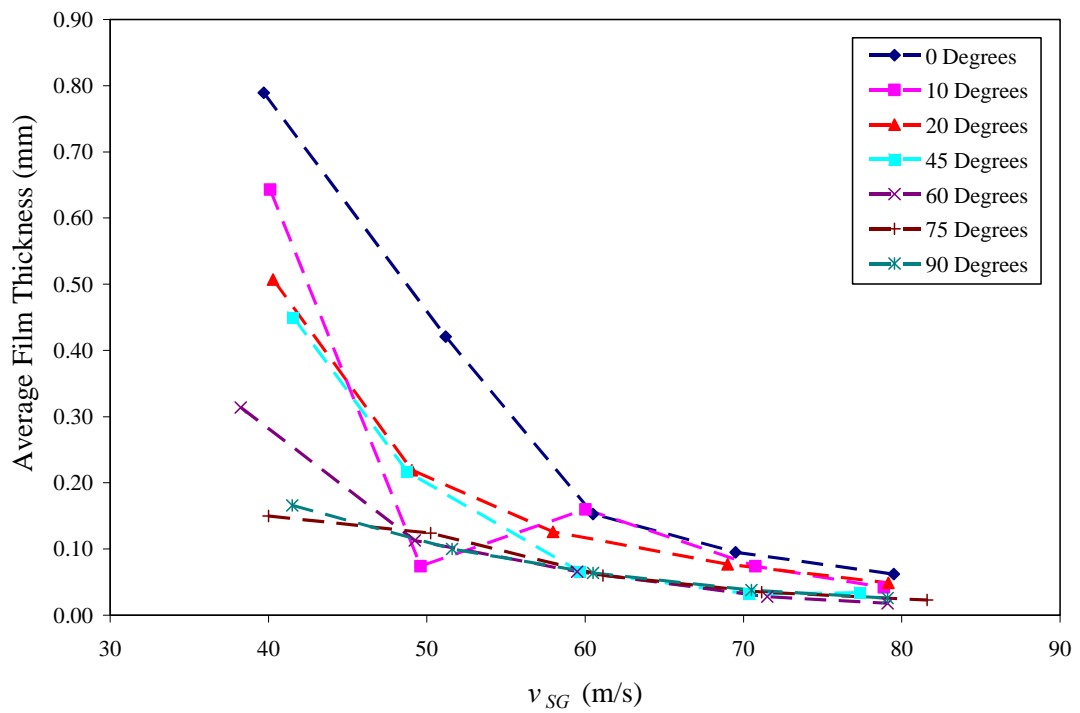


Figure 23: Average Bottom Film Thickness for $v_{SL} = 0.02$ m/s

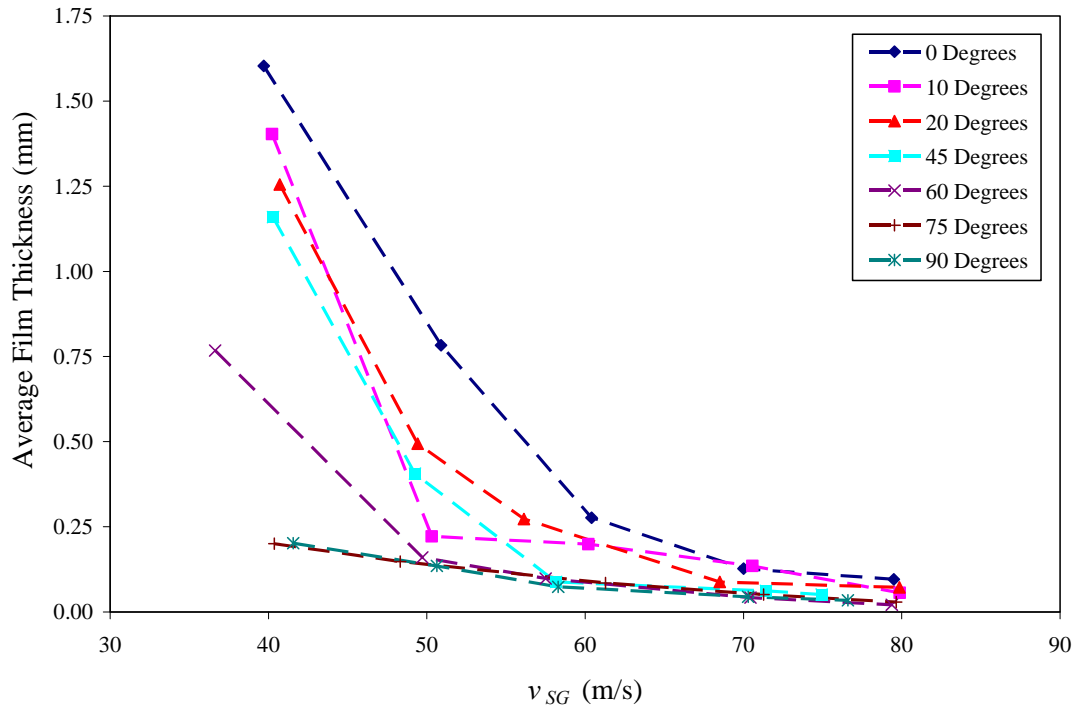


Figure 24: Average Bottom Film Thickness for $v_{SL} = 0.04$ m/s

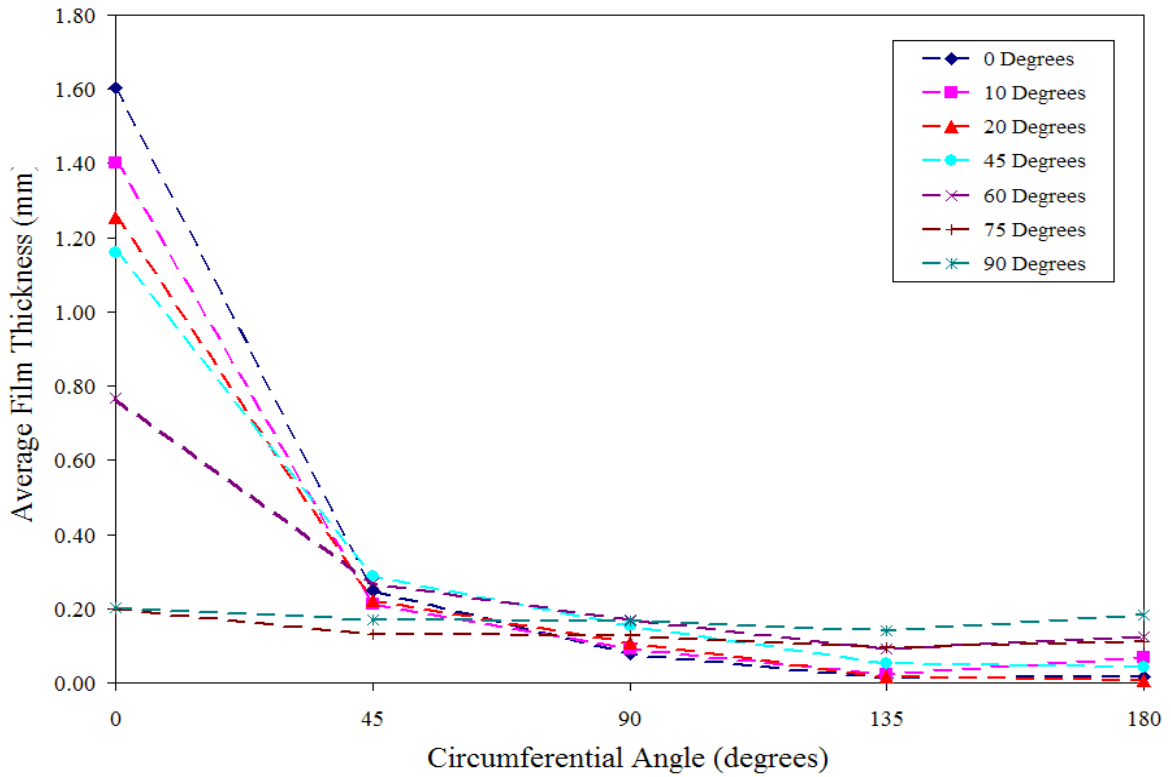


Figure 25: Circumferential Film Thickness for $v_{SL} = 0.04$ m/s, $v_{SG} = 40$ m/s

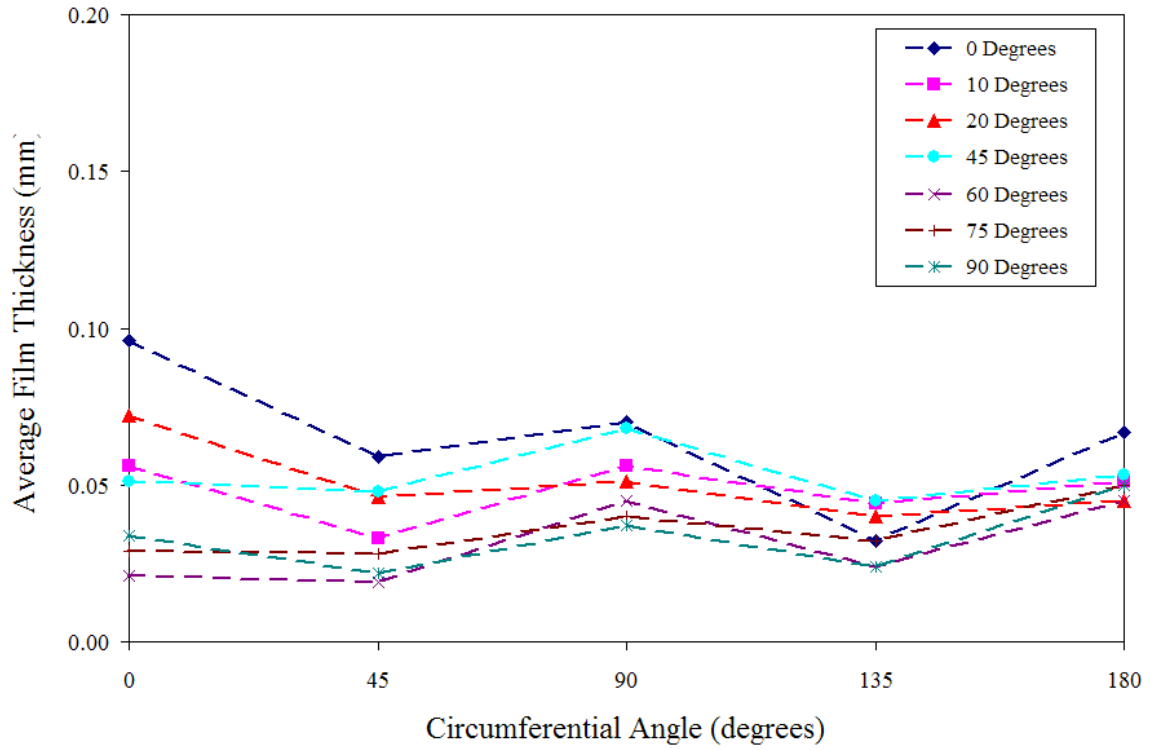


Figure 26: Circumferential Film Thickness for $v_{SL} = 0.04$ m/s, $v_{SG} = 80$ m/s

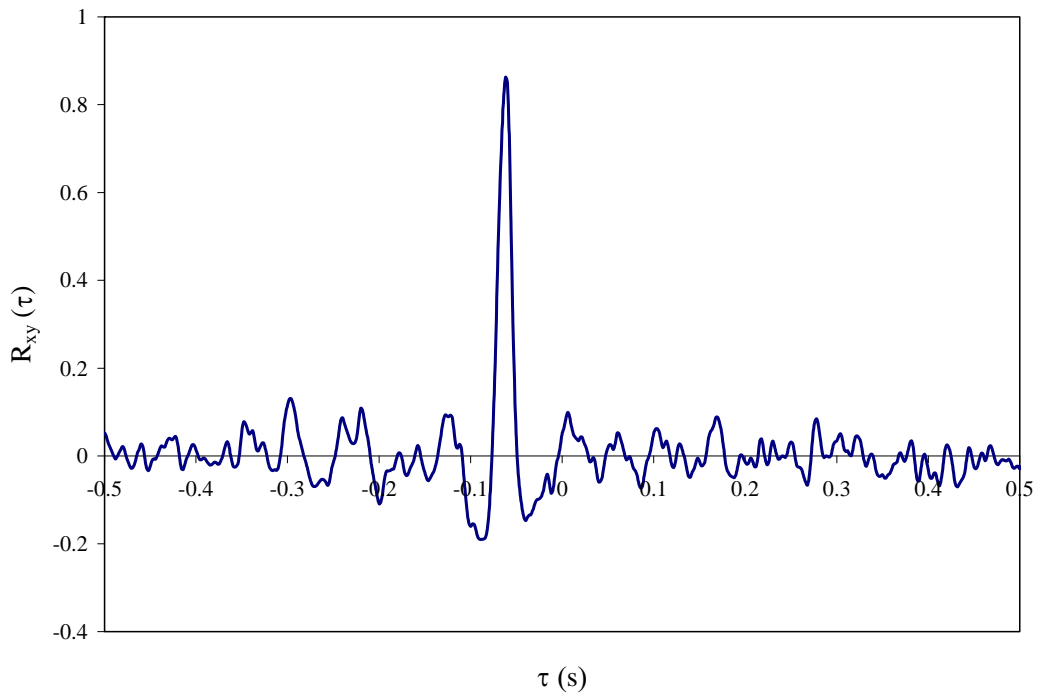


Figure 27: Cross-Correlation Result, $v_{SL} = 0.04$ m/s, $v_{SG} = 80$ m/s, $\theta = 0^\circ$

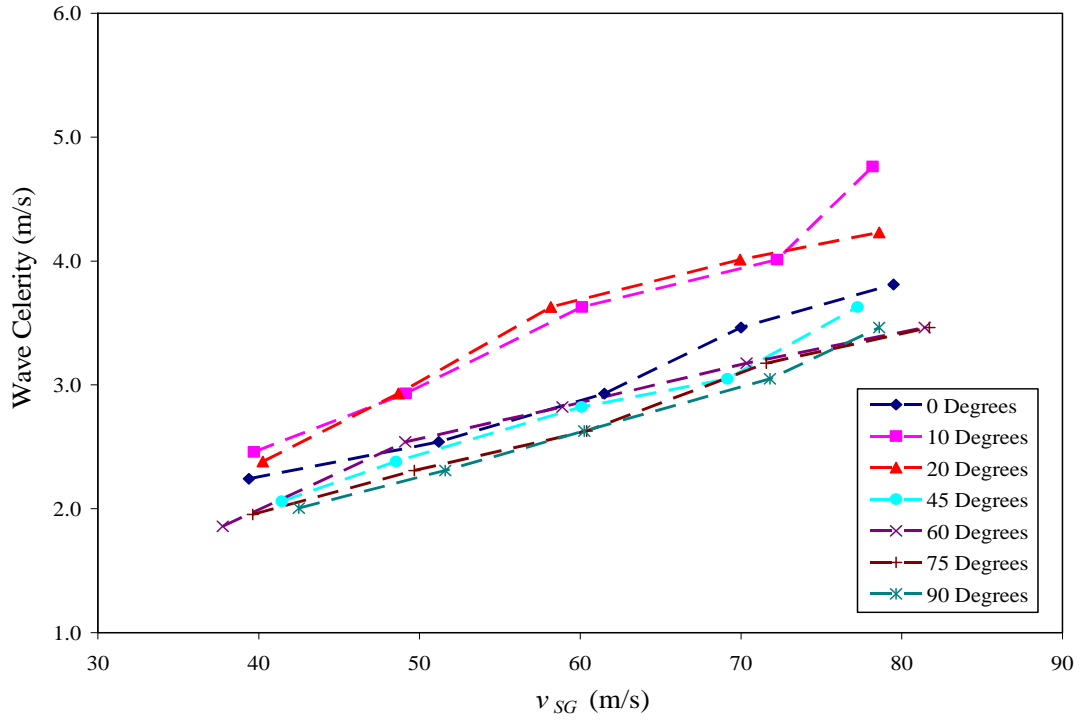


Figure 28: Wave Celerity Results for $v_{SL} = 0.0035$ m/s

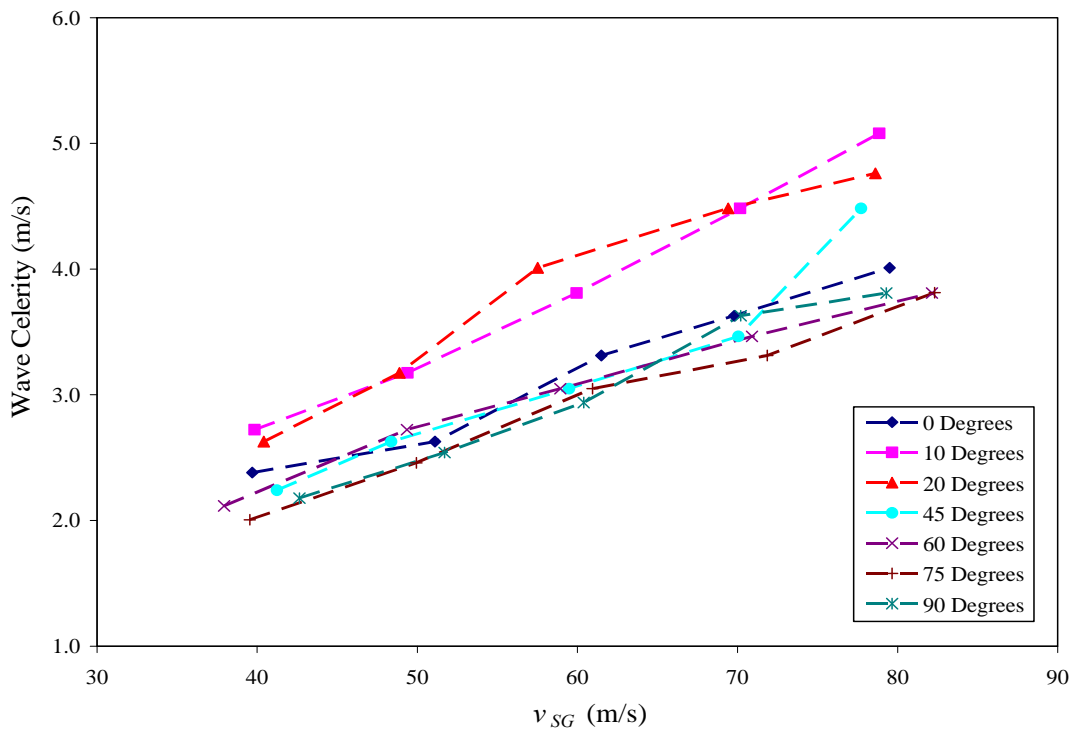


Figure 29: Wave Celerity Results for $v_{SL} = 0.01$ m/s

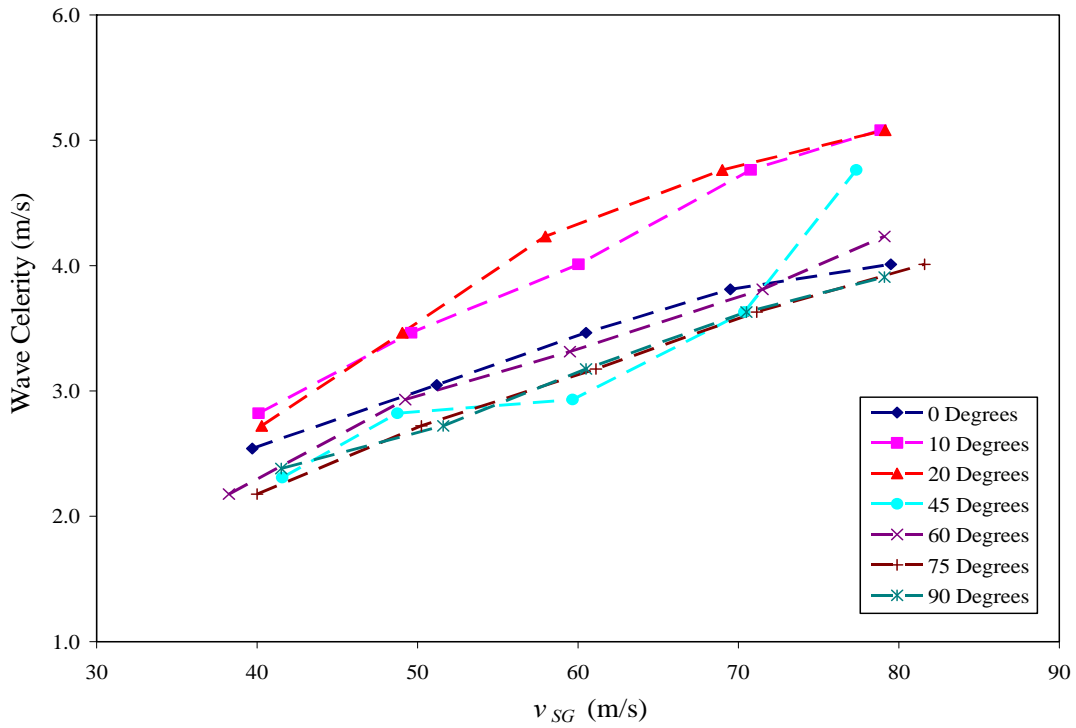


Figure 30: Wave Celerity Results for $v_{SL} = 0.02$ m/s

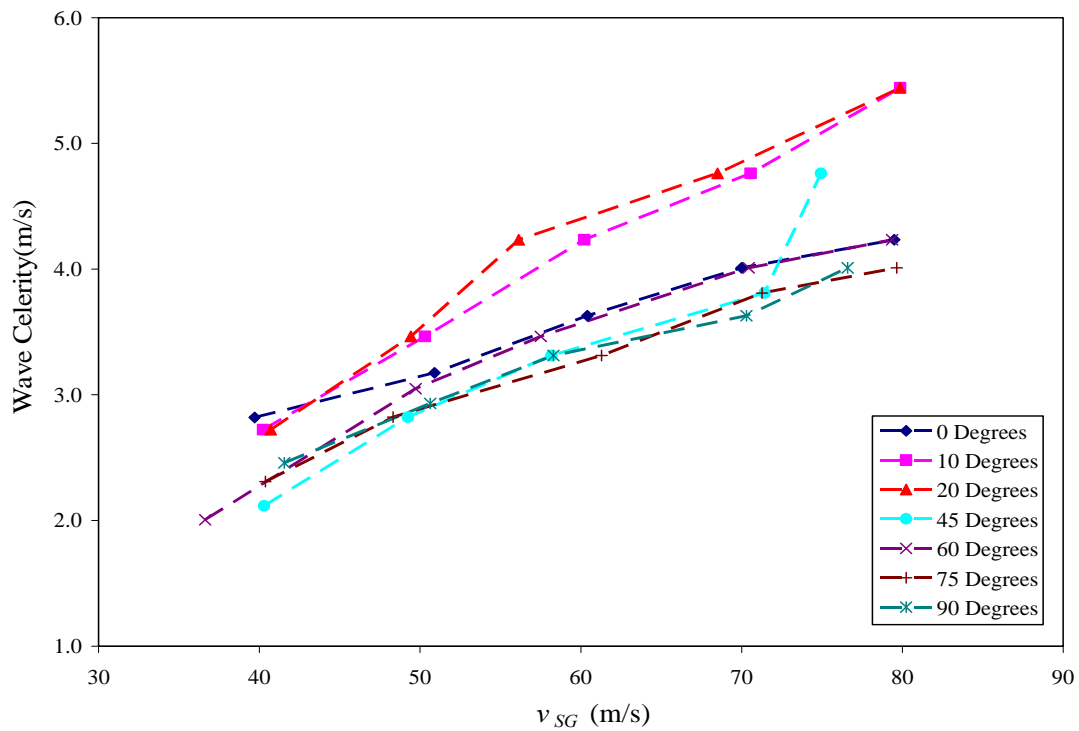


Figure 31: Wave Celerity Results for $v_{SL} = 0.04$ m/s

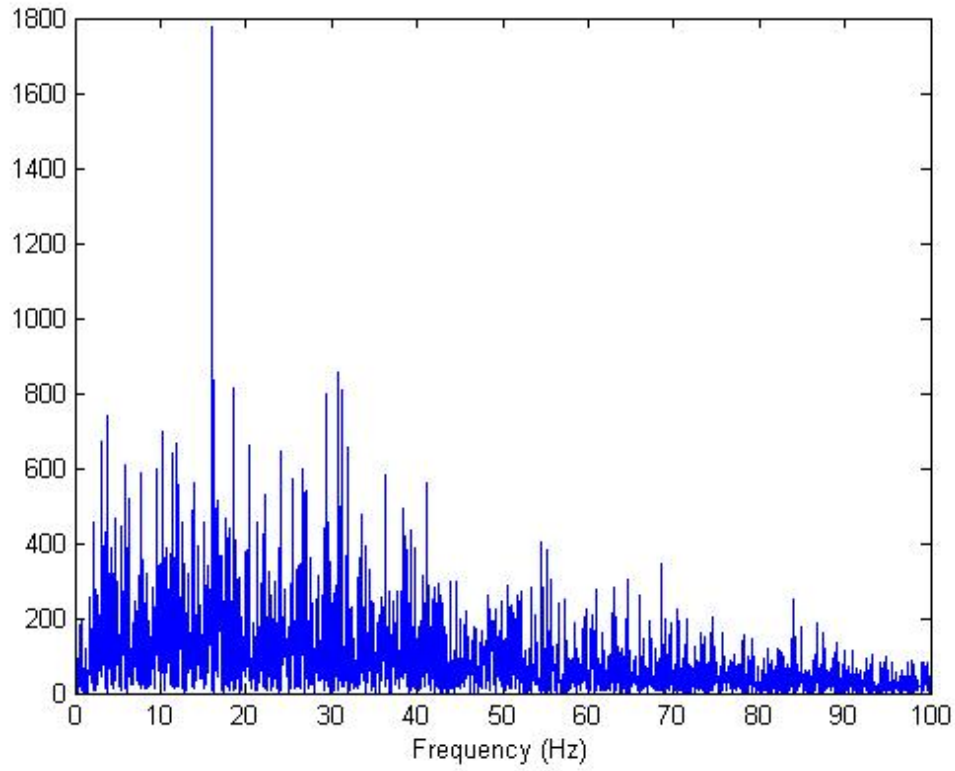


Figure 32: MATLAB Power Spectrum for $v_{SL} = 0.04$ m/s, $v_{SG} = 50$ m/s

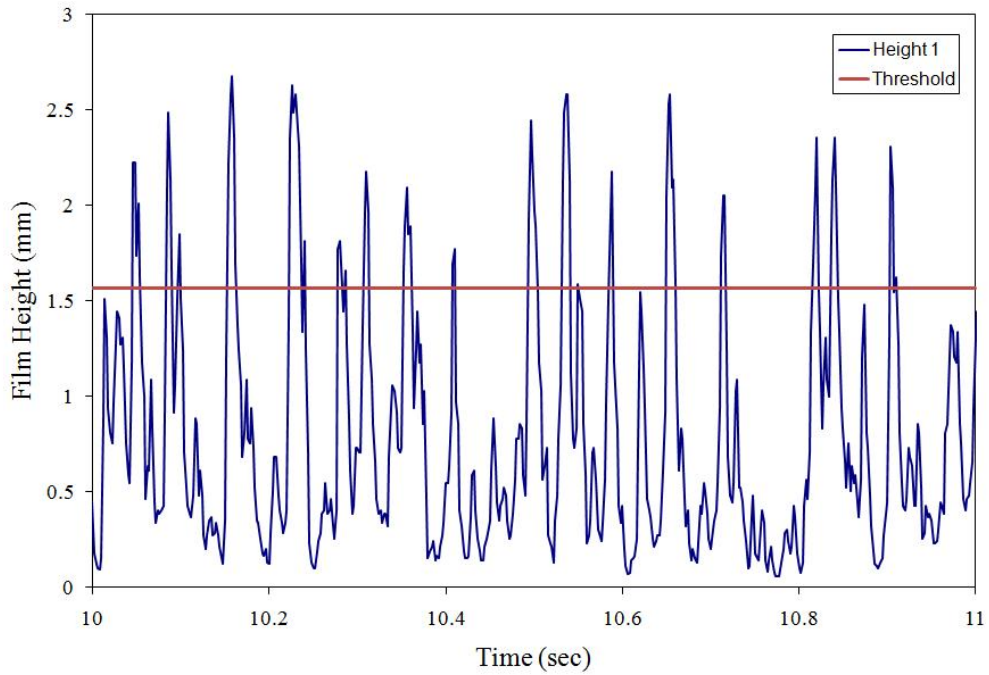


Figure 33: Liquid Film Height Time Trace for $v_{SL} = 0.04$ m/s, $v_{SG} = 50$ m/s

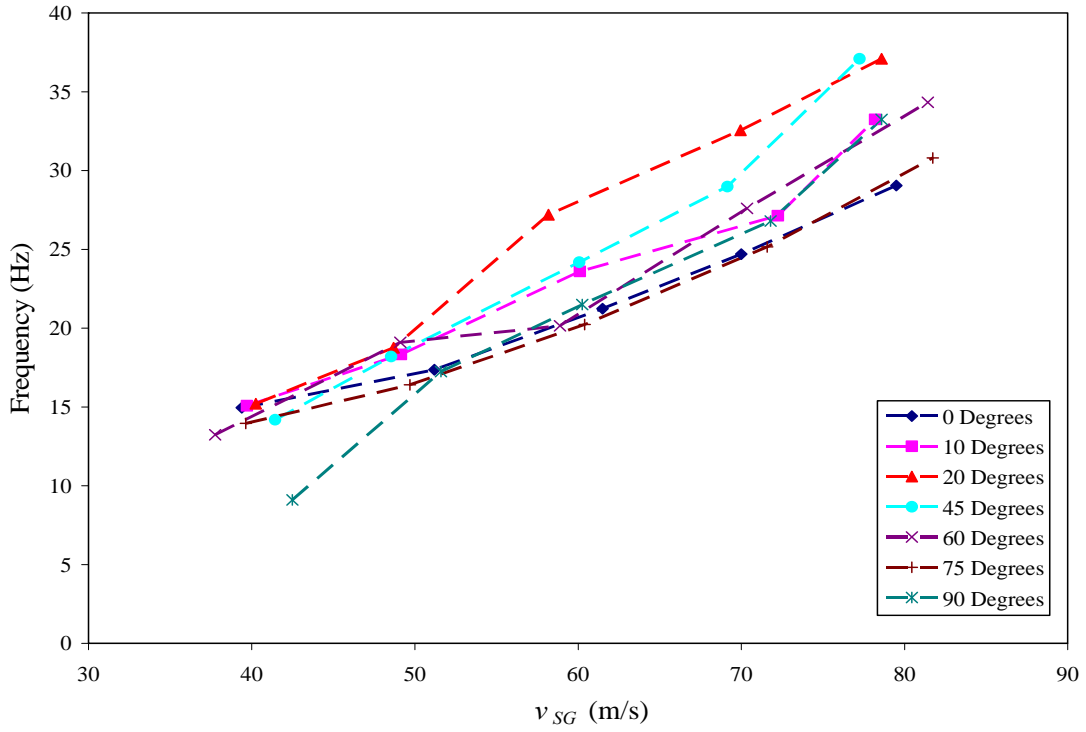


Figure 34: Wave Frequency Results for $v_{SL} = 0.0035$ m/s

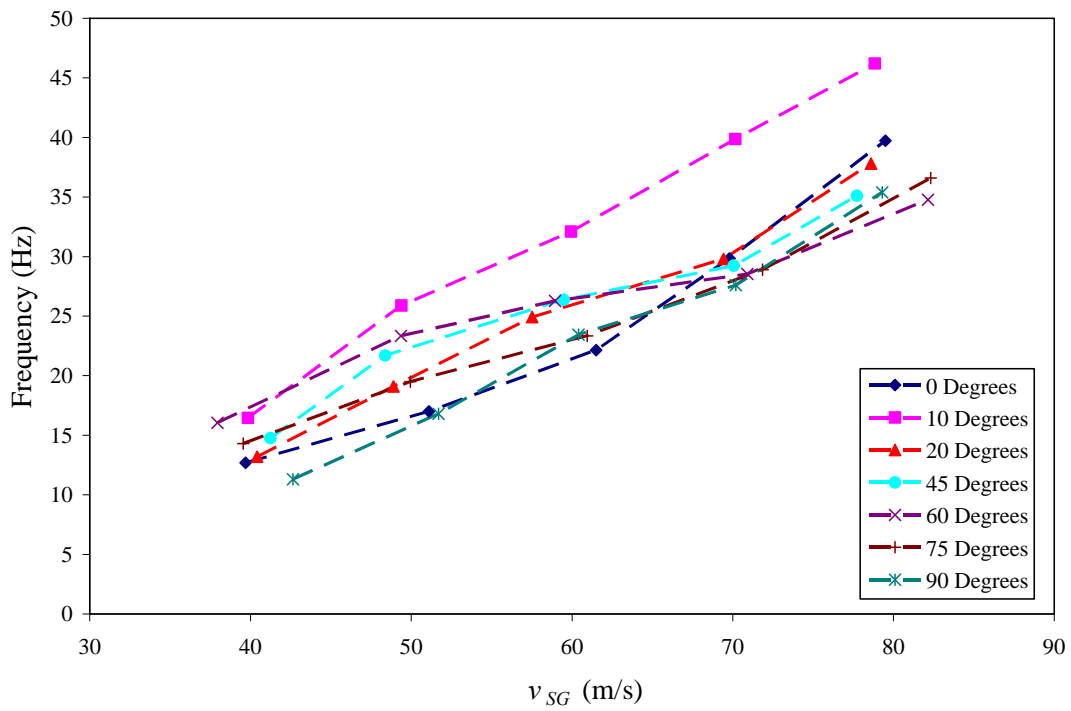


Figure 35: Wave Frequency Results for $v_{SL} = 0.01$ m/s

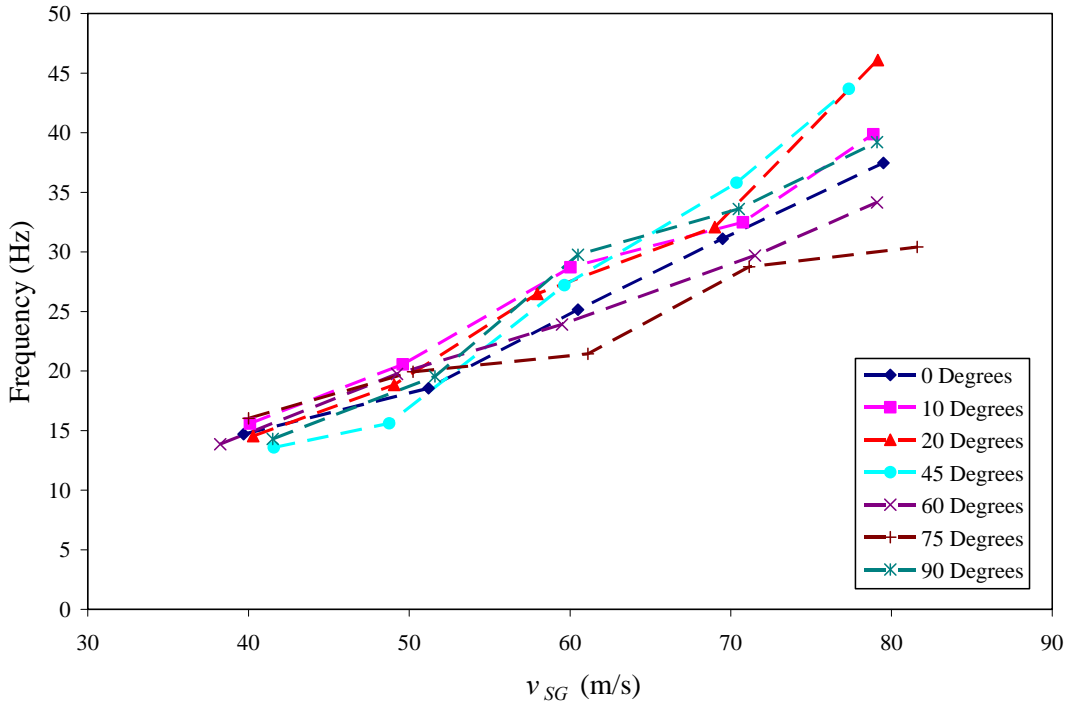


Figure 36: Wave Frequency Results for $v_{SL} = 0.02$ m/s

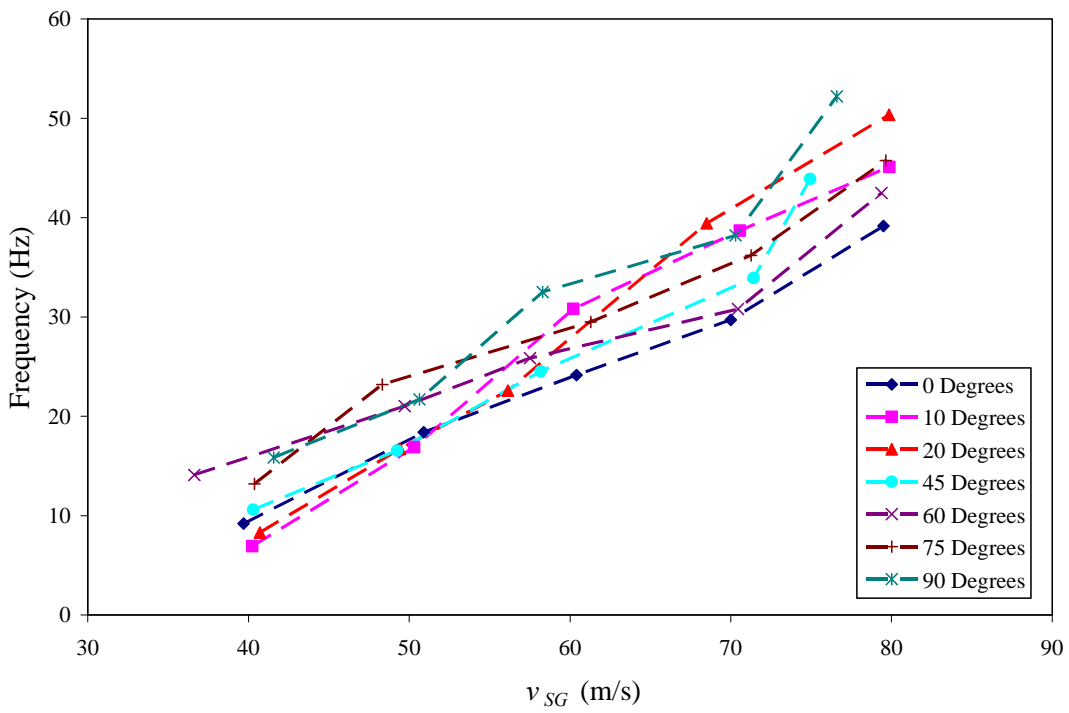


Figure 37: Wave Frequency Results for $v_{SL} = 0.04$ m/s

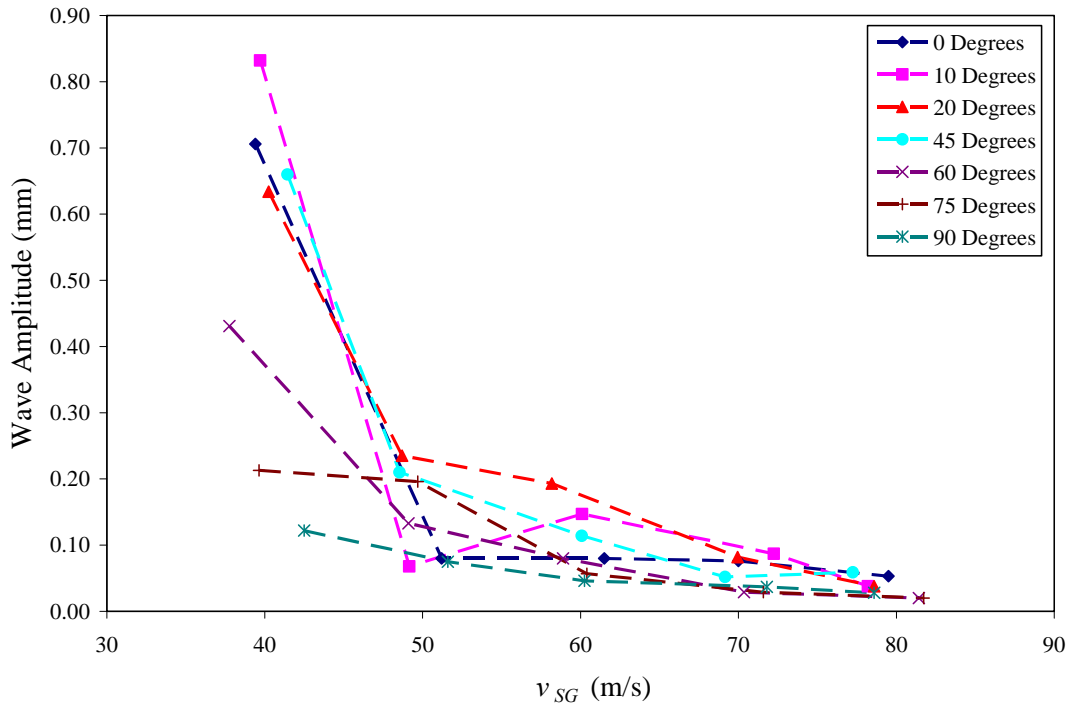


Figure 38: Wave Amplitude Results for $v_{SL} = 0.0035$ m/s

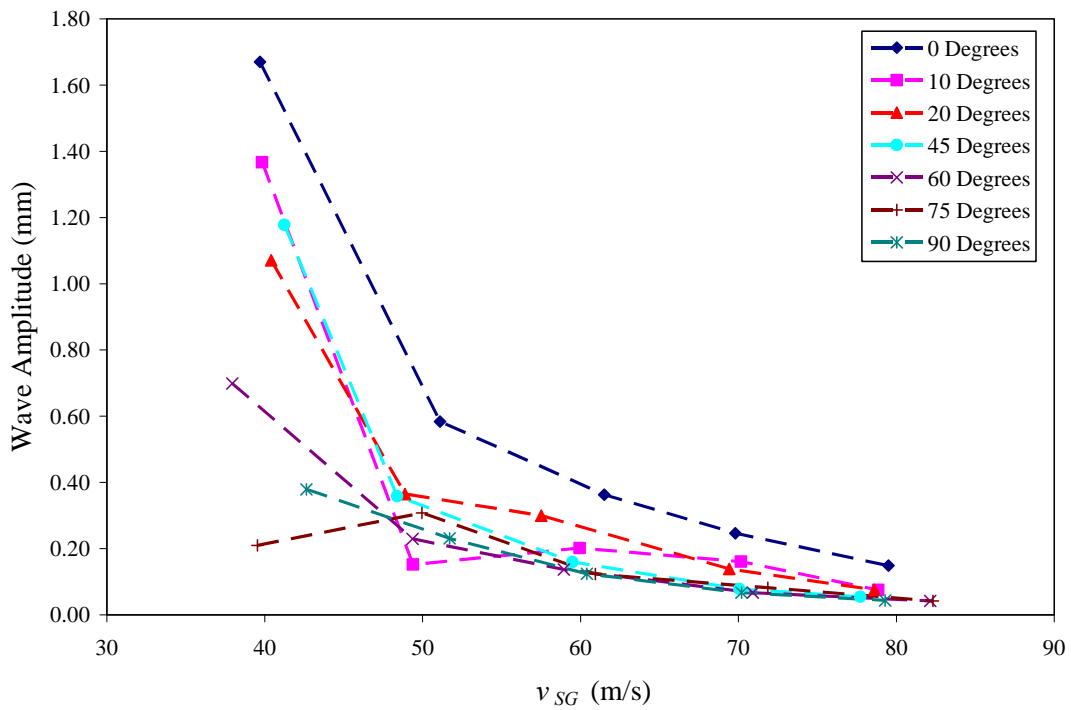


Figure 39: Wave Amplitude Results for $v_{SL} = 0.01$ m/s

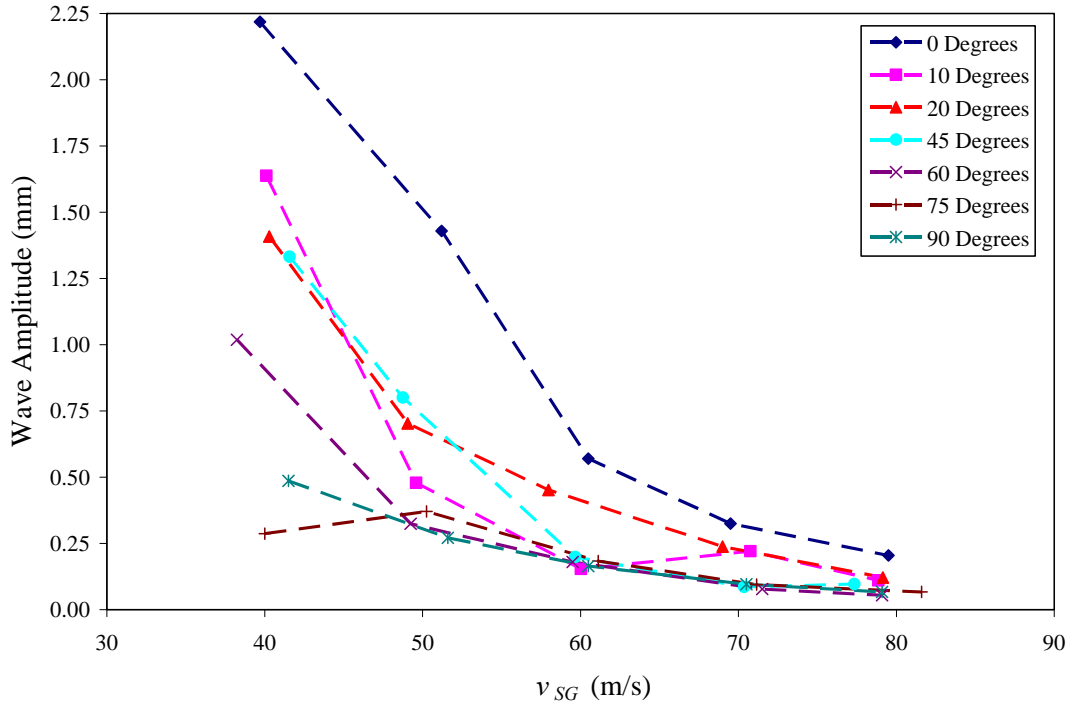


Figure 40: Wave Amplitude Results for $v_{SL} = 0.02$ m/s

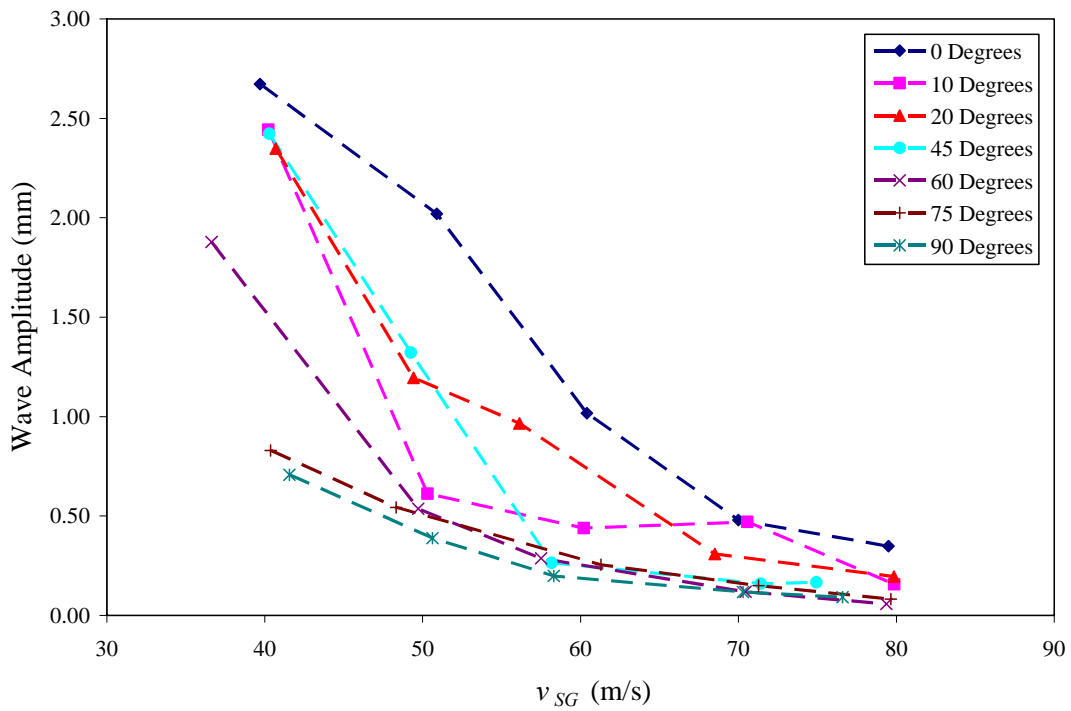


Figure 41: Wave Amplitude Results for $v_{SL} = 0.04$ m/s

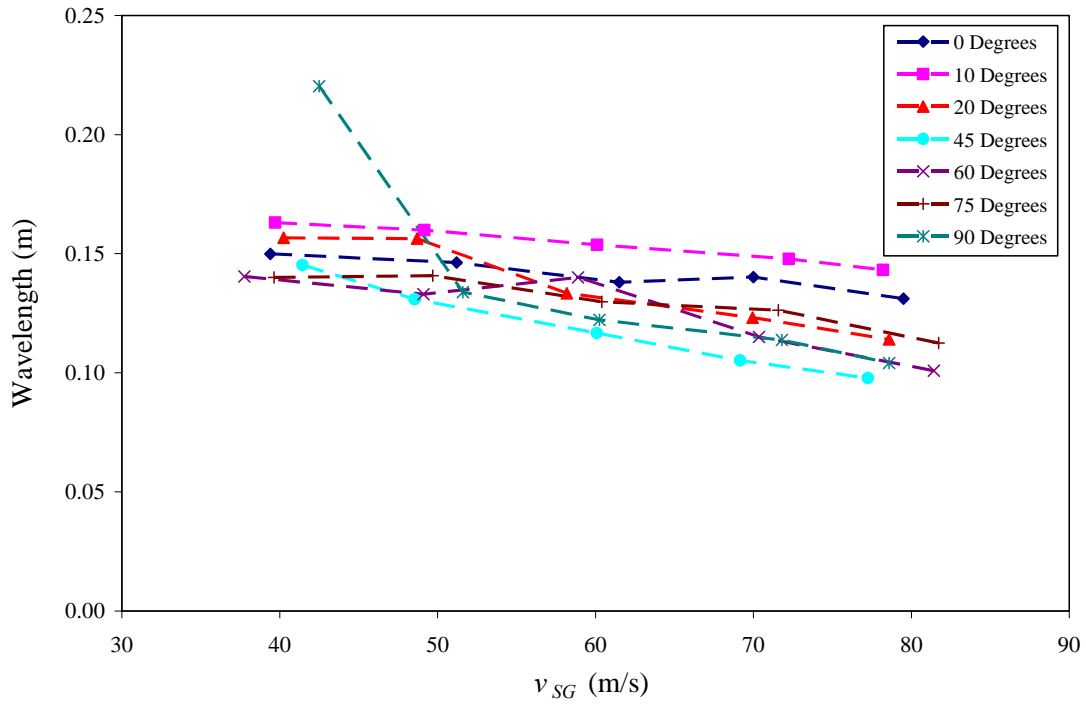


Figure 42: Wavelength Results for $v_{SL} = 0.0035$ m/s

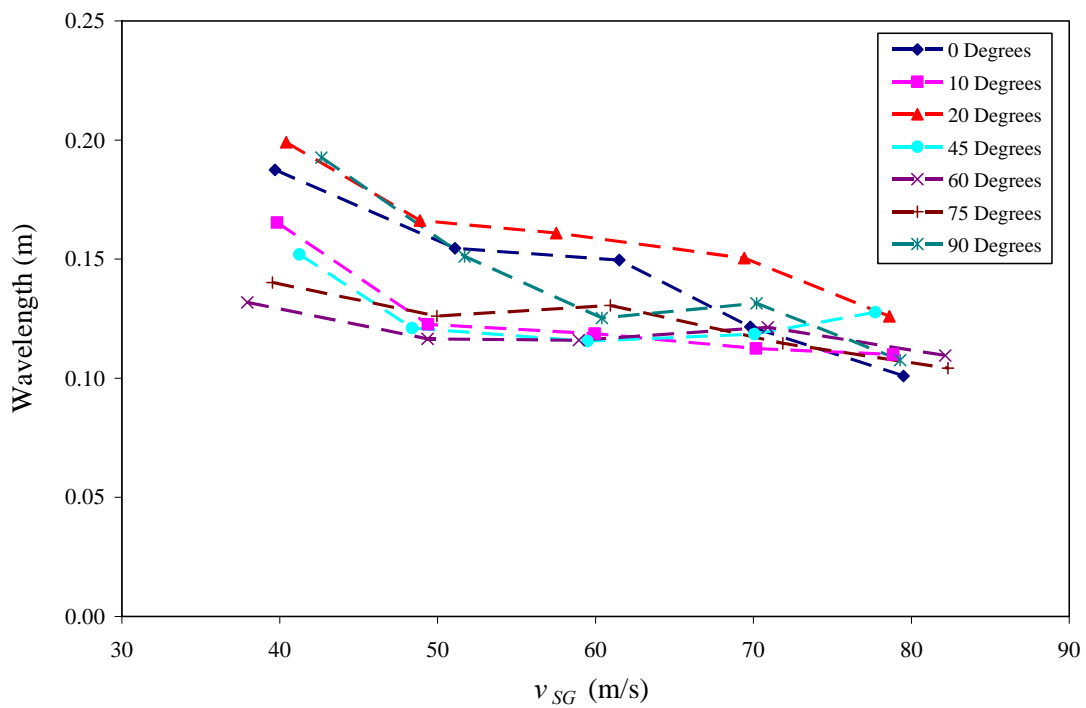


Figure 43: Wavelength Results for $v_{SL} = 0.01$ m/s

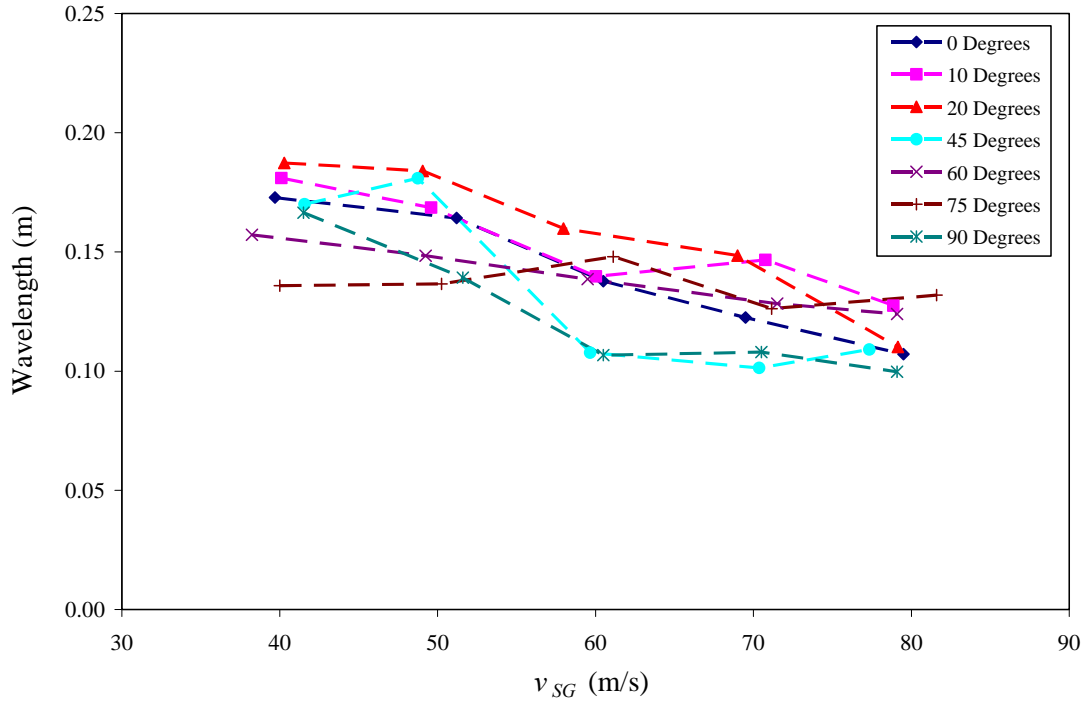


Figure 44: Wavelength Results for $v_{SL} = 0.02$ m/s

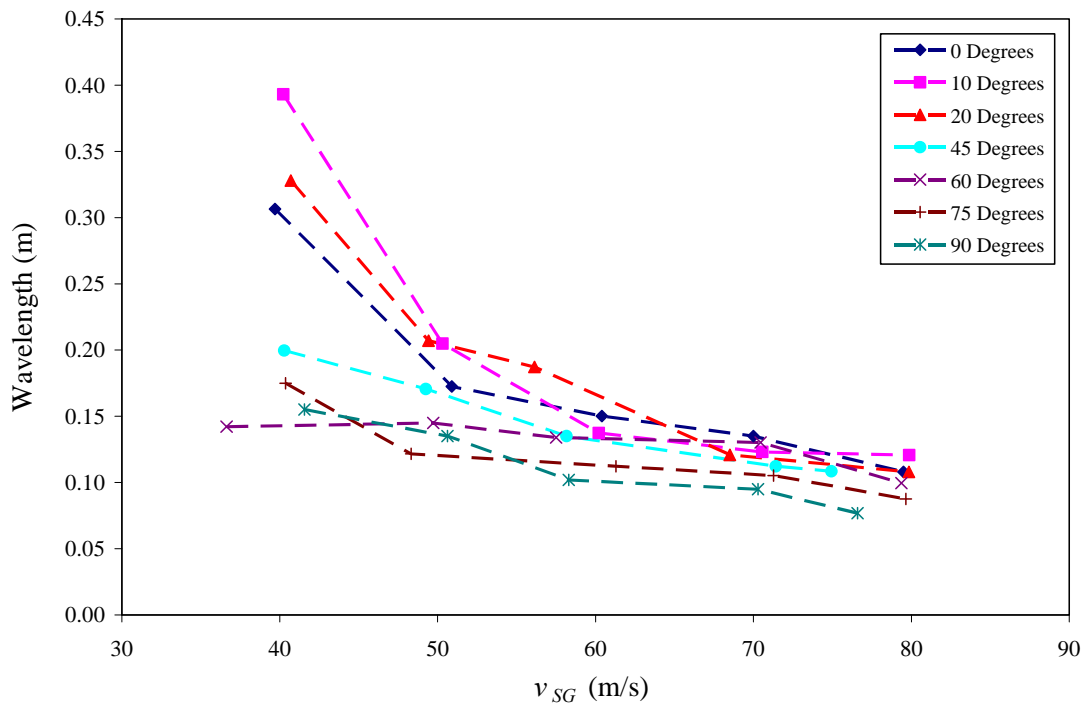


Figure 45: Wavelength Results for $v_{SL} = 0.04$ m/s

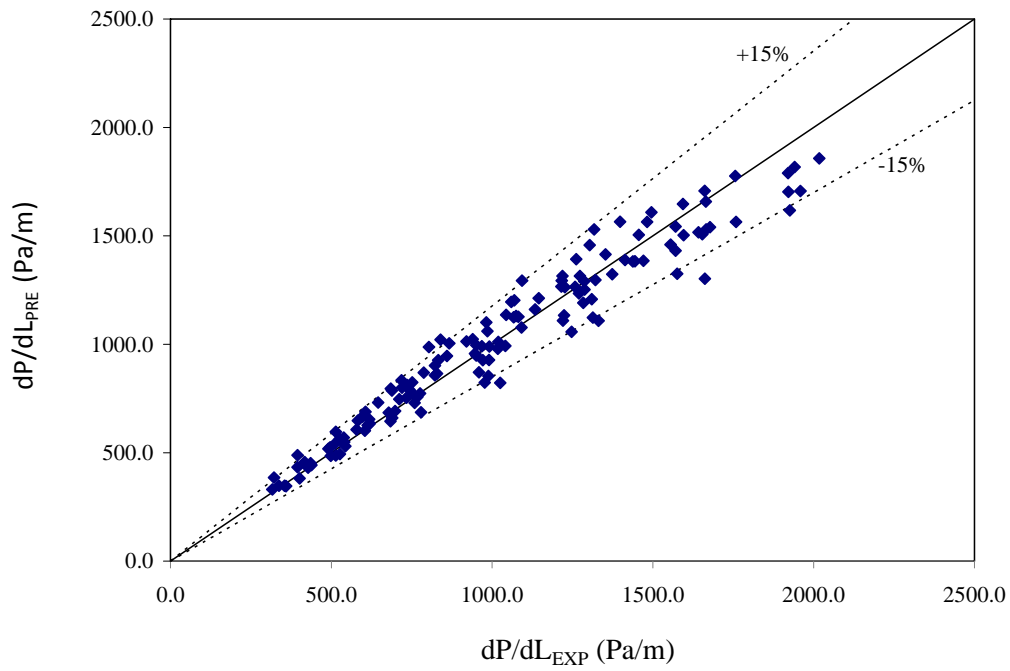


Figure 46: Pressure Gradient Comparison with TUFFP Unified Model Predictions

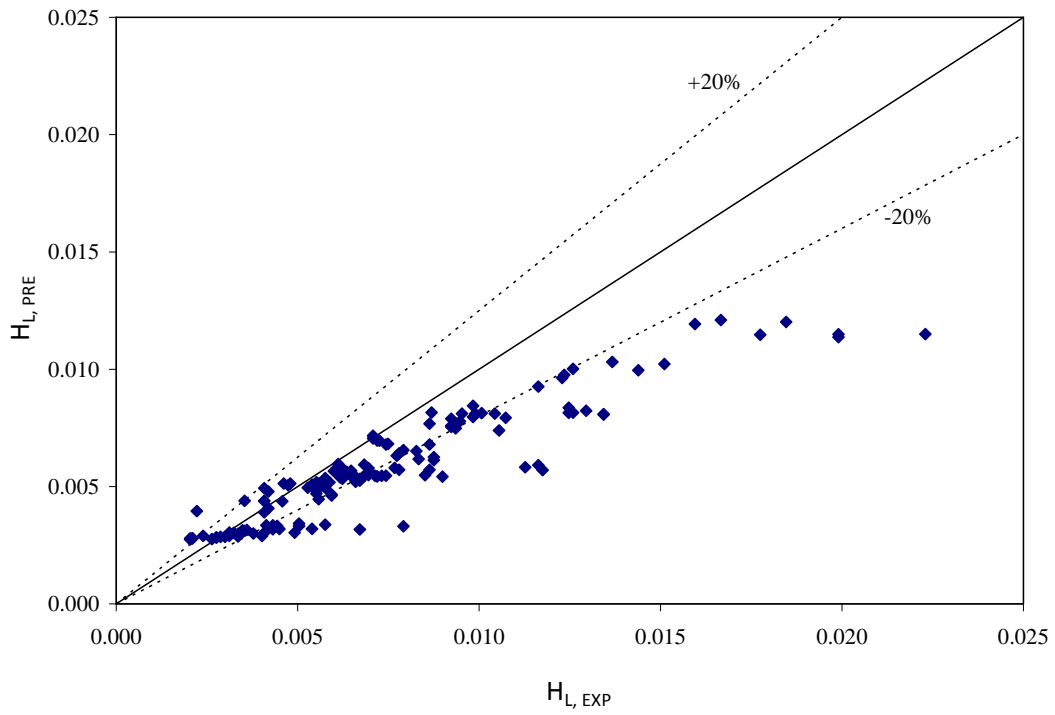


Figure 47: Liquid Holdup Comparison with TUFFP Unified Model Predictions



Fluid Flow Projects

Executive Summary of Research Activities

Cem Sarica

Advisory Board Meeting, September 30, 2009

Upward Multiphase Flow in a Vertical Annulus

- ◆ **Significance**
 - Production Through Annulus
 - Liquid Loading Problem
- ◆ **Objective**
 - Significant Improvements in Multiphase Flow Modeling Since 1985
 - Development of an Improved Mechanistic Model for Vertical Annulus
- ◆ **Past Studies**
 - Caetano
 - ▲ Thorough Experimental and Modeling Study in 1985

Upward Multiphase Flow in a Vertical Annulus ...



◆ Current Study

- Developed a New Model Based on Unified Modeling Approach
- New Model Outperforms the Original Unified Model



Fluid Flow Projects

Modeling of Gas-Liquid Flow in Upward Vertical Annuli

Tingting Yu

Advisory Board Meeting, September 30, 2009

Outline

- ◆ Objectives
- ◆ Introduction
- ◆ Hydrodynamic Models for Individual Flow Patterns
- ◆ Flow Pattern Transition Models
- ◆ Performance Analysis
- ◆ Recommendations



Objectives

- 
- ◆ **Theoretically Investigate Gas-Liquid Flow in Upward Vertical Concentric and Eccentric Annuli**
 - ◆ **Develop New Model**
 - ◆ **Validate Model with Experimental Data**



Significance

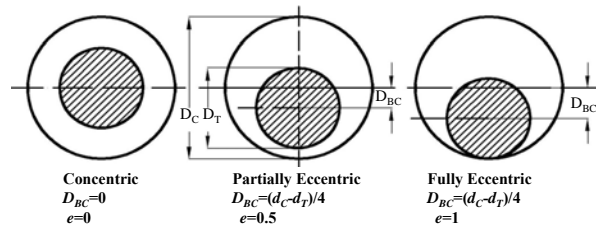
- 
- ◆ **Flow through Annuli Encountered in Many Applications**
 - **Gas Well Production**
 - **Wells under Various Types of Artificial Lifts**
 - ◆ **Oil Wells of High Production Rates Produce through Casing-Tubing Annulus**



Introduction

- ◆ Annulus Formed by Two Circular Pipes
- ◆ Two Geometrical Parameters

$$K = \frac{d_T}{d_C} \quad e = \frac{2D_{BC}}{(d_C - d_T)}$$



Fluid Flow Projects

Advisory Board Meeting, September 30, 2009

Reference Diameter

- ◆ Representative Diameter

$$d_R = \sqrt{d_C^2 - d_T^2}$$

- ◆ Hydraulic Diameter

$$d_H = d_C - d_T$$



Fluid Flow Projects

Advisory Board Meeting, September 30, 2009

Literature Review Summary

- ◆ Vertical Annulus Flow Model by Caetano (1986)
- ◆ Lage *et al.* (2000) and Omurlu *et al.* (2007) Mechanistic Models for Horizontal Annulus Flow
- ◆ Several Advances in Upward Pipe Flow Modeling to be Applied in Annulus Flow



Modeling of Annulus Flow

- ◆ Existing Model Predictions of Liquid Holdup and Pressure Gradient of Annulus Flow Not Satisfactory
- ◆ New Model Developed by Taking Annulus Configuration into Account
- ◆ Model Based on Zhang *et al.* (2003) Unified Modelling Approach



Flow Patterns

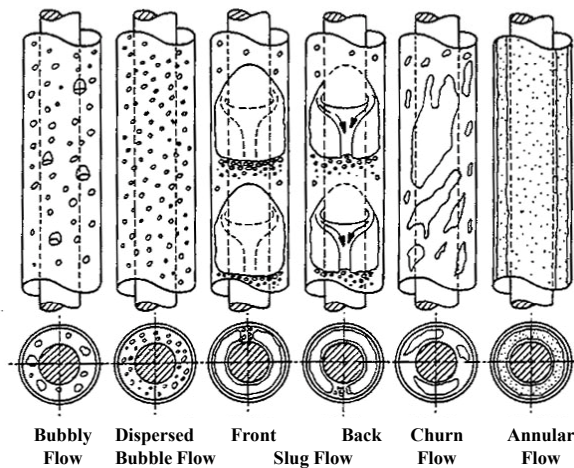
- ◆ **Bubble Flow**
 - Bubbly and Dispersed Bubble
- ◆ **Intermittent Flow**
 - Slug and Churn
- ◆ **Separated Flow**
 - Annular



Fluid Flow Projects

Advisory Board Meeting, September 30, 2009

Flow Patterns in Concentric Annulus



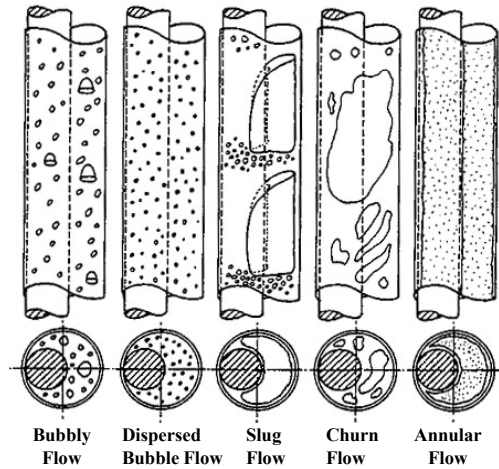
Caetano (1986)



Fluid Flow Projects

Advisory Board Meeting, September 30, 2009

Flow Patterns in Fully Eccentric Annulus



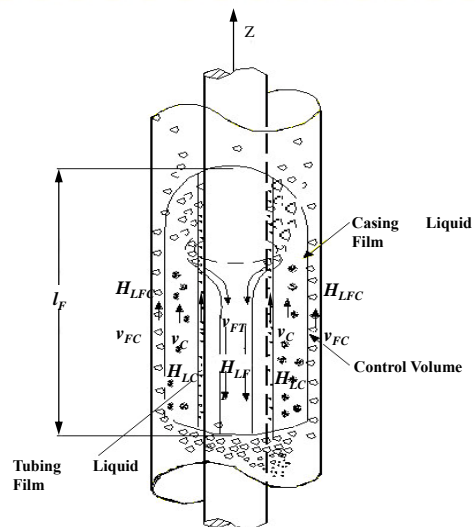
Caetano (1986)



Fluid Flow Projects

Advisory Board Meeting, September 30, 2009

Control Volume



Fluid Flow Projects

Advisory Board Meeting, September 30, 2009

Slug Flow Model

◆ Mass Conservation

➤ Liquid in Film Zone

$$H_{LS}(v_T - v_S) = H_{LFC}(v_T - v_{FC}) + H_{LFT}(v_T - v_{FT})$$

➤ Gas in Film Zone

$$(1 - H_{LS})(v_T - v_S) = (1 - H_{LFC} - H_{LFT})(v_T - v_C)$$



Slug Flow Model ...

◆ Continuity Equations

➤ Liquid in Slug Unit

$$l_U v_{SL} = l_S H_{LS} v_S + l_F (H_{LFC} v_{FC} + H_{LFT} v_{FT})$$

➤ Gas in Slug Unit

$$l_U v_{SG} = l_S (1 - H_{LS}) v_S + l_F (1 - H_{LFC} - H_{LFT}) v_C$$



Slug Flow Model ...

◆ Momentum Equation for Liquid Film

➤ Casing Liquid Film

$$\frac{(P_2 - P_1)}{l_F} = \frac{\rho_L (v_{FC} - v_T)(v_{FC} - v_S)}{l_F} + \frac{\tau_{IC} S_{IC}}{H_{LFC} A} - \frac{\tau_{FC} S_{FC}}{H_{LFC} A} - \rho_L g \sin \theta$$

➤ Tubing Liquid Film

$$\frac{(P_2 - P_1)}{l_F} = \frac{\rho_L (v_{FT} - v_T)(v_{FT} - v_S)}{l_F} + \frac{\tau_{IT} S_{IT}}{H_{LFT} A} - \frac{\tau_{FT} S_{FT}}{H_{LFT} A} - \rho_L g \sin \theta$$



Slug Flow Model ...

◆ Momentum Equation for Gas Core

$$\frac{(P_2 - P_1)}{l_F} = \frac{\rho_C (v_T - v_C)(v_S - v_C)}{l_F} + \frac{\tau_{IT} S_{IT} + \tau_{IC} S_{IC}}{(1 - H_{LFT} - H_{LFC}) A} - \rho_C g \sin \theta$$



Slug Flow Model ...

◆ Combined Momentum Equation for Casing Liquid Film

$$\frac{\rho_L(v_{FC} - v_T)(v_{FC} - v_S) - \rho_C(v_C - v_T)(v_C - v_S)}{l_F} - \frac{\tau_{FC} S_{FC}}{H_{LFC} A}$$

$$+ \frac{\tau_{IT} S_{IT}}{(1 - H_{LFC} - H_{LFT}) A} + \tau_{IC} S_{IC} \left(\frac{1}{H_{LFC} A} + \frac{1}{(1 - H_{LFC} - H_{LFT}) A} \right)$$

$$+ (\rho_C - \rho_L) g \sin \theta = 0$$



Slug Flow Model ...

◆ Combined Momentum Equation for Tubing Liquid Film

$$\frac{\rho_L(v_{FT} - v_T)(v_{FT} - v_S) - \rho_C(v_C - v_T)(v_C - v_S)}{l_F} - \frac{\tau_{FT} S_{FT}}{H_{LFT} A}$$

$$+ \frac{\tau_{IC} S_{IC}}{(1 - H_{LFC} - H_{LFT}) A} + \tau_{IT} S_{IT} \left(\frac{1}{H_{LFT} A} + \frac{1}{(1 - H_{LFC} - H_{LFT}) A} \right)$$

$$+ (\rho_C - \rho_L) g \sin \theta = 0$$



Annular Flow Model

◆ Momentum Equation for Casing Film

$$0 - \frac{\tau_{FC} S_{FC}}{H_{LFC} A} + \frac{\tau_{IT} S_{IT}}{(1 - H_{LFC} - H_{LFT}) A} + \tau_{IC} S_{IC} \left(\frac{1}{H_{LFC} A} + \frac{1}{(1 - H_{LFC} - H_{LFT}) A} \right) + (\rho_C - \rho_L) g \sin \theta = 0$$



Annular Flow Model ...

◆ Momentum Equation for Tubing Film

$$0 - \frac{\tau_{FT} S_{FT}}{H_{LFT} A} + \frac{\tau_{IC} S_{IC}}{(1 - H_{LFC} - H_{LFT}) A} + \tau_{IT} S_{IT} \left(\frac{1}{H_{LFT} A} + \frac{1}{(1 - H_{LFC} - H_{LFT}) A} \right) + (\rho_c - \rho_L) g \sin \theta = 0$$



Churn Flow Model

◆ Combined Momentum Equation for Liquid Film and Gas Pocket

$$\frac{\rho_L(v_T - v_F)(v_S - v_F) - \rho_C(v_T - v_C)(v_S - v_C)}{l_F} + \frac{\tau_C S_C}{(1 - H_{LF})A} - \frac{\tau_F S_F}{H_{LF}A} + \tau_I S_I \left(\frac{1}{H_{LF}A} + \frac{1}{(1 - H_{LF})A} \right) - (\rho_L - \rho_C)g \sin\theta = 0$$

◆ Slug Length

$$l_S = 4d_R$$



Bubble Flow Model

◆ Bubbly Flow Model

$$v_O = 1.53 \left[\frac{(\rho_L - \rho_G)g\sigma}{\rho_L^2} \right]^{1/4} H_L^n \quad v_S = \frac{v_{SG}}{1 - H_L} - \frac{v_{SL}}{H_L}$$

◆ Dispersed Bubble Model

➤ Homogeneous Flow



Flow Pattern Transitions ...

◆ Transition from Slug Flow to Churn Flow

➤ Kaya (1998) Model

$$v_{SG} = 2.76(1.2v_{SL} + v_o)$$

$$v_o = (0.35 \sin \theta + 0.54 \cos \theta) \left(\frac{g(\rho_L - \rho_g)d_R}{\rho_L} \right)^{1/2}$$



Closure Relationships

- ◆ Film Liquid Holdup Ratio
- ◆ Slug Translational Velocity
- ◆ Wall Friction Factor
- ◆ Interfacial Friction Factor
- ◆ Liquid Entrainment Fraction in Gas Core
- ◆ Slug Liquid Holdup
- ◆ Slug Length



Film Liquid Holdup Ratio

◆ Caetano's (1986) Liquid Film Holdup Equations

$$H_{LFT} = \frac{4\delta_T}{d_C} K \left(\frac{1 + \frac{\delta_T}{d_T}}{1 - K^2} \right) \quad H_{LFC} = \frac{4\delta_C}{d_C} \left(\frac{1 + \frac{\delta_C}{d_C}}{1 - K^2} \right)$$

$$\frac{H_{LFT}}{H_{LFC}} = \frac{\delta_T}{\delta_C} K \quad \frac{\delta_T}{\delta_C} = \frac{W_T'}{(2\pi - W_T')K}$$

$$W_T' = \frac{1}{(1 - K^2)} \left(2 * \sin^{-1}(K) + 2K\sqrt{1 - K^2} - K^2\pi \right)$$



Slug Translational Velocity

◆ Nicklin (1962)

$$v_T = C_S v_S + v_D$$

➤ C_S Coefficient

$C_S = 1.3$ for Turbulent Flow

$C_S = 2.0$ for Laminar Flow

$C_S = 2.0 - 0.7(\text{Re} - 2000)/2000$ for Transition

➤ Drift velocity (Hasan and Kabir (1992))

$$v_D = 0.345(1 + 0.1K)\sqrt{gd_c(\rho_L - \rho_G)/\rho_L}$$



Wall Friction Factor

◆ Friction Factor for Shear Stress at Wall

$$f = C \operatorname{Re}^{-n}$$

$$C = 16, n = 1 \quad \text{Laminar}$$

$$C = 0.046, n = 0.2 \quad \text{Turbulent}$$

◆ Caetano's Friction Factor

$$f_{CA} = \frac{16}{\operatorname{Re}} \frac{(1-K)^2}{\left[\frac{1-K^4}{1-K^2} - \frac{1-K^2}{\ln(1/K)} \right]} \quad \text{Laminar}$$



Wall Friction Factor ...

◆ Caetano's Friction Factor ...

$$\frac{1}{\left\{ f_{CA} \left(\frac{F_P}{F_{CA}} \right)^{0.45 \exp[-(\operatorname{Re}-3000)/10^6]} \right\}^{1/2}} = \quad \text{Turbulent}$$

$$4.0 \log \left\{ \operatorname{Re} \left[f_{CA} \left(\frac{F_P}{F_{CA}} \right)^{0.45 \exp[-(\operatorname{Re}-3000)/10^6]} \right]^{1/2} \right\} = -0.40$$



Interfacial Friction Factor

◆ Ambrosini et al. (1991) Correlation for Annular Flow

$$f_I = f_G \left(1 + 13.8 We_G^{0.2} Re_G^{-0.6} (h_F^+ - 200 \sqrt{\rho_G / \rho_L}) \right)$$

$$We_G = \frac{\rho_G v_C^2 d_R}{\sigma} \quad Re_G = \frac{\rho_G v_C d_R}{\mu_G}$$

$$h_F^+ = \frac{\rho_G \delta_C v_C^*}{\mu_G} \quad v_C^* = \sqrt{\tau_I / \rho_G}$$

$$f_G = 0.046 Re_G^{-0.2}$$



Interfacial Friction Factor ...

◆ Andritsos et al. (1987) Correlation for Slug Flow

$$f_I = f_C \left(1.0 + 15.0 \left(\frac{2\delta}{d_R} \right)^{0.5} \left(\frac{v_{SG}}{v_{SG,t}} - 1.0 \right) \right)$$

$$v_{SG,t} = 5.0 \sqrt{\frac{\rho_a}{\rho_g}}$$



Liquid Entrainment Fraction

♦ Wallis *et al.* (1969) Correlation

$$f_E = 1 - \exp[-0.125(\phi - 1.5)]$$

$$\phi = 10^4 \frac{v_{SG} \mu_G}{\sigma} \left(\frac{\rho_G}{\rho_L} \right)^{0.5}$$



Slug Liquid Holdup

Zhang *et al.* (2003) Model

$$H_{LS} = \frac{1}{1 + \frac{T_{sm}}{3.16[(\rho_L - \rho_G)g\sigma]^{1/2}}}$$

$$T_{sm} = \frac{1}{C_e} \left(\begin{array}{l} f_S / 2\rho_S v_S^2 + \\ \frac{d_R \rho_L (H_{LFC} + H_{LFT})(v_T - v_{FC})(v_S - v_{FC})}{4 l_S} \\ + \frac{d_R \rho_C (1 - H_{LFC} - H_{LFT})(v_T - v_C)(v_S - v_C)}{4 l_S} \end{array} \right)$$

$$C_e = \frac{2.5 - |\sin(\theta)|}{2}$$



Slug Length

- ◆ **Taitel *et al.* (1980) and Barnea and Brauner (1985)**

$$l_S = (32.0 \cos^2 \theta + 16.0 \sin^2 \theta) d_R$$



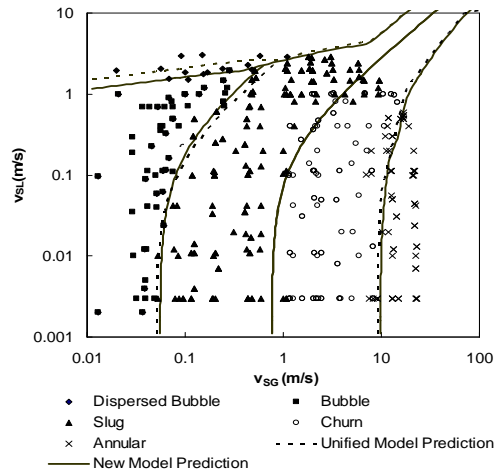
Experimental Data

- ◆ **Experimental Information**

- **Caetano (1986) Test Facility: 16-m (52.493-ft) Long with 76.2-mm (3-inch) I.D. Casing and 42.2 (1.66-inch) O.D. Tubing**
- **Experimental Fluids: Air, Water and Kerosene**
- **Annulus Configuration: Concentric and Fully Eccentric Annulus**



Flow Pattern Map



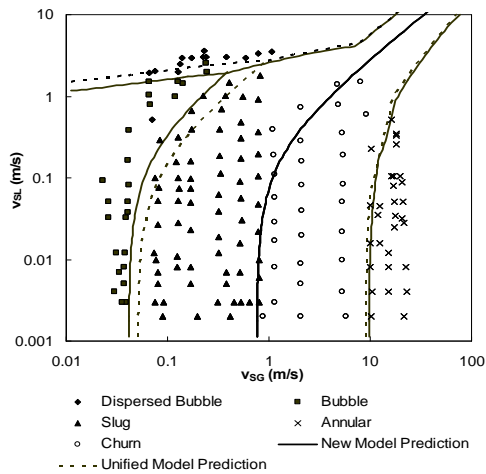
Air and Water Flow in Concentric Annulus



Fluid Flow Projects

Advisory Board Meeting, September 30, 2009

Flow Pattern Map ...



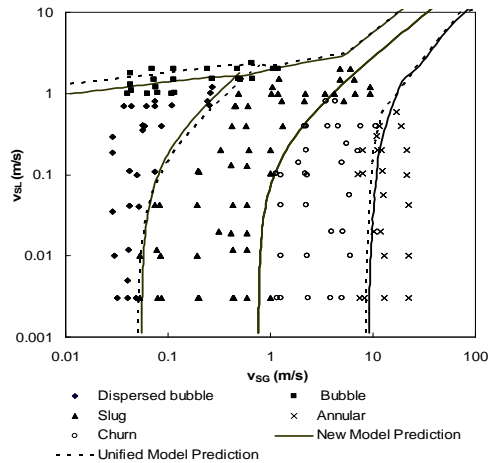
Air and Water Flow in Fully Eccentric Annulus



Fluid Flow Projects

Advisory Board Meeting, September 30, 2009

Flow Pattern Map ...



Air and Kerosene Flow in Concentric Annulus



Fluid Flow Projects

Advisory Board Meeting, September 30, 2009

Flow Pattern Transition Model Performance

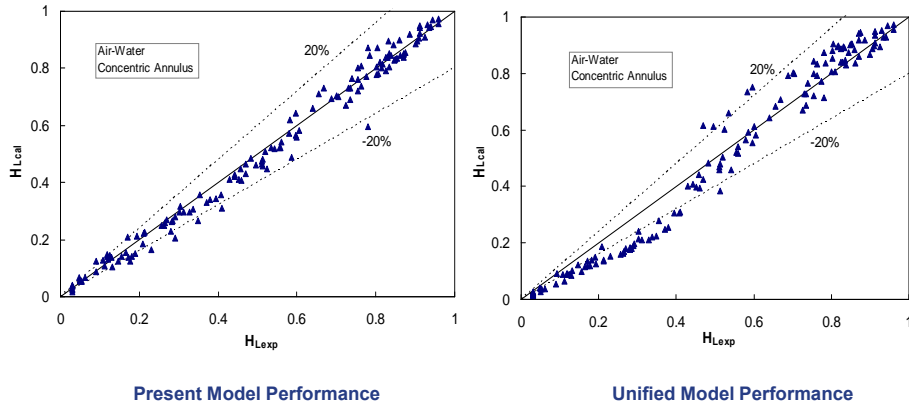
- ◆ Bubbly/Slug Flow Pattern Transition Work Well for All Flow Conditions
- ◆ Dispersed Bubble Flow Pattern Transition Performs Well Except for Air and Kerosene
- ◆ Slug/Churn Flow Pattern Transition Model Performs Not Well at Higher Liquid Flow Rate
- ◆ Annular Flow Pattern Transition Model Predicts Higher Transition Velocity



Fluid Flow Projects

Advisory Board Meeting, September 30, 2009

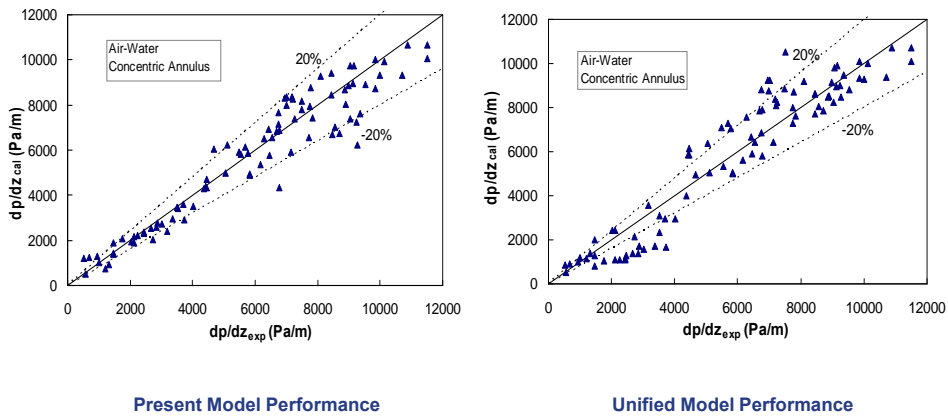
Liquid Holdup Prediction



 Fluid Flow Projects

Advisory Board Meeting, September 30, 2009

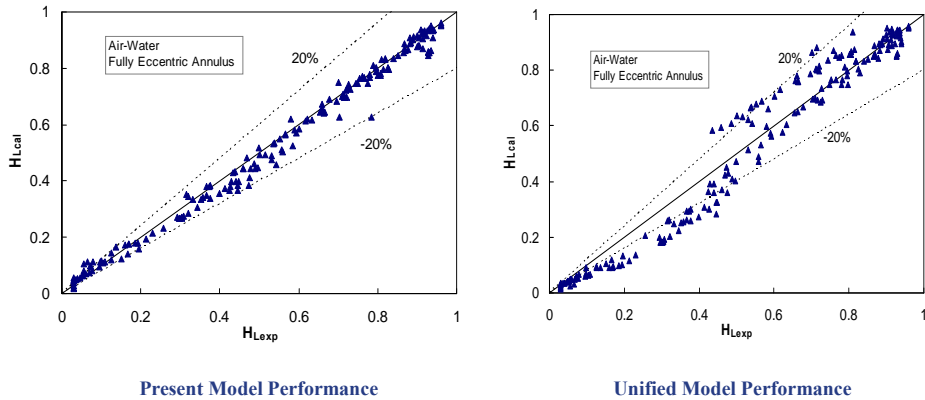
Pressure Gradient Prediction



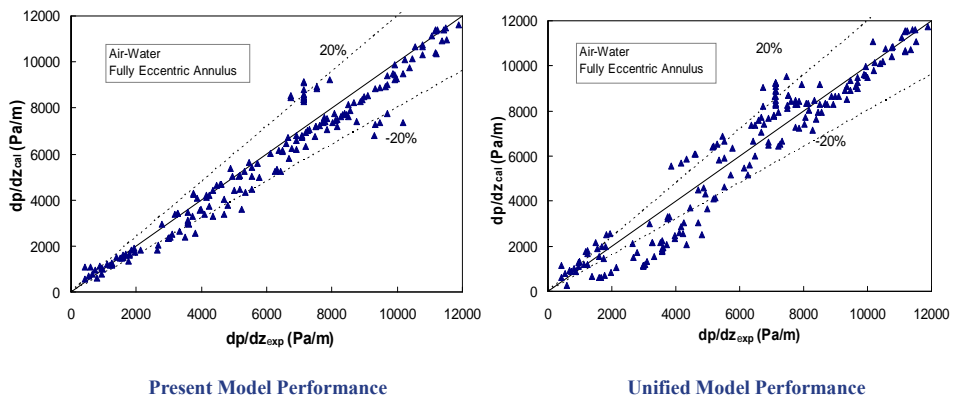
 Fluid Flow Projects

Advisory Board Meeting, September 30, 2009

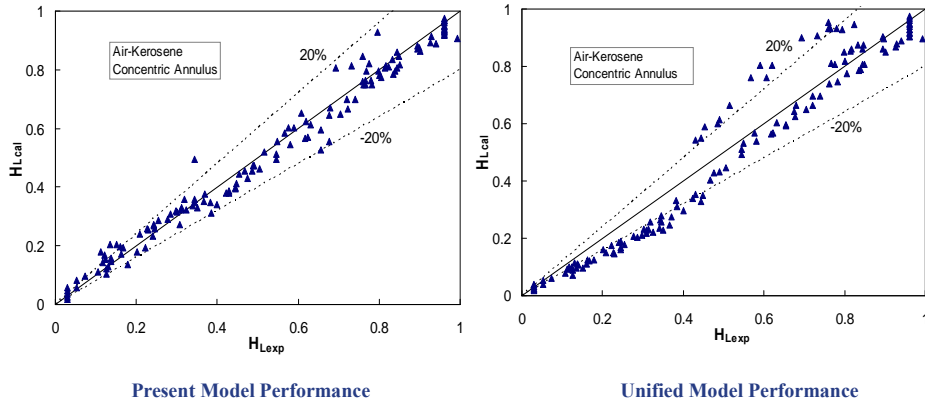
Liquid Holdup Prediction



Pressure Gradient Prediction



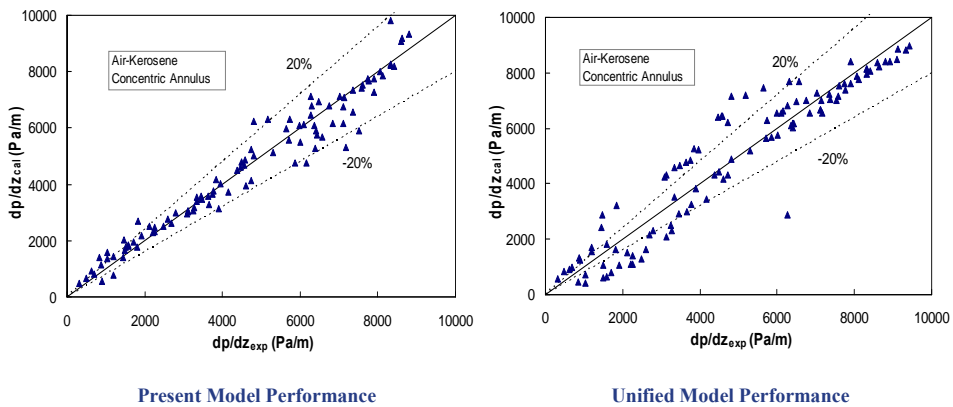
Liquid Holdup Prediction



 Fluid Flow Projects

Advisory Board Meeting, September 30, 2009

Pressure Gradient Prediction



 Fluid Flow Projects

Advisory Board Meeting, September 30, 2009

Evaluation Criteria

◆ Relative Error

$$e_i = \left[\left(\frac{V_{cal} - V_{exp}}{V_{exp}} \right) \times 100 \right]$$

◆ Actual Error

$$e_j = (V_{cal} - V_{exp})$$



Evaluation Criteria ...

◆ Average Relative Error

$$\varepsilon_1 = \frac{1}{N} \sum_{i=1}^N (e_i)$$

◆ Absolute Average Relative Error

$$\varepsilon_2 = \left[\frac{1}{N} \sum_{j=1}^N |e_{rj}| \right] \times 100$$

◆ Standard Deviation about the Average Relative Error

$$\varepsilon_3 = \sqrt{\frac{\sum_i (e_i - \varepsilon_1)^2}{N-1}}$$



Evaluation Criteria ...

◆ Average Actual Error

$$\varepsilon_4 = \frac{1}{N} \sum_{j=1}^N (e_j)$$

◆ Absolute Average Actual Error

$$\varepsilon_5 = \frac{1}{N} \sum_{j=1}^N |e_j|$$

◆ Standard Deviation about the Average Actual Error

$$\varepsilon_6 = \sqrt{\frac{\sum_{j=1}^N (e_j - \varepsilon_4)^2}{N-1}}$$



Model Evaluation with Liquid Holdup

Comparisons	Statistical Parameters					
	ε_1	ε_2	ε_3	$\varepsilon_4 (-)$	$\varepsilon_5 (-)$	$\varepsilon_6 (-)$
H_{Lnew_wc}	-1.6	8.2	11.9	-0.009	0.026	0.035
$H_{Lunified_wc}$	-10.2	15.8	18.1	-0.012	0.050	0.062
H_{Lnew_kc}	1.6	9.6	15.3	-0.006	0.030	0.042
$H_{Lunified_kc}$	-8.7	16.7	18.5	-0.013	0.064	0.079
H_{Lnew_we}	0.9	8.4	16.3	-0.007	0.026	0.055
$H_{Lunified_we}$	-8.0	14.8	18.3	-0.011	0.053	0.069



Model Evaluation with Pressure Gradient

Comparisons	Statistical Parameters					
	ε_1	ε_2	ε_3	ε_4 (Pa/m)	ε_5 (Pa/m)	ε_6 (Pa/m)
dp/dz_{new_wc}	-2.5	11.2	15.5	-164.3	648.3	961.4
$dp/dz_{unified_wc}$	-2.6	19.1	25.5	67.5	895.7	1189.8
dp/dz_{new_kc}	4.3	11.8	17.1	46.3	416.9	599.8
$dp/dz_{unified_kc}$	2.5	22.6	31.3	33.6	671.3	874.36
dp/dz_{new_we}	-3.3	11.4	15.8	-249.9	585.0	797.3
$dp/dz_{unified_we}$	-3.4	20.0	26.4	-70.1	824.5	1012.1



Slug Flow Model Evaluation with Liquid Holdup

Comparisons	Statistical Parameters					
	ε_1	ε_2	ε_3	ε_4 (-)	ε_5 (-)	ε_6 (-)
H_{Lnew_wc}	-5.2	6.7	7.1	-0.03	0.038	0.041
$H_{Lunified_wc}$	0.7	10.5	13.4	0.003	0.056	0.071
H_{Lnew_kc}	-6.6	8.4	7.6	-0.032	0.045	0.042
$H_{Lunified_kc}$	0.03	15.0	18.3	0.005	0.079	0.096
H_{Lnew_we}	-4.9	5.8	6.4	-0.035	0.039	0.042
$H_{Lunified_we}$	2.1	13.0	15.4	0.020	0.073	0.081



Slug Flow Model Evaluation with Pressure Gradient

Comparisons	Statistical Parameters					
	ε_1	ε_2	ε_3	ε_4 (Pa/m)	ε_5 (Pa/m)	ε_6 (Pa/m)
dp/dz_{new_wc}	-5.2	10.2	11.3	-416.6	704.3	820.0
$dp/dz_{unified_wc}$	3.8	14.1	17.3	171.8	803.3	935.5
dp/dz_{new_kc}	1.1	11.8	13.1	-69.3	591.6	689.2
$dp/dz_{unified_kc}$	7.5	18.0	22.5	297.4	751.1	909.1
dp/dz_{new_we}	-4.7	6.8	7.0	-332.9	431.7	432.3
$dp/dz_{unified_we}$	0.3	15.4	19.4	32.7	856.9	980.7



Fluid Flow Projects

Advisory Board Meeting, September 30, 2009

Churn Flow Model Evaluation with Liquid Holdup

Comparisons	Statistical Parameters					
	ε_1	ε_2	ε_3	ε_4 (-)	ε_5 (-)	ε_6 (-)
H_{Lnew_wc}	-7.2	11.8	13.2	-0.02	0.03	0.03
$H_{Lunified_wc}$	-31.0	30.1	7.1	-0.08	0.08	0.03
H_{Lnew_kc}	-4.7	9.0	9.3	-0.02	0.02	0.02
$H_{Lunified_kc}$	-31.9	31.9	9.4	-0.08	0.08	0.04
H_{Lnew_we}	7.1	11.4	13.8	0.01	0.02	0.02
$H_{Lunified_we}$	-26.1	26.1	5.4	-0.06	0.06	0.03



Fluid Flow Projects

Advisory Board Meeting, September 30, 2009

Churn Flow Model Evaluation with Pressure Gradient

Comparisons	Statistical Parameters					
	ε_1	ε_2	ε_3	ε_4 (Pa/m)	ε_5 (Pa/m)	ε_6 (Pa/m)
dp/dl_{new_wc}	-3.5	9.1	12.4	-153.5	249.1	299.7
$dp/dl_{unified_wc}$	-40.6	40.6	14.4	-1084.5	1084.5	464.2
dp/dl_{new_kc}	-10.7	15.6	14.7	-427.3	492.6	467.8
$dp/dl_{unified_kc}$	-35.5	38.0	23.7	-1012.5	1146.2	840.7
dp/dl_{new_we}	7.5	11.8	12.4	62.5	270.0	359.5
$dp/dl_{unified_we}$	-34.0	36.1	21.8	-619.7	757.5	575.1



Annular Flow Model Evaluation with Liquid Holdup

Comparison	Statistical Parameters					
	ε_1	ε_2	ε_3	ε_4 (-)	ε_5 (-)	ε_6 (-)
H_{Lnew_wc}	11.0	14.8	13.8	0.009	0.011	0.010
$H_{Lunified_wc}$	-29.0	29.4	9.5	-0.023	0.025	0.016
H_{Lnew_kc}	20.0	26.2	25.1	0.02	0.027	0.030
$H_{Lunified_kc}$	-2.0	43.4	59.0	-0.02	0.032	0.031
H_{Lnew_we}	9.2	21.3	23.2	0.006	0.012	0.013
$H_{Lunified_we}$	-20.0	30.0	32.5	-0.016	0.020	0.021



Annular Flow Model Evaluation with Pressure Gradient

Comparison	Statistical Parameters					
	ε_1	ε_2	ε_3	ε_4 (Pa/m)	ε_5 (Pa/m)	ε_6 (Pa/m)
dp/dz_{new_wc}	-0.15	19.5	23.6	193.0	507.2	679.5
$dp/dz_{unified_wc}$	11.4	13.3	12.5	226.9	250.0	201.9
dp/dz_{new_kc}	11.3	25.5	27.9	103.1	324.9	378.6
$dp/dz_{unified_kc}$	39.0	44.1	33.9	395.8	573.7	589.3
dp/dz_{new_we}	3.8	14.1	19.6	60.9	180.6	240.2
$dp/dz_{unified_we}$	18.4	25.9	23.7	156.5	344.1	363.7



Bubble Flow Model Performance

Comparison	Statistical Parameters					
	ε_1	ε_2	ε_3	ε_4 (-)	ε_5 (-)	ε_6 (-)
H_L						
H_{Lnew_wc}	0.03	2.5	3.2	7.8E-08	0.021	0.027
H_{Lnew_kc}	-1.0	3.0	4.6	-0.010	0.026	0.038
H_{Lnew_we}	20.0	26.2	25.1	0.02	0.027	0.030
dp/dz	ε_1	ε_2	ε_3	ε_4 (Pa/m)	ε_5 (Pa/m)	ε_6 (Pa/m)
dp/dz_{new_wc}	6.3	9.6	8.8	477.4	773.9	730.8
dp/dz_{new_kc}	-1.4	4.4	4.8	-160.4	342.9	343.7
dp/dz_{new_we}	11.0	12.6	12.0	514.4	1061.3	1071.2



Dispersed Bubble Flow Model Performance

Comparison	Statistical Parameters					
	ε_1	ε_2	ε_3	$\varepsilon_4 (-)$	$\varepsilon_5 (-)$	$\varepsilon_6 (-)$
H_L						
$H_{L_{new_wc}}$	2.9	3.7	4.2	0.025	0.031	0.033
$H_{L_{new_kc}}$	-3.2	3.8	3.3	-0.027	0.032	0.027
$H_{L_{new_we}}$	1.1	1.5	1.2	0.010	0.012	0.010
dp/dz	ε_1	ε_2	ε_3	ε_4 (Pa/m)	ε_5 (Pa/m)	ε_6 (Pa/m)
dp/dz_{new_wc}	-1.8	5.4	7.1	-247.8	574.6	750.8
dp/dz_{new_kc}	-4.7	4.7	1.2	-421.2	421.2	113.8
dp/dz_{new_we}	7.3E-05	2.4	2.9	6.9	263.1	321.4



Concluding Remarks

- ◆ **New Model Performs Well and Better than Zhang *et al.* (2003) Unified Model**
- ◆ **Big Error Points Exist Due to Inaccuracy of Flow Pattern Prediction**
- ◆ **Annular Flow Model Still Needs to be Evaluated and Improved**



Recommendations

- 
- ◆ **Experimental Investigation on: Interfacial Friction Factor, Liquid Entrainment Fraction and Liquid Film Distribution**
 - ◆ **Effect of Hydraulic Diameter of Liquid Films and Gas Core**
 - ◆ **Effect of Viscosity on Flow Pattern Transition Models**
 - ◆ **Extend Study to Different Annulus Eccentricity and Inclination Angles**





Fluid Flow Projects

Executive Summary of Research Activities

Cem Sarica

Advisory Board Meeting, September 30, 2009

Three-phase Flow Studies

- ◆ **Significance**
 - Good Understanding of Gas-Oil Flow
 - Poor Understanding of Gas-Oil-Water Flow
- ◆ **Objective**
 - Development of Improved Prediction Models
- ◆ **Past Studies**
 - Oil-Water
 - ▲ Trallero (1994), Horizontal
 - ▲ Flores (1996), Vertical and Deviated
 - ▲ Alkaya (1999), Inclined

Three-phase Flow Studies ...

◆ Past Studies ...

➤ Three-phase

- ▲ Keskin (2007), Experimental Horizontal Three-phase Study
- ▲ Zhang and Sarica (2005), Three-phase Mechanistic Model Development
- ▲ Need to More Research on Oil-Water Flow

➤ Recent Oil-Water Studies with Emphasis on Droplets

- ▲ Vielma (2006), Horizontal Flow
- ▲ Atmaca (2007), Inclined Flow

Three-phase Flow Studies ...

◆ Current Study (Oil-Water Flow Modeling in Pipelines)

➤ Progress

- ▲ New Modeling Approach Based on Energy Minimization
- ▲ Performs Better than Other Models When Compared with Data



Fluid Flow Projects

Modeling of Hydrodynamics and Dispersions in Oil-Water Pipe Flow

Anoop Kumar Sharma

Advisory Board Meeting, September 30, 2009

Outline

- ◆ Introduction & Objectives
- ◆ Modeling
- ◆ Model Validation
- ◆ Conclusions and Recommendations

Introduction

- ◆ **Oil-water Flow is Encountered in Various Processes in Petroleum Industry**
- ◆ **Existing Predictive Models**
 - **Do not Properly Represent Physics**
 - **Can not Capture Gradual Transition between Flow Patterns**

Objectives

- ◆ **Development of a Better Model for Oil-water Flow**
- ◆ **Validation of Model Using Available Experimental Data**

Modeling

◆ Working Principle

- A System Stabilizes to Its Minimum Total Energy

Modeling ...

◆ Segregated Layers

- Combined Momentum Balance Equation $\rightarrow 0$
- Total Energy \rightarrow Minimum

◆ Full Dispersion

- Total Energy \rightarrow Minimum

Modeling ...

◆ Transition to Dispersion

➤ Can D_{MAX} be Accommodated in Continuous Phase?

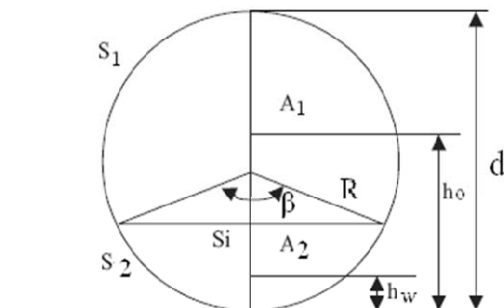
◆ Angeli and Hewitt (2000)

$$d_{SM} v_C^{1.8} = 2 \times 10^{-8} \times (4 f_C)^{-3.12}$$

$$d_{MAX} v_C^{1.8} = 4.2 \times 10^{-8} \times (4 f_C)^{-3.13}$$

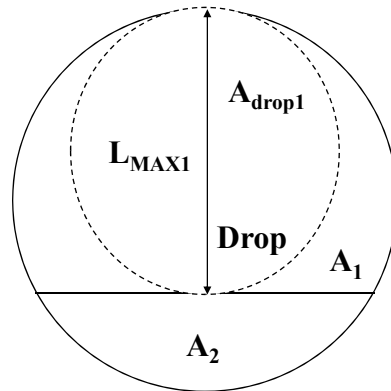
Modeling ...

◆ Pipe Geometry



Modeling ...

◆ Transition to Dispersion



$$\left(\frac{A_{drop1}}{A_1} \right) \leq H_{INV1}$$

$$d_{MAX1} \leq L_{MAX1}$$

Modeling ...

◆ Mixture Property Calculation

➤ Density

$$\rho_1 = \rho_o(1 - H_{D1}) + \rho_w H_{D1}$$

$$\rho_2 = \rho_w(1 - H_{D2}) + \rho_o H_{D2}$$

➤ Viscosity (Brinkman Correlation)

$$\mu_1 = \mu_o(1 - H_{D1})^{-2.5}$$

$$\mu_2 = \mu_w(1 - H_{D2})^{-2.5}$$

Modeling ...

◆ Inversion Point (Zhang and Sarica, 2006)

$$H_{O,INV} = \frac{\left(\frac{\mu_O}{\mu_W}\right)^{0.4}}{1 + \left(\frac{\mu_O}{\mu_W}\right)^{0.4}}$$

Modeling ...

◆ Continuity Equation

$$q_{O,T} = A_1(1 - H_{D1})v_1 + A_2H_{D2}v_2$$

$$q_{W,T} = A_2(1 - H_{D2})v_2 + A_1H_{D1}v_1$$

Modeling ...

◆ Combined Momentum Equation

$$F = -\frac{\tau_{W2}S_2}{A_2} + \frac{\tau_{W1}S_1}{A_1} + \tau_I S_I \left(\frac{1}{A_1} + \frac{1}{A_2} \right) +$$

$$(\rho_1 - \rho_2)g \sin(\theta) = 0$$

Modeling ...

◆ Interfacial Shear Stress

$$\tau_I = \left[\rho_{MIX} C_f (\tau_1 H_1 + \tau_2 H_2) \right]^{1/2} (v_1 - v_2)$$

$$\rho_{MIX} = (\rho_1 H_1 + \rho_2 H_2)$$

$$C_f = \left(\frac{f_1 H_1 + f_2 H_2}{2} \right)$$

$$H_1 = \left(\frac{A_1}{A_1 + A_2} \right) \quad H_2 = \left(\frac{A_2}{A_1 + A_2} \right)$$

Modeling ...

◆ Total Potential Energy

$$PE = A_1 \rho_1 g h_1 + A_2 \rho_2 g h_2$$

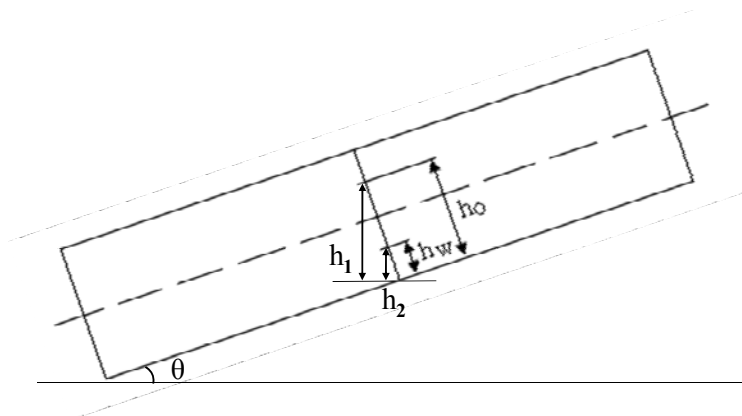
$$h_1 = h_o \cos(\theta)$$

$$h_2 = h_w \cos(\theta)$$

$$h_o = \frac{d}{2} \left[1 + \frac{4}{3} \frac{\sin^3\left(\frac{\beta}{2}\right)}{(2\pi - \beta - \sin(\beta))} \right] \quad h_w = \frac{d}{2} \left[1 - \frac{4}{3} \frac{\sin^3\left(\frac{\beta}{2}\right)}{(\beta - \sin(\beta))} \right]$$

Modeling ...

◆ Side View of Pipe



Modeling ...

◆ Total Kinetic Energy

$$KE = \frac{1}{2} A_1 \rho_1 v_1^2 + \frac{1}{2} A_2 \rho_2 v_2^2$$

◆ Total Surface Energy

$$SE = \sigma \left[d \sin\left(\frac{\beta}{2}\right) + \frac{6 A_1 H_{D1}}{d_{SM1}} + \frac{6 A_2 H_{D2}}{d_{SM2}} \right]$$

Modeling ...

◆ Total Energy

$$TE = SE + KE + PE$$

Modeling ...

◆ Pressure Gradient Calculation

➤ Segregated Flow Patterns

▲ Two Fluid Model (Trallero Oil-Water, 1995)

➤ Fully Dispersed Flow Patterns

▲ Homogeneous Model

Modeling ...

◆ Homogeneous Model

$$\left(\frac{dP}{dL}\right) = \left(\frac{dP}{dL}\right)_{Friction} + \left(\frac{dP}{dL}\right)_{Gravitational}$$

$$\left(\frac{dP}{dL}\right)_{Friction} = \frac{2f_M \rho_M v_M^2}{d}$$

$$\left(\frac{dP}{dL}\right)_{Gravitational} = \rho_M g \sin(\theta)$$

Model Validation

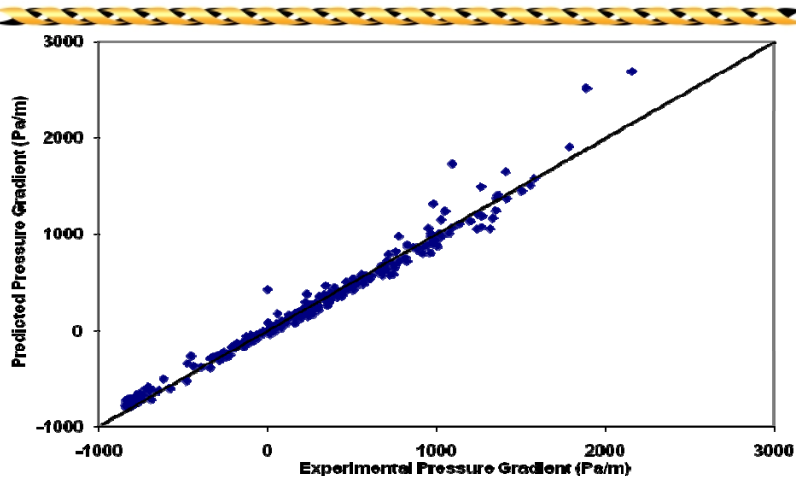
- ◆ Trallero (1995)
- ◆ Alkaya (2000)
- ◆ Abduvayt (2006)
- ◆ Atmaca (2007)

Model Validation...

◆ Statistical Parameters

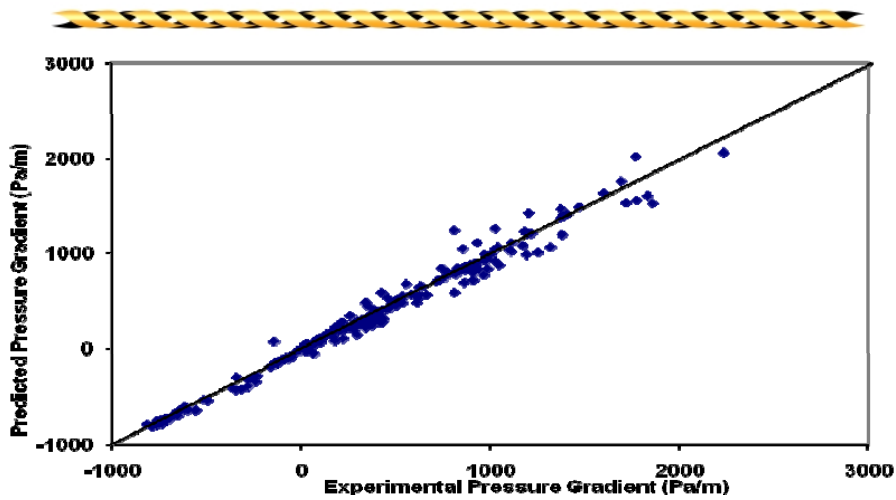
Definitions
$e_{ri} = \left(\frac{\text{Predicted value} - \text{Measured Value}}{\text{Measure Value}} \right) \times 100$
$e_i = \text{Predicted value} - \text{Measured Value}$
$\varepsilon_1 = \left[\frac{1}{N} \right] \sum_{i=1}^N e_{ri}$
$\varepsilon_2 = \left[\frac{1}{N} \right] \sum_{i=1}^N e_{ri} $
$\varepsilon_3 = \sqrt{\frac{\sum_{i=1}^N (e_{ri} - \varepsilon_1)^2}{N - 1}}$
$\varepsilon_4 = \left[\frac{1}{N} \right] \sum_{i=1}^N e_i$
$\varepsilon_5 = \left[\frac{1}{N} \right] \sum_{i=1}^N e_i $
$\varepsilon_6 = \sqrt{\frac{\sum_{i=1}^N (e_i - \varepsilon_4)^2}{N - 1}}$

Model Validation ...



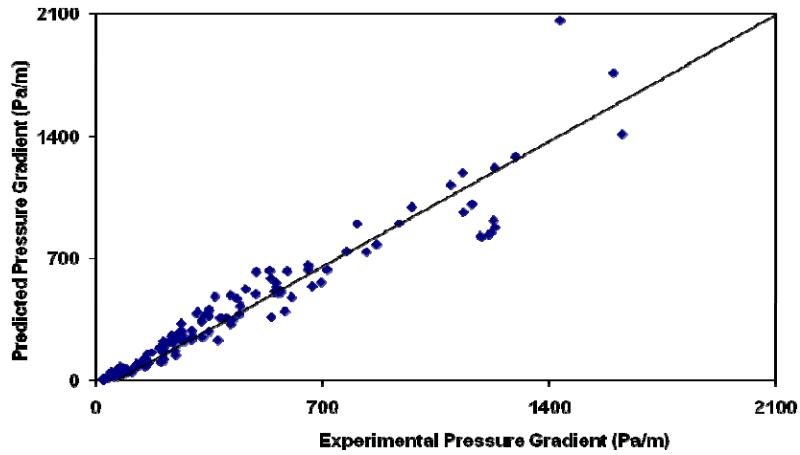
Model Predictions of Pressure Gradient Compared with Experimental Data of Atmaca (2007)

Model Validation ...



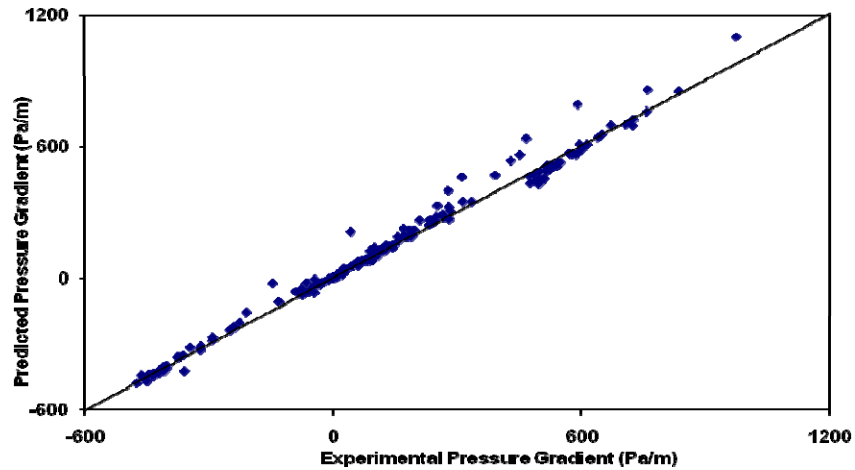
Model Predictions of Pressure Gradient Compared with Experimental Data of Alkaya (2000)

Model Validation ...



Model Predictions of Pressure Gradient Compared with Experimental Data of Trallero (2000)

Model Validation ...



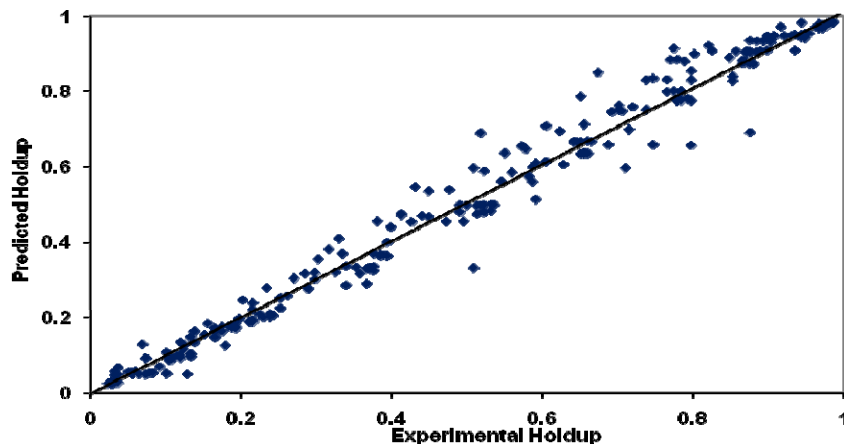
Model Predictions of Pressure Gradient Compared with Experimental Data of Abduvayt (2006)

Model Validation ...

Statistical Parameters for Pressure Gradient Predictions by Current Model Compared with Experimental Measurements

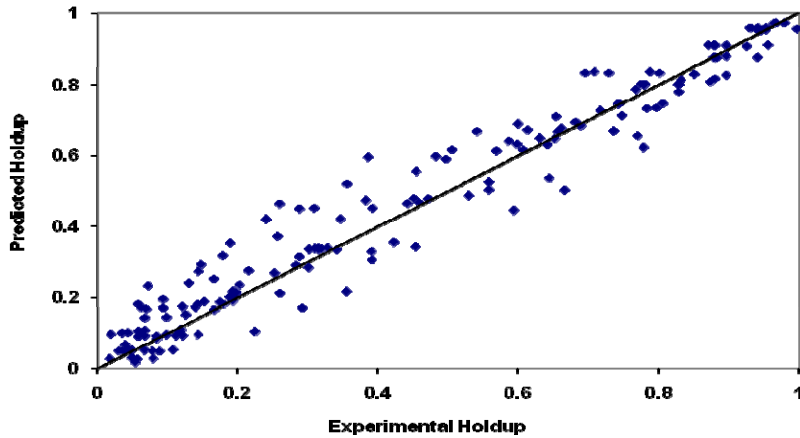
	ε_1 (%)	ε_2 (%)	ε_3 (%)	ε_4 (Pa/m)	ε_5 (Pa/m)	ε_6 (Pa/m)
Atmaca (2007)	-6.79	14.65	30.16	-0.48	49.48	87.07
Alkaya (2000)	-1.85	16.33	33.39	-21.61	47.08	76.17
Trallero (1995)	-25.27	29.12	26.23	-33.83	55.54	91.37
Abduvayt (2006)	16.01	36.77	105.44	7.75	21.58	36.33

Model Validation ...



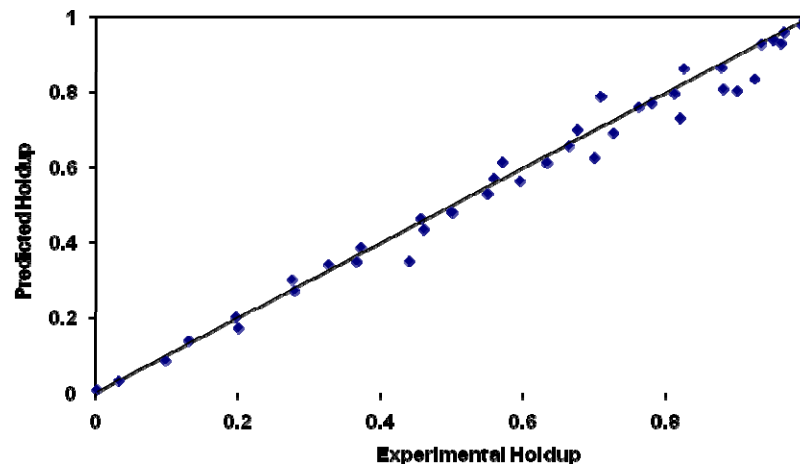
Model Predictions of Holdup Compared with Experimental Data of Atmaca (2007)

Model Validation ...



Model Predictions of Holdup Compared with Experimental Data of Alkaya (2000)

Model Validation ...



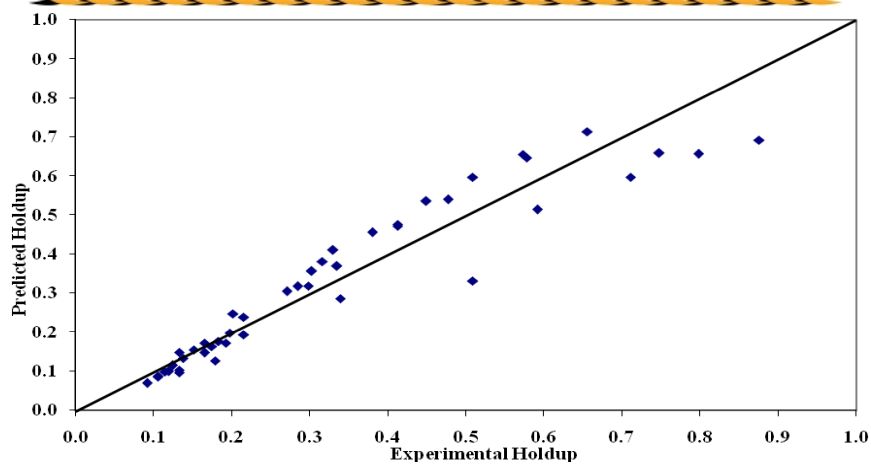
Model Predictions of Holdup Compared with Experimental Data of Trallero (1995)

Model Validation ...

Statistical Parameters for Holdup Predictions by Current Model Compared with Experimental Studies

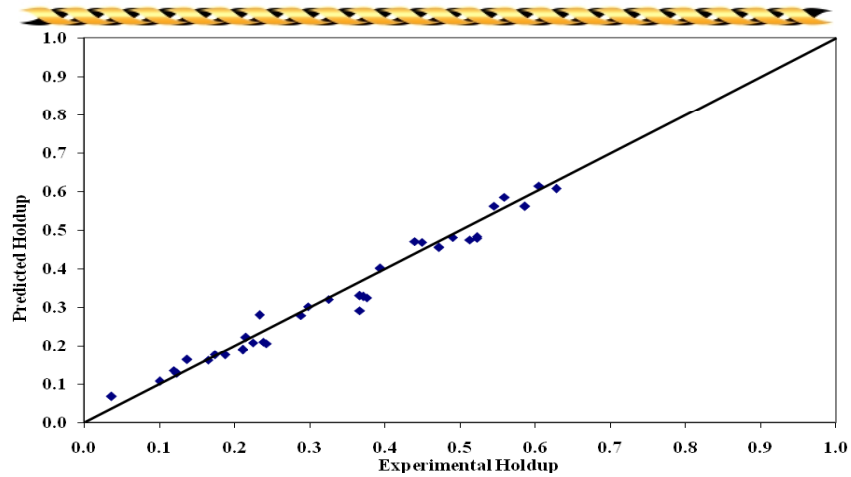
	ε_1 (%)	ε_2 (%)	ε_3 (%)	ε_4	ε_5	ε_6
Atmaca (2007)	0.47	9.73	15.58	0.01	0.03	0.05
Alkaya (2000)	16.45	27.79	51.81	0.02	0.05	0.07
Trallero (1995)	13.06	15.74	58.43	0.03	0.04	0.05

Model Validation ...



Model Predictions of Holdup for Stratified Flow Pattern Compared with Experimental Data of Atmaca (2007)

Model Validation ...



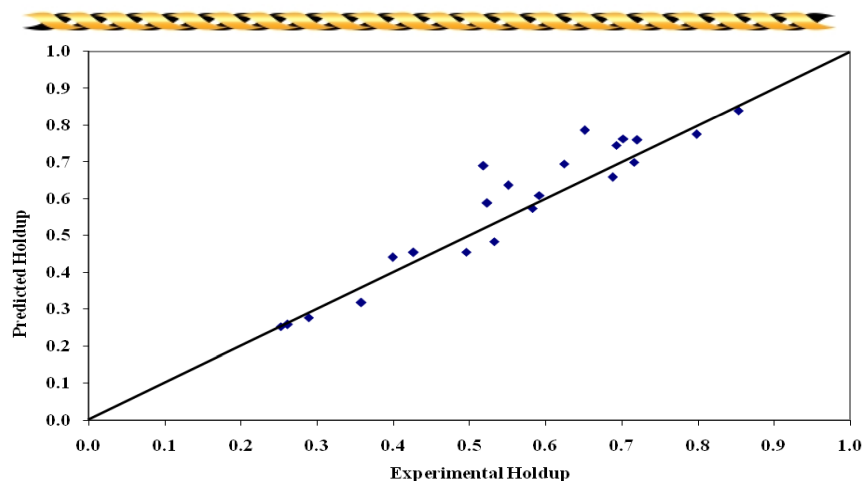
Model Predictions of Holdup for Dual Dispersion Flow Pattern Compared with Experimental Data of Atmaca (2007)



Fluid Flow Projects

September 30, 2009

Model Validation ...



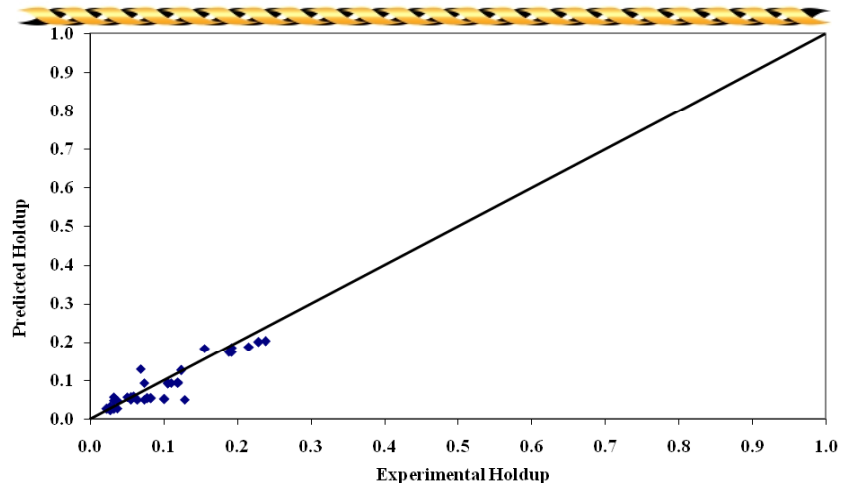
Model Predictions of Holdup for Oil in Water Dispersion and Oil Layer Flow Pattern Compared with Experimental Data of Atmaca (2007)



Fluid Flow Projects

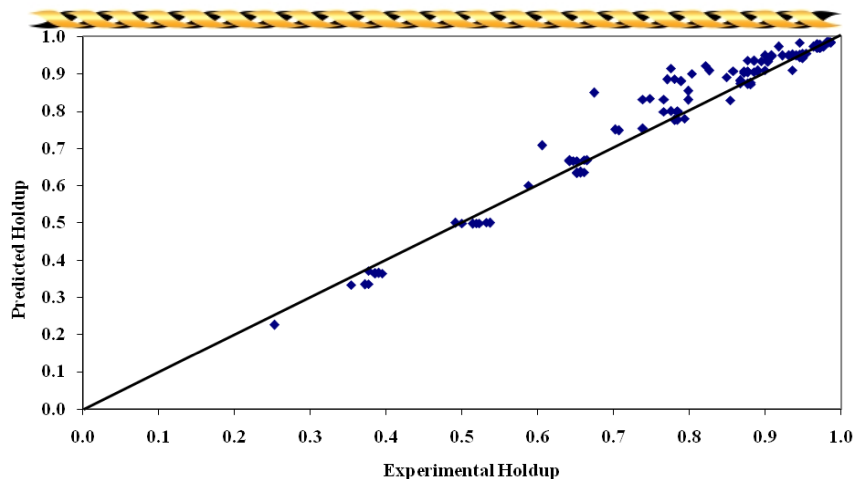
September 30, 2009

Model Validation ...



Model Predictions of Holdup for Water in Oil Dispersion Flow Pattern Compared with Experimental Data of Atmaca (2007)

Model Validation ...

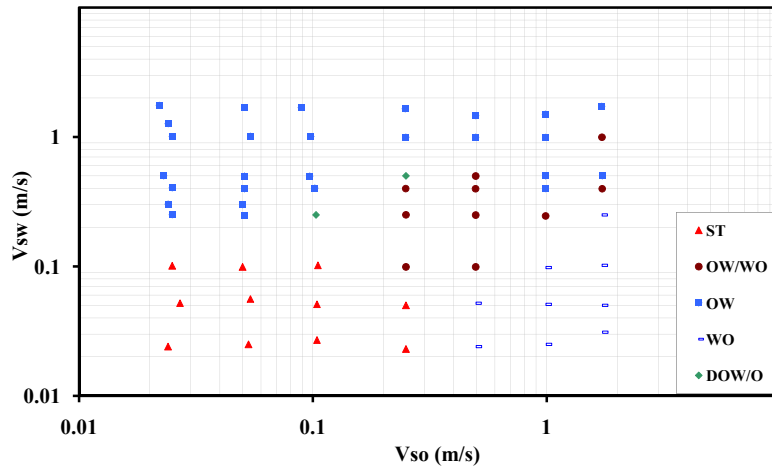


Model Predictions of Holdup for Oil in Water Dispersion Flow Pattern Compared with Experimental Data of Atmaca (2007)

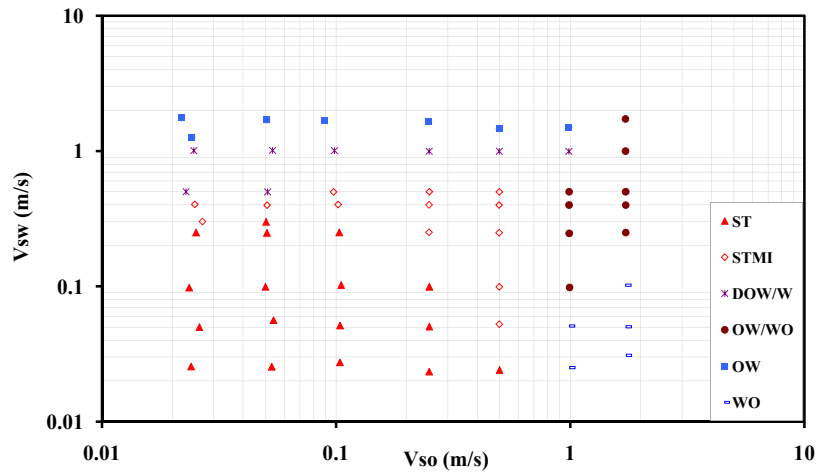
Model Validation

- ◆ Different Inclination Angle
 - No Significant Differences for Pressure Gradient and Holdup Comparisons
 - Given in the Appendix of Thesis

Model Validation ...

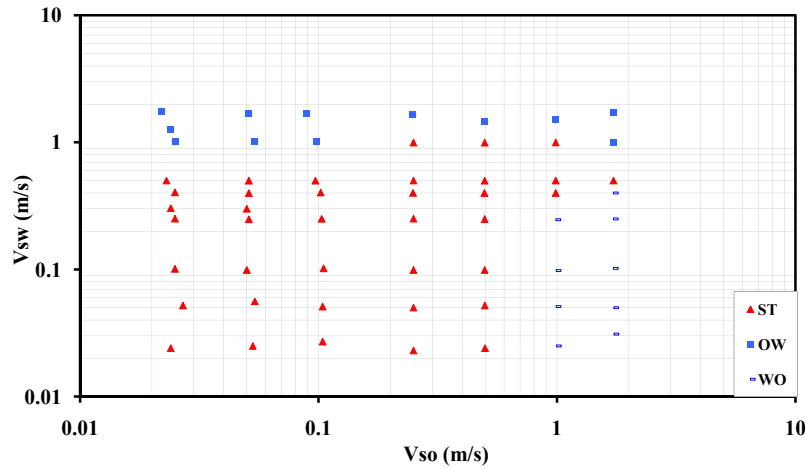


Model Validation ...



Flow Pattern Map Observed by Atmaca (2007) for Horizontal Flow

Model Validation ...



Flow Pattern Map Predicted by Unified Model for Horizontal Flow

Model Validation ...

Pressure Gradient Predictions by Unified Model and Current Model Compared with Atmaca (2007) Data

	ε_1 (%)	ε_2 (%)	ε_3 (%)	ε_4 (Pa/m)	ε_5 (Pa/m)	ε_6 (Pa/m)
Unified Model	2.5	20.6	40.7	41.5	63.6	99.4
Current Model	-7.0	14.8	30.4	-0.4	49.4	86.9

Water Holdup Predictions by Unified Model and Current Model Compared with Atmaca (2007) Data

	ε_1 (%)	ε_2 (%)	ε_3 (%)	ε_4 (-)	ε_5 (-)	ε_6 (-)
Unified Model	-2.94	8.93	13.21	-0.02	0.03	0.04
Current Model	0.47	9.73	15.58	0.01	0.03	0.05

Model Validation ...

Pressure Gradient Predictions by Unified Model and Current Model Compared with Alkaya (2000) Data

	ε_1 (%)	ε_2 (%)	ε_3 (%)	ε_4 (Pa/m)	ε_5 (Pa/m)	ε_6 (Pa/m)
Unified Model	3.26	21.10	45.10	21.81	57.53	126.02
Current Model	-1.85	16.33	33.39	-21.61	47.08	76.17

Water Holdup Predictions by Unified Model and Current Model Compared with Alkaya (2000) Data

	ε_1 (%)	ε_2 (%)	ε_3 (%)	ε_4 (-)	ε_5 (-)	ε_6 (-)
Unified Model	17.02	28.56	55.47	0.00	0.05	0.08
Current Model	16.45	27.79	51.81	0.02	0.05	0.07

Model Validation ...

Pressure Gradient Predictions by Unified Model and Current Model Compared with Abduvayt (2006) Data

	ε_1 (%)	ε_2 (%)	ε_3 (%)	ε_4 (Pa/m)	ε_5 (Pa/m)	ε_6 (Pa/m)
Unified Model	17.27	35.93	102.16	15.71	28.45	115.22
Current Model	16.01	36.77	105.44	7.75	21.58	36.33

Model Validation ...

Pressure Gradient Predictions by Unified Model and Current Model Compared with Trallero (1995) Data

	ε_1 (%)	ε_2 (%)	ε_3 (%)	ε_4 (Pa/m)	ε_5 (Pa/m)	ε_6 (Pa/m)
Unified Model	-7.08	18.17	24.07	2.79	48.16	93.23
Current Model	-25.27	29.12	26.23	-33.83	55.54	91.37

Water Holdup Predictions by Unified Model and Current Model Compared with Trallero (1995) Data

	ε_1 (%)	ε_2 (%)	ε_3 (%)	ε_4 (-)	ε_5 (-)	ε_6 (-)
Unified Model	7.22	14.31	59.30	-0.01	0.03	0.04
Current Model	13.06	15.74	58.43	0.03	0.04	0.05

Conclusions

- ◆ **Modeling Approach is Simple and Basic**
- ◆ **Uses Single Criterion for Prediction**
 - **Different from Various Previous Models**
- ◆ **Captures Gradual Changes in Flow Configuration**
- ◆ **Useful for Modeling Near Horizontal Flow**
- ◆ **Model Gives Extensive Information**

Conclusions ...

- ◆ **Model Validation are Very Encouraging**
 - **Excellent Prediction of Pressure Gradient**
 - **Holdup Predictions Comparable to Unified Model**
 - **Flow Pattern Map Predictions Closer to Observed**
 - **Predicted Flow Pattern Maps Follows General Trends Very Well**

Recommendations

- ◆ **Better Closure Relationships**
 - **Droplet Size Correlations**
 - **Viscosity Correlation**
- ◆ **Criteria of Onset of Entrainment**
 - **Conservative**
 - **Promotes Prediction of Dispersion**

Recommendations ...

- ◆ **By Better Estimation of Energy in Intermittent Flow**
 - **Model Can be Extended to Gas-Liquid Flow**
 - **Model Can be Extended to Higher Inclinations**

Modeling of Hydrodynamics and Dispersions in Oil-Water Pipe Flow

Anoop Kumar Sharma

PROJECT COMPLETETION DATES:

Literature Review.....	Completed
Model Development.....	Completed
Model Validation.....	Completed
Final Report and Thesis.....	Completed

Objectives

The objectives of this study are:

- Development of a better model for oil-water flow which captures the physics behind the process, especially for transitions between flow patterns, and
- Validation of the model using available experimental data.

Introduction

The flow of two immiscible liquids is encountered in a diverse range of processes and equipment, particularly in the petroleum industry, where mixtures of oil and water are often transported in pipes over long distances. Accurate prediction of oil-water flow characteristics, such as flow pattern, water holdup and pressure gradient, is important in many engineering applications. However, despite their importance, liquid-liquid flow has not been explored to the same extent as gas-liquid flow. The density difference between the phases in a liquid-liquid system is relatively small. However, the viscosity ratio encountered can extend over several orders of magnitude. Moreover, oils and oil-water emulsions can show either a Newtonian or non-Newtonian rheological behavior. Therefore, concepts of gas-

liquid two-phase flow cannot be readily applied to liquid-liquid systems.

Existing models are based on first predicting flow patterns and then calculation of design parameters such as pressure gradient and holdup. This approach results in artificially abrupt changes and forces the flow to conform to a particular flow pattern. This study focuses on facilitating gradual changes in flow configuration, therefore resulting in better predictions of the design parameters.

Model Development

A comprehensive model is developed to predict the oil-water flow in horizontal and slightly inclined pipes. The new model is based on the principle that a system stabilizes to its minimized total energy, including the fluid flowing in the pipe. Chakrabarti *et al.* (2005) used a similar approach for pressure prediction for a horizontal, segregated flow pattern. In this model, for each inlet condition, the total energy is minimized. Moreover, for the segregated flow pattern, the continuity equation and combined momentum balance equation are also solved. For full dispersion conditions, only total energy is minimized and the continuity equation is solved.

The following assumptions are made for the model:

- Smooth interface and smooth pipe,

- Negligible surface energy in between the pipe wall and fluids,
- Homogeneous dispersion, and
- Steady-state flow.

For all flow patterns under consideration, including dispersion, the mixture properties for each phase can be calculated with the following:

$$\rho_1 = \rho_o(1-H_{D1}) + \rho_w H_{D1}, \quad (1)$$

$$\rho_2 = \rho_w(1-H_{D2}) + \rho_o H_{D2}, \quad (2)$$

$$\mu_1 = \mu_w(1-H_{D1})^{-2.5}, \quad (3)$$

$$\mu_2 = \mu_w(1-H_{D2})^{-2.5}. \quad (4)$$

Where, subscripts 1 and 2 represent layer 1 (oil continuous phase) and layer 2 (water continuous phase), respectively. Subscripts D, o, w represents dispersed phase, pure oil phase and pure water phase, respectively. H, μ and ρ represents the holdup, viscosity and density, respectively. Equations 3 and 4 use the Brinkman viscosity correlation to calculate the viscosity of dispersions. Although the model uses the Brinkman viscosity correlation, other mixture viscosity correlations can also be used. H_{D1} and H_{D2} will vary from 0 to the phase inversion point. The inversion point in this model is calculated by using Eq. 5, as used by Zhang *et al.* (2003).

$$H_{O,INV} = \frac{\left(\frac{\mu_O}{\mu_W}\right)^{0.4}}{1 + \left(\frac{\mu_O}{\mu_W}\right)^{0.4}}. \quad (5)$$

Where $H_{O,INV}$ is the holdup of the dispersed phase (oil) in an oil-water dispersion at which inversion takes place. The velocity of each layer can be calculated by simultaneously solving continuity equations for both oil and water.

$$q_{O,T} = A_1(1-H_{D1})v_1 + A_2H_{D2}v_2. \quad (6)$$

$$q_{W,T} = A_2(1-H_{D2})v_2 + A_1H_{D1}v_1. \quad (7)$$

Where, $q_{O,T}$, $q_{W,T}$, v_1 and v_2 are the total inlet flow rate of oil and water and velocities of the oil

continuous and the water continuous phases, respectively. A_1 and A_2 are areas corresponding to oil continuous and water continuous phases as shown in Fig. 1, respectively.

Trallero (1995) presented a two-fluid model to predict pressure drop in two-phase segregated flow. The two-fluid model solves the combined momentum equation to predict the pressure drop. Assuming smooth, equilibrium, horizontal stratified flow, the following momentum balance equations can be derived for each phase (phases 1 and 2):

$$-A_1\left(\frac{dP}{dL}\right)_1 - \tau_{W1}S_1 - \tau_I S_I - \rho_1 A_1 g \sin(\theta) = 0. \quad (8)$$

$$-A_2\left(\frac{dP}{dL}\right)_2 - \tau_{W2}S_2 + \tau_I S_I - \rho_2 A_2 g \sin(\theta) = 0. \quad (9)$$

$$F = -\frac{\tau_{W2}S_2}{A_2} + \frac{\tau_{W1}S_1}{A_1} + \tau_I S_I \left(\frac{1}{A_1} + \frac{1}{A_2}\right) + (\rho_1 - \rho_2)g \sin(\theta) = 0. \quad (10)$$

Where, A , S and $\left(\frac{dP}{dL}\right)$ denote area, perimeter and pressure gradient, respectively. F represents the combined momentum. Subscripts 1, 2 and I represent the oil continuous phase, water continuous phase and the interface, respectively. θ is the inclination angle from horizontal. τ_{W1} , τ_{W2} , τ_I are oil, water and interfacial shear stresses, respectively. These can be expressed in terms of the corresponding fluid friction factors f_1 , f_2 and f_I .

$$\tau_{W1} = \frac{f_1 \rho_1 v_1^2}{2}. \quad (11)$$

$$\tau_{W2} = \frac{f_2 \rho_2 v_2^2}{2}. \quad (12)$$

The fanning friction factor can be expressed for any phase j , assuming a smooth pipe wall.

$$f_j = C \left(\frac{d_j v_j \rho_j}{\mu_j} \right)^{-n}. \quad (13)$$

Where, coefficient C and exponent n are equal to 16 and 1 for laminar flow and to 0.046 and 0.2 for turbulent flow. Equivalent hydraulic diameters are determined on the basis of which phase is faster.

For $v_1 > v_2$,

$$d_1 = \frac{4A_1}{S_1 + S_I}. \quad (14)$$

$$d_2 = \frac{4A_2}{S_2}. \quad (15)$$

For $v_1 < v_2$,

$$d_1 = \frac{4A_1}{S_1}. \quad (16)$$

$$d_2 = \frac{4A_2}{S_2 + S_I}. \quad (17)$$

For $v_1 \approx v_2$,

$$d_1 = \frac{4A_1}{S_1}. \quad (18)$$

$$d_2 = \frac{4A_2}{S_2}. \quad (19)$$

In the model, the interfacial shear stress (τ_I) is calculated using Eq. 20, as proposed by Zhang *et al.* (2005).

$$\tau_I = [\rho_{MIX} C^* (\tau_1 H_1 + \tau_2 H_2)]^{1/2} (v_1 - v_2). \quad (20)$$

$$\rho_{MIX} = (\rho_1 H_1 + \rho_2 H_2). \quad (21)$$

$$C_f = \left(\frac{f_1 H_1 + f_2 H_2}{2} \right). \quad (22)$$

$$H_1 = \left(\frac{A_1}{A_1 + A_2} \right). \quad (23)$$

$$H_2 = \left(\frac{A_2}{A_1 + A_2} \right). \quad (24)$$

h_o and h_w shown in Fig. 1 are the centroid of the oil continuous phase and water continuous phase from the pipe base, respectively:

$$h_o = \frac{d}{2} \left[1 + \frac{4}{3} \frac{\sin^3\left(\frac{\beta}{2}\right)}{(2\pi - \beta - \sin(\beta))} \right]. \quad (25)$$

$$h_w = \frac{d}{2} \left[1 - \frac{4}{3} \frac{\sin^3\left(\frac{\beta}{2}\right)}{(\beta - \sin(\beta))} \right]. \quad (26)$$

For inclined pipe, the height of the centroids of oil and water continuous phases from the bottom, as shown in Fig. 2, will be

$$h_1 = h_o \cos(\theta). \quad (27)$$

$$h_2 = h_w \cos(\theta). \quad (28)$$

The total pressure energy per unit length of pipe can be calculated as:

Total Potential Energy (PE) = PE of water continuous phase + PE of oil continuous phase. (29)

$$PE = A_1 \rho_1 g h_1 + A_2 \rho_2 g h_2. \quad (30)$$

The total kinetic energy per unit length of pipe can be calculated as:

Total Kinetic Energy (KE) = KE of water continuous phase + KE of oil continuous phase. (31)

$$KE = \frac{1}{2} A_1 \rho_1 v_1^2 + \frac{1}{2} A_2 \rho_2 v_2^2. \quad (32)$$

The total surface energy per unit length can be calculated as:

Total Surface Energy (SE) = SE of interface + SE of water droplets in oil phase + SE of oil droplets in water phase. (33)

$$SE = \sigma \left[d \sin\left(\frac{\beta}{2}\right) + \frac{6 A_1 H_{D1}}{d_{SM1}} + \frac{6 A_2 H_{D2}}{d_{SM2}} \right]. \quad (34)$$

Where, σ , d_{SM1} and d_{SM2} are the interfacial tension between oil and water, Sauter Mean Diameter (SMD) of the water droplets and SMD of the oil droplets. SMD can be estimated by several different models and correlations. In this model, the correlations of Angeli and Hewitt (2000) are used to estimate Maximum Diameter (d_{MAX}) and SMD (d_{SM}).

$$d_{SM} v_C^{1.8} = 2 \times 10^{-8} \times (4f_C)^{-3.12}. \quad (35)$$

$$d_{MAX} v_C^{1.8} = 4.2 \times 10^{-8} \times (4f_C)^{-3.13}. \quad (36)$$

Where, v_C and f_C are continuous phase velocity and friction factor (Fanning), respectively.

Finally, the total energy of the system is:

$$TE = SE + KE + PE. \quad (37)$$

The pressure gradient is calculated by the two-fluid model for all flow patterns in which two distinct phases are present in the pipe. For fully dispersed flow, the pressure gradient is calculated from a homogeneous model as follows,

$$\left(\frac{dP}{dL}\right) = \left(\frac{dP}{dL}\right)_{Friction} + \left(\frac{dP}{dL}\right)_{Gravitational}. \quad (38)$$

$$\left(\frac{dP}{dL}\right)_{Friction} = \frac{2f_M \rho_M v_M^2}{d}. \quad (39)$$

$$\left(\frac{dP}{dL}\right)_{Gravitational} = \rho_M g \sin(\theta). \quad (40)$$

Where, f_M , ρ_M and v_M are the friction factor of the mixture, mixture density and mixture velocity, respectively.

The model first takes all the inputs, including fluid properties, superficial velocities of the oil and water, etc. The model then varies β from 0° to 360° and calculates TE and F for the system. The solution is the condition where the total energy is minimum ($TE \rightarrow Minimum$) and combined momentum equation is near zero ($F \rightarrow 0$) simultaneously. For the two cases of full dispersions, i.e. $\beta = 0^\circ$ (dispersion of water in oil) and $\beta = 360^\circ$ (dispersion of oil in water), the model does not consider the combined momentum equation ($F=0$) and only considers the minimization

of total energy. For Reynolds number smaller than 1000, it is assumed that the flow will be laminar and the continuous phase will have a negligible amount of turbulent energy, if any, to cause any dispersion. Hence, the continuous phase remains in segregated form. To determine whether there is any dispersion for Reynolds number higher than 1000, d_{MAX} is calculated and compared with the maximum distance (L_{MAX}) between the interface and pipe wall across the continuous phase, as shown in Fig. 3.

$$d_{MAX} \leq L_{MAX} \quad (41)$$

Moreover, to avoid inversion, the maximum cross section area swept by the biggest droplet should not cross the inversion point of dispersed phase holdup in the continuous phase.

$$\left(\frac{A_{drop}}{A}\right) \leq H_{INV}. \quad (42)$$

Where, A_{drop} , A and H_{INV} represents the cross sectional area of the drop, cross sectional area of the layer where the drop exists and the holdup of the dispersed phase at the inversion point below which the particular droplet dispersion is stable, respectively. These assumptions are very reasonable, conservative and biased towards the dispersions. If either of the conditions is not satisfied then it is not possible to have dispersions and the continuous phase still remains in segregated form. If the continuous phase can accommodate d_{MAX} , then the hold-up of the dispersed phase (H_D) is varied from 0 to the phase inversion point and for each case both TE and F are minimized. This is done simultaneously in both layers.

Results and Discussions

A VBA code was written for the model. The flow chart for the model is shown in Fig. 4. The model is validated against available experimental data. Model predictions are compared with results of oil-water experimental studies performed by Atmaca (2007), Alkaya (2000), Trallero (1995) and Abduvayt (2006). In this chapter the model predictions are compared and validated in different aspects including pressure gradient, holdup and flow pattern. Statistical evaluation parameters are defined in Table 1.

Pressure Gradient

Pressure gradient data from different experimental studies are compared with current model predictions for near horizontal inclinations. In Fig. 5, the predicted pressure gradients are compared with Atmaca's (2007) experimental pressure gradients, for inclination angles of 0° , 1° , 2° , -1° , -2° , and -5° . In Fig. 6, the predicted pressure gradients are compared with the Alkaya (2000) experimental pressure gradients, for inclination angles of 0° , 1° , -1° , 5° , and -5° . In Fig. 7, the predicted pressure gradients are compared with the Trallero (1995) experimental pressure gradients, for horizontal oil-water flows. In Fig. 8, the predicted pressure gradients are compared with the Abduvayt (2006) experimental pressure gradients, for inclination angles of 0° , 0.5° , -0.5° , 3° , and -3° . It is seen in the above graphs that the data points are quite close to the 45° line. This indicates that the current model performs very well in pressure gradient predictions. Error analysis of the current model predictions is given in Table 2.

Holdup

Holdup data from different experimental studies are compared with current model predictions for near horizontal inclinations. In Fig. 9, water holdup predictions of the current model are compared with the Atmaca (2007) experimental data for inclination angles of 1° , 2° , -1° , -2° and -5° . In Fig. 10, water holdup predictions of the current model are compared with the Alkaya (2000) experimental data for inclination angles of 1° , 5° , -1° , -5° and horizontal. In Fig. 11, water holdup predictions of the current model are compared with the Trallero (1995) experimental data for horizontal flow. It is seen in Figs. 9 to 11 that the current model predicts holdup with good accuracy for Atmaca (2007), Alkaya (2000) and Trallero (1995) data where average holdup was measured using trapping technique. Error analysis of the current model predictions is given in Table 3.

Comparisons of the current model predictions with Atmaca (2007) data for different flow patterns are shown in Figs. 12 - 16. Some deviation is observed in holdup predictions for stratified flow pattern. This

might be because of inaccuracies in the estimation of interfacial shear stress in current model. More work is needed to correctly estimate the interfacial shear stress. Some cluster of data points in fully dispersed flow patterns (OW and WO) are off the 45° line. This is because the experimentally observed flow patterns are not fully dispersed corresponding to these data points. The model predicts fully dispersed flow pattern for these data points because the criteria for the onset of entrainment is conservative and biased towards dispersion. This leads the model to over predict dispersions in flow and hence cause errors in prediction of holdup.

Flow Pattern

Flow pattern predictions are compared with experimentally observed flow patterns. Fig. 17 shows the flow pattern map observed by Atmaca (2007) for horizontal flow and Fig. 18 shows the flow pattern map predicted by the current model for the same data. In Figs. 17-19, ST, STMI, DOW/W, DOW/O, O/W and W/O denote stratified, stratified mixing, dispersion of oil in water with water layer, dispersion of oil in water with oil layer, dispersion of oil in water and dispersion of water in oil, respectively. The flow pattern maps are showing general flow patterns trend very well. The flow pattern map heavily depends on the droplet size correlations and how we are defining the criteria for onset of entrainment.

Comparison with Unified Model

The current model predictions are also compared with the Zhang and Sarica (2006) *Unified Model* predictions. The current model uses a single criterion of minimization of energy to predict flow pattern map, holdup as well as pressure gradient. The unified model first predict flow pattern and then predicts pressure gradient and holdup according to the respective flow pattern. The error analysis of pressure gradient and holdup predictions by the unified model and current model for Atmaca (2007) data, Alkaya (2000) data, Abduvayt (2006) data and Trallero (1995) data are given in Tables 4 to 10. The current model performs very well in both pressure gradient predictions and holdup predictions. The

current model predictions are on par with the unified model and in many occasions its performance is more accurate than the unified model. The flow pattern maps predicted by current model and the unified model are shown for horizontal flow observations from Atmaca (2007) in Fig. 18 and Fig. 19, respectively. The corresponding observed flow pattern map is shown in Fig. 17. The predictions of current model are closer to the actual observed flow patterns than unified model predictions. Another drawback of unified model is that it can predict only three flow patterns: ST, OW and WO.

Conclusions

The concept of minimization of total energy is very simple, basic and can be applied to any flowing condition in the pipe. Unlike existing oil-water flow models, the current model does not have strict different criteria for different flow pattern transitions. The model does not force the flow to conform to a particular flow pattern and captures the gradual changes in flow configuration. Therefore, this results in better predictions of the design parameters.

The model gives extensive information about the flow, e.g. flow pattern (including dual dispersions, single layer dispersions), droplet size information, holdup and dispersed phase holdup for individual layers and pressure gradient. It can predict six different flow patterns namely: Stratified Smooth (ST), Dispersion of Oil in Water and Oil layer (DOW/W), Dispersion of Water in Oil and Water layer (DWO/W), Dual Dispersion (OW/WO), Dispersion of Oil in Water (OW) and Dispersion of Water in Oil (WO). Unlike other present models, it captures the gradual changes of the flow behaviors during the transition from stratified to fully dispersed flow). It is evident from the results and comparisons that the model estimates the pressure gradient and flow pattern very well. The model predictions are on par with the Zhang and Sarica (2006) unified model. In some cases the current model predicts more accurately.

The model is sensitive to the closure relationships such as droplet size, mixture viscosity, and onset of entrainment. The flow pattern map heavily depends on the droplet size correlations and the criteria for

onset of entrainment. Any improvements in estimation of droplet size can be translated into better predictions of the current model. The criteria used in current model are quite conservative and biased towards formation of dispersions. Better correlation or model for estimation of emulsion viscosity can be very useful to estimate the pressure gradient in the current model.

The minimization of energy approach works well for liquid-liquid near horizontal flow. It is because in liquid-liquid flow with simple assumptions and under steady state condition the formula for estimation of the energy will remain the same in space as well as in time. The method can be extended to gas-liquid flow provided proper methods for estimation of all different types of energies are formulated for all gas-liquid flow patterns. The concept of energy minimization can be applied to all inclinations provided proper methods for estimation of all different types of energies are formulated for all liquid-liquid flow patterns. Once these hurdles are overcome the model can be used as unified model which can predict flow behavior for all fluids at all inclinations.

It is evident from the results and comparisons that the model estimates the pressure gradient and flow pattern very well on the basis of the minimization of total energy. The concept of minimization of total energy is very simple, basic and can be applied to any flowing condition in the pipe. It can be a very useful tool for modeling behavior at near-horizontal angles. It gives extensive information about the flow, e.g. pressure gradient, flow pattern (including dual dispersions, single layer dispersions), droplet size information, holdup and dispersed phase holdup for individual layers. Unlike existing oil-water flow models, the current model does not have strict different criteria for different flow pattern transitions. The model does not force the flow to conform to a particular flow pattern and captures the gradual changes in flow configuration, therefore resulting in better predictions of the design parameters.

More work need to be done, and there is ample room to improve model predictions. The model is very sensitive to the closure relationships, especially the

droplet size correlations. The mixture viscosity closure relationship is also very crucial for the model. Any improvements in these will be directly reflected in the model's performance.

Nomenclature

<u>Symbol</u>	<u>Description</u>	<u>Unit</u>
A	Area	m ²
C	Constant	/
d	Diameter (pipe, droplet and hydraulic)	m
DOW/O	Dispersion of oil in water and oil	/
DOW/W	Dispersion of oil in water and water	/
DWO/O	Dispersion of water in oil and oil	/
DWO/W	Dispersion of water in oil and water	/
e_{ri}	Relative error	/
e_i	Actual error	/
f	Friction factor	/
F	Residual of combined momentum balance equation	Pa.m
h	Height of centroid from base of pipe	m
H	Holdup	/
KE	Kinetic energy per unit length	J/m
L	Length	m
N	Number of elements in a population, sample size	/
OW	Oil dispersed in water	/
$\left(\frac{dp}{dL}\right)$	Total pressure gradient	Pa/m
PE	Potential energy per unit length	J/m
R	Radius of pipe	m
S	Perimeter	m
SE	Surface energy per unit length	J/m

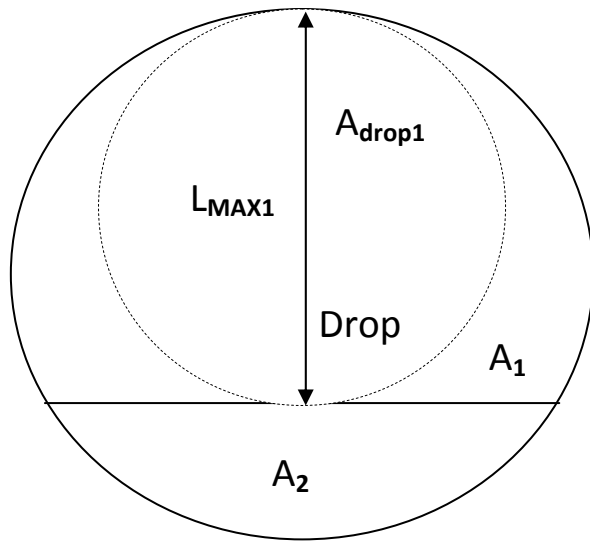
<u>Symbol</u>	<u>Description</u>	<u>Unit</u>
ST	Stratified	/
ST&MI	Stratified mixing	/
TE	Total energy per unit length	J/m
TRANS	Transition	/
v	Velocity	m/s
WO	Water dispersed in oil	/
β	Angle subtended by interface at the center of pipe	degree
$\varepsilon_1 - \varepsilon_6$	Statistical perimeters	/
θ	Inclination angle	degree
ρ	Density	kg/m ³
σ	Surface tension	N/m
τ	Shear stress	Pa
τ_I	Interfacial shear stress	Pa
τ_W	Wall shear stress	Pa
μ	Viscosity	Pa.s

Subscripts

<u>Symbol</u>	<u>Description</u>	<u>Unit</u>
1	Phase one (oil continuous phase)	/
2	Phase two (water continuous phase)	/
C	Continuous phase	/
D	Dispersed phase	/
drop	Droplet	/
I	Interfacial	/
INV	Inversion point	/
M	Mixture	/
max	Maximum	/
MIX	Mixture	/
o	Oil	/
w	Water	/
S	Superficial velocity	/
T	Total	/

References

- Abduvayt, P., Manabe, R., Watanabe, T. and Arihara, N., "Analysis of Oil/Water-Flow Tests in Horizontal, Hilly Terrain and Vertical Pipes," *SPE Production Operations* (2006), 123-133.
- Angeli, P. and Hewitt, G. F., "Drop Size Distribution in Horizontal Oil-Water Dispersed Flows," *Chemical Engineering Science* (2000), **55**, 3133-3143.
- Alkaya, B., "Oil-Water Flow Patterns and Pressure Gradients in Slightly Inclined Pipes," M.S. Thesis, The University of Tulsa (2000).
- Atmaca S., "Characterization of Oil-Water Flow in Horizontal and Slightly Inclined Pipes," M.S. Thesis, The University of Tulsa (2007).
- Brinkman, H. C., "The Viscosity of Concentrated Suspensions and Solutions," *J. Chem. Phys.* (1952), **20**, 571-581.
- Chakrabarti, D. P., Das, G., Ray, S., "Pressure Drop in Liquid-Liquid Two Phase Horizontal Flow: Experiment and Prediction," *Chem. Eng. & Tech.* (2005), **28**, 1003-1009.
- Trallero, J. L., "Oil-Water Flow Patterns in Horizontal Pipes," Ph.D. Dissertation, The University of Tulsa (1995).
- Vielma, M., "Characterization of Oil-Water Flow in Horizontal Pipes" M.S. Thesis, The University of Tulsa (2007).
- Zhang, H.-Q., "A Unified Approach for Interfacial Shear in Multiphase Flow," *TUFFP Advisory Board Meeting (October 6, 2005)*, **65**, 109-116.
- Zhang, H.-Q., and Sarica, C., "Unified Modeling of Gas/Oil/Water Pipe Flow- Basic Approaches and Preliminary Validation", *SPE Projects Facilities & Construction* (2006), **1** (2), 1-7.



$$\left(\frac{A_{drop1}}{A_1} \right) \leq H_{INV1}$$

$$d_{MAX1} \leq L_{MAX1}$$

Figure 3: Transition Criteria for Onset of Entrainment

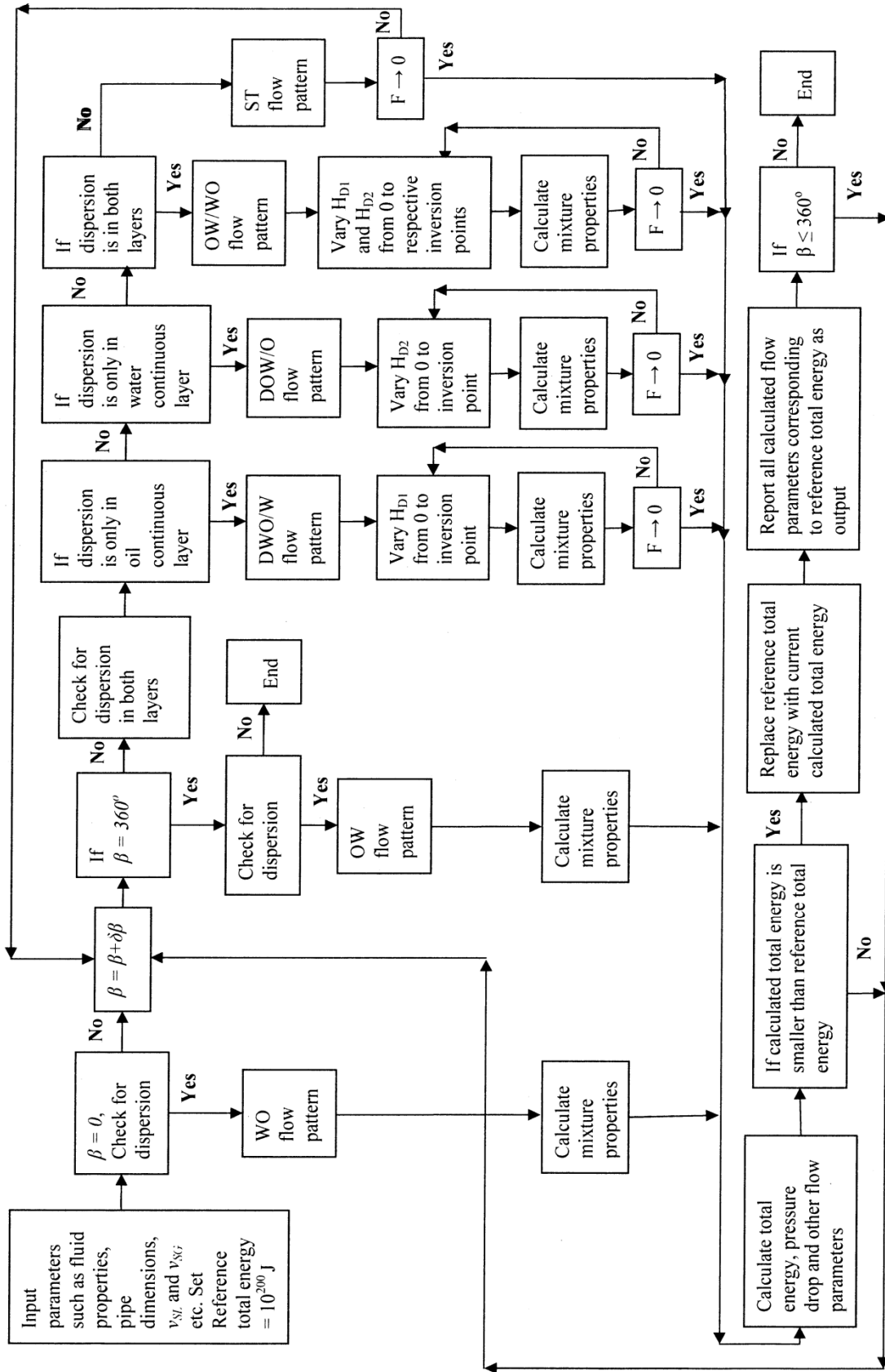


Figure 4: Model Flow Chart

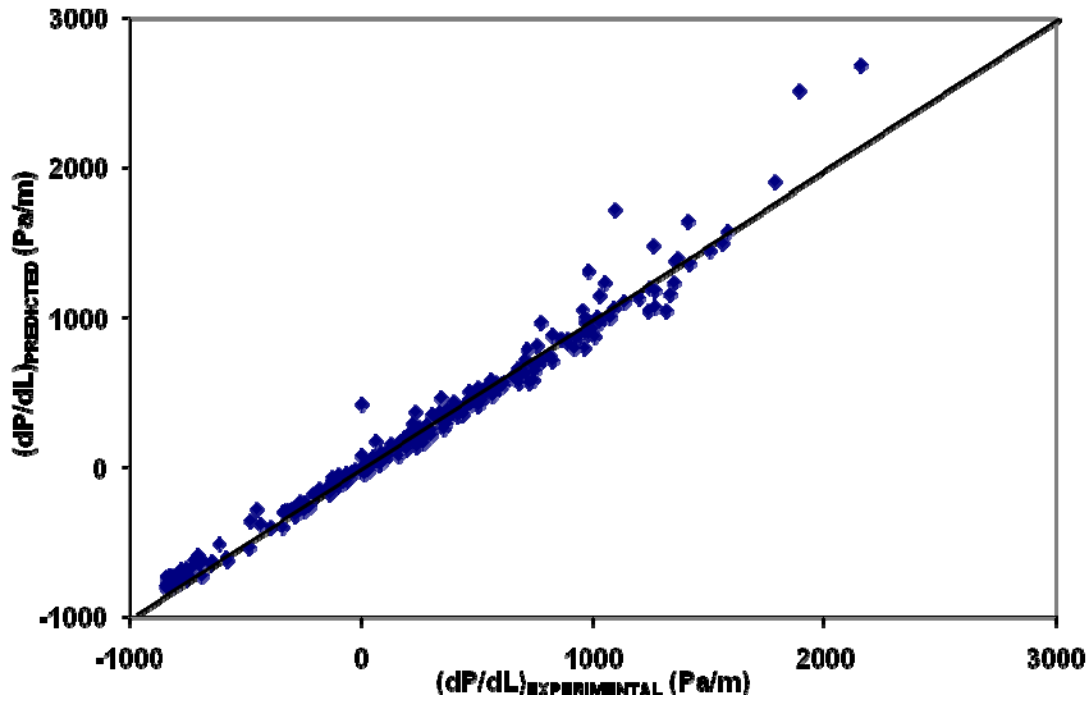


Figure 5: Model Predictions of Pressure Gradient Compared with Experimental Data of Atmaca (2007)

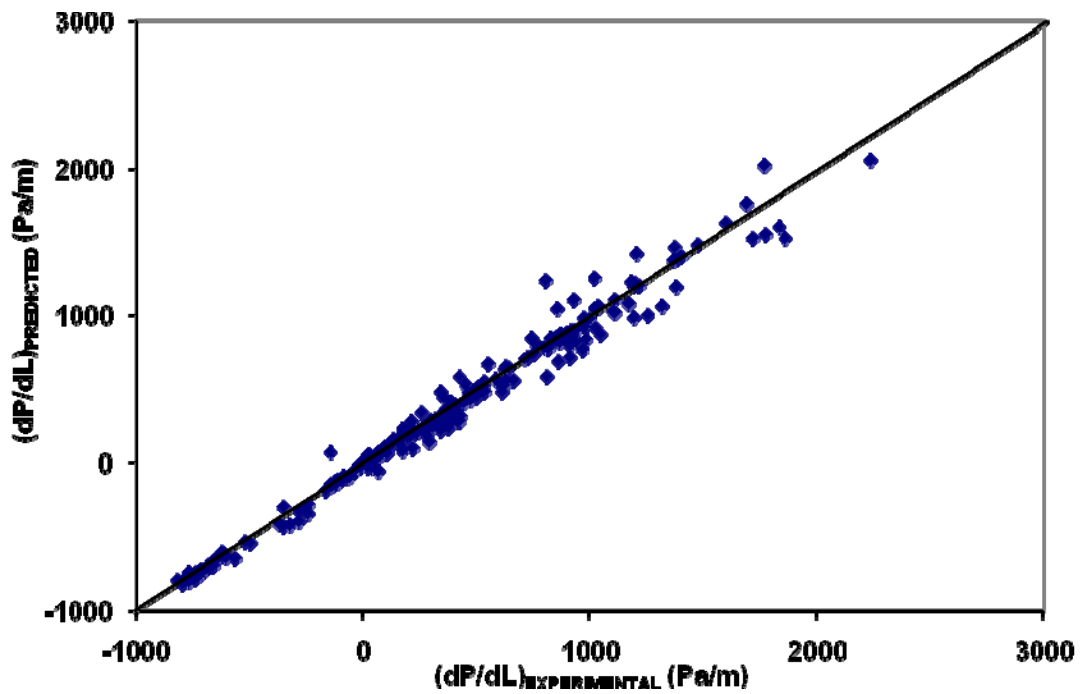


Figure 6: Model Predictions of Pressure Gradient Compared with Experimental Data of Alkaya (2000)

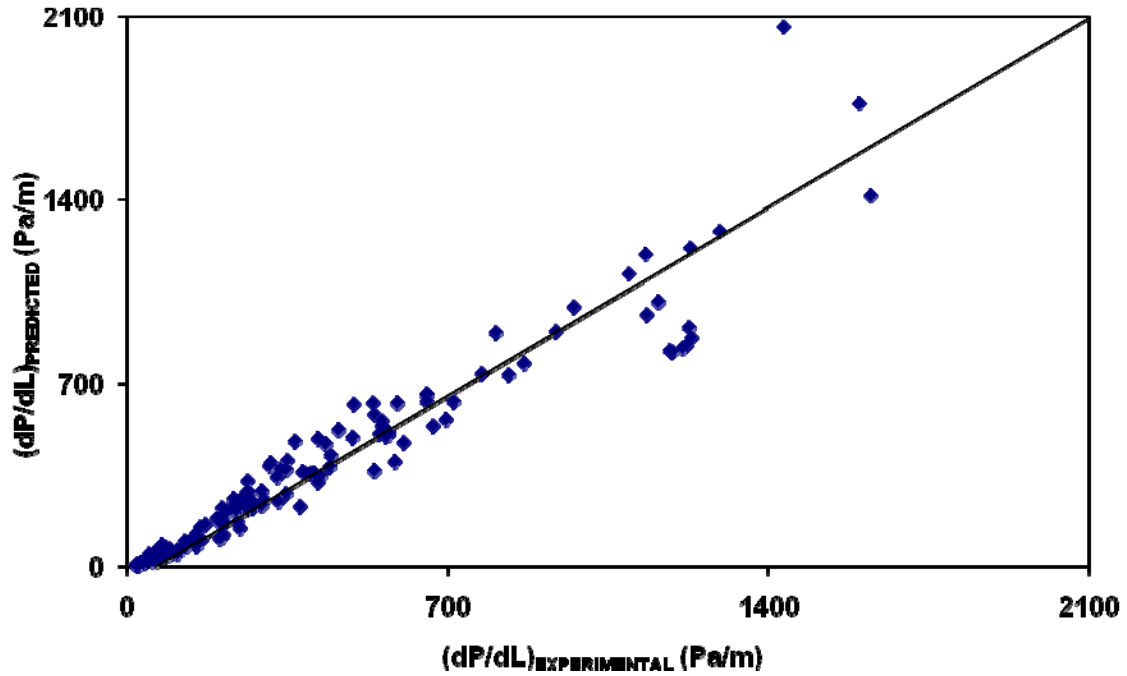


Figure 7: Model Predictions of Pressure Gradient Compared with Experimental Data of Trallero (2000)

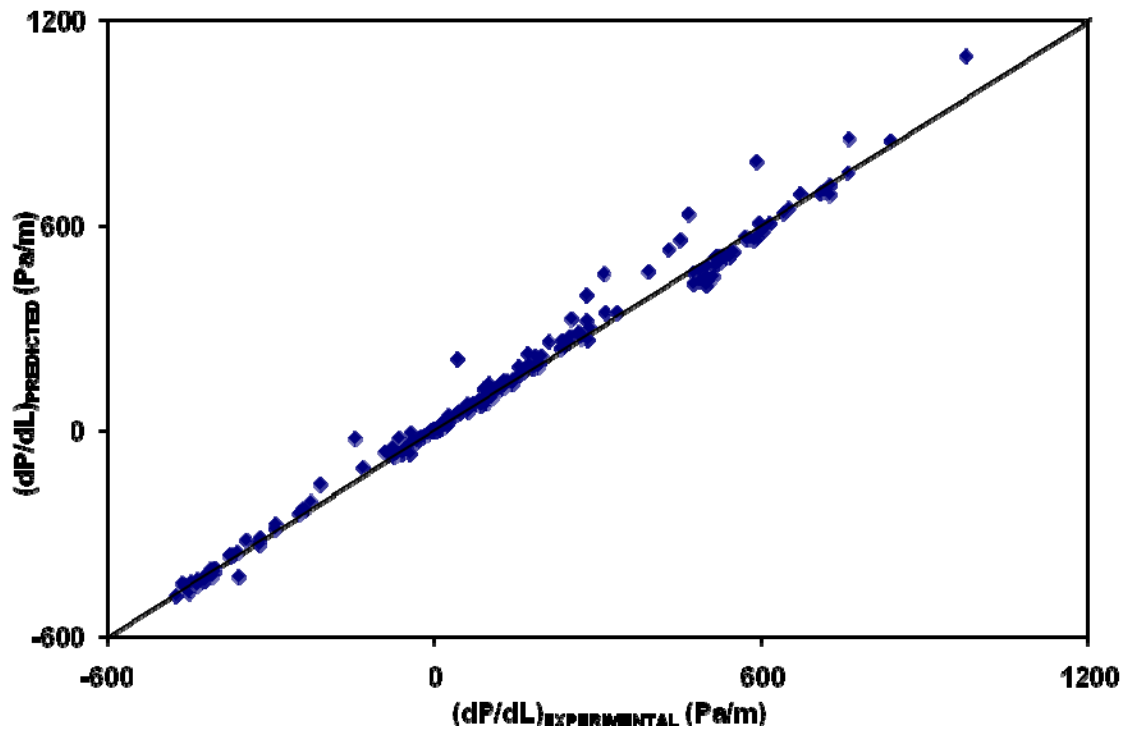


Figure 8: Model Predictions of Pressure Gradient Compared with Experimental Data of Abduvayt (2006)

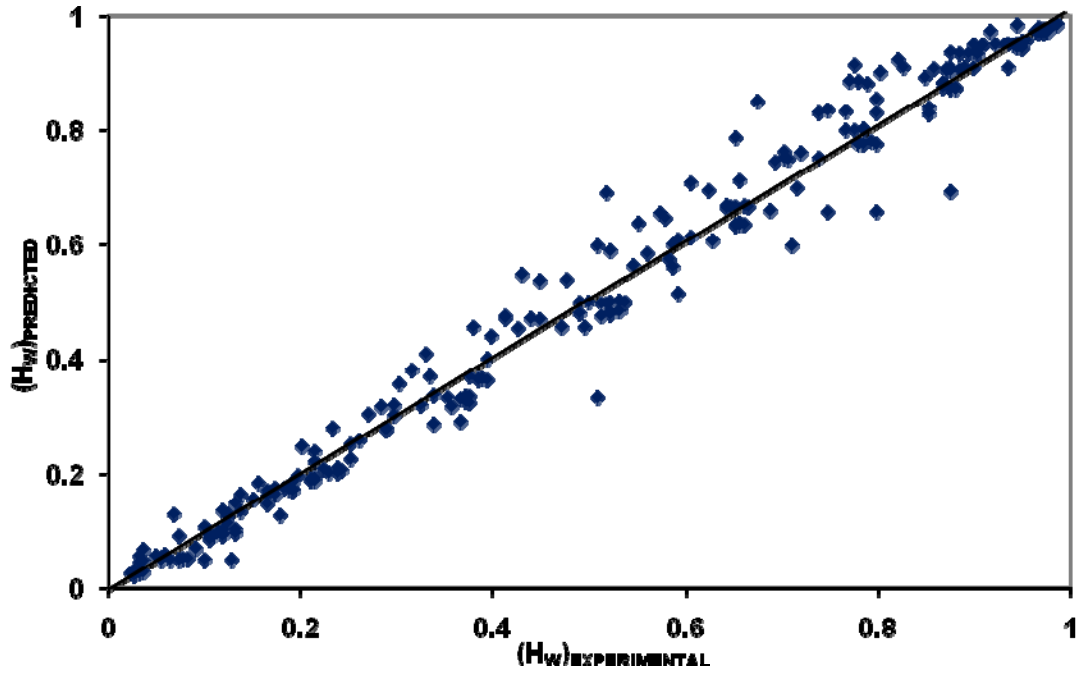


Figure 9: Model Predictions of Water Holdup Compared with Experimental Data of Atmaca (2007)

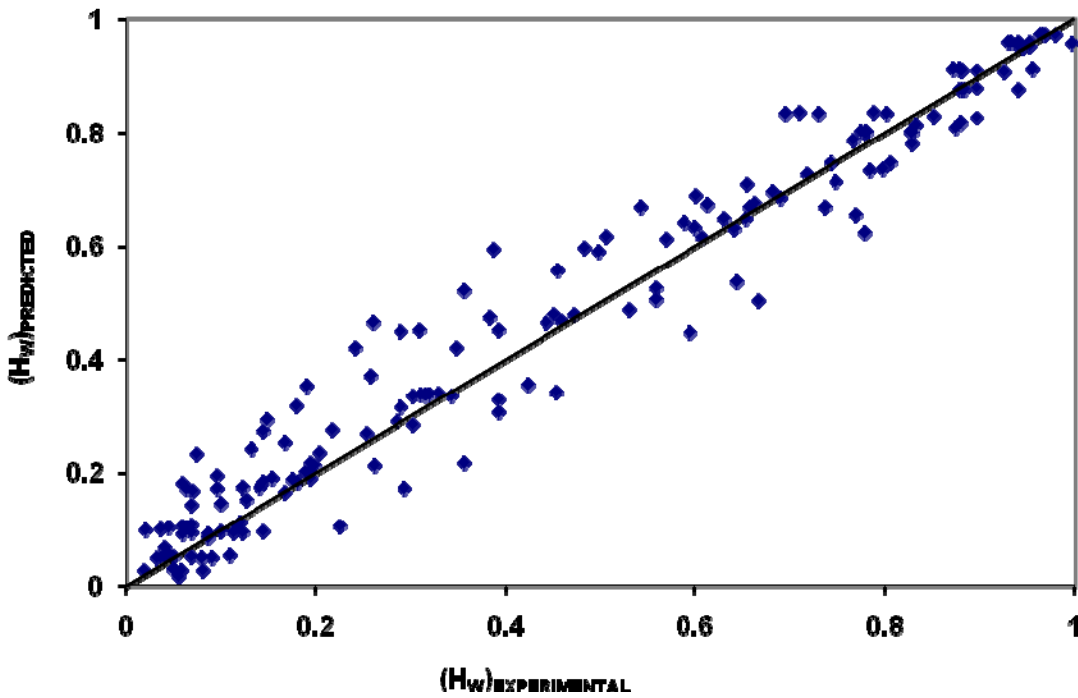


Figure 10: Model Predictions of Water Holdup Compared with Experimental Data of Alkaya (2000)

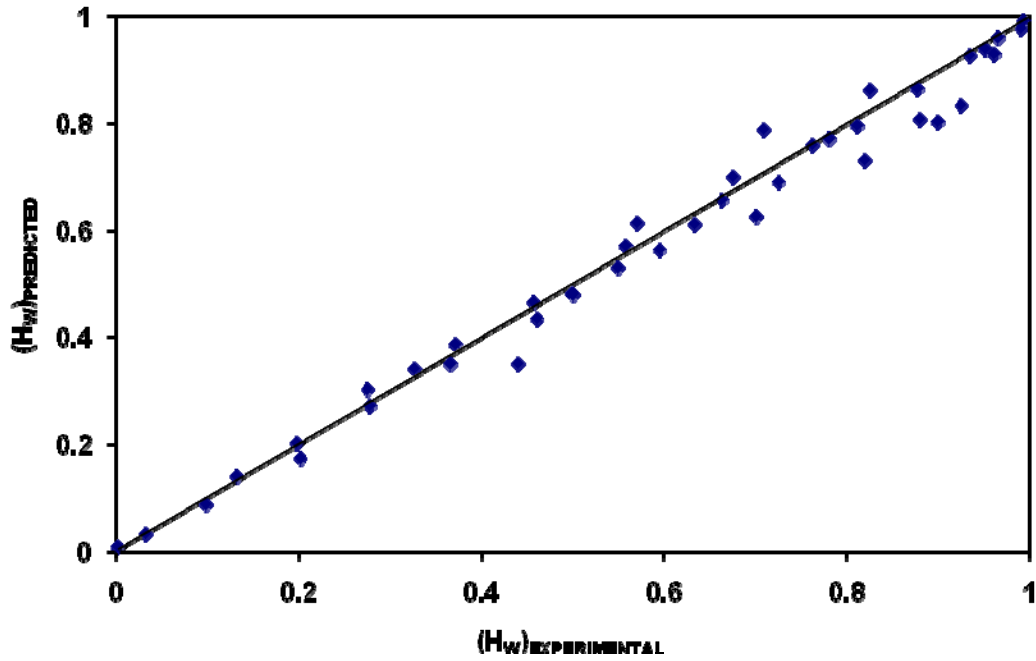


Figure 11: Model Predictions of Water Holdup Compared with Experimental Data of Trallero (1995)

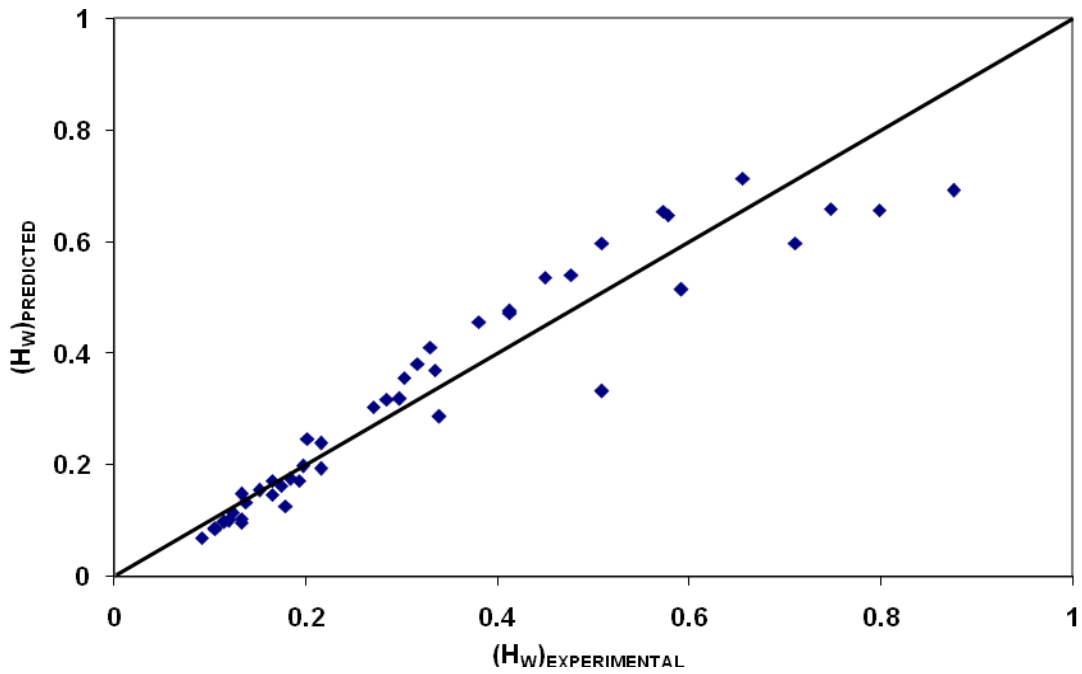


Figure 12: Model Predictions of Water Holdup for Stratified Flow Pattern Compared with Experimental Data of Atmaca (2007)

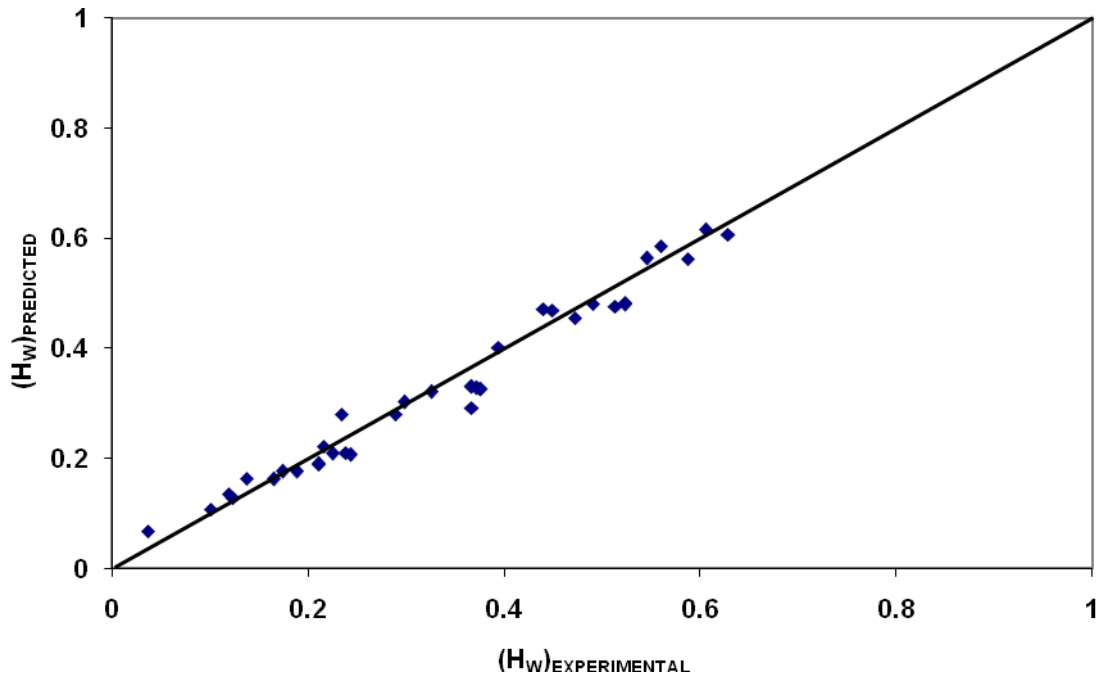


Figure 13: Model Predictions of Water Holdup for Dual Dispersion Flow Pattern Compared with Experimental Data of Atmaca (2007)

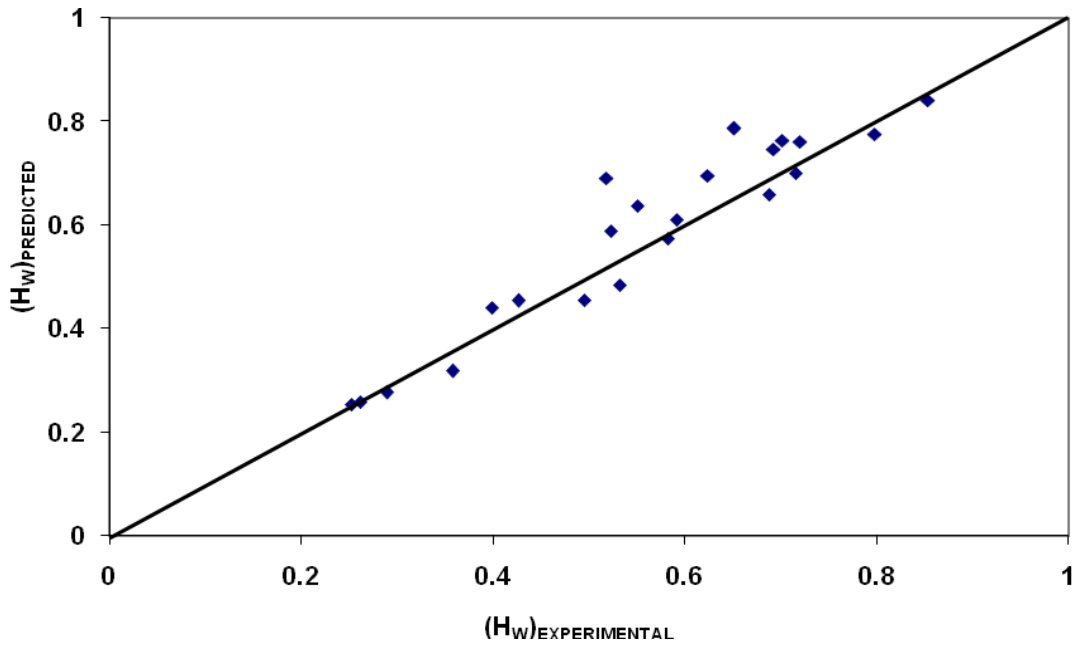


Figure 14: Model Predictions of Water Holdup for Oil in Water Dispersion and Oil Layer Flow Pattern Compared with Experimental Data of Atmaca (2007)

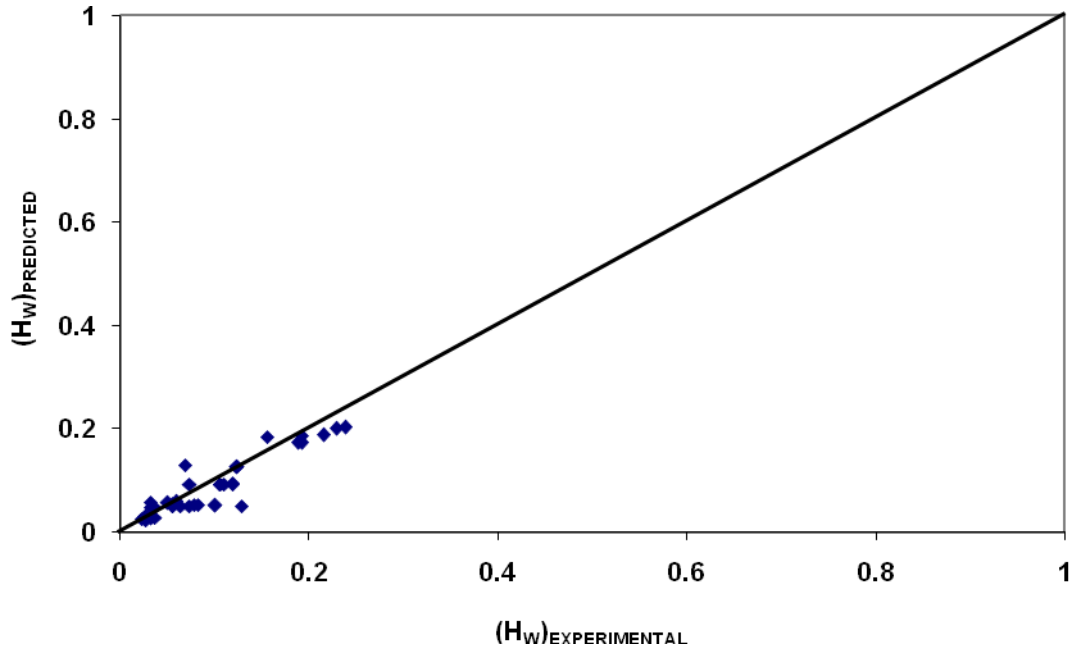


Figure 15: Model Predictions of Water Holdup for Water in Oil Dispersion Flow Pattern Compared with Experimental Data of Atmaca (2007)

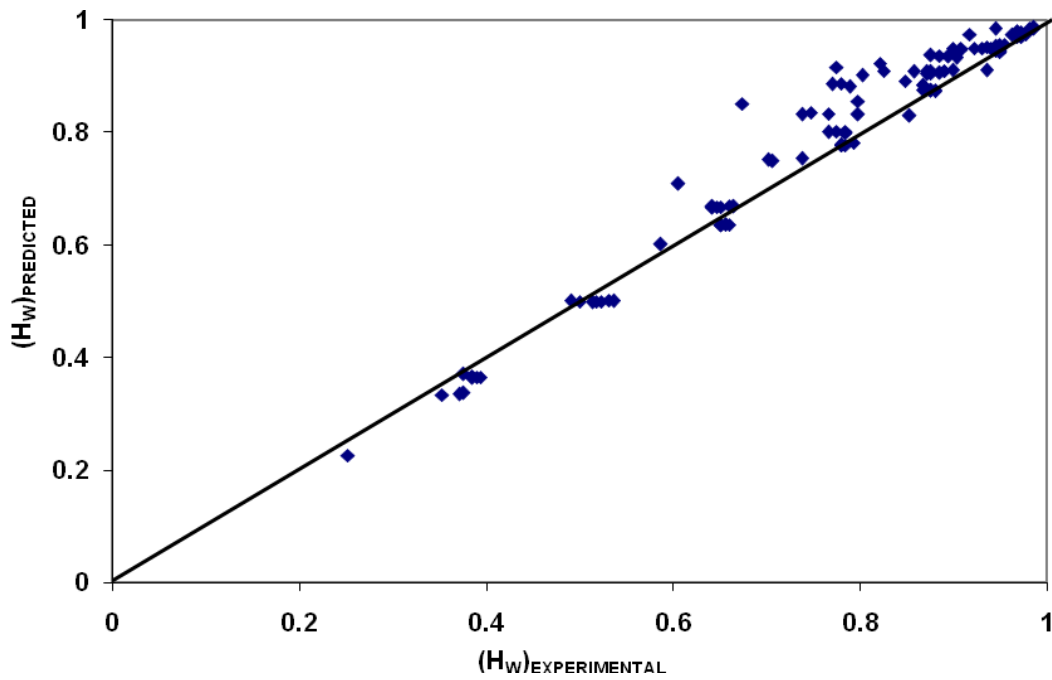


Figure 16: Model Predictions of Water Holdup for Oil in Water Dispersion Flow Pattern Compared with Experimental Data of Atmaca (2007)

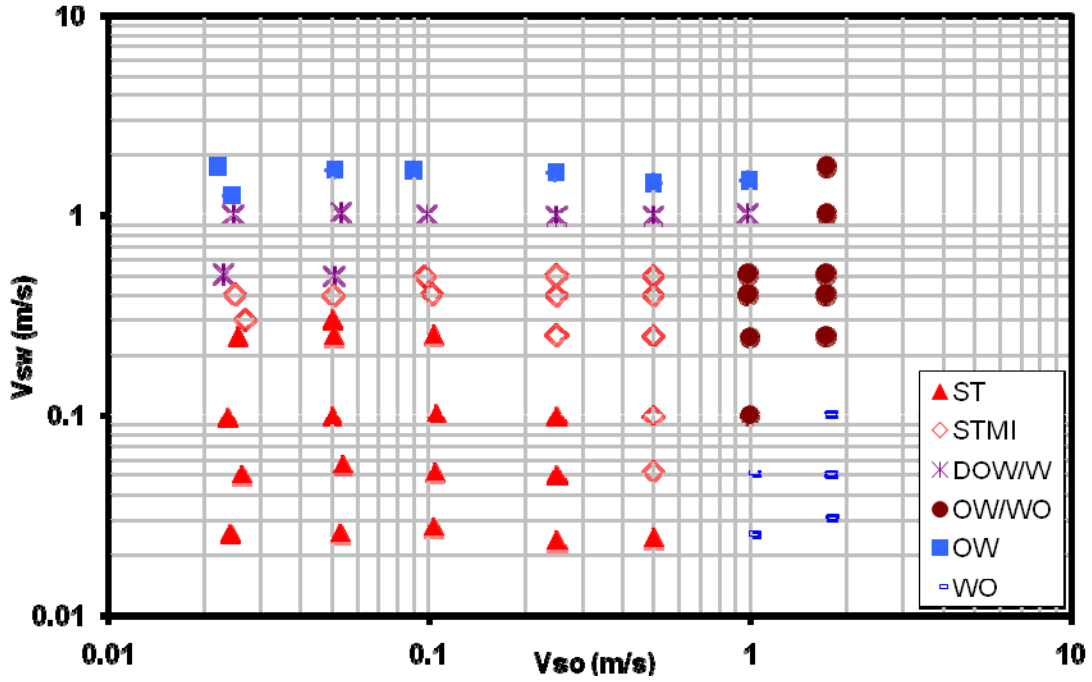


Figure 17: Flow Pattern Map Observed by Atmaca (2007) for Horizontal Flow

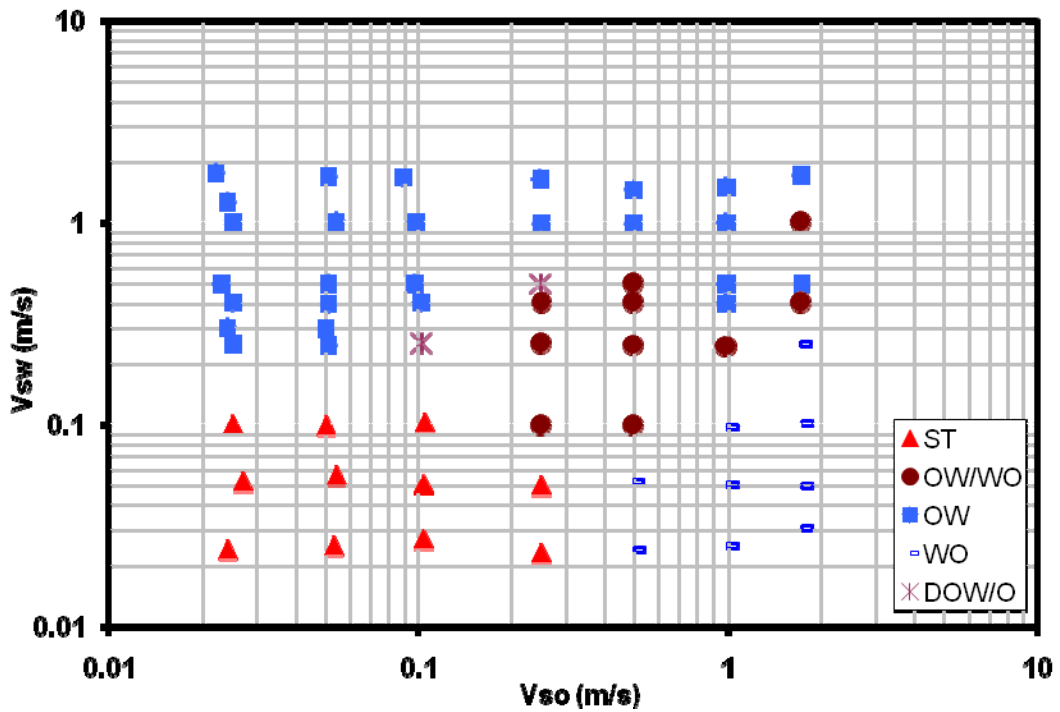


Figure 18: Flow Pattern Map Predicted by Present Model for Horizontal Flow for Atmaca (2007) Data

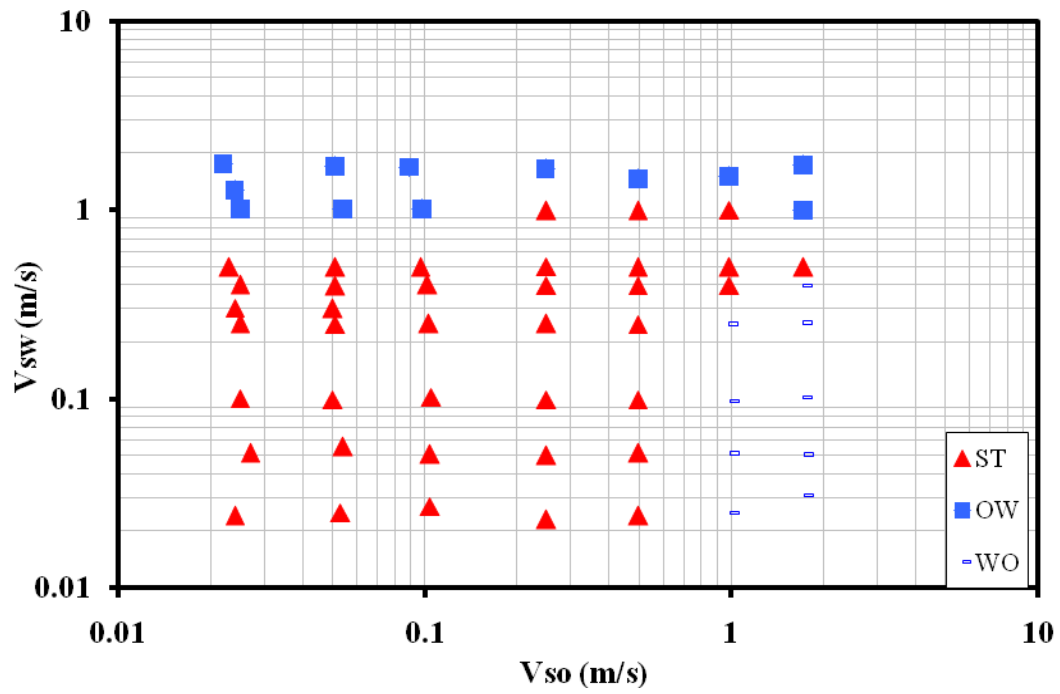


Figure 19: Flow Pattern Map Predicted by Unified Model for Horizontal Flow Corresponding to Atmaca (2007) Data

Table 1: Statistical Parameters

Definitions
$\epsilon_{1i} = \left(\frac{\text{Predicted value} - \text{Measured Value}}{\text{Measure Value}} \right) \times 100$
$\epsilon_1 = \text{Predicted value} - \text{Measured Value}$
$\epsilon_2 = \left[\frac{1}{N} \right] \sum_{i=1}^N \epsilon_{1i}$
$\epsilon_3 = \left[\frac{1}{N} \right] \sum_{i=1}^N \epsilon_{1i} $
$\epsilon_4 = \sqrt{\frac{\sum_{i=1}^N (\epsilon_{1i} - \epsilon_2)^2}{N-1}}$
$\epsilon_5 = \left[\frac{1}{N} \right] \sum_{i=1}^N \epsilon_i$
$\epsilon_6 = \left[\frac{1}{N} \right] \sum_{i=1}^N \epsilon_i $
$\epsilon_7 = \sqrt{\frac{\sum_{i=1}^N (\epsilon_i - \epsilon_5)^2}{N-1}}$

Table 2: Statistical Parameters for Pressure Gradient Predictions by Current Model Compared with Experimental Measurements

	ϵ_1 (%)	ϵ_2 (%)	ϵ_3 (%)	ϵ_4 (Pa/m)	ϵ_5 (Pa/m)	ϵ_6 (Pa/m)
Atmaca (2007)	-6.79	14.65	30.16	-0.48	49.48	87.07
Alkaya (2000)	-1.85	16.33	33.39	-21.61	47.08	76.17
Trallero (1995)	-25.27	29.12	26.23	-33.83	55.54	91.37
Abduvayt (2006)	16.01	36.77	105.44	7.75	21.58	36.33

Table 3: Statistical Parameters for Water Holdup Predictions by Current Model Compared with Experimental Studies

	ε_1 (%)	ε_2 (%)	ε_3 (%)	ε_4 (-)	ε_5 (-)	ε_6 (-)
Atmaca (2007)	0.47	9.73	15.58	0.01	0.03	0.05
Alkaya (2000)	16.45	27.79	51.81	0.02	0.05	0.07
Trallero (1995)	13.06	15.74	58.43	0.03	0.04	0.05

Table 4: Pressure Gradient Predictions by Unified Model and Current Model Compared with Atmaca (2007) Data

	ε_1 (%)	ε_2 (%)	ε_3 (%)	ε_4 (Pa/m)	ε_5 (Pa/m)	ε_6 (Pa/m)
Unified Model	2.5	20.6	40.7	41.5	63.6	99.4
Current Model	-7.0	14.8	30.4	-0.4	49.4	86.9

Table 5: Water Holdup Predictions by Unified Model and Current Model Compared with Atmaca (2007) Data

	ε_1 (%)	ε_2 (%)	ε_3 (%)	ε_4 (-)	ε_5 (-)	ε_6 (-)
Unified Model	-2.94	8.93	13.21	-0.02	0.03	0.04
Current Model	0.47	9.73	15.58	0.01	0.03	0.05

Table 6: Pressure Gradient Predictions by Unified Model and Current Model Compared with Alkaya (2000) Data

	ε_1 (%)	ε_2 (%)	ε_3 (%)	ε_4 (Pa/m)	ε_5 (Pa/m)	ε_6 (Pa/m)
Unified Model	3.26	21.10	45.10	21.81	57.53	126.02
Current Model	-1.85	16.33	33.39	-21.61	47.08	76.17

Table 7: Water Holdup Predictions by Unified Model and Current Model Compared with Alkaya (2000) Data

	ε_1 (%)	ε_2 (%)	ε_3 (%)	ε_4 (-)	ε_5 (-)	ε_6 (-)
Unified Model	17.02	28.56	55.47	0.00	0.05	0.08
Current Model	16.45	27.79	51.81	0.02	0.05	0.07

Table 8: Pressure Gradient Predictions by Unified Model and Current Model Compared with Abdvayt (2006) Data

	ε_1 (%)	ε_2 (%)	ε_3 (%)	ε_4 (Pa/m)	ε_5 (Pa/m)	ε_6 (Pa/m)
Unified Model	17.27	35.93	102.16	15.71	28.45	115.22
Current Model	16.01	36.77	105.44	7.75	21.58	36.33

Table 9: Pressure Gradient Predictions by Unified Model and Current Model Compared with Trallero (1995) Data

	ε_1 (%)	ε_2 (%)	ε_3 (%)	ε_4 (Pa/m)	ε_5 (Pa/m)	ε_6 (Pa/m)
Unified Model	-7.08	18.17	24.07	2.79	48.16	93.23
Current Model	-25.27	29.12	26.23	-33.83	55.54	91.37

Table 10: Water Holdup Predictions by Unified Model and Current Model Compared with Trallero (1995) Data

	ε_1 (%)	ε_2 (%)	ε_3 (%)	ε_4 (-)	ε_5 (-)	ε_6 (-)
Unified Model	7.22	14.31	59.30	-0.01	0.03	0.04
Current Model	13.06	15.74	58.43	0.03	0.04	0.05



Fluid Flow Projects

Executive Summary of Research Activities

Cem Sarica

Advisory Board Meeting, September 30, 2009

Three-phase Hilly Terrain Flow

◆ Significance

- Valleys and Hills may Act as Local Separation Devices for Fluids
- Location, Amount and Residence Time of Water in a Pipe can have Significant Impact on Flow Assurance Issues such as Hydrate Formation and Corrosion

Three-phase Hilly Terrain Flow ...

◆ Past Studies

- Hilly Terrain Flow of Two Phases has been Studied Extensively
 - ▲ Al-Safran, 1999 and 2003
 - ▲ Others Outside of TUFFP
- No Available Research is Found on Three-phase Flow

Three-phase Hilly Terrain Flow ...

◆ Current Project

- Objectives
 - ▲ Observe Flow Behavior and Identify Flow Characteristics
 - ▲ Develop Predictive Tools (Closure Relationships or Models)

Three-phase Hilly Terrain Flow ...



◆ Status

- Testing is Complete
- Data Analysis and Model Evaluation are Underway



Fluid Flow Projects

Slug Flow Evolution of Gas-Oil-Water Flow in Hilly-Terrain Pipelines

Gizem Ersoy Gokcal

Advisory Board Meeting, September 30, 2009

Outline

- ◆ Introduction
- ◆ Objectives
- ◆ Experimental Study
- ◆ Preliminary Modeling
- ◆ Project Schedule

Introduction

Hilly-Terrain Pipelines Cause

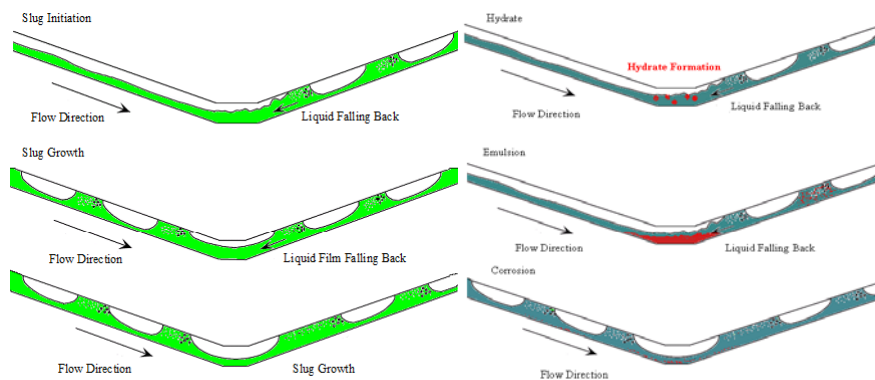
- ◆ **Operational Problems**
 - Flooding of Downstream Facilities
 - Severe Pipe Corrosion
 - Structural Instability of Pipelines
- ◆ **Flow Assurance Problems**
 - Hydrates
 - Emulsions
 - Paraffin Deposition
 - Corrosion



Introduction ...

Hydrodynamics

Flow Assurance



Objectives

- ◆ Investigate Gas-Oil-Water Flow in Hilly-Terrain Pipelines
- ◆ Develop Closure Models for Flow in Hilly-Terrain Pipelines on
 - Three-Phase Slug Initiation and Dissipation
 - Mixing Status of Phases

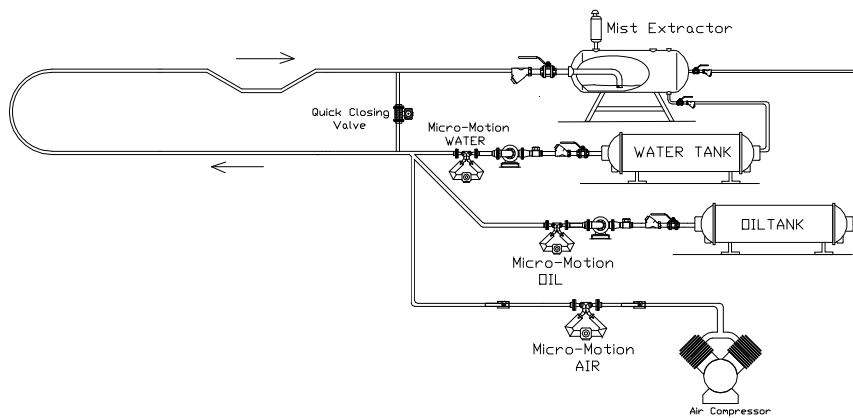
Experimental Study

- ◆ Experimental Facility
- ◆ Instrumentation
- ◆ Data Acquisition System
- ◆ Test Fluids
- ◆ Testing Ranges
- ◆ Uncertainty Analysis
- ◆ Experimental Results

Experimental Facility

- ◆ Extended to 69-m (226-ft) Long
- ◆ 50.8-mm (2-in.) ID Pipes
- ◆ Single Hilly-Terrain Unit
 - 9.7-m (32-ft) Long Downhill
 - 1.5-m (5-ft) Long Horizontal
 - 9.7-m (32-ft) Long Uphill Sections (L/D=413)
- ◆ $\pm 1^\circ$, $\pm 2^\circ$, $\pm 5^\circ$ of Inclination Angles

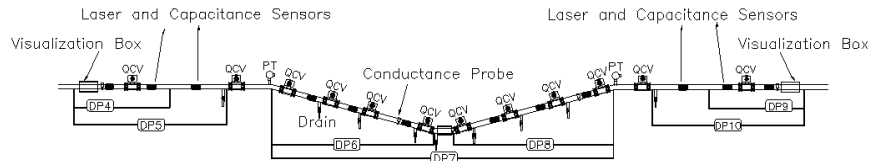
Experimental Facility



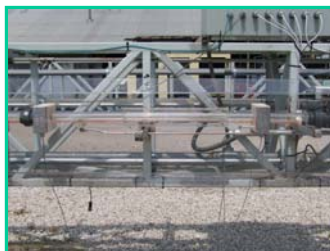
Experimental Facility ...



Test Section



Experimental Facility ...



Instrumentation

- ◆ **Pressure & Differential Pressure Transducers**

- Pressure Drop
- Identification of Flow Patterns
- Connected to High-Speed DAQ

- ◆ **Quick-Closing Valves**

- Average Gas, Oil, Water Holdups

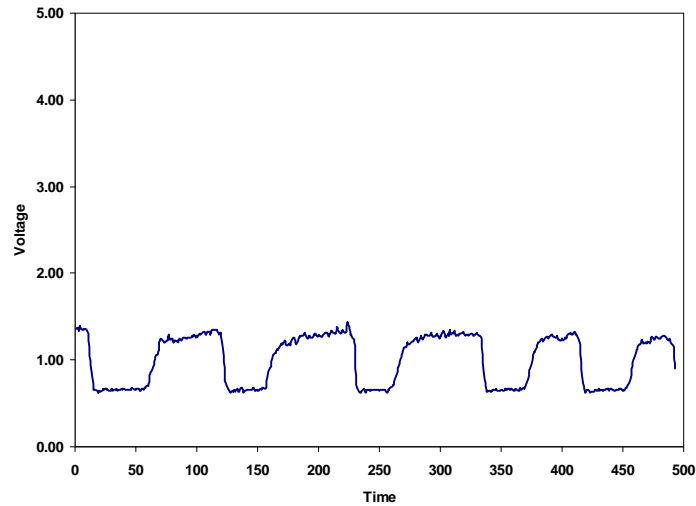
Instrumentation ...

- ◆ **Laser Sensors**

- Slug Flow Characteristics
- Connected to High-Speed DAQ
- Tested for Three-Phase Slug Flow



Instrumentation ...



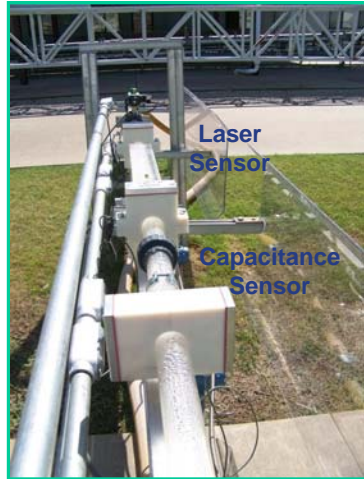
Instrumentation ...

◆ Capacitance Sensors

- Slug Flow Characteristics
- Connected to High-Speed DAQ
- Tested for Oil-Water and Three-Phase Slug Flow



Instrumentation ...

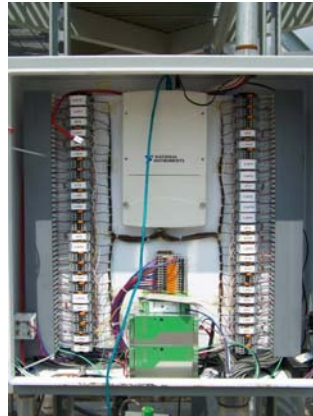


Instrumentation ...

- ◆ **Cameras**
 - **Identification of Flow Patterns**
 - **Slug Characteristics**
 - **Oil-Water Mixing Status**
 - **Validation of Laser and Capacitance Sensors**

Data Acquisition System

- ◆ Lab VIEW™ 7.1 Software
- ◆ High-Speed Data Acquisition



Test Fluids

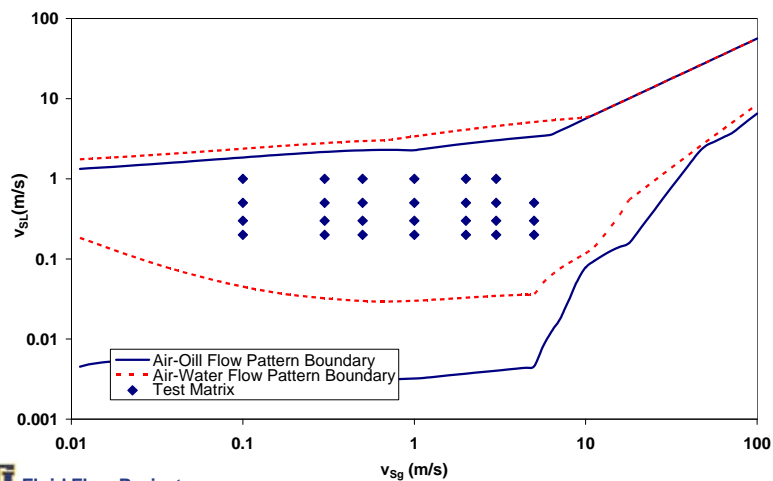
- ◆ Air - Mineral Oil - Water
- ◆ Tulco Tech-80 Mineral Oil
 - API: 33.2°
 - Density: 858.75 kg/m³ @ 15.6 °C (60°F)
 - Viscosity: 13.5 cP @ 40 °C (104 °F)
 - Surface Tension: 29.14 dynes/cm @ 25.1 °C (77.2 °F)

Testing Ranges

- ◆ Superficial Oil Velocity
 - 0.04 – 1 m/s
- ◆ Superficial Water Velocity
 - 0.025 – 1 m/s
- ◆ Superficial Gas Velocity
 - 0.1 – 5 m/s
- ◆ Water Fraction
 - 20%, 40%, 60%, 80%
 - 0% and 100% for Preliminary Tests
- ◆ Hilly-Terrain Unit
 - 5° for Valley Configuration

Testing Ranges ...

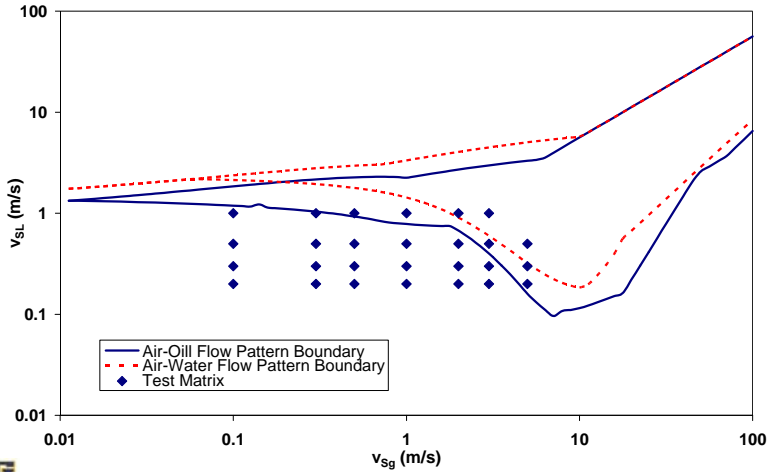
Unified Horizontal Flow Pattern Map



Testing Ranges ...



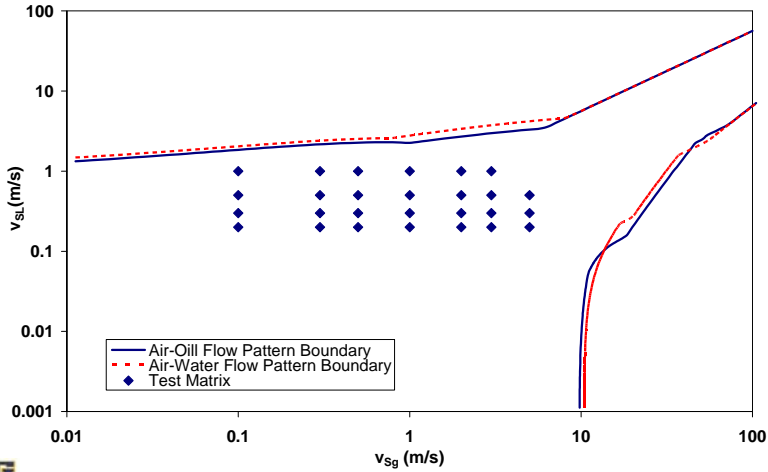
Unified Flow Pattern Map for -5° Inclination Pipe



Testing Ranges ...



Unified Flow Pattern Map for +5° Inclination Pipe

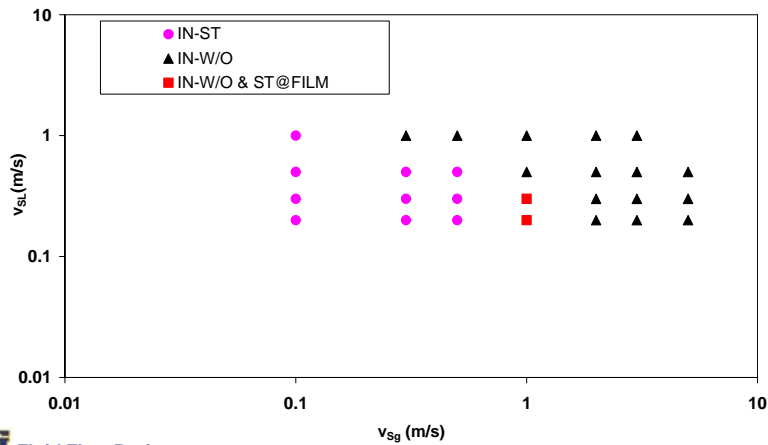


Uncertainty Analysis

Measured Parameter	Random Uncertainty	Systematic Uncertainty	Combined Uncertainty
Pressure	±0.16%	±0.04%	±0.35%
Pressure Drop	±0.01%	±0.04%	±3.19%
Temperature	±0.03%	±1.02%	±2.1%
Slug Frequency	±0.76% (LSR)	N/A	±0.76%
	+0.77% (CAP)	N/A	+0.77%
Oil Flow Rate	±0.17%	±0.10%	±0.35%
Water Flow Rate	±0.15%	±0.10%	±0.31%

Experimental Results

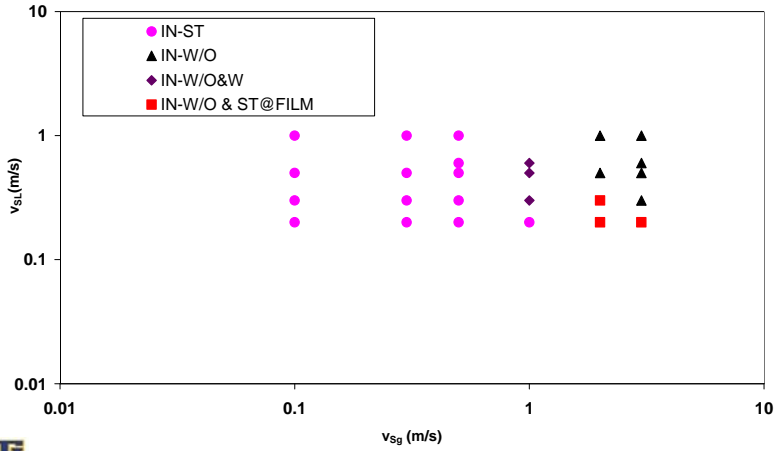
HORIZONTAL GAS-OIL-WATER FLOW PATTERN MAP for 20% WATER CUT



Experimental Results ...



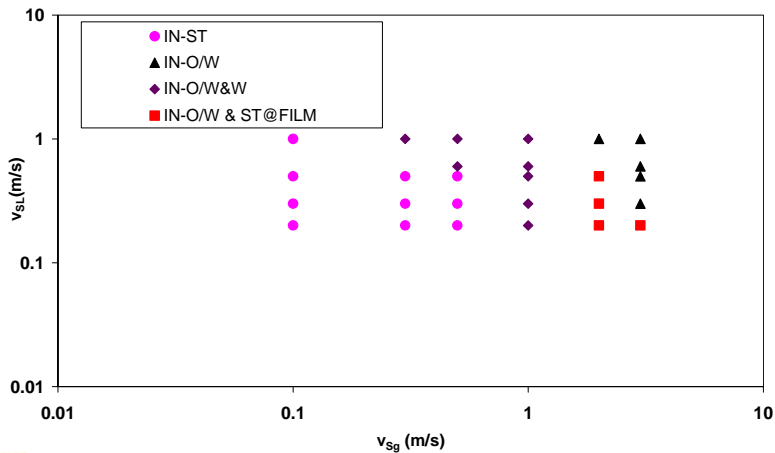
HORIZONTAL GAS-OIL-WATER FLOW PATTERN MAP for 40% WATER CUT



Experimental Results ...



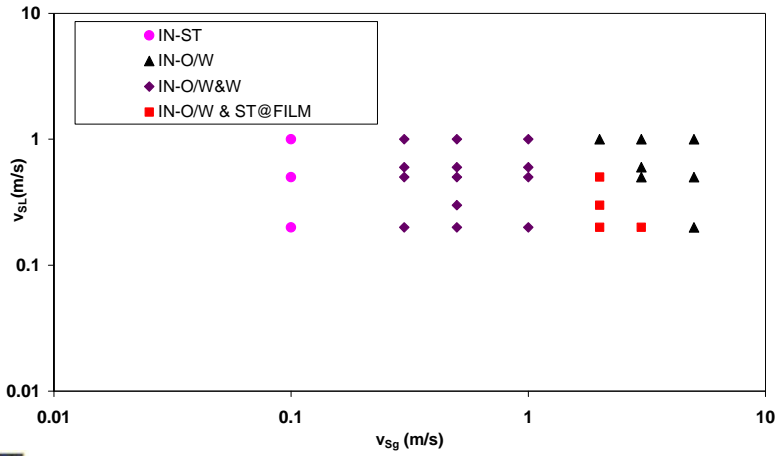
HORIZONTAL GAS-OIL-WATER FLOW PATTERN MAP for 60% WATER CUT



Experimental Results ...



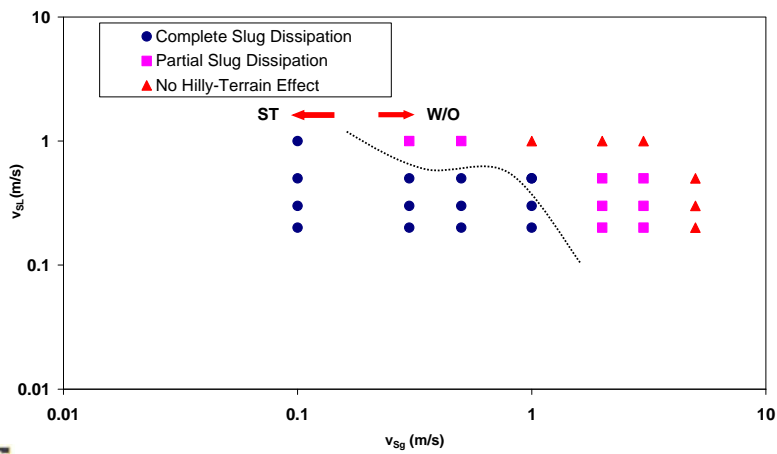
HORIZONTAL GAS-OIL-WATER FLOW PATTERN MAP for 80% WATER CUT



Experimental Results

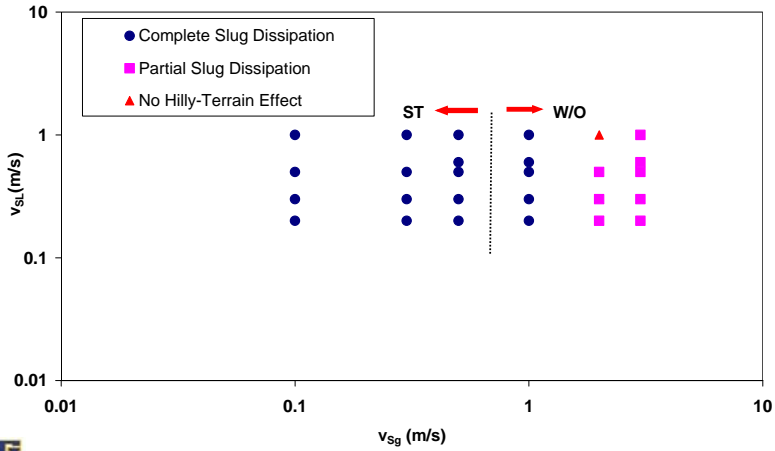


SLUG DISSIPATION at DOWNWARD INCLINED SECTION for 20% WATER CUT



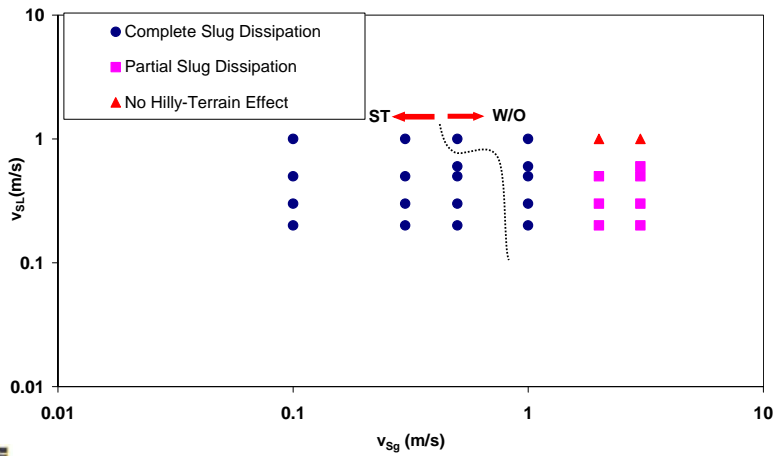
Experimental Results ...

SLUG DISSIPATION at DOWNWARD INCLINED SECTION for 40% WATER CUT



Experimental Results ...

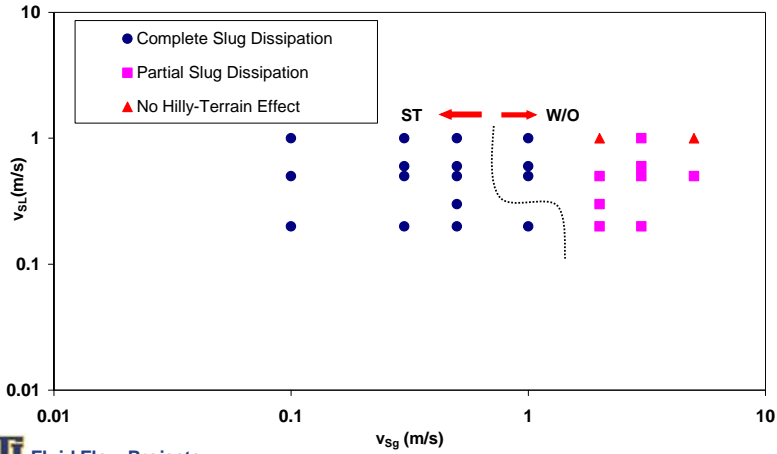
SLUG DISSIPATION at DOWNWARD INCLINED SECTION for 60% WATER CUT



Experimental Results ...



SLUG DISSIPATION at DOWNWARD INCLINED SECTION for 80% WATER CUT



Videos



Data Processing

- ◆ Data Processing Big Challenge
- ◆ Data Collected for 10 Minutes at Various Frequencies for 14 Laser Sensors and 6 Capacitance Sensors
- ◆ Two Large Excel Macro Programs are Written to Process Data

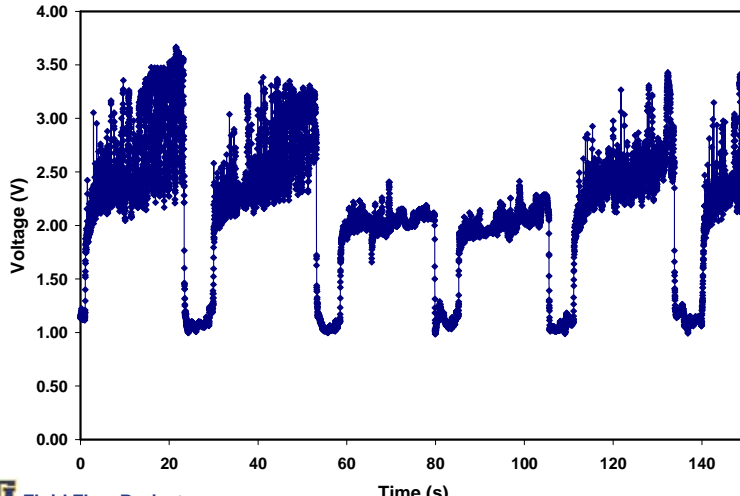
Data Processing ...

- ◆ First Macro
 - Filters Raw Signal
 - Calculate Slug Frequency
 - Record Beginning and End Times for Each Slug for Each Sensor
- ◆ Second Macro
 - Apply Cross-Correlation Technique on Raw Signal
 - Calculate Translational Velocity

Data Processing ...



Raw Output Signal



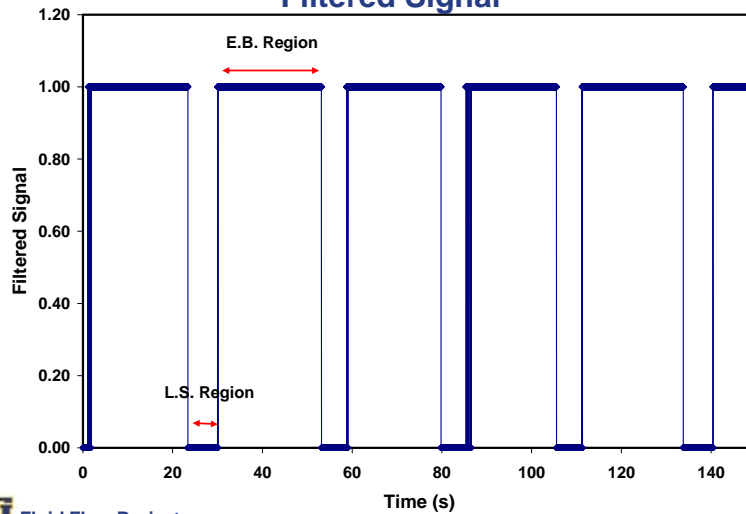
Fluid Flow Projects

Advisory Board Meeting, September 30, 2009

Data Processing ...



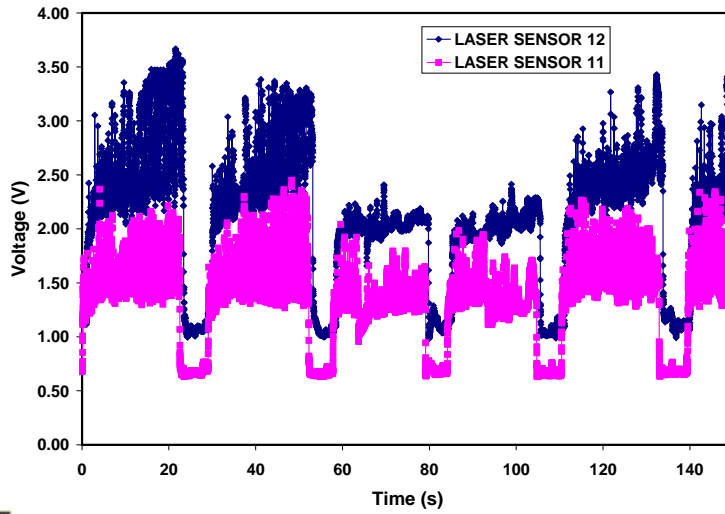
Filtered Signal



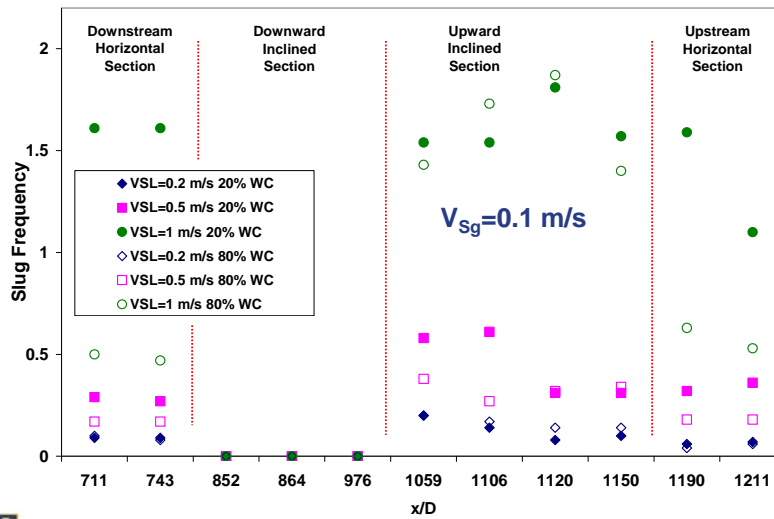
Fluid Flow Projects

Advisory Board Meeting, September 30, 2009

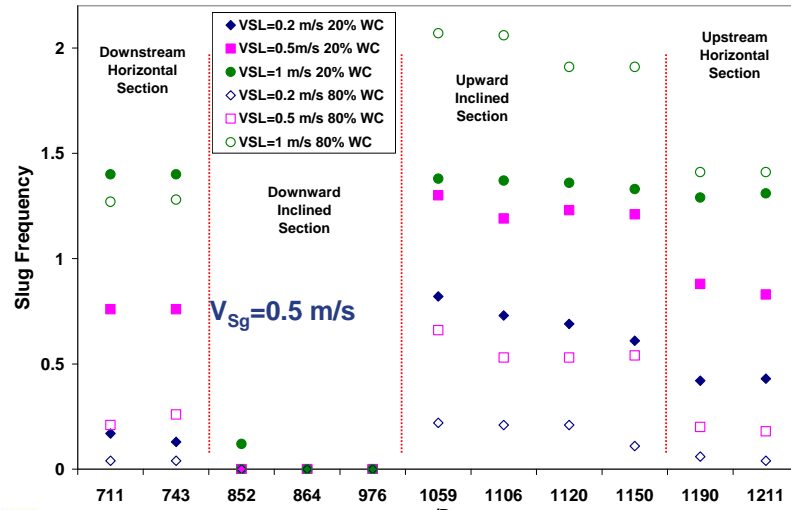
Data Processing ...



Experimental Results ...



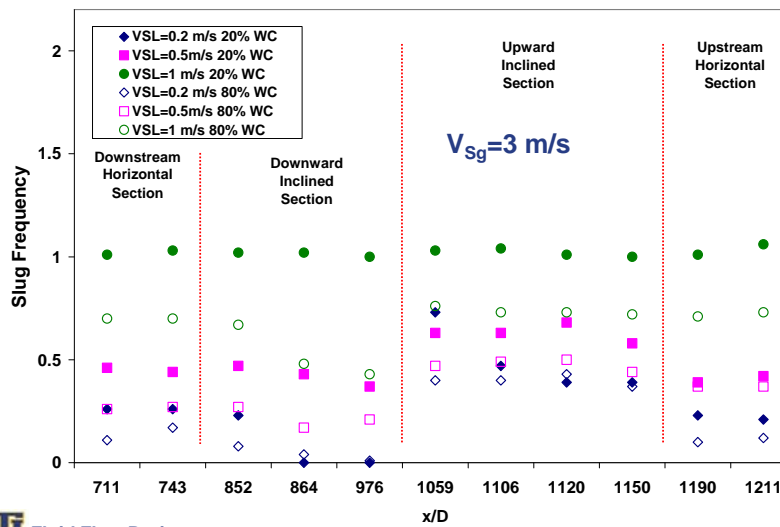
Experimental Results ...



Fluid Flow Projects

Advisory Board Meeting, September 30, 2009

Experimental Results ...



Fluid Flow Projects

Advisory Board Meeting, September 30, 2009

Preliminary Modeling

◆ Challenges:

- Lack of Studies Addressing Gas-Oil-Water Flow in Hilly-Terrain Pipelines
- Significance of Experimental Data
 - ▲ Observation of Physical Phenomena
 - ▲ Validation of Models

◆ Identified Flow Regions of Slug Initiation, Growth and Dissipation with Mixing Status of Liquid Phases

Preliminary Modeling ...

◆ Testing and Modification of Existing Two-Phase Slug Initiation and Dissipation Model (Underway)

- Zhang (2000) Model Taken as Reference for Three-Phase Flow Study
 - ▲ Requires Experimental Data for Closure Relations
 - ▲ Slug Tracking Based on Slug Length

Preliminary Modeling ...

- Investigate Effects of:
 - ▲ Phase Distribution on Slug Characteristics
 - ▲ Slip Velocity

Project Schedule

- | | |
|---------------------|---------------|
| ◆ Model Development | December 2009 |
| ◆ Model Validation | December 2009 |
| ◆ Final Report | December 2009 |

Questions & Comments



Slug Flow Evolution of Gas-Oil-Water Flow in Hilly-Terrain Pipelines

Gizem Ersoy Gokcal

PROJECTED COMPLETION DATES:

Literature Review	Completed
Facility Modifications	Completed
Preliminary Testing	Completed
Testing	Completed
Data Analysis	Completed
Model Development	December 2009
Model Validation	December 2009
Final Report	December 2009

Objective

The general objectives of this project are:

- to conduct experiments on three-phase gas-oil-water flow in hilly-terrain pipelines,
- to develop closure models for three-phase slug initiation, dissipation and mixing status of phases,
- to validate developed closure models with experimental results.

Introduction

In the petroleum industry, slug flow is the most complex and dominant flow pattern in horizontal and near-horizontal pipes. Numerous studies have been carried out on slug flow in pipelines. Although slug flow in horizontal and inclined pipes has been studied extensively, slug flow in hilly-terrain pipelines which are common in both onshore and offshore production and transportation systems, is still not completely understood.

A hilly-terrain pipeline is a pipeline consisting of horizontal, upward inclined, and downward inclined sections. The standard engineering design method for hilly-terrain pipelines has been to divide the pipeline into various sections of constant slopes, and apply steady state flow models to simulate flow behavior in each section. However, the lack of understanding of how flow characteristics change when these sections are interconnected in hilly-terrain pipelines, prevents enhancing pipeline and downstream facility designs. Some of the most

common problems hilly-terrain pipeline causes are operational problems, flooding of downstream facilities, severe pipe corrosion and structural instability of the pipeline, as well as production loss and poor reservoir management due to unpredictable wellhead pressures.

With the challenging field conditions, three-phase gas-oil-water flow becomes more common in oil production. The understanding of three-phase flow is crucial for flow assurance problems such as hydrates, emulsions and paraffin deposition. Corrosion and erosion also depend on the characteristics of three-phase flow in pipes. However, very limited amount of work on three-phase flow has been conducted due to the difficulties of oil-water and gas-liquid flow characterizations.

In the open literature, no studies addressing three-phase slug flow in hilly-terrain pipelines could be found. Since slug flow is such a frequently encountered flow pattern in three-phase flow, a study of slug characteristics for three-phase flow in hilly-terrain pipelines is very crucial for production and pipeline transportation. However, the complexity of slug flow increases from two-phase to three-phase flow. The increased complexity in slug flow necessitates transient solutions, supported by closure models. These closure models should focus especially on the phase distribution throughout the flow, and oil-water interactions, as well as the slug flow characteristics. In this study, these models will be examined and studied.

Experimental Study

Experimental Facility and Flow Loop

The experimental work is being conducted using the TUFFP facility for gas-oil-water flow located at the University of Tulsa North Campus Research Complex. The gas-oil-water facility was previously used by Atmaca (2007) for characterization of oil-water flow in inclined pipes. The facility consists of a closed circuit loop with storage tanks, progressive cavity pumps, heat exchangers, metering sections, filters, test section and separator.

For oil and water phases, there are two storage tanks equipped with valves to control the flow rates. Two progressive cavity pumps are used to maintain the liquid flow rates. There are manual bypass valves after the pumps to obtain low flow rates, and pressure relief valves for excessive pressure control. Copper-tube type heat exchangers are used to control the temperature of the fluid during the tests. After the heat exchangers, manual bypass valves allow the fluids to be pumped back to the respective tanks.

Two separate metering sections are equipped with Micro Motion™ Coriolis flow meters to measure mass flow rates and densities of the fluids, and with temperature transducers for monitoring the temperatures of the fluids. Oil and water flow through filters after the metering section. At the inlet of the test section gas, oil and water flow through the mixing tee to form the gas-oil-water three-phase co-current flow. After the fluids flow through the test section, the mixture is directed to the separator where pressure is set at 20 psig.

The test section is attached to an inclinable boom that makes inclined flow in the loop possible. However, during the three-phase hilly-terrain study, the boom will not be used and the part of the flow loop that is mounted on the boom stay horizontal.

Significant modifications are needed to flow loop to make enough space for the hilly-terrain section and instrumentation. The original gas-oil-water flow loop consisted of two 21.1-m (69.3-ft) long runs connected with a U-shaped bend to reduce the disturbance of the flow pattern due to a sharp turn. The current test section consists of a 21.1-m (69.3-ft) long upstream branch and a 46.7-m (153.2-ft) long downstream branch connected with a 1.2-m (4-ft) long U-shaped PVC bend as shown in Fig. 1. Both of the branches are made of transparent pipes with 50.8-mm (2-in.) diameter.

The upstream branch of the test section consists of a 13.8-m (45.3-ft) long flow developing section ($L/D=272.0$), two pressure drop sections 1.17-m (3.83-ft) and 2.79-m (9.3-ft) long, one long pressure drop section combining the two short sections, and one 3.1-m (10.2-ft) long fluid trapping section ($L/D=108$). The entire upstream branch is placed on the boom.

The downstream branch of the test section consists of a 13.8-m (45.3-ft) long flow developing section ($L/D=272.0$), a 6-m (19.7-ft) long horizontal section with two short pressure drop sections 4.2-m (14-ft) and 2.13-m (7-ft) long, in addition to a 21-m (68.9-ft) long hilly-terrain section ($L/D=413.4$) followed by a 6-m (19.7-ft) long horizontal section.

The hilly-terrain section simulates a hilly-terrain unit of 9.5 m (31.3 ft) downhill followed by a 1.9 m (6.2 ft) horizontal and 9.5 m (31.3 ft) uphill sections. The inclination angles are $\pm 1^\circ$, $\pm 2^\circ$ and $\pm 5^\circ$ for the valley configurations.

The horizontal section immediately downstream of the hilly-terrain section was designed and built similar to the horizontal section immediately upstream of the hilly-terrain section.

The 21.1-m long section of the downstream branch is placed on the inclined boom as in the original gas-oil-water facility. The rest of the downstream branch, which is 25.6 m long, is supported by an aluminum base. Schematic diagram of the test section is given in Fig. 2.

Some hazards have been identified through a facility hazard analysis. Polycarbon protective glass is installed around the test section to provide protection in case of a rupture. In addition, the existing equipment such as pumps, flow meters, separator and storage tanks are checked and made operational.

Instrumentation and Data Acquisition

Capacitance sensors, quick closing valves temperature transducers, laser sensors, and pressure and differential pressure transducers are installed along the facility to measure the operating temperature, pressure, differential pressure, total liquid holdup and spatial distribution of the phases.

For data acquisition, Lab View™ 7.1 is used. New hardware, including a high speed data acquisition system is used for absolute and differential pressure transducers and laser and capacitance sensors. With

the instruments connected to high speed data acquisition system, slug flow characteristics are captured and compared more efficiently. For most of the test matrix, a sampling rate of 100 sample/s is found to be acceptable. For high flow rates, the sampling rate can be increased based on the three-phase slug characteristics. The existing program for the low speed data acquisition is updated for three-phase gas-oil-water flow in hilly-terrain studies. A sampling rate of 1 sample/s is selected to collect data for this data acquisition system. The data logging for each test is ten minutes.

Test Fluids

For the experiments of three-phase flow in a hilly-terrain pipeline, fresh water, air and refined mineral oil were chosen as the testing fluids. The refined oil, Tulco Tech 80, was chosen based on its easy separation. The physical properties of Tulco Tech 80 are given below:

- API gravity: 33.2°
- Density: 858.75 kg/m³ @ 15.6°C
- Viscosity: 13.5 cp @ 40°C
- Surface tension: 29.14 dynes/cm @ 25.1°C
- Interfacial tension with water: 16.38 dynes/cm @ 25.1°C
- Pour point temperature: -12.2°C
- Flash point temperature: 185°C

The properties of Tulco Tech 80 were measured by Chevron labs. As shown in Figs. 3 and 4, the density and viscosity changes with temperature at three different flow rates were measured, respectively.

Experimental Ranges

In this study, 108 tests were conducted for three-phase air-oil-water flow in hilly-terrain pipelines with an inclination angle of $\pm 5^\circ$ for valley configuration. Although the facility can be modified to run at $\pm 1^\circ$, $\pm 2^\circ$ and $\pm 5^\circ$ for the valley configurations, the inclination angle for the hilly-terrain unit is set to $\pm 5^\circ$ due to time constraints. This inclination angle is decided to observe the most significant changes in three-phase slug flow. The testing ranges for the three-phase hilly-terrain experiments on the gas-oil-water flow loop are as follows:

Superficial gas velocity: 0.1-5.0 m/s

Superficial oil velocity: 0.04-1 m/s

Superficial water velocity: 0.02-1 m/s

Water fraction: 20, 40, 60 and 80 %

The lower limits of superficial velocities were decided on by the accuracies of the Micro Motion™ flow meters. The higher limits were set by the pressure gradient and facility limits.

The test matrix was arranged in order to include both the flow regime transition from stratified to slug flow and the phase distributions from low water cut to high water cut. For each water cut value, twenty seven data points were taken.

The observed three-phase flow patterns based on the test matrix for this study are Intermittent-Stratified (IN-ST), Intermittent-Oil Continuous (IN-OC) and Intermittent-Water Continuous (IN-WC) as described in Keskin et al (2007).

Test Program

A typical test program for gas-oil-water flow in a hilly-terrain pipeline starts with varying the gas flow rate, keeping the oil and water flow rates and water fraction constant. Then, tests are repeated for several oil and water flow rates at constant water fraction, and continued with various water fractions.

Uncertainty Analysis

Experimental data are crucial to understand and analyze the physical process. Therefore, the quality of the data should be investigated before drawing any conclusions on the behavior of the system. Every measurement inherits error by nature. “Error is the difference between the measurement and the true value” (Dieck, 2002). However, the true value of the error is not known in any measurement. Uncertainty analysis is used as a method to estimate the limits of the error and show the reliability of the experimental data.

An error consists of random error (precision) and systematic error (bias). Random error is related to the scattered data around its average value. Random error can be represented by a distribution such as Normal, Gaussian, etc. Systematic error is the difference between the average measured value and the true value. Systematic error is constant during experiments and can not be observed in the data. Sources of systematic error are calibration errors, scale-reading errors, and data acquisition errors. Based on errors, random uncertainty estimates the limits of random errors and systematic uncertainty

estimated the limits of systematic errors. The combination of random and systematic uncertainty analysis shows the reliability of the experimental data.

In this study, uncertainty analysis on calculated parameters is also conducted by applying uncertainty propagation. In the following subsections, random, systematic and combined uncertainty and uncertainty propagation are explained briefly.

Random Uncertainty

When measurement of a parameter is repeated N times, a population with N points is obtained. The sample standard deviation of this population is calculated as follow:

$$S_x = \sqrt{\frac{\sum_{i=1}^N (X_i - \bar{X})^2}{N-1}} \quad (1)$$

The sample standard deviation S_x of the data shows the scattering of the data around its average in the N data points. In data analysis, researchers are more interested on the scatter of the mean values. The standard deviation of population average is calculated with the following equation,

$$S_{\bar{X}} = \frac{S_x}{\sqrt{N}} \quad (2)$$

$S_{\bar{X}}$ is called as the random uncertainty with a confidence level of 68%. Since for uncertainty analysis, sample data is used instead of total population, a ‘‘Student’s t ’’ distribution is selected for the desired accuracy. With a selected 5% significance level, the random uncertainty can be stated as follows: $\bar{X} - t_{95} S_{\bar{X}} \leq X \leq \bar{X} + t_{95} S_{\bar{X}}$. This means that the difference between the measured and the true values is expected to be within a specified range, $\pm t_{95} S_{\bar{X}}$, 95 times out of 100.

Systematic Uncertainty

Because of their nature, systematic errors are constant for the duration of experiments. Their effects can not be observed or detected in the experimental data. Therefore, experimental data can not be used for systematic uncertainty. Systematic errors results from various error sources. For this

study, only calibration of instruments is considered as major sources of uncertainty. For pressure, differential pressure, and temperature measurements, the systematic uncertainty was calculated from calibration errors in this study. For liquid holdup measurements the systematic uncertainty was estimated based on experience.

Each source of the elemental systematic uncertainty, b_i , needs to be combined by using the following equation,

$$B_R = \left[\sum_{i=1}^N (b_i)^2 \right]^{1/2} \quad (3)$$

B_R is the combined systematic uncertainty component of the uncertainty analysis. The systematic uncertainty is always assumed to have a 95% confidence level.

Combination of Random and Systematic Uncertainties

When reporting the experimental data, a combination of random and systematic uncertainties is calculated and presented to describe the quality of data. The combined uncertainty can be calculated by:

$$U_{95} = \pm t_{95} \left[(B/2)^2 + (S_{\bar{X}})^2 \right]^{1/2} \quad (4)$$

To apply the formula and combine uncertainties, the confidence level of each uncertainty should be the same and be in the desired confidence level. In the uncertainty analysis the desired accuracy and the systematic uncertainty has a confidence level of 95%.

On the other hand, random uncertainty ($S_{\bar{X}}$) has a confidence level of 68%. First, the systematic uncertainty is divided by 2, which is the Student’s t value with infinite degree of freedom to convert 95% to 65%. After the combined uncertainty is calculated, the t_{95} is used to convert the combined uncertainty confidence level to the 95%. It should be noted that the uncertainty values presented with this analysis shows the maximum possible uncertainties during all the experiments.

Uncertainty Propagation

When a parameter is calculate from measured parameters, the uncertainties of the measured parameters propagate for the calculated parameter. There are three common methods to calculate uncertainty propagation: the Taylor’s Series uncertainty propagation, ‘‘Dithering’’ and Monte

Carlo Simulation. In this uncertainty analysis, Taylor's series uncertainty propagation was performed for superficial velocities.

If y is a function of independent variables a, b, c, \dots , the uncertainty of y will be described as a function of independent uncertainties of a, b, c, \dots , and are expressed as follows:

$$U_y = \sqrt{\left[\left(\frac{\partial y}{\partial a}\right)^2 (U_a)^2 + \left(\frac{\partial y}{\partial b}\right)^2 (U_b)^2 + \left(\frac{\partial y}{\partial c}\right)^2 (U_c)^2 + \dots\right]} \quad (5)$$

Table 1 shows the uncertainty analysis results for the measurements in gas-oil-water hilly-terrain facility.

Experimental Results

Experiments on hilly-terrain effects on three-phase slug flow characteristics are conducted. Experimental data contains visual observations, differential pressure, average holdup, slug frequency and length. Observed three-phase flow patterns, pressure drop and liquid holdup were presented at the spring of 2009. In the following subsections, the changes in slug characteristics vs. water cut are presented and discussed.

Three-Phase Flow Patterns

Three-phase gas-oil-water slug flow experiments have been conducted for 20, 40, 60 and 80% water cuts at various flow rates. Three-phase flow patterns have been observed using the video system at the facility. Three-phase flow pattern maps for the horizontal section before hilly-terrain section are shown in Figs. 5-8. For the operational water cuts, slug dissipation at the downward inclined section is shown in Figs. 9-12. For the slug dissipation analysis, flow pattern maps are divided into three categories.

The first category, Complete Slug Dissipation, is the most common case. It is observed mainly at low and moderate flow rates. In this category, slug flow completely dissipates along the downhill section of the hilly-terrain unit. Most of this category shows Intermittent-Stratified three-phase flow at the horizontal section before the hilly-terrain section. For the Partial Slug Dissipation region, as the second category, the slug flow still survives at downhill section. However, slug frequency decreases. For high superficial gas and liquid velocities slug flow is not affected significantly by the downward inclination. This region corresponds to No Hilly-

Terrain Effect as the third region. For the second and third category, liquid phases mix and result in oil and water continuous cases based on the water cut. For the operational conditions and pipelined geometry, it has been observed that none of the Intermittent-Stratified cases at horizontal section before the hilly-terrain section could maintain slug flow at the downward inclined section.

Slug Frequency

The three-phase slug flow characteristics are investigated by using laser and capacitance sensors in addition to the cameras. The slug characteristics are measured with a sampling frequency of 100 Hz per sensor for time duration of 600 s to acquire statistical information. Due to the large amount of experimental data obtained by the laser and capacitance sensors, two Excel macro programs are developed and used to analyze the data automatically.

During the three-phase slug flow tests, it has been observed that air entrainment at the slug body increases with superficial gas velocity. The existence of the air bubbles in slug flow effects the performance of the sensors by creating jumps on the output signals. A disregard value is defined to filter these jumps from the output signals in the first Excel macro program. Before running the program for each test, the raw output signals are examined to determine voltage thresholds that are used to differentiate between the slug body and elongated bubble for each sensor output. It is found from the experimental results that the output signal for liquid slug region is higher than elongated bubble region for oil continuous flow. On the other hand, the output signal for elongated bubble region is higher than slug region for the experiments with water continuous flow. For oil continuous cases, the first macro then identifies the liquid slug region as "1" when the output signal is higher than the specified threshold value. When the output signal is lower, they are regarded as elongated bubble region and registered as "0". Based on this analysis, slugs are counted by the program. For the water continuous cases slug region is defined as "0" and elongated bubble region as "1". The rest of the analysis is similar to oil continuous cases. During the signal process, slugs are assumed and analyzed as rectangles (horizontal lines) and film regions as horizontal lines (rectangles) for the oil (water) continuous case. As a final step, the macro determines slug frequency by dividing the number of slugs detected by the laser or capacitance sensors by the test duration and records the time that each slug passes from each sensor.

The time differences that the slug front and back takes to travel from one sensor to another are also detected and given as an output by the first Excel macro program. The time difference that is taken by a slug front and back to travel from one sensor to another is defined as Δt_f and Δt_b , respectively. Since the distance between each two sensors are known, slug front and back velocities can be calculated as

$$v_f = \frac{\Delta x}{\Delta t_f} \quad (6)$$

and

$$v_b = \frac{\Delta x}{\Delta t_b}, \quad (7)$$

respectively. Slug growth and dissipation can be analyzed with the relative magnitudes of the slug front and back velocities to each other. No change in slug length (or frequency) can be observed if the slug front and back velocities are similar to each other. Slug growth is observed in the cases where slug front velocity is bigger than the slug back velocity. Slugs dissipate when the slug back velocity is bigger than slug front velocity and there is enough pipe length for the flow to be developed fully.

In the second Excel macro program, cross correlation technique is used to find critical time lag to calculate the slug translational velocity. The cross-correlation is a standard method to measure of the extent to which two signals (or series) correlate with each other as a function of the time displacement between them.

Consider two time series, $x(t_n)$ and $y(t_n)$, where $n = 0, 1, 2, \dots, N-1$. The cross-correlation coefficient is defined as:

$$R_{xy}(\tau) = \frac{C_{xy}(\tau)}{\sqrt{C_x(0)C_y(0)}}, \quad (8)$$

If the signals are identical, the cross correlation will be one, and if they are completely dissimilar, the cross correlation will be zero. In Eqs. 9 and 10, $x(\tau)$ and $y(\tau)$ are time series data when τ is the temporal lag. When the time series $x(\tau)$ and $y(\tau)$ are identical, the correlation coefficient is called auto-correlation coefficient,

$$C_{xy}(\tau) = \frac{1}{N-\tau} \sum_{n=1}^{N-\tau} x(t_n)y(\tau+t_n). \quad (9)$$

$$C_x(0) = \frac{1}{N} \sum_{n=1}^N x(t_n)^2 = \overline{x^2}. \quad (10)$$

The critical time lag is defined by the value of τ where the cross correlation coefficient is maximum. Based on this analysis, the second Excel macro program finds the critical time lag and translational velocity for each test and for each sensor couples. The output signals from laser and capacitance sensors are used for cross-correlating between different pairs of laser sensors and capacitance sensors that are at the same segment of the test facility, i.e., between LSR1-LSR2, LSR3-LSR4, LSR5-LSR6, LSR5-LSR7, LSR8-LSR9 and CS3-CS4. Then, the translational velocity is easily calculated from the following equation and by the second program automatically:

$$v_t = \frac{\Delta L_{LS2 \rightarrow LS1}}{\tau}. \quad (11)$$

The time difference for a slug to travel from one sensor to another is defined as Δt_s and calculated by the first Excel macro program for each test. Slug length is calculated by multiplying translational velocity with Δt_s and can be expressed as:

$$l_s = \Delta t_s * v_t. \quad (12)$$

Figures 13-15 show the results of processed laser sensors' data along the test facility for various superficial gas and liquid velocities for 20 and 80% water cuts. Figure 13 shows the resultant frequency changes for the superficial gas velocity of 0.1m/s. This case shows effect of water cut at low superficial gas velocity. For all of the tests in this figure, intermittent-stratified three-phase flow is seen at the horizontal section before the hilly-terrain section. At the downward inclined section, complete slug dissipation is observed for all cases. With the beginning of upward inclined section, slugs are initiated with the liquid accumulation at the elbow section. However, most of the initiated slugs cannot survive until the end of upward inclined section and liquid fallback is observed. Therefore, at the upward inclined section, first an increase and then a decrease in slug frequency is observed. The decrease in frequency is observed to be at the higher parts of the upward inclined section for the higher liquid velocity. For the low operational conditions, water cut effect on slug frequencies is not significant. However, effect of water cut is more visible when superficial liquid velocity is increased.

When the superficial gas velocity is increased, the effect of water cut on slug frequency can be seen more clearly in Fig. 14. For the tests with $V_{SL}=0.2$ and 0.5 m/s for 20% water cut, intermittent-stratified flow was observed for the downstream horizontal section. On the other hand, the rest of tests show oil and water continuous slug flow for 20% and 80% water cut, respectively. For the lower superficial liquid velocities of 0.2 and 0.5 m/s, the trends of frequencies are similar for each water cut. However, for $V_{SL}=1$ m/s, frequency trends for both water cuts show different behavior. The oil-water mixing status between two cases might result in this observation.

When superficial gas velocity increases, water cut effects start to become less significant. In Fig. 15, with the exception of the high superficial liquid velocity test for 20 % water cut, partial slug dissipation is observed at downward inclined section. For the upward section close to the elbow, slug frequency increases due to slug initiation. Slug frequency stays constant along the upward section due to the operational conditions. When the frequency values before and after the hilly-terrain section are compared, the change in frequency is less significant than the tests with lower superficial gas velocities. For the test with $V_{SL}=1$ m/s with 20% water cut, three-phase slug flow maintains a constant frequency along the pipe which is not affected by the hilly-terrain geometry.

Preliminary Modeling Study

As it is briefly discussed at the previous section, different cases of flow were identified for slug dissipation, initiation and growth along the hilly-terrain section (Al-Safran, 2003). As a first step to model three-phase effects on slug growth and initiation mechanisms, these flow cases will be improved by including the three-phase flow patterns.

At low flow rates, it has been observed that phases are mostly mixed in the slug body and segregated fluids exist at the film region. With the increase in water cut, wave growth and coalescence mechanisms in the film region will be analyzed and slug initiation models will be investigated. Although slug tracking model by Taitel and Barnea (1999) can predict the two-phase slug length distribution along a hilly-terrain pipeline, it requires measured slug length distributions at the entrance and at the lower dip to simulate the flow behavior. In an earlier study by Zheng (1991), the effects of a hilly-terrain pipeline configuration on two-phase flow characteristics are

investigated. A simple slug-tracking model is proposed that follows the behavior of all individual slugs for a rather simple geometry consisting of a single hilly-terrain unit. His model is based on sink/source concept at the pipeline connections, where an elbow accumulates liquid as a sink and releases liquid as a source. However, the model requires improvement on slug dissipation mechanism. Zhang *et al.* (2000) investigated two-phase slug dissipation in downward flow section of a hilly-terrain pipeline. Experiments were conducted for inclination angles of 1° , 2° , 5° , 10° and 20° . Slug flow in downward inclined pipes was grouped in terms of change in slug frequency. Based on previous studies, Zhang (2000) used the entire liquid film and gas pocket in the film zone as a control volume for developing two-phase slug flow enabling the momentum exchange between slug body and liquid film. Unsteady continuity and momentum equations are derived for the control volume relative to a coordinate system moving with translational velocity, V_t . It is assumed that, the slug frequency of an unsteady slug flow may change while the slug length remains constant. The liquid mass in the disappearing slug units are distributed to each liquid film of the remaining slugs. This two-phase modeling approach for developing slugs will be compared with three-phase experimental data and the continuity and momentum equations will be modified and rearranged for three-phase flow. The analysis of this model is expected to improve the TUFFP unified hydrodynamic model.

For the model development, closure relationships such as liquid holdup in the slug body are needed. Three-phase gas-oil-water slug flow data will be analyzed considering the changes in water cut. Using the experimental findings, the closure models for slug length and frequency, translational velocity, slug holdup will be investigated and developed if possible. These closure models will be integrated into three-phase momentum equations.

Accumulation of water at low spots in pipelines can cause serious corrosion and hydrate problems. As an auxiliary study, water level in downward and upward flow in the hilly-terrain section and the segregation of water phase will be observed and analyzed. At the elbow of the hilly-terrain unit, the water accumulation and critical values of mixture velocity to sweep the water phase will be studied with different water cuts and mixture velocities.

The experimental database on three-phase flow is very limited and the literature shows a lack of studies that address modeling of three-phase gas-oil-water

flow in hilly-terrain pipelines. Therefore, the experimental work plays a significant role in the modeling study. The resulting models will be validated with experimental data and compared with a multiphase flow simulator, OLGA®.

Near Future Activities

The modeling study including the model validation is expected to be finished by December 2009. The final report will also be submitted by December 2009.

Nomenclature

b_i systematic uncertainty from the i th
systematic error source

B_R combined systematic uncertainty
 N number of data point in sample
 S_X standard deviation of a data sample
 $S_{\bar{X}}$ random uncertainty
 t_{95} Student's t
 U_{95} combined uncertainty with 95% confidence
 \bar{X} sample average
 X_i the i th data point in sample

References

- Al-Safran, E.: "An Experimental and Theoretical Investigation of Slug Flow Characteristics in the Valley of a Hilly Terrain Pipeline," Ph.D. Dissertation, U. of Tulsa, Tulsa, OK (2003).
- Atmaca S.: "Characterization of Oil-Water Flow in Horizontal and Slightly Inclined Pipes," M.S. Thesis, The University of Tulsa (2007).
- Dieck, R. H.: "Measurement Uncertainty: Methods and Application," Third Edition, ISA, (2002).
- Keskin, C., Zhang, H.Q., Sarica, C.: "Identification and Classification of New Three-Phase Gas/Oil/Water Flow Patterns," SPE 110221, presented at SPE ATCE, Anaheim, California (2007).
- Taitel, Y. and Barnea, D.: "Slug Tracking in Hilly Terrain Pipelines," Paper Presented in SPE ATCE, Houston, TX (1999).
- Zhang, H.-Q., Al-Safran, E., Jayawardena, S., Redus, C., Sarica, C. and Brill, J.: "Modeling of Slug Dissipation and Generation in Gas-Liquid Hilly-Terrain Pipe Flow," ASME J. Energy Res. Tech., vol. 125, pp. 161-168 (2003).
- Zhang, H.-Q. and Sarica, C.: "Unified Modeling of Gas/Oil/Water Pipe Flow – Basic Approaches and Preliminary Validation," SPE 95749, presented at SPE ATCE, Dallas, TX (2005).
- Zhang, H.-Q., Wang, Q., Sarica, C. and Brill, J.P.: "Unified Model for Gas-Liquid Pipe Flow via Slug Dynamics-Part 1: Model Development," ASME J. Energy Res. Tech., vol. 125 (4), pp.266 (2003).
- Zhang, H.-Q., Yuan, H., Redus, C.L., and Brill, J.P.: "Observation of Slug Dissipation in Downward Flow," presented at ETCE/OMAE 2000, New Orleans, February, 14-17, 2000.
- Zheng, G.: "Two-Phase Slug Flow in Hilly-Terrain Pipelines," Ph.D. Dissertation, U. of Tulsa, Tulsa, OK (1991).

Table 1: Uncertainty Analysis Results for Gas-Oil-Water Hilly-Terrain Facility

Instrument	Random	Systematic	Combined
PT 3	±0.16%	±0.04	±0.35%
PT 4	±0.00%	±0.04	±1.31%
PT 5	±0.00%	±0.04	±1.31%
PT 6	±0.00%	±0.04	±1.36%
PT 7	±0.00%	±0.04	±1.41%
DP 1	±0.01%	±0.04	±2.76%
DP 2	±0.01%	±0.04	±0.01%
DP 3	±0.01%	±0.04	±0.01%
DP 4	±0.01%	±0.04	±1.98%
DP 5	±0.01%	±0.04	±2.81%
DP 6	±0.01%	±0.04	±3.19%
DP 7	±0.01%	±0.04	±2.49%
DP 8	±0.01%	±0.04	±2.98%
DP 9	±0.01%	±0.04	±2.23%
DP 10	±0.01%	±0.04	±2.79%
TT 5	±0.03%	±1.02%	±2.10%
TT 7	±0.04%	±0.68%	±0.94%
LSR 1	±0.03%	N/A	±0.03%
LSR 2	±0.04%	N/A	±0.04%
LSR 3	±0.03%	N/A	±0.03%
LSR 4	±0.04%	N/A	±0.04%
LSR 5	±0.03%	N/A	±0.03%
LSR 6	±0.76%	N/A	±0.76%
LSR 7	±0.02%	N/A	±0.02%
LSR 8	±0.10%	N/A	±0.10%
LSR 9	±0.06%	N/A	±0.06%
LSR 10	±0.03%	N/A	±0.03%
LSR 11	±0.02%	N/A	±0.02%
LSR 12	±0.02%	N/A	±0.02%
LSR 13	±0.03%	N/A	±0.03%
LSR 14	±0.07%	N/A	±0.07%
CAP 3	±0.51%	N/A	±0.51%
CAP 4	±0.46%	N/A	±0.46%
CAP 5	±0.10%	N/A	±0.10%
CAP 6	±0.04%	N/A	±0.04%
CAP 7	±0.18%	N/A	±0.18%
CAP 8	±0.77%	N/A	±0.77%
WFM	±0.15%	±0.10%	±0.31%
OFM	±0.17%	±0.10%	±0.35%
GFM	±0.19%	±0.10%	±0.38%
Hw	N/A	±5-10%	±5-10%
Ho	N/A	±5-10%	±5-10%
V _{sw}	±0.05%	±0.10%	±0.12%
V _{so}	±0.05%	±0.10%	±0.11%
V _{sg}	±0.08%	±0.11%	±0.24%

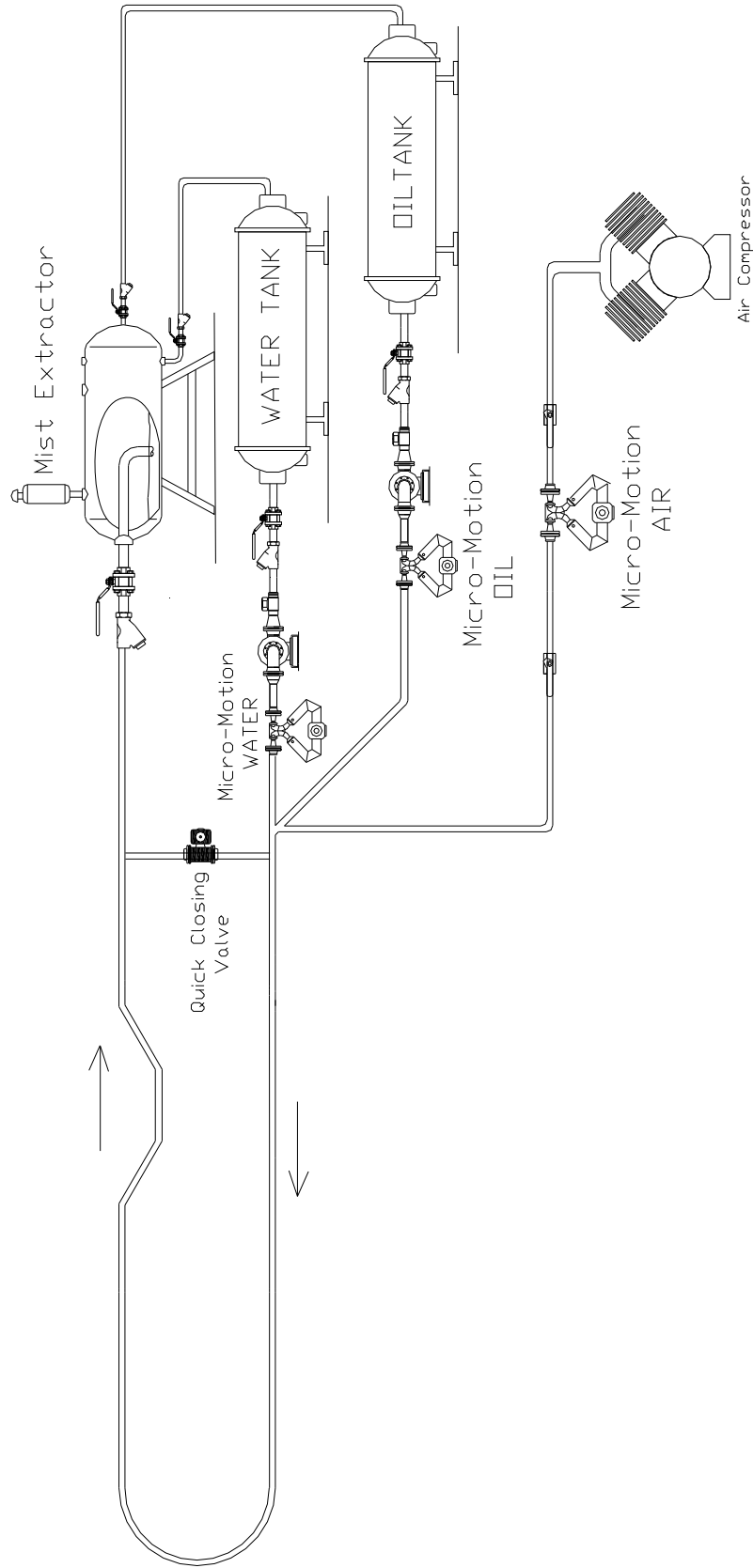


Figure 1: Gas-Oil-Water Facility Schematic

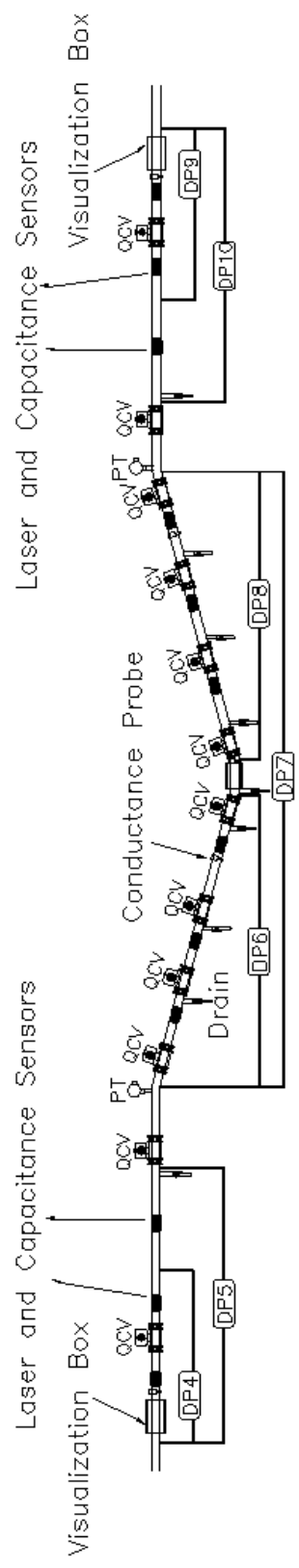


Figure 2: Schematic of Downstream Branch of Test Section

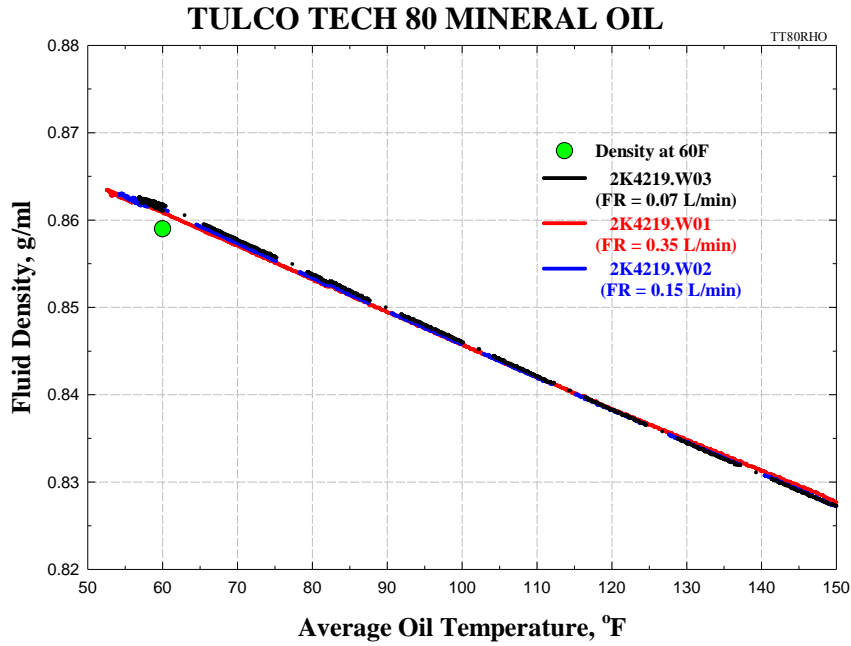


Figure 3: Tulco Tech 80 Oil Density vs. Temperature

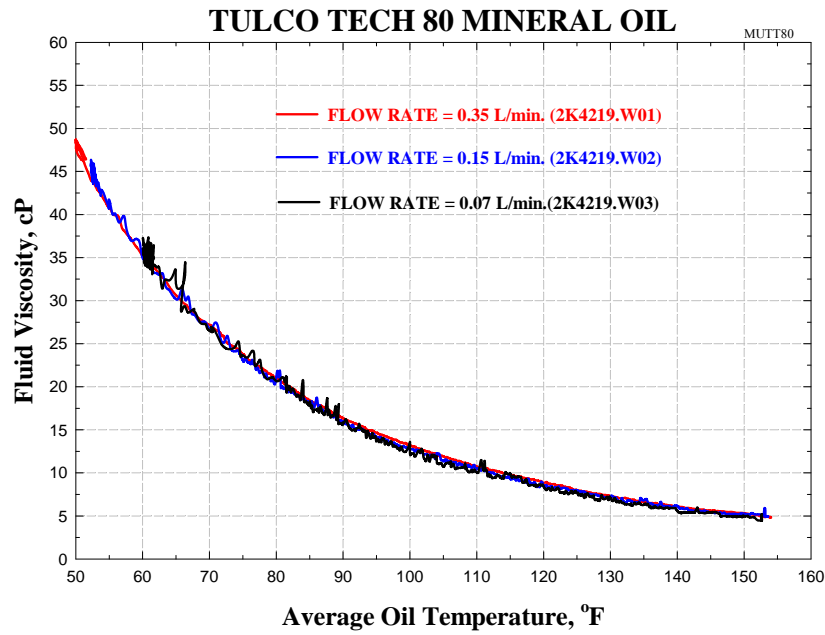


Figure 4: Tulco Tech 80 Oil Viscosity vs. Temperature

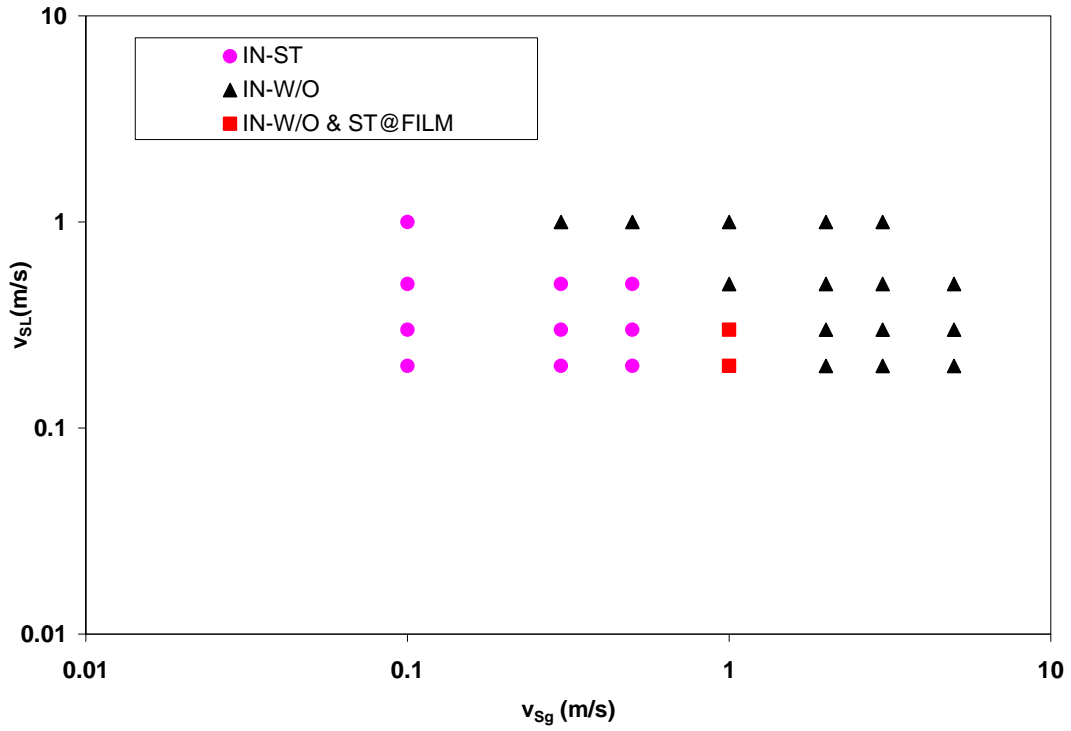


Figure 5: Horizontal Gas-Oil-Water Flow Pattern Map for 20% Water Cut

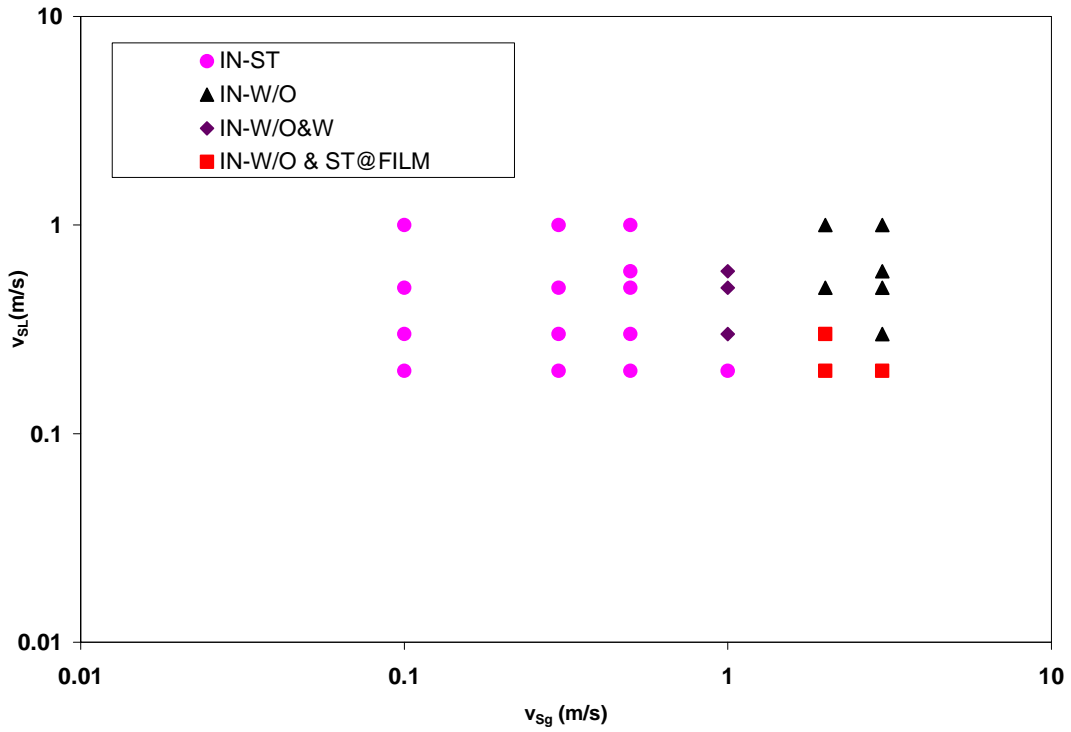


Figure 6: Horizontal Gas-Oil-Water Flow Pattern Map for 40% Water Cut

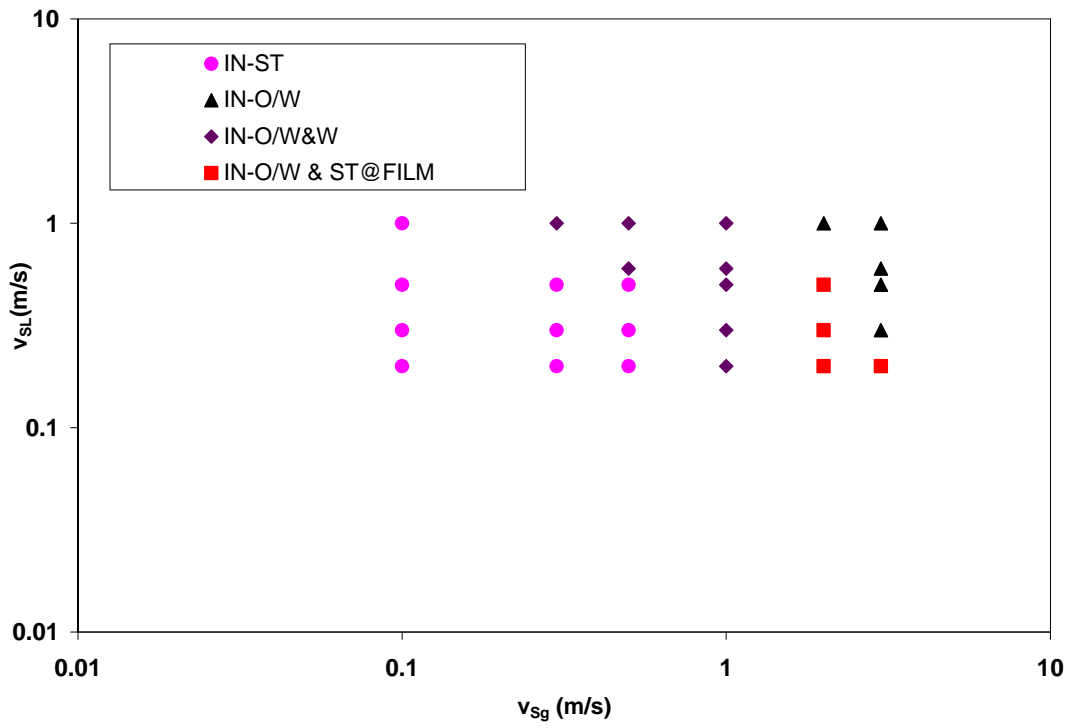


Figure 7: Horizontal Gas-Oil-Water Flow Pattern Map for 60% Water Cut

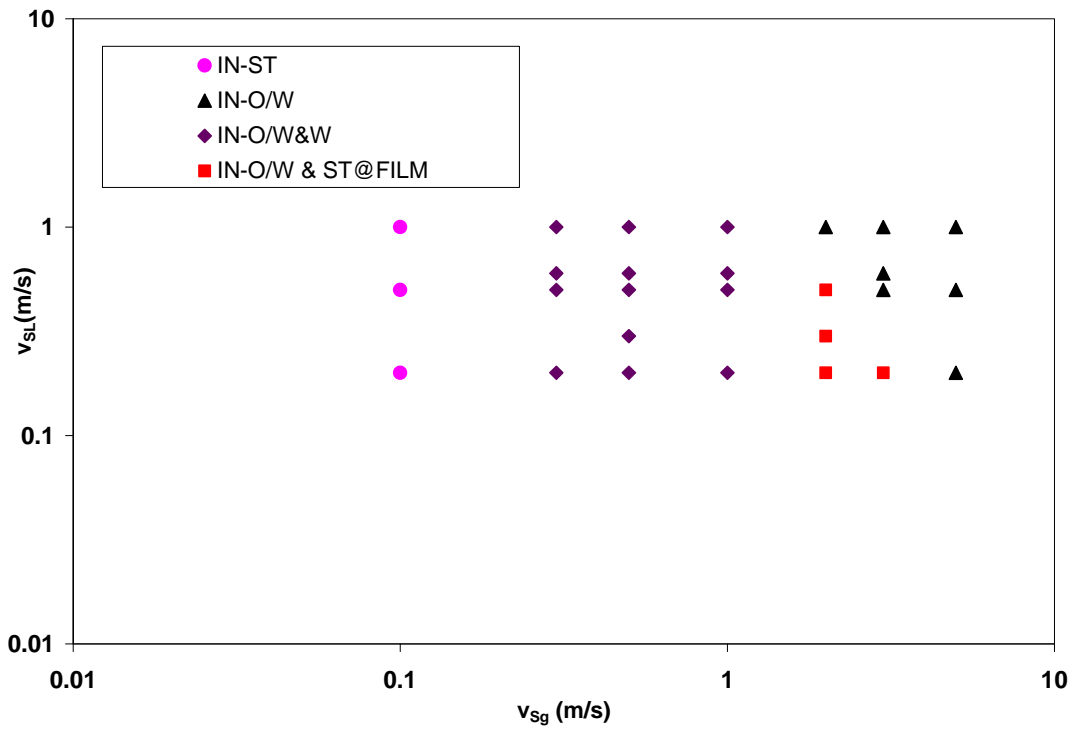


Figure 8: Horizontal Gas-Oil-Water Flow Pattern Map for 80% Water Cut

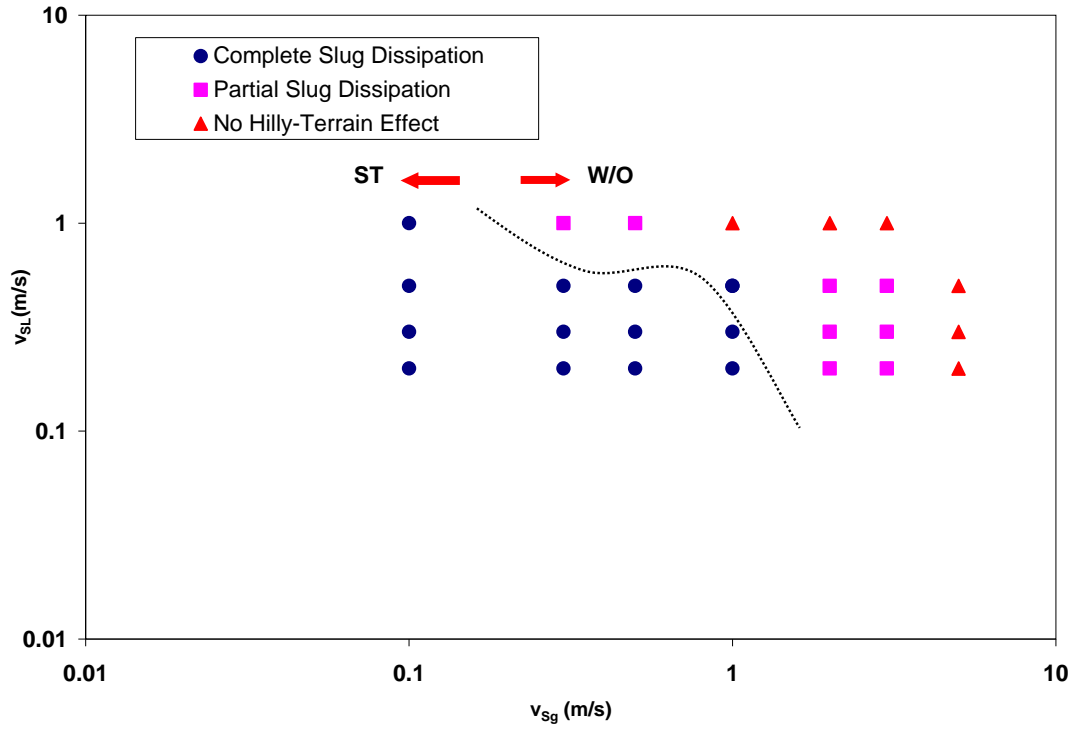


Figure 9: Slug Dissipation at the Downward Inclined Section for 20% Water Cut

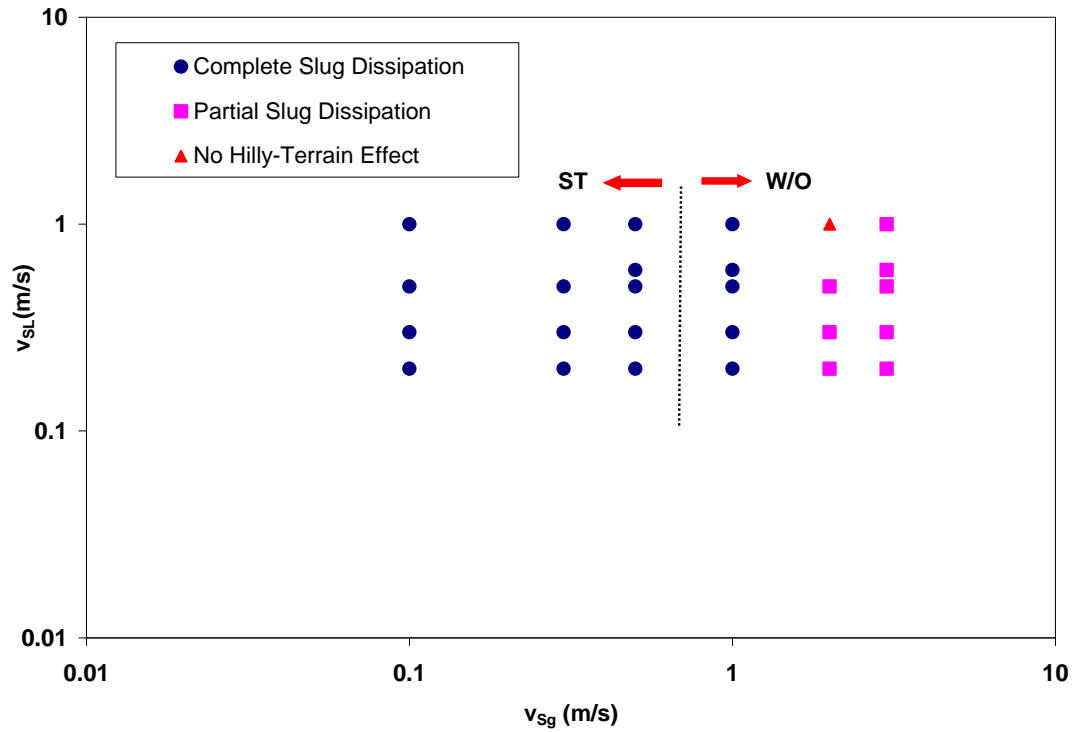


Figure 10: Slug Dissipation at the Downward Inclined Section for 40% Water Cut

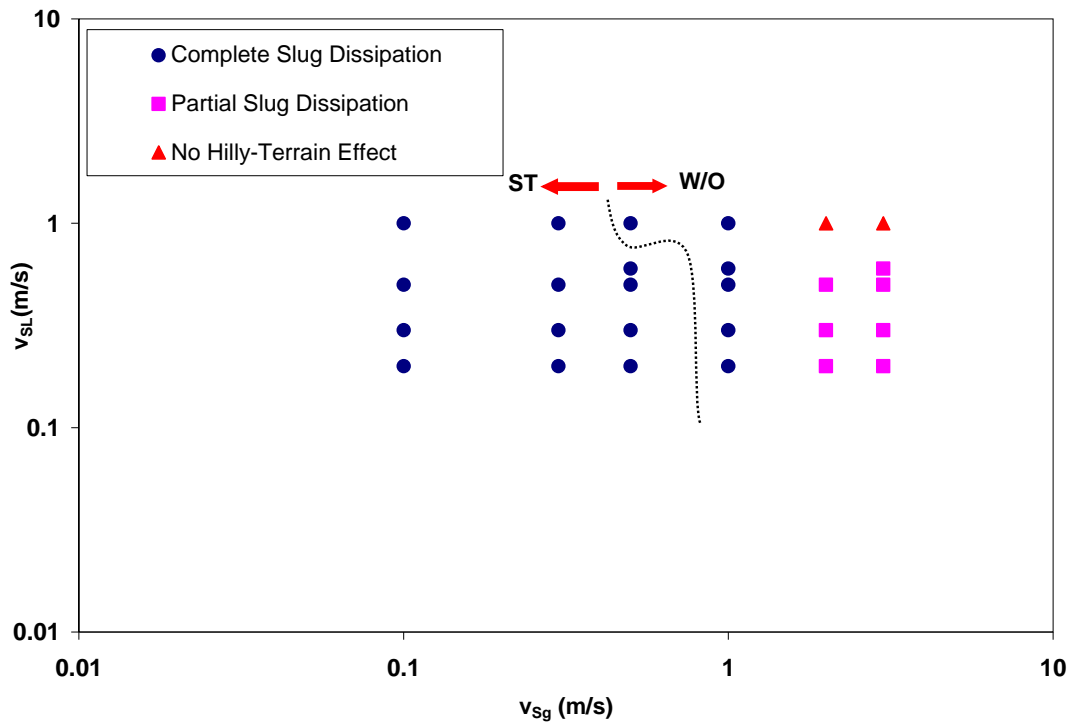


Figure 11: Slug Dissipation at the Downward Inclined Section for 60% Water Cut

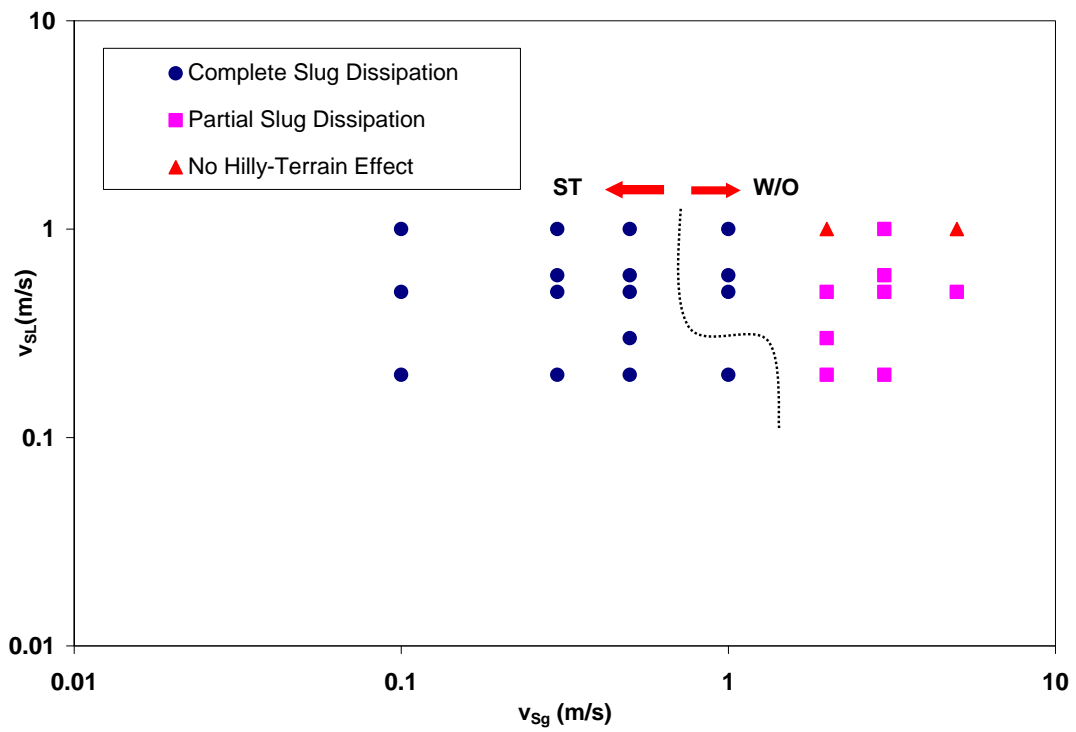


Figure 12: Slug Dissipation at the Downward Inclined Section for 80% Water Cut

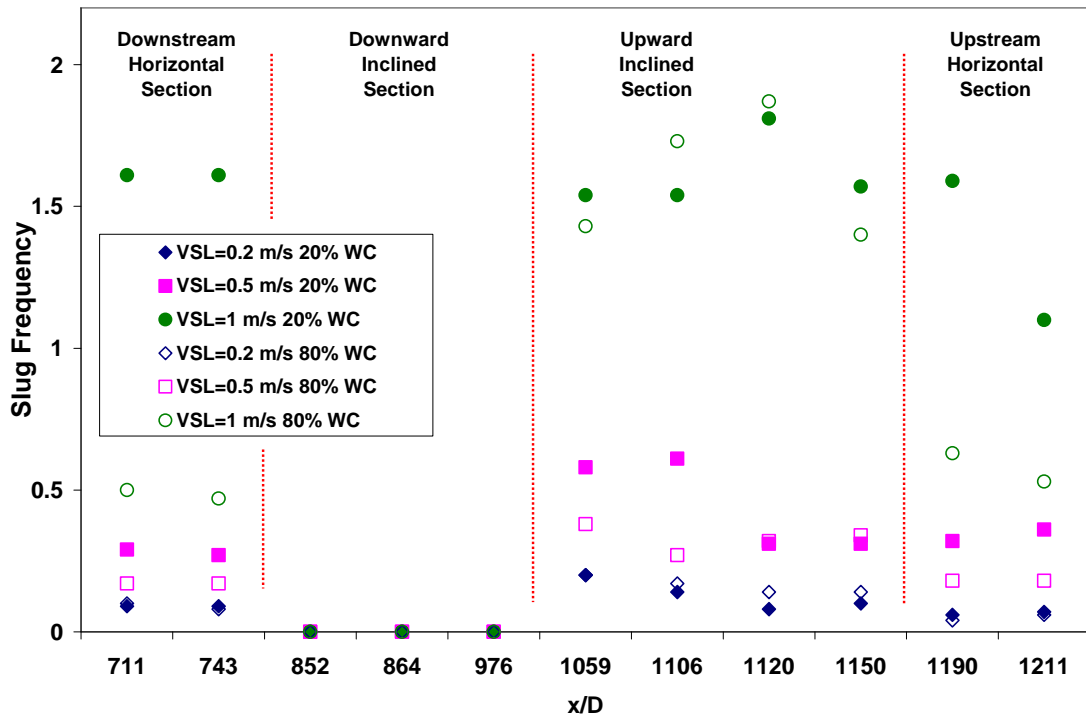


Figure 13: Slug Frequency for $V_{Sg} = 0.1$ m/s

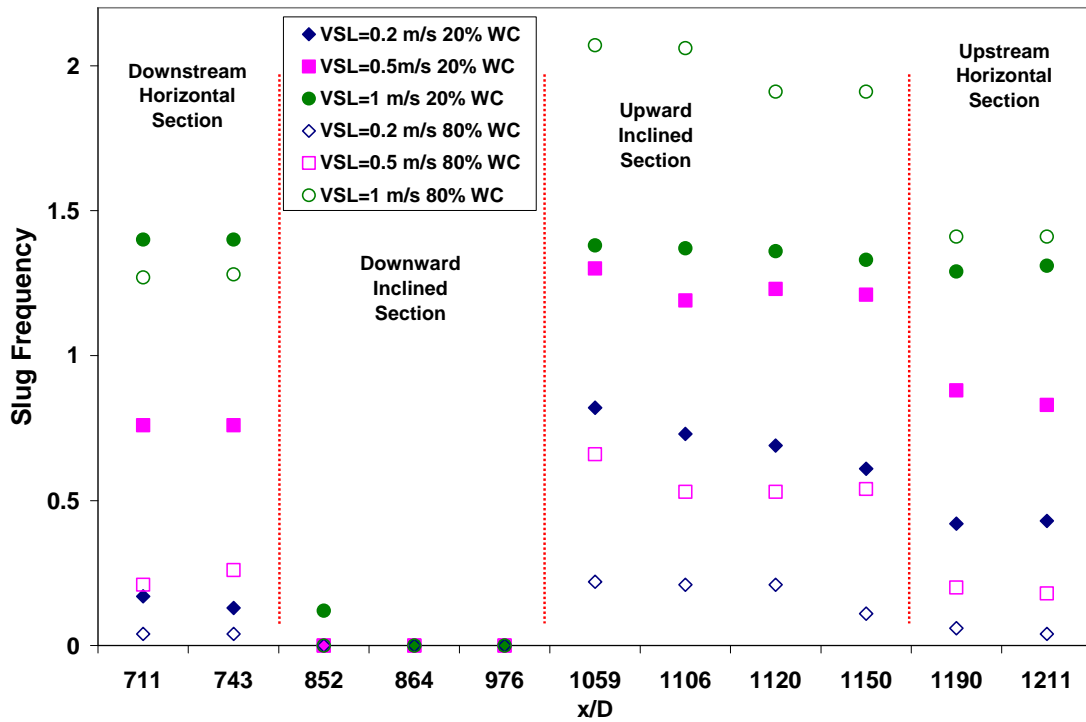


Figure 14: Slug Frequency for $V_{Sg} = 0.5$ m/s

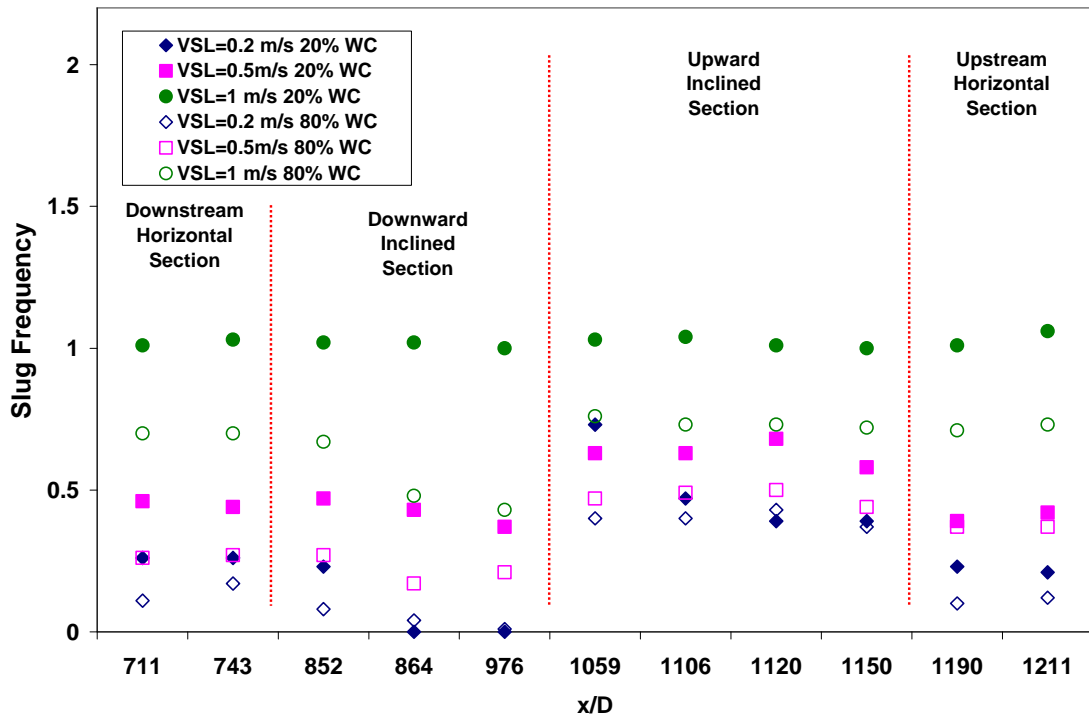


Figure 15: Slug Frequency for $V_{sg} = 3 \text{ m/s}$



Fluid Flow Projects

Executive Summary of Research Activities

Cem Sarica

Advisory Board Meeting, September 30, 2009

High Viscosity Multiphase Flow

- ◆ **Significance**
 - **Discovery of High Viscosity Oil Reserves**
- ◆ **Objective**
 - **Development of Better Prediction Models**
- ◆ **Past Studies**
 - **First TUFFP Study by Gokcal (2005)**
 - ▲ Existing Models Perform Poorly for Viscosities Between 200 and 1000 cp
 - ▲ Significantly Different Flow Behavior
 - ✦ Dominance of Slug Flow
 - **Recent Study by Gokcal (2008)**
 - ▲ New Drift Velocity and Translational Velocity Closure Models
 - ▲ New Slug Frequency Correlation



High Viscosity Multiphase Flow ...



◆ Current Study (Status)

- Slug Liquid Holdup Closure Relationship Development
- Slug Length Closure Relationship Development
- Drift Velocity Study

High Viscosity Multiphase Flow ...



◆ Slug Liquid Holdup

- Literature Review Mostly Complete
- Liquid Holdup Measurement Methods are Under Study
 - ▲ Differential Pressure
 - ▲ Quick Closing Valves

High Viscosity Multiphase Flow ...



◆ Slug Length Study

- Shorter Slug Lengths are experimentally Observed
- Detailed Probabilistic/Deterministic Slug Length Study is Underway

High Viscosity Multiphase Flow ...



◆ Drift Velocity Study

- Diameter Effects on Drift Velocity
 - ▲ 3 in. ID. Tests Completed
 - ▲ No Significant Effect Observed
- Next, 6 in. ID. Tests will be Performed



Fluid Flow Projects

Effects of High Oil Viscosity on Slug Liquid Holdup in Horizontal Pipes

Ceyda Kora

Advisory Board Meeting, September 30, 2009

Outline

- ◆ Objectives
- ◆ Introduction
- ◆ Literature Survey
- ◆ Experimental Facility
- ◆ Experimental Study
- ◆ Near Future Tasks
- ◆ Project Schedule



Objectives

- 
- ◆ Investigate Slug Liquid Holdup for High Viscosity Oil and Gas Flow
 - ◆ Develop Closure Models for Slug Liquid Holdup

Introduction

- 
- ◆ Increase in Oil Consumption
 - ◆ Decline in Discoveries of Low Viscosity Hydrocarbon Resources
 - ◆ Previous Studies Based on Low Viscosity Oils

Introduction ...

- ◆ **Gokcal (2005, 2008) Studies**
 - **Intermittent Flow Observed as Dominant Flow Pattern**
 - **Significant Effect of High Viscosity Oil on Slug Flow Characteristics Observed**
 - **TUFFP Unified Model Modified for High Viscosity Oil-Gas Flow**

Literature Review Summary

- ◆ **Available Multiphase Flow Models Developed for Low Viscosity Liquids**
- ◆ **Few Studies Include Liquid Viscosity Effect on Slug Characteristics**
- ◆ **Limited Experimental Data on High Viscosity Oil Multiphase Flow**

Experimental Facility



 Fluid Flow Projects

Advisory Board Meeting, September 30, 2009

Experimental Facility ...

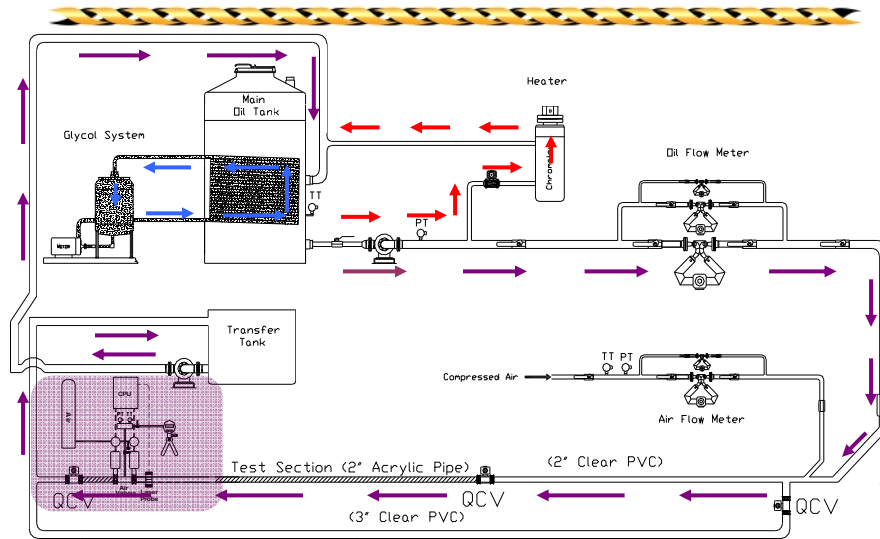
◆ Modifications

- Oil Transfer Tank
- Additional Oil Pump
- 2-in 62-ft Test Section
- 32-ft Clear PVC and 30-ft Acrylic Pipe
- 3-in Clear PVC Return Pipe

 Fluid Flow Projects

Advisory Board Meeting, September 30, 2009

Experimental Facility ...



 Fluid Flow Projects

Advisory Board Meeting, September 30, 2009

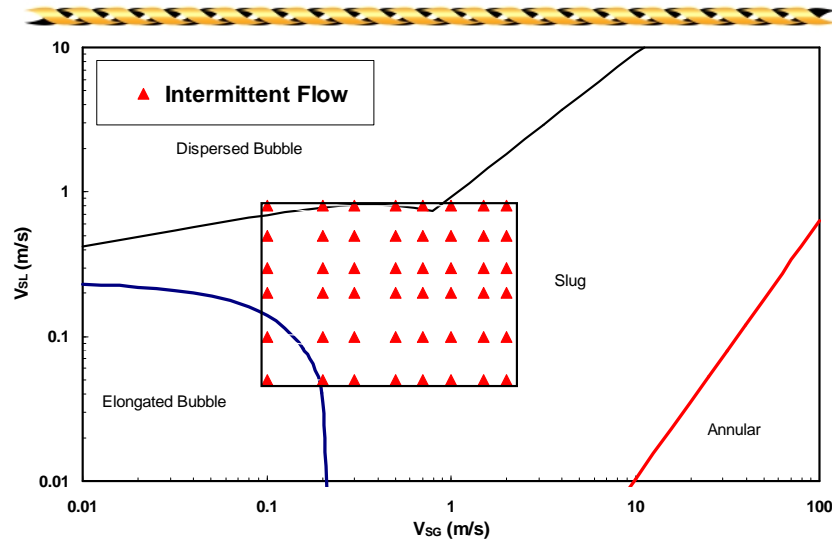
Test Fluids

- ◆ Citgo Sentry 220
 - Mineral Oil
 - API Gravity: 27.6
 - Viscosity: 0.22 Pa-s @ 40 °C
 - Specific Gravity: 0.89 @ 25 °C
- ◆ Air

 Fluid Flow Projects

Advisory Board Meeting, September 30, 2009

Testing Range



Testing Range ...

- ◆ Superficial Liquid Velocity
 - 0.05 – 0.8 m/s
- ◆ Superficial Gas Velocity
 - 0.1 – 2 m/s
- ◆ Temperatures and Viscosities
 - 21.1 – 37.8 °C (70 – 100 °F)
 - 0.587 – 0.181 Pa·s
- ◆ Inclination
 - Horizontal

Experimental Study

- ◆ Quick-Closing Valves
- ◆ Differential Pressure Sensor

Quick-Closing Valves ...

- ◆ No Proper Methods in Literature
- ◆ Non-Intrusive Measurement Technique
- ◆ Easy to Construct
- ◆ Affordable Cost

Quick-Closing Valves



 Fluid Flow Projects

Advisory Board Meeting, September 30, 2009

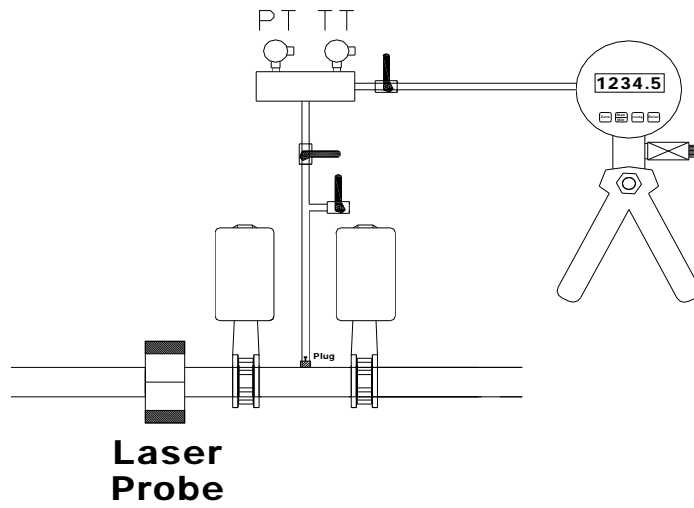
Quick-Closing Valves ...

 [Video](#)

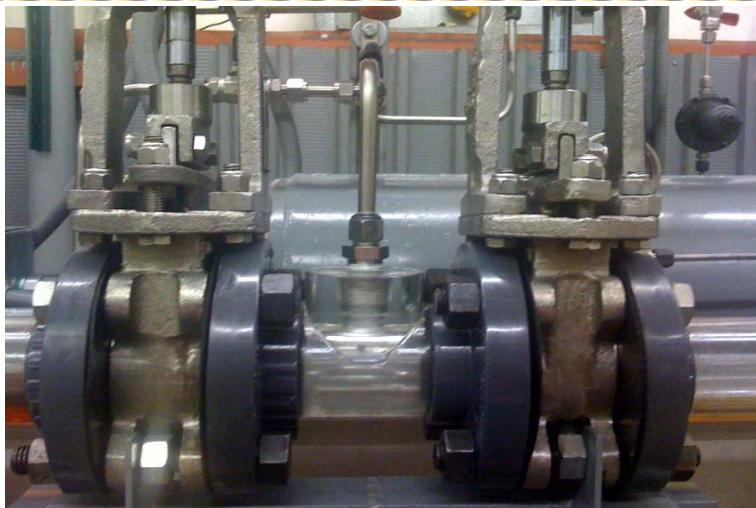
 Fluid Flow Projects

Advisory Board Meeting, September 30, 2009

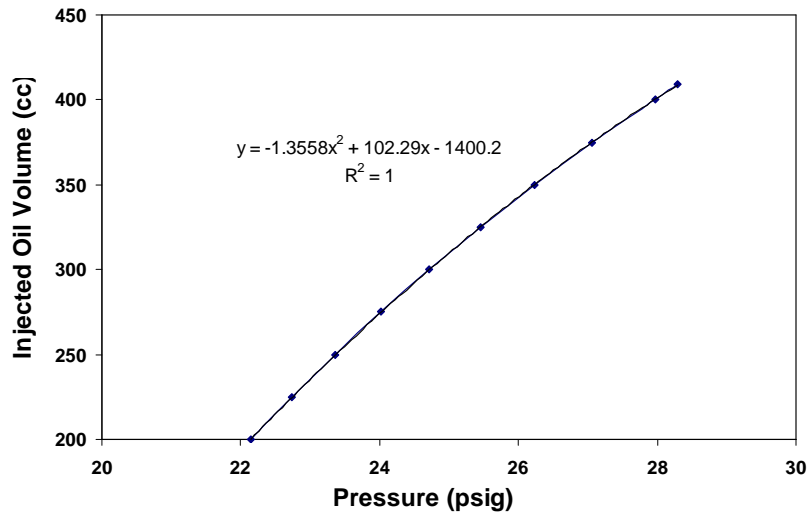
Quick-Closing Valves ...



Quick-Closing Valves ...



Quick-Closing Valves ...

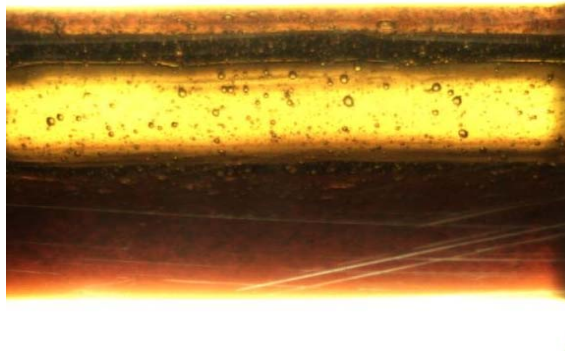


Quick-Closing Valves ...

- ◆ QCVs Close at Same Time
- ◆ Trapping Time of QCVs Adjustable
- ◆ Managed to Capture Only Liquid Slugs
- ◆ Videos Recorded with High Speed Camera

Quick-Closing Valves ...

💧 Liquid Film Height



Differential Pressure Sensor

- 💧 Theoretically Proper for Slug Liquid Holdup Measurements
- 💧 Impulse Line Problem Solved with Flush Diaphragm Pressure Transducers

Differential Pressure Sensor ...



Differential Pressure Sensor ...

- ◆ **Already Built**
- ◆ **Will be Placed Close to Trap Section**
- ◆ **Increase the Number of Data Points**
- ◆ **Better Holdup Prediction for Front and Tail Parts of Liquid Slug**

Preliminary Experiments

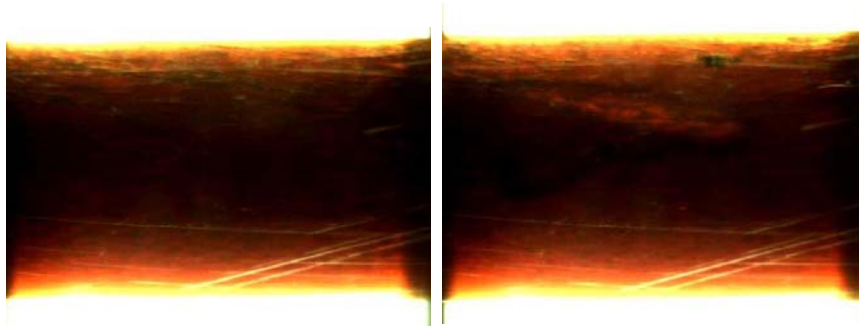
- ◆ 25 Data Points with QCV System
- ◆ At 70 °F
- ◆ Horizontal
- ◆ $v_{SL} = 0.5 \text{ m/s}$ and 0.8 m/s
- ◆ $v_{SG} = 0.5 \text{ m/s}, 1 \text{ m/s}, 1.5 \text{ m/s}$

Preliminary Experiments ...

- ◆ Challenges
 - Time
 - Bubble Size Difference in Liquid Slug

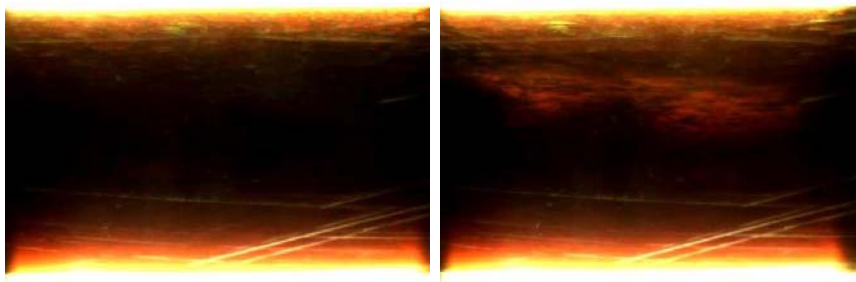
Preliminary Experiments ...

◆ $v_{SL} = 0.5 \text{ m/s}$ $v_{SG} = 1 \text{ m/s}$



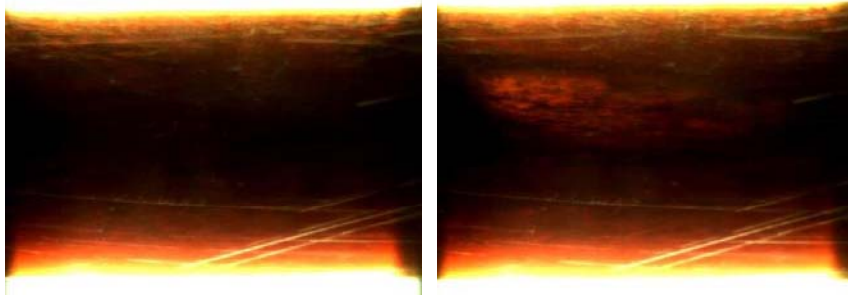
Preliminary Experiments ...

◆ $v_{SL} = 0.5 \text{ m/s}$ $v_{SG} = 1.5 \text{ m/s}$



Preliminary Experiments ...

◆ $v_{SL} = 0.8 \text{ m/s}$ $v_{SG} = 1 \text{ m/s}$



Preliminary Experiments ...

- ◆ Divide Data into Two Groups
- ◆ Collect more Data for Higher Flow Rates
- ◆ Compare Results with Differential Pressure Sensor

Future Tasks

- ◆ **Completion of Facility Modifications for Differential Pressure Sensor**
- ◆ **Calibration of Differential Pressure Sensor**
- ◆ **Conduct Experiments with Quick Closing Valves and Differential Pressure Sensor**
- ◆ **Collect Liquid Film Height Data**

Future Tasks ...

- ◆ **Record Videos with High Speed Video Camera for Each Flow Rate and Temperature**
- ◆ **Evaluate Data Acquired From Quick Closing Valves and Differential Pressure Sensor**
- ◆ **Compare Acquired Data with Predictions of Existing Correlations**

Project Schedule



◆ Literature Review	Completed
◆ Facility Modifications	Completed
◆ Preliminary Testing	Underway
◆ Testing	April 2010
◆ Data Analysis	June 2010
◆ Final Report	August 2010

Questions & Comments



Effects of High Oil Viscosity on Slug Liquid Holdup in Horizontal Pipes

Ceyda Kora

PROJECTED COMPLETION DATES:

Literature Review	Completed
Facility Modifications	Completed
Preliminary Testing	Underway
Testing	April 2010
Data Evaluation	June 2010
Final Report	August 2010

Objectives

The main objectives of this study are,

- Investigation of slug liquid holdup for high viscosity oil and gas flow,
- Development of closure models for slug liquid holdup.

Introduction

High viscosity oils are produced and transported from many fields all over the world. Because of the increased consumption of hydrocarbon resources and decline in discoveries of low viscosity oils, the importance of high viscosity oil has increased. It is important to design a proper production system in order to eliminate operational problems for high oil viscosity fields. Available multiphase flow models are primarily developed for low viscosity liquids. TUFFP has been studying the high viscosity oil multiphase flow in a systematic way since 2005, and has made significant progress towards the improvements in high viscosity oil multiphase flow prediction.

The first experimental study at TUFFP on high viscosity oil was completed by Gokcal (2005). The effects of high oil viscosity on oil-gas two-phase flow behavior were investigated and significant changes in flow behavior were encountered. Gokcal (2005) observed intermitted flow (slug and elongated bubble) as

the dominant flow pattern for high viscosity oil and air flow. Slug characteristics should be examined in detail for better understanding of high liquid viscosity effect.

An experimental and theoretical investigation of slug flow for high oil viscosity in horizontal pipes was completed by Gokcal in 2008. Gokcal (2008) developed models for drift velocity, transitional velocity and slug frequency by taking into account the viscosity effect. Slug liquid holdup was not studied due to a lack of proper instrumentation. Gokcal was only able to measure average liquid holdup in his study. Therefore, investigation of slug liquid holdup for high viscosity oil and gas two phase flow is crucial.

The most challenging part of this study is to measure the gas void fraction in liquid slugs. For the prediction of slug liquid holdup, a new quick-closing valve system has been developed. As a second measurement technique, differential pressure sensor has been built and will be placed to test section. Preliminary experiments have been started with the quick-closing valve system. High viscosity oil and air two-phase flow experiments will continue to collect slug liquid holdup data at different flow rates and temperatures for horizontal pipe.

Literature Review

There has been significant research reported in the literature on slug holdup. Most of the studies focused on low oil viscosity. There exist some efforts investigating the effects of viscosity on

slug liquid holdup. However, these studies are not adequate to fully understand the effect of high viscosity on slug liquid holdup. Many of these studies were reviewed at the March 2009 Advisory Board meeting. Since the experimental results of slug liquid holdup will be compared with the existing slug liquid holdup correlations, the literature review will be an ongoing task until the end of this study.

Preliminary experimental results are compared with three different liquid holdup correlations and a mechanistic model.

The first empirical correlation, most commonly used, is given by Gregory *et al.* (1978) given with Eq. 1. Gregory *et al.* conducted experiments on liquid holdup in slugs with two different horizontal diameters pipe: 2.58 cm and 5.12 cm. In this correlation, they assumed the slug to be homogenous. However, they suggested that the gas fraction in a slug changes with position.

$$H_L = \frac{1}{1 + \left(\frac{v_m}{8.66}\right)^{1.39}} \quad (1)$$

The second is the dimensionless correlation proposed by Gomez *et al.* (2000) for inclination angles from horizontal to upward vertical (Eqs. 2-3). This correlation included the mixture velocity, liquid viscosity, pipe diameter, and inclination angle. They established their empirical correlation by considering inclination angle and Reynolds number. Although this empirical correlation considers the liquid viscosity through a Reynolds number, it was not validated for high viscosity oils.

$$H_{LS} = 1.0e^{-(0.45\theta_r + 2.48 \cdot 10^{-6} \text{Re}_S)} \quad (2)$$

$$\text{Re}_S = \frac{\rho_L V_M D}{\mu_L} \quad (3)$$

The empirical correlation of Abdul-Majeed (2000) for slug liquid holdup in horizontal and slightly inclined two-phase flow is the third correlation given by Eqs. 4-6. This correlation is the function of mixture velocity, liquid viscosity and inclination angle. Abdul-Majeed (2000) claimed that slug liquid holdup is significantly affected by liquid viscosity and inclination angle.

$$H_{LS} = (1.009 - C v_M) A \quad (4)$$

$$C = 0.006 + 1.3377 \left(\frac{\mu_G}{\mu_L} \right) \quad (5)$$

$$A = 1.0 (\theta \leq 0) \quad (6)$$

A mechanistic model to predict the slug holdup is proposed by Zhang *et al.* (2003). It is given with Eqs. 7-9. It is based on the slug dynamics. This model is modified in an ad-hoc fashion based on Gokcal (2005) data. If the Reynolds number is less than 5000, the momentum term for gas entrapment is multiplied by $\text{Re}/5000$.

$$H_{LS} = \frac{1}{1 + \frac{T_{sm}}{3.16 [(\rho_L - \rho_G) g \sigma]^{1/2}}} \quad (7)$$

$$T_{SM} = \frac{1}{C_C} \left[\frac{f_S}{2} \rho_S v_M^2 + \frac{d}{4} \frac{\rho_L H_{LF} (v_T - v_F) (v_M - v_F)}{l_S} \right] \quad (8)$$

$$C_C = \frac{2.5 - |\sin(\theta)|}{2} \quad (9)$$

Experimental Study

Facility

An existing TUFFP indoor high viscosity facility has been modified for this study (Fig. 1). This facility was previously used by Gokcal (2005 and 2008) to investigate the effects of high oil viscosity on slug flow characteristics. Recently, further modifications have been done in the facility in order to prevent the oil accumulation in the horizontal dip section of the return pipe which may cause artificial fluctuations in low flow rates. Moreover, visible sections were increased for the better observation through the flow loop.

There are four main parts of the facility: metering section, test section, heating system and cooling system. The test section was redesigned as an 18.9-m (62-ft) long, 50.8-mm (2-in.) ID pipe including a clear PVC section and a transparent acrylic pipe section. A 9.15-m (30-ft) long transparent acrylic pipe section is used to observe the flow behavior visually. This section is connected to a 76.2-mm (3-in.) ID return pipe with a flexible hose. The old steel return pipe was changed with clear PVC pipe and the level

of the return pipe was set parallel to the test section at the same height. An oil transfer tank (1.32 m³) is added to the end of return pipe. Return pipe is connected to this tank with a flexible hose, and + 1° inclination from horizontal is given to eliminate the concerns about possible terrain type slugging. 3-hp progressing cavity pump is also placed to the outlet of the new tank which sends oil back to the main tank (3.03 m³) through the riser. From main storage tank, oil is pumped by a 20-hp screw pump to the test section. A dry rotary screw air compressor delivers compressed air to the system. Before entering the test section, two fluids were mixed at a mixing tee. Micro Motion™ mass flow meters are used to meter the mass flow rates and densities of oil and air. There is no special separation system. Air and oil are gravity segregated in the oil tank, and separated air is released to the atmosphere through a ventilation system. The inclination of the test section can be set from -2° to 2° from horizontal by adjusting the heights of the stands.

The test oil viscosity is very sensitive to temperature changes. The temperature measurements are imperative to determine the viscosity of the oil during experiments. Therefore, it is crucial to conduct experiments at a constant temperature. Existing heating and cooling systems are be used to control temperature. Resistance Temperature Detector (RTD) transducers already exist in the facility to measure temperatures during experiments. Pressure transducers and differential pressure transducers are located at various points to monitor the pressure and pressure drop during experiments.

Previously developed data acquisition program is used for the high viscosity facility. Pressure, differential pressure, temperature, flow rates, superficial gas and superficial liquid velocities are monitored on the PC of the facility during the experiments.

Test Fluids

The previously used high viscosity oil (Citgo Sentry 220) and air were selected again for this study. Following are the typical properties of the oil:

Gravity: 27.6 °API
Viscosity: 0.220 Pa·s @ 40 °C
Density: 889 kg/m³ @ 15.6 °C

The oil viscosity vs. temperature behavior is shown in Fig. 2.

Testing Range

In this study, a large number of data points will be collected at various oil and gas velocities and different oil viscosities corresponding to different temperatures. Since most of the slug characteristics were determined by Gokcal (2008) in the previous project of TUFFP, his test matrix will be used as the starting point of this study. Superficial oil velocities range from 0.05 to 0.8 m/sec. Superficial air velocities range from 0.1 to 2 m/sec. The viscosity of Citgo Sentry 220 oil is very sensitive to temperature changes. Therefore, experiments will be conducted at four different temperatures: 70, 80, 90, and 100 °F and 0.587, 0.378, 0.257, and 0.181 Pa·s oil viscosities correspond to these temperatures, respectively. The test section inclination will be kept as 0° from horizontal. The testing range can be expanded to higher oil and air superficial velocities after the completion of Gokcal's test matrix within the limitations of the facility.

Current Effort

Slug liquid holdup measurement techniques in the literature had been examined for high viscosity oil and gas two-phase flow. In previous studies, several instruments and methods were used, such as impact probes, quick-closing valves, conductance sensors, capacitance sensors, hot-film anemometry and gamma ray densitometers. The issues about these methods were discussed at the March 2009 Advisory Board meeting. It was concluded that a non-intrusive method is required to reduce the uncertainty of the slug liquid holdup prediction. For this purpose, a new quick-closing valve system was designed and constructed for this study.

Quick-Closing Valves System

Gokcal (2008) proposed that the slug length for high viscosity oil-air flow is changing between 8D-13D. Therefore, the optimum distance between quick-closing valves was determined as 8 inches considering slug lengths for various flow rates and instrumental limitations. A dedicated CPU was used for this system. A laser sensor was placed before the first valve in order to distinguish slug body from elongated bubble.

When the laser sensor detects the slug front, after a period of time, the dedicated CPU closes the quick-closing-valves. This period of time is readjusted each time according to different flow rates after several capturing trials. A by-pass system was added to the system for continuity of flow. Three old and two new quick-closing valves on the test section work synchronously for this purpose. Since the drainage of high viscosity oil is a slow process, a new measurement technique is needed to measure slug liquid holdup after a representative sample is captured. A schematic view of this system is shown in Fig. 3.

When liquid slug is trapped by quick-closing valves, this action is recorded by high speed video camera to verify that only liquid slug is captured in the trap section. There is a hole on top of the trap section to connect it to an empty closed 50.8-mm (2 in) ID acrylic pipe section with a steel tube including a valve in the middle of it. During flow and trapping process, a plug is placed to this hole. After a representative liquid slug is trapped, this plug is taken off and steel tube is connected to both sections and tightened. In order to ensure the pressures of both sections are equal to the atmospheric pressure, the valve between these two sections and the discharge valve are kept open for a while. After closing the both valves, the pressure of the empty pipe section is increased to 30 psig with a sensitive pressure calibrator. Then, the valve between two sections is opened, and this pressure value is recorded. The change in the pressure from 30 psig to this new pressure value is used to calculate slug liquid holdup. Calibration of this system was repeated three times to convert this pressure difference to holdup data.

For the calibration of this system, trap section is cleaned and quick-closing valves are closed. High viscosity oil is injected to trap section from the hole on top of it with a syringe. Calibration of the 30 cc syringe was done with micro-pipette and two different graduated cylinders. Pressure data are recorded starting from empty trap section to full trap section for each 25 cc increment of high viscosity oil volume. Each time after tube connections are done and the pressures of both sections are equalized to atmospheric pressure, pressure of the empty acrylic pipe section is increased to 30 psig. The valve in the middle of two sections is opened, and the new pressure data is noted. By using these data points, oil volume in the trap section

versus pressure graph is plotted. It is expected that slug liquid holdup will be over 0.8 for high viscosity oil and air flow. Therefore, for the final calibration curve the pressure data after 200 cc are plotted for the better match of the curve and its trend line (Fig. 4). The equation of the trend line is used to calculate oil volume in the trapped section with the recorded pressure value after trapping the liquid slug. As the oil volume in the trap section is calculated with this equation, slug liquid holdup can also be estimated by dividing calculated oil volume to volume of the trap section.

In order to verify this equation, different parts of slugs are captured by quick-closing valves. Using the same procedure, pressure data are recorded for each trapped slug part. Oil volume in the trap section is calculated from the equation with the new pressure data. For comparison, oil is injected to trap section to find out how much oil is needed to reach full trap section volume. Calculated oil volume is compared with the injected oil volume. Difference between these two volumes is around 2 cc corresponding to holdup of ± 0.005 for each trial.

Gokcal (2008) did not study the liquid film height in two phase high viscosity oil and air flow. The new quick-closing valve system can also be used to measure the liquid film height in this study. Since the drainage of high viscosity oil is very slow, there always exists a liquid film on top of the pipe during the flow. An accurate thickness prediction for the upper film is not possible due to pipe curvature. However, with the newly developed method, when the liquid film is captured by quick-closing valves, oil volume of the liquid film can be calculated with the mentioned procedure. Then, the liquid height can be calculated. In addition, during the flow, pictures of the slugs are taken by high speed video camera. From these pictures, the film height can be estimated considering the proportion between the pipe diameter and oil-air interface height. Image processing software may be needed to identify the interface between oil and air during flow. As a result, thickness of the upper oil film can be predicted by combining the results of two techniques.

Differential Pressure Sensor

Before the last Advisory Board meeting, the feasibility of measuring differential pressure across the cross section of the pipe was tested for

liquid holdup measurement since, theoretically, this method is very promising. During the testing, however, some mechanical problems with the transmission lines had been encountered. Drainage of oil and penetration of gas bubbles into the transmission lines were observed while slugs were passing. In order to solve this problem, two flush diaphragm pressure transducers were ordered. Following are some of specifications of the flush diaphragm pressure transducers:

Range: 0-6 psig

Accuracy: 0.5% BFSL

Operating Temperature Range: -51 to 93°C (-60 to 200°F)

Thermal Sensitivity Effect: $\pm 0.02\%/^{\circ}\text{C}$ ($\pm 0.01\% \text{ rdg}/^{\circ}\text{F}$)

Differential pressure sensor is ready and will be placed to test section after Advisory Board meeting. The differential pressure sensor will be located as close as possible to trap section in order to make the results of two methods comparable. After calibration of this method is completed, slug liquid holdup is also going to be measured with this instrument for different flow rates and temperatures.

Preliminary Experiments

Preliminary experiments have been conducted with the new quick-closing valve system and some challenges are identified.

Firstly, the holdup measurement is a very time consuming process. It takes at least 30 minutes to record just a single data point. Secondly, each time only 8 inch liquid slug can be trapped by quick-closing valves. At high flow rates, apart from many tiny gas bubbles, there are some big bubbles in the liquid slug. This makes slug liquid holdup lower compared to other data points. In order to solve this problem, number of data points can be increased or data points can be divided into two groups according to the bubble sizes. The optimum number of data points was determined as 10 considering statistical calculations and time limitation. The differential pressure sensor is expected to be a solution for this problem. With differential pressure sensor, it is possible to collect more data points for the same flow rates in a short time.

Before the facility modification, 25 data points are collected for high flow rates at 70 °F. The

superficial liquid velocity is set at 0.5 and 0.8 m/s. The superficial air velocity is set at 0.5, 1 and 1.5 m/s.

Gregory's empirical correlation slightly underestimates slug liquid holdup. On the other hand, the results of Gomez and Abdul-Majeed's correlations are very close to each other and they slightly overestimate slug liquid holdup. Finally, TUFFP Unified slug liquid holdup correlation performs better than the other correlations for low flow rates, however, it needs to be improved for better prediction of high flow rates (Fig. 5 and Table-1).

Near Future Tasks

The main future tasks are:

- Completion of facility modifications
- Calibration of differential pressure sensor
- Conduct experiments with quick-closing valve system and differential pressure sensor
- Evaluation of the acquired data from new quick-closing valve system and differential pressure sensor
- Collect data for liquid film height
- Compare experimental data with existing correlations.

Nomenclature

d = pipe diameter [m]

H = holdup

Re = Reynolds number

v = velocity [m/s]

f = friction factor

Greek Letters

μ = viscosity [kg/ms]

ρ = density [kg/m³]

σ = surface tension [N/m]

θ = inclination angle [°]

Subscripts

G = gas phase

L = liquid phase

LS = liquid slug

M = mixture

S = slug

LF = liquid film

F = film

C = gas core

T = translational velocity

References

Abdul-Majeed, G.: “Liquid Slug Holdup in Horizontal and Slightly Inclined Two-Phase Slug Flow,” *Journal of Petroleum Science and Engineering*, 27, pp. 27–32 (2000).

Al-safran, E.: “Prediction of Slug Liquid Holdup in Horizontal Pipes,” *Journal of Energy Resources Technology* Volume 131, Issue 2 (2009).

Gregory, G.A., Nicholson, M.K., Aziz, K.: “Correlation of the Liquid Volume Fraction in The Slug for Horizontal Gas–Liquid Slug Flow,” *International Journal of Multiphase Flow*, 4, 33–39 (1978).

Gokcal, B.: “Effects of High Oil Viscosity on Two-Phase Oil-Gas Flow Behavior in Horizontal Pipes,” MSc.Thesis, The University of Tulsa, Tulsa, OK (2005).

Gokcal, B.: “An Experimental and Theoretical Investigation of Slug Flow for High Oil Viscosity in Horizontal Pipes,” Ph.D. Dissertation, The University of Tulsa, Tulsa, OK (2008).

Gokcal, B.: “An Experimental and Theoretical Investigation of Slug Flow for High Oil Viscosity in Horizontal Pipes,” TUFFP ABM (September 2008a), pp. 47-76 (2008).

Gomez, L.E., Shoham, O., Taitel, Y.: “Prediction of Slug Liquid Holdup: Horizontal to Upward Vertical Flow,” *International Journal of Multiphase Flow*, 26, 517–521 (2000).

Zhang H., Wang O., Sarica C., Brill J. P.: “Unified Model for Gas-Liquid Pipe Flow via Slug Dynamics—Part I: Model Development,” *Journal of Energy Resources Technology*, Volume 125, Issue 4, 226 (2003).

Table 1: Slug Liquid Holdup Prediction and Comparison with Gregory, Gomez and Abdul-Majeed Slug Holdup Correlations

Slug Liquid Holdup							
V _{SL} (m/s)	V _{SG} (m/s)	Temperature (°F)	Measured	Gregory	Gomez	Abdul-Majeed	TUFFP Unified
0.51	0.51	70.17	0.974	0.951	1.000	1.003	0.977
0.51	1	70.28	0.974	0.919	1.000	1.000	0.950
0.51	1.51	70.77	0.950	0.883	1.000	0.997	0.913
0.81	0.53	71.22	0.964	0.930	1.000	1.001	0.960
0.81	1.01	71.56	0.968	0.897	1.000	0.998	0.927

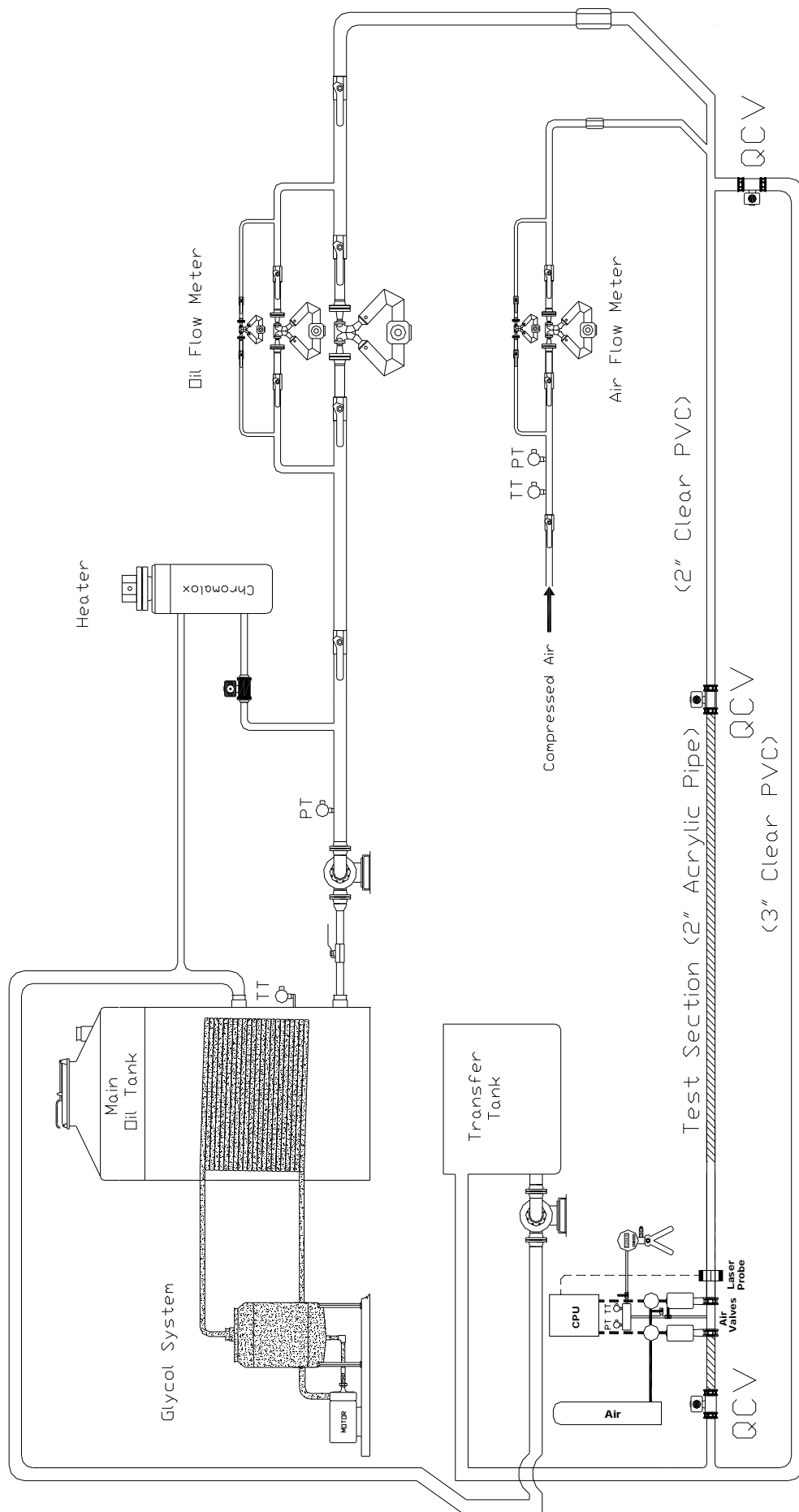


Figure 1: Schematic of High viscosity facility of the Tulsa University Fluid Flow Projects (TUFPF)

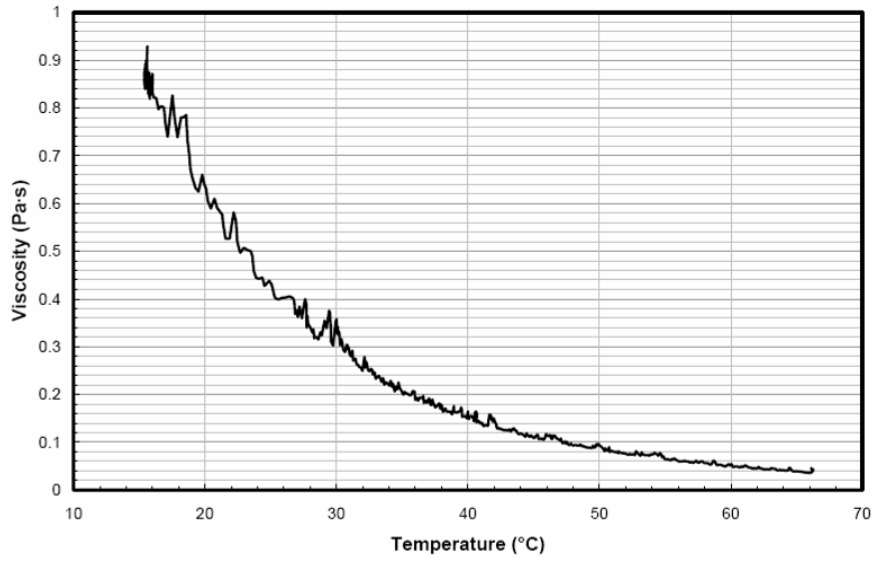


Figure 2: Viscosity vs. Temperature for Citgo Sentry 220 Oil

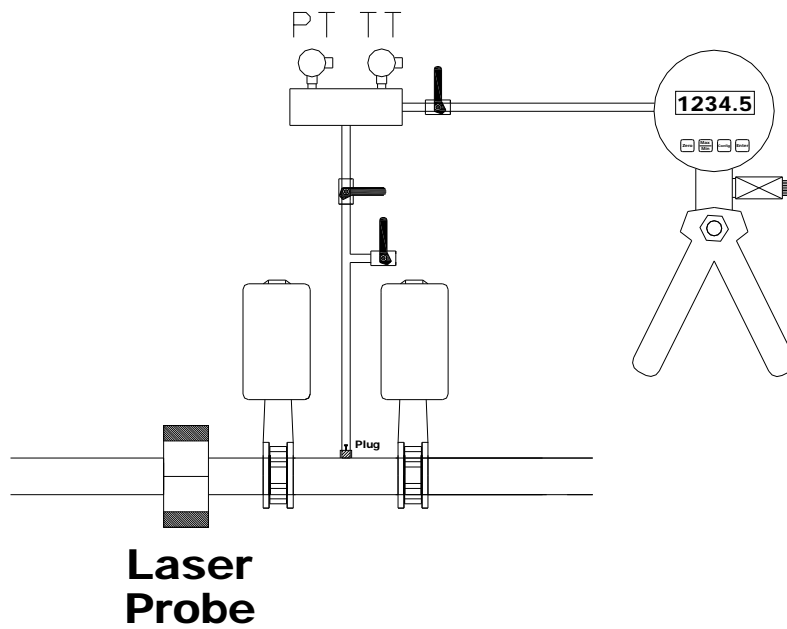


Figure 3: Schematic of New Quick-Closing Valve System

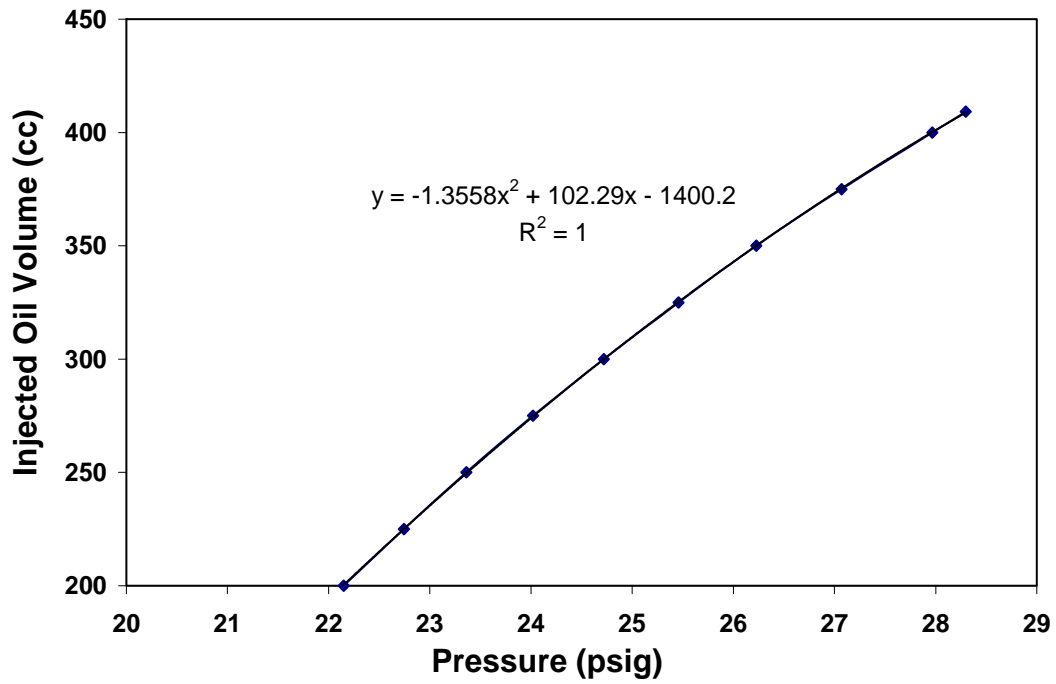


Figure 4: Calibration Curve of Pressure Volume (PV) Holdup Measurements

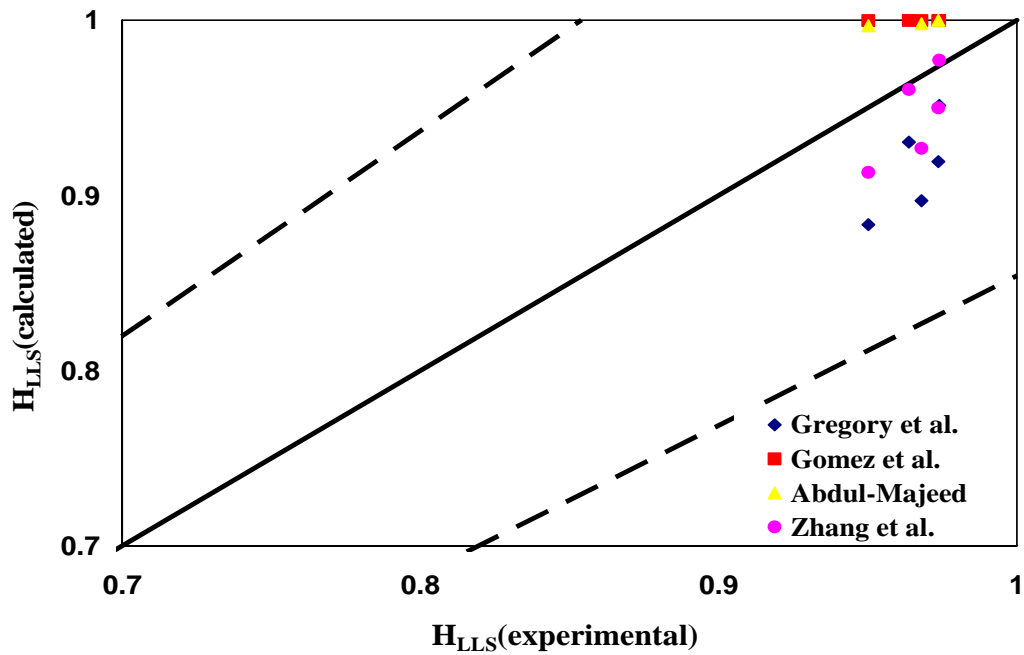


Figure 5: Performance of Gregory (1978), Gomez (2000) and Abdul-Majeed (2000) Correlations for Slug Liquid Holdup Prediction



Fluid Flow Projects

Investigation of High Viscosity Oil Two-Phase Slug Length in Horizontal Pipes

Eissa Alsafran (KU/KOC)

Advisory Board Meeting, September 30, 2009

Outline

- ◆ Introduction
- ◆ Flow Visualization
- ◆ Data Analysis
- ◆ Physical Viscosity Effect
- ◆ Theoretical Viscosity Effect
- ◆ Future Work

Significance

◆ Pipeline Design (Sizing and Routing)

- Pressure Drop
- Liquid Volume

◆ Facility/Equipment Design

- Instantaneous Liquid Rate at Pipe Outlet is 5-20X of Average Rate
- Slug Catchers
- Multiphase Pumps
- Multiphase Meters

Significance ...

◆ Flow Assurance

- Terrain Slugging
- Erosion/Corrosion

◆ Mechanical Integrity

- Piping System
- System Components

Literature Review

- ◆ No Literature is Found on High Viscosity Oil Two-phase Slug Length
- ◆ Low Viscosity Oil Slug Length is Strongly Correlated to Pipe Diameter, and Insensitive to Other Parameters
- ◆ Low Viscosity Oil Slug Length
 - Smallest Near the “Center” of Slug Flow Region on Flow Pattern (FP) Map
 - L_s Increases Near Transition Boundaries

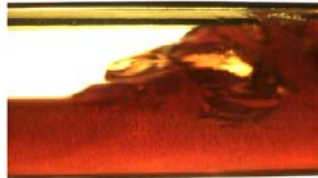
Literature Review ...

- ◆ High Viscosity Effect on Liquid Holdup in Film and Slug Regions-Direct Relationship
- ◆ High Viscosity Effect on Slug Frequency-Inverse Relationship
- ◆ Increase of Slug Frequency and Slug Liquid Holdup Results in Short Slugs

Flow Visualization

◆ Slug Zone ($v_{SL}=0.01$ m/s, $v_{Sg}=1.5$ m/s)

➤ Slug Front



$\mu=0.590$ Pa.s



$\mu=0.182$ Pa.s

Flow Visualization ...

➤ Slug body



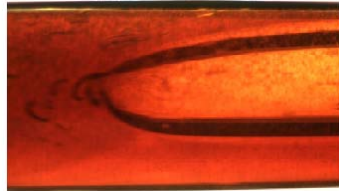
$\mu=0.590$ Pa.s



$\mu=0.182$ Pa.s

Flow Visualization ...

➤ Slug Tail



$\mu=0.590$ Pa.s



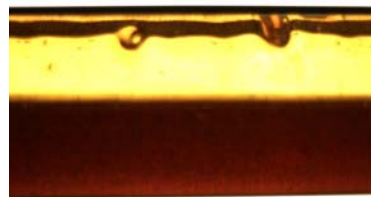
$\mu=0.182$ Pa.s

Flow Visualization ...

◆ Film Region ($v_{SL}=0.1$ m/s, $v_{Sg}=2$ m/s, $\mu=0.26$ Pa.s)



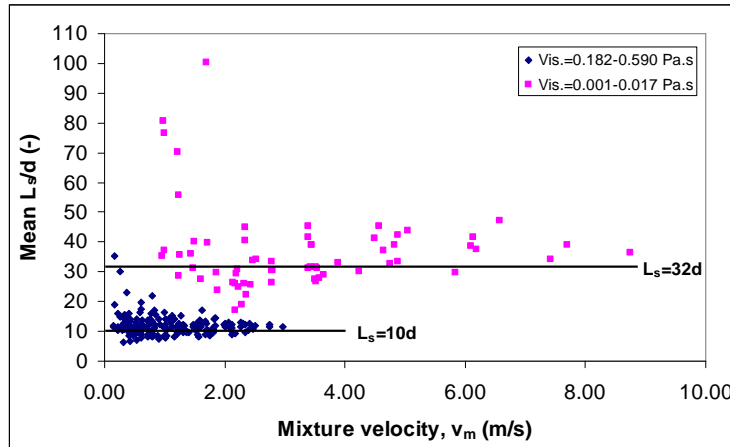
Developing film



Developed film

Data Analysis

- Comparison (Kouba (1986), BP Loop (2001), Alsafran (2003), Gokcal (2008))

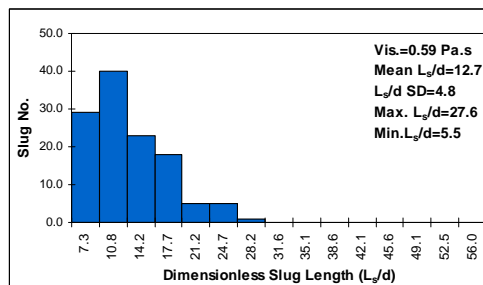
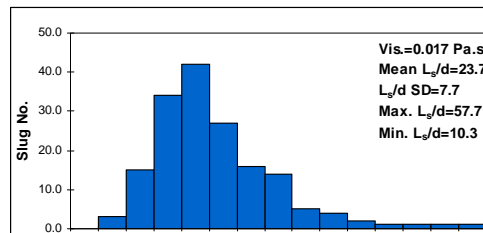


Data Analysis ...

- Comparison (Low Viscosity vs. High Viscosity)

$$v_{SL}=0.3 \text{ m/s}$$

$$v_{Sg}=1.5 \text{ m/s}$$



Data Analysis ...

- ◆ Analysis of Variance (ANOVA) to Test the Following Hypothesis:

$$H_0 : \mu_{low} = \mu_{mid} = \mu_{high}$$

- Calculate p-value and Set Sig. Level ($\alpha=0.10$), i.e. 90% Confidence
- Calculated p-value < α , Thus Reject H_0

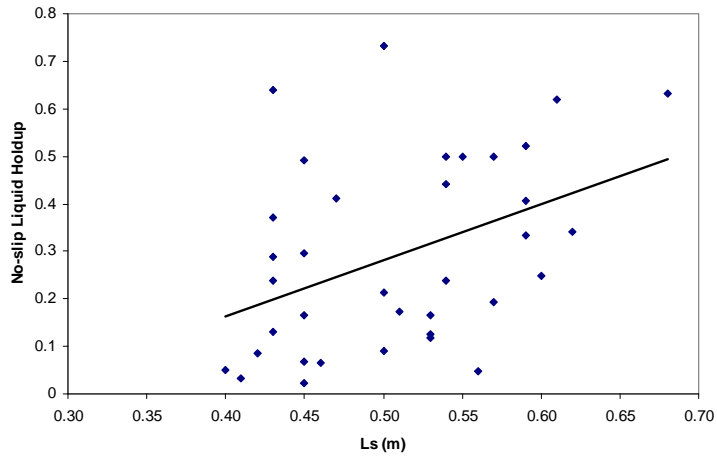
Data Analysis ...

- ◆ Partial Correlation Coefficient Analysis

$$r_{yx_1(x_2)} = \frac{r_{yx_1} - r_{yx_2} r_{x_1x_2}}{\sqrt{(1 - r_{x_1x_2}^2)}}$$

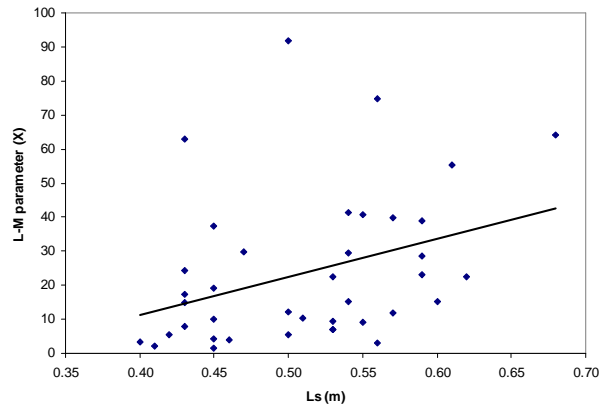
- Significant Correlation with No-slip Liquid Holdup in Pipe

Data Analysis ...



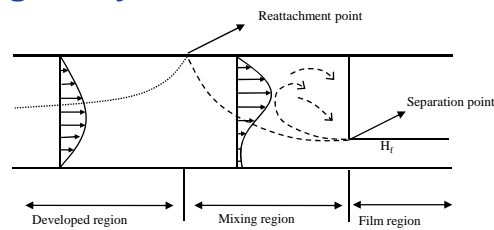
Data Analysis ...

- Significant Correlation with Lockhart-Martinelli Parameter (X)



Physical Modeling

♦ Dukler *et al.* (1985) Proposed Minimum Slug Length Physical Model



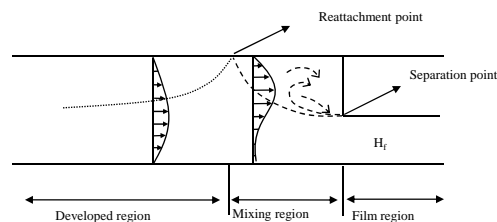
- Sudden Expansion at Separation Point
- New Wall Boundary at Reattachment Point
- Downstream a Fully Developed Velocity Profile is Formed

Physical Modeling ...

♦ Proposed High Viscosity Liquid Physical Model

- Thick Film-Less Expansion (Jet Velocity)
- Less (Short) Front Mixing Intensity
- Smaller Velocity Profile and Maximum Velocity

$$v_z = \frac{\Delta P \times R^2}{4\mu L} \left[1 - \left(\frac{r}{R} \right)^2 \right]$$



Theoretical Viscosity Effect

$$L_s = \frac{v_s}{\nu_s (H_{LLS} - H_{LTBe})} \left[\left(\frac{W_L}{\rho_L A_p v_s} - H_{LTBe} \right) + c(H_{LLS} - H_{LTBe}) \right]$$

First Term: $\left[\frac{v_s \downarrow}{\nu_s \uparrow (H_{LLS} \uparrow - H_{LTBe} \uparrow) \downarrow} \right] \downarrow$

Second Term: $\left[\left(\frac{W_L \rightarrow}{\rho_L (\rightarrow) A_p (\rightarrow) v_s (\downarrow)} \right) \uparrow - H_{LTBe} \uparrow \right] \downarrow$

Third Term: $\left[c (\rightarrow) (H_{LLS} \uparrow - H_{LTBe} \uparrow) \right] \downarrow$

Thus, Slug Length Decreases with Increasing Liquid Viscosity

Future Work

- ◆ Further Characterize Two-Phase Flow Behavior in Slug and Film Regions
- ◆ Analyze Experimental Data for Correlating Parameters and Trends
- ◆ Investigate the Best Fit Probabilistic Distribution for High Viscosity Oil
- ◆ Modify/Develop Minimum Slug Length Model for High Viscosity Oil

Investigation of High Viscosity Two-Phase Slug Length in Horizontal Pipes

Eissa Al-Safran

Objective

The objectives of this project are as follows:

- Understand the effect of high viscosity liquid on average slug length and slug length distribution.
- Develop a high viscosity two-phase slug length physical model.
- Develop a predictive mathematical slug length model.

Background

Gas-Liquid two phase flow in pipes occurs at production and transportation facilities for oil and gas. The most common type of flow patterns in field operation for horizontal and near horizontal pipelines is the slug flow pattern. Slug flow is described by alternating liquid slugs and gas intervals, both of which when combined form what is called slug unit. Among all the slug flow characteristics, slug length is one of the most critical characteristic for system proper design and safe operation. For example, average slug length is important and preferred (over slug frequency) input parameter for mechanistic models to predict liquid holdup and pressure gradient. Furthermore, long slugs often cause operational problems, flooding of downstream facilities, severe pipe corrosion, structural instability of the pipeline, as well as production loss and poor reservoir management due to unpredictable wellhead pressures. Although several investigators studied the average and slug length distribution in pipes for light oil, a recent literature search on high viscosity two-phase slug length revealed no detailed conducted studies. However, few studies were found on the effect of high viscosity liquid on other two-phase slug flow characteristics such as liquid holdups and frequency, which can be related, implicitly, to slug length.

Nadler and Mewes (1995) experimentally investigated the liquid viscosity effect on liquid holdup in the slug unit, film region and slug zone in

the aerated slug flow region. They used three fluid systems, air/light oil ($\mu_o=17$ mPa.s), air/heavy oil systems ($\mu_o = 34$ mPa.s) and air/water systems. In general, their results revealed that by increasing liquid viscosity, a significant increase of liquid holdup in the slug unit and film region is observed, while less significant increase of liquid holdup in the slug zone is observed. The observed directly proportional relationship between film liquid holdup and liquid viscosity is explained by the increase of interfacial and wall shear forces on the liquid film. A significant difference in slug unit and film liquid holdup is observed between air/light oil and air/water systems; which is attributed to the difference in surface tension and densities of the two systems. Abdul-Majeed (2000) developed an empirical correlation for slug liquid holdup as a function of liquid viscosity. He reported that slug liquid holdup is significantly affected by and is directly proportional to liquid viscosity. Brauner and Ullmann (2004) developed a Taylor bubble wake model of gas entrainment from Taylor bubble to slug body to predict the slug liquid holdup in vertical, inclined and horizontal pipes. Their model takes into account the effect of liquid viscosity which predicts that the bubble entrainment decreases (slug liquid holdup increases) with increasing liquid viscosity. Slug frequency was also investigated for the high viscosity two-phase flow. A recent study by Gokcal *et al.* (2009) shows that slug frequency increases with increasing liquid viscosity for which they developed an empirical slug frequency correlation.

The above literature review suggests that under the condition of high liquid viscosity, slugs are less aerated and more frequent. Theoretically, these two characteristics result in short slugs. Furthermore, experimental data (Kouba (1990), Kokal (1987), Marcano (1996), Rothe (1986), Brandt and Fuchs (1989), and El-Oun (1990)) on light oil showed the inverse relationship between slug frequency and slug length, and between the slug liquid holdup and slug length. Therefore, from the limited literature review on high viscosity oil and the previous knowledge and experimental data on the relationships among slug

flow characteristics, one can speculate an inverse relationship between liquid viscosity and slug length.

Flow Visualization

The data of study is acquired by Gokcal (2008) using TUFFP high viscosity two-phase flow loop. In this section, flow visualization is presented for different parts of the slug flow, namely slug back and front, slug body, and film region at different viscosities. The purpose of this is to characterize and better understand the slug flow structure under the effect of high liquid viscosity to be able to relate the slug/film structure to slug length.

Slug Zone.

Figure 1 shows the slug front, slug body and slug back for two different liquid viscosities flows, 0.590 Pa.s, and 0.182 Pa.s at $v_{sg}=1.5$ m/s and $v_{sl}=0.1$ m/s. The low liquid viscosity slug (Slug-B) shows turbulence and mixing in the slug front. On the other hand, the high viscosity slug front is less turbulent with a top boundary layer moving faster than the slug body and entraining large bubbles. It is evident from the slug front pictures that viscosity affects the scooping process at the slug front. The middle pictures of Fig. 1 illustrate the slug body for the same slug which shows the impact of the gas entrainment in the slug front on the slug body. Slug (A) shows a large gas pocket entrained in the slug front which grows further as small bubbles merge in it. This large bubble is a result of the scooping process at the slug front which entrains large bubbles. As the gas pocket grows, it splits the large slug to two shorter slugs, this is one of the mechanism generating short slugs. On the other hand, low viscosity slug body shows relatively small entrained bubbles due to the high turbulence and mixing in the slug front which causes bubbles fragmentation generating small bubbles. The lower pictures of Fig. 1 show the slug tail for the same slugs shown previously. The high viscosity slug (Slug-A) shows a long bubble nose accelerated by the wake of entrained large gas pocket which leads to short slugs and eventually to slug dissipation. The lower viscosity slug back shows a sharper, less developed and deformed bubble nose. The location of the bubble nose in low viscosity liquid condition with respect to the pipe centerline is asymmetric as oppose to the symmetric geometry in the high viscosity condition. In summary, Fig. 1 shows that liquid viscosity significantly affects the slug.

Film Zone.

Similar to the slug zone, high viscosity liquid significantly affects the liquid film characteristics in the Taylor bubble region. Experimental observations and video recordings show that the film height is significantly large and aerated as oppose to the low liquid viscosity condition. Furthermore, it is observed that the film region has two distinct sub-regions, namely developing and developed regions. The developing region is observed within 5D-10D from the Taylor bubble nose. It is characterized, in addition to its axial flow, by a secondary spherical film flow increasing the film height in this developing region. The second developed section is far away of the slug zone and can be characterized by a stratified film layer. However, in the case of high liquid viscosity, a thin film layer is observed at the top wall of the pipe similar to annular flow configuration (Fig 2). Under certain condition of high superficial gas velocity, this layer is observed to be wavy. Further characterization of the film is underway; which may change the conventional modeling approach of the film zone in a slug unit.

Data Analysis

In this section, the average slug length and slug length distributions of high viscosity liquid will be presented and compared with low viscosity liquid slug length. The purpose of this comparison is to illustrate the effect of the liquid viscosity and its magnitude on slug length. Figure 3 illustrates the evolution of the dimensionless average slug length with mixture velocity for high and low viscosity liquids. As observed by Gokcal *et al.* (2008a and 2008b) and Colmenares *et al.* (2001), high viscosity liquid average slug length is shorter than that of low viscosity liquid. Figure 3 further shows a decreasing slug length trend at low values mixture velocity followed by a constant average slug length around 10D for a high viscosity liquid. Similar to the low viscosity liquid slug length trend, high viscosity average slug length shows insensitivity to operational conditions. In addition, the critical mixture velocity beyond which average slug length remains constant for high viscosity liquid is in the order of 0.5 m/s, while it is 1 m/s for light oil condition.

Figure 4 display the slug length distribution for low (0.017 Pa.s) and high (0.59 Pa.s) liquid viscosities for superficial gas and liquid velocities of 1.5 m/s and 0.3 m/s, respectively. It is not only the shape of the overall distribution that is different but also the statistical parameters are significantly different. For example, the light oil distribution is Log Normal with

a wide range of slug length from 14D to 58D. Conversely, the high viscosity slug length is a truncated Normal distribution with a minimum stable slug length of around 7.5D. In addition, the statistical parameter of the high viscosity slug length distribution, namely mean slug length, standard deviation, maximum and minimum slug lengths are approximately one half of the statistical values of light oil distribution.

Inferential Statistical Analysis.

Although the above data analysis is carried out on sample data acquired in the experimental study of Gokcal (2008), using probability theory, the analysis can be generalized by extending it to a population with a given confidence interval. Analysis of Variance (ANOVA) is carried out to investigate the existence of a significant difference in the mean slug length of light, medium and heavy liquids. ANOVA tests the following null hypothesis: $H_0: \mu_{\text{low vis.}} = \mu_{\text{mid. vis.}} = \mu_{\text{high vis.}}$ (μ is the population mean slug length). The null hypothesis will not be rejected unless the sample data provide convincing evidence that it is false. A significance level has to be selected based on which one decides to reject or accept the null hypothesis. The significance level will be compared with the P-value (calculated by ANOVA) and if the P-value is less than the significant level, the null hypothesis will be rejected; otherwise there is not enough evidence to reject the null hypothesis. In this study, we selected a value of 0.1 significance level ($\alpha=0.1$) meaning that there is 10% probability that Type I error is committed (Type I error is when true hypothesis is rejected). In other words, we will be 90% confident that our statement about the null hypothesis is true. The value of the significance level depends on how much one can tolerate falling in Type I error.

ANOVA separates the total variation in the data into two groups, namely variation within groups and variation between groups. Then, ANOVA calculates the two variations and compares them. If the variation between the groups is significantly greater than the variation within groups, then the two population means are significantly (to a level of 10%) unequal. A detailed mathematical formulation of ANOVA may be found in Hethcote and Rhinehart, (1991). The result of the ANOVA analysis is to reject the null hypothesis, indicating that in a population scale the mean slug length of low, medium and high viscosity liquids are significantly different. This emphasizes the effect of liquid viscosity on slug length. Further statistical analysis is

under way to conduct Posteriori test to find the relation between each two pairs of averages.

Partial Correlation.

The purpose of partial correlation analysis is to investigate the existence of significant correlation(s) between the slug length and other independent variables when the common variance of the independent variables is extracted. In general, the partial correlation coefficient is defined as follows.

$$r_{yx_1(x_2)} = \frac{r_{yx_1} - r_{yx_2} r_{x_1x_2}}{\sqrt{(1 - r_{x_1x_2}^2)}} \quad (1)$$

In general terms, Eq. 1 is the partial correlation coefficient between variable y and x_1 when the effect of variable x_2 is extracted. This analysis revealed a significant correlation between average slug length and no-slip liquid holdup in the pipe. Physically, the no-slip liquid holdup is strongly related to the actual liquid holdup in the pipe which is the primary reason for higher slug frequency and thus shorter slugs (Fig. 5).

Furthermore, a significant relationship was found between average slug length and the ratio of the superficial liquid to superficial gas frictional pressure drops (Lockart and Martinelli parameter), defined as

$$X = \frac{\sqrt{\left(\frac{dp}{dL}\right)_{SL}}}{\sqrt{\left(\frac{dp}{dL}\right)_{Sg}}} \quad (2)$$

Figure 6 shows the relationship. Further analysis is underway to physically explain the relationships and find a model to relate them to the average slug length.

Physical and Theoretical Viscosity Effect

Average slug length is found to be more or less constant, approximately, 30D (Dukler and Hubbard (1975), and Nicholson *et al.* (1978)). A fully developed slug is defined as a stable slug with a constant liquid pickup and shed back rates. In a stable slug, the velocity profile at the tail of the slug is fully developed with a maximum velocity close to 1.2 of the slug velocity (Fabre, (1994)). Therefore, if a short slug has a developing velocity profile at its back, the trailing bubble velocity will be accelerated to overtake the leading bubble dissipating the short slug in between. This slug dissipation (bubble

overtaking) process will continue until all the slugs in the pipe are long enough to develop a fully developed velocity profile. This process is the one that controls the slug length and establish stable slug length.

Dukler *et al.* (1985) developed a physical model for the minimum slug length in which the interaction between the film and slug front is simulated as a sudden expansion of a conduit flow into a large reservoir (Fig. 7). As the liquid separates from the film to the slug front it goes into a recirculation process formed between the separation point and the reattachment point, known as the slug mixing zone and characterized by vortices and high local velocity. At the reattachment point, a new wall boundary layer is developed ending the turbulence structure region. Downstream of the reattachment point, the “memory” of the severe separation effect is vanished and a new developed velocity profile is formed with lower maximum velocity. Dukler *et al.* (1985) found that the minimum stable slug length in horizontal pipe is in the order of 20D; however, experimental slug length data were found to be between 20D-40D.

In another work by Taitel *et al.* (1980) and Barnea and Brauner (1985), the developed slug length is modeled and found equal to a distant by which a jet absorbed by liquid and a fully developed velocity profile is established. According to their approach, a minimum slug length of 32D was obtained in horizontal flow.

According to the above modeling, two hydrodynamic parameters can be deduced which control the minimum stable slug length, namely the film height, which controls the sudden expansion or jet velocity, and the time for the redevelopment of fully developed velocity profile, i.e. the length of slug mixing region. Liquid viscosity affects both parameters as discussed in the flow visualization section and shown in Figs. 1 and 2. In the case of high viscosity liquid (Fig. 8), the film height in front of the slug is promoted (thick) indicating shorter mixing zone and reattachment distant which shortens the slug length to achieve a fully developed velocity profile. Furthermore, downstream of the reattachment point, the velocity profile and centerline maximum velocity are smaller because they are inverse functions of liquid viscosity in laminar flow. This can be shown by the laminar velocity profile and maximum velocity in horizontal pipe flow derived from momentum conservation law as follows.

$$v_z = \frac{\Delta P \times R^2}{4\mu L} \left[1 - \left(\frac{r}{R} \right)^2 \right]. \quad (3)$$

$$v_{z,\max} = \frac{\Delta P \times R^2}{4\mu L}. \quad (4)$$

The proposed physical model in Fig. (8) indicates that the change in slug flow characteristics due to high liquid viscosity result in shorter stable slug lengths.

Theoretically, the slug length can be derived from mass and momentum conservation laws across the slug and film regions (Dukler and Hubbard (1975)) as follows.

$$L_s = \frac{v_s}{v_s (H_{LLS} - H_{LTBe})} \times \left[\left(\frac{W_L}{\rho_L A_p v_s} - H_{LTBe} \right) + c(H_{LLS} - H_{LTBe}) \right]. \quad (5)$$

From Eq. 5 the effect of liquid viscosity can be implicitly related to the slug length through the slug flow characteristics, namely v_s , $v_{s,}$ H_{LLS} and H_{LTBe} . From our experimental observation shown in Fig. 2, the liquid holdup in Taylor bubble, H_{LTBe} , is promoted as well as the slug liquid holdup, H_{LLS} , yet the increase in the film holdup is greater than in slug zone (Nadler and Mewes (1995)). Thus, the effect on their difference ($H_{LLS}-H_{LTBe}$) is inversely proportional to liquid viscosity. Furthermore, it is experimentally observed and theoretically investigated (Gokcal (2009)) that slug frequency increases with increasing liquid viscosity. If we look at each term of Eq. 5 and its relationship to the slug length as liquid viscosity increases, the following is found.

1st term of Eq. 5:

$$\left[\frac{v_s \downarrow}{v_s \uparrow (H_{LLS} \uparrow - H_{LTBe} \uparrow \downarrow)} \right] \downarrow$$

2nd term of Eq. 5:

$$\left[\left(\frac{W_L \rightarrow}{\rho_L (\rightarrow) A_p (\rightarrow) v_s (\downarrow)} \right) \uparrow - H_{LTBe} \uparrow \right] \downarrow$$

3rd term of Eq. 5:

$$\left[c(\rightarrow) (H_{LLS} \uparrow - H_{LTBe} \uparrow) \right] \downarrow$$

The above analysis shows the significant inverse effect of liquid viscosity on slug length.

Future Work

- Further characterize the liquid behavior in film zone including the developing and developed sections to come up with a physical model.
- Further analyze the experimental data for correlating parameters and trends.
- Investigate the best fit probabilistic distribution and model it for high viscosity oil.
- Develop/modify existing slug length correlation.
- Modify Dukler *et al.* (1985) physical model for the minimum slug length to account for high viscosity liquids.

Nomenclature

A=	pipe cross sectional area
c=	constant
H=	liquid holdup, liquid height
L=	length
p=	pressure
r=	correlation coefficient, pipe radial direction
R=	pipe radius
v=	velocity

W=	mass rate
x=	arbitrary variable
X=	Lockhart and Martinelli parameter
y=	arbitrary variable

Subscripts

f=	film
L=	liquid
LS=	liquid slug
max=	maximum
o=	oil
P=	pipe
S=	slug
Sg=	superficial gas
SL=	superficial liquid
TBe=	Taylor bubble equilibrium
z=	axial direction

Greek

μ =	viscosity, population mean.
ρ =	density
ν =	slug frequency

References

- Abdul-Majeed G.: "Liquid Slug Holdup in Horizontal and Slightly Inclined Two-Phase Slug Flow," *J. Pet. Sci. and Eng.* 27, 27-32, (2000).
- Brandt, I., and Fuchs, P.: "Liquid Holdup in Slugs: Some Experimental Results From the SINTIF Two-Phase Flow Laboratory," BHRG Multiphase Proceedings, Nice, France (1989).
- Brauner, N. and Ullmann, A.: "Modeling of Gas Entrainment from Taylor Bubbles. Part A: Slug Flow," *Int. J. of Multiphase Flow*, 30, 239-272, (2004).
- Colmenares, J., Ortega, P., Padino, J., and Trallero, J.L.: "Slug Flow Model for the Prediction of Pressure Drop for High Viscosity Oils in a Horizontal Pipeline," SPE 71111, Presented at SPE International Thermal Operations and Heavy Oil Symposium, Margarita Island, Venezuela, March 12-14 (2001).
- Dukler, A.E. and Hubbard, M.G.: "A Model for Gas-Liquid Slug Flow in Horizontal and Near Horizontal Tubes", *I&EC Fundamentals*, 14, pp. 337-347 (1975).
- Dukler, A., Moalem-Maron, D., and Brauner, N.: "A Physical Model for Predicting the Minimum Stable Slug Length," *Chem. Eng. Sci.* 40, 1379-1385 (1985).

El-Oun, Z.: "Gas-Liquid Two-Phase Flow in Pipelines," SPE 20645, Presented at SPE ATCE, New Orleans, LA, (1990).

Fabre, J., Grenier, P. and Gadoin, E.: "Evolution of Slug Flow in Long Pipe," BHRG Production Technology Conference, Cannes, France (1993).

Gokcal, B., Al-Sarkhi, A., Sarica, C. and Al-Safran, E.: "Prediction of Slug Frequency for High-Viscosity Oils in Horizontal Pipes," SPE 124057, To Be presented in SPE/ATCE =, New Orleans, LA, (2009).

Gokcal, B., Wang, Q., Zhang, H. Q., and Sarica, C.: "Effects of High Oil Viscosity on Oil-Gas Flow Behavior in Horizontal Pipes," SPE 102727, *SPE Projects, Facilities & Construction Journal*, June, (2008a).

Gokcal, B.: An Experimental and Theoretical Investigation of Slug Flow for High Oil Viscosity in Horizontal Pipes. Ph.D. Dissertation, The University of Tulsa, Tulsa, Oklahoma, (2008b).

Hethea, R. and Rhinehart, R.: Applied Engineering Statistics, Marcel Dekker Inc., (1991).

Kokal, S.: "An Experimental Study of Two-Phase Flow in Inclined Pipes," Ph.D. Dissertation, The University of Calgary, Calgary, Canada, (1987).

Scott, L. and Kouba, G.: "Advances in Slug Flow Characterization for Horizontal and Slightly Inclined Pipelines," SPE20628, Presented in SPE/ATCE, New Orleans, LA., (1990).

Marcano, R.: "Slug Characteristics for Two-Phase Horizontal Flow," M.S. Thesis, The University of Tulsa, Tulsa, OK, (1996).

Nadler M. and Mewes D.: "Effect of the Liquid Viscosity on the Phase Distribution in Horizontal Gas-Liquid Slug Flow" *Int. J. of Multiphase Flow*, 21, No. 2, 253-266, (1995).

Nicholson, K., Aziz, K., and Gregory, G.: "Intermittent Two Phase Flow in Horizontal Pipes, Predictive Models," *Can. J. Chem. Eng.*, 56, 653-663, (1978).

Rothe, P., Crowley, C. and Sam, R.: "Investigation of Two-Phase Flow in Horizontal Pipes at large Pipe Size and High Gas Density," AGA Pipe Research Committee Project, PR-172-507, (1986).

Taitel, Y., Barnea, D., and Dukler, A.: "Modeling Flow Pattern Transition for Steady Upward Gas-Liquid Flow in Vertical Tube," *AIChE J.* 26, 345-354 (1980).

Barnea, D., and Brauner, N.: "Holdup of the Liquid Slugs in Two Phase intermittent Flow," *Int. J. Multiphase Flow* 11, 43-49 (1985).

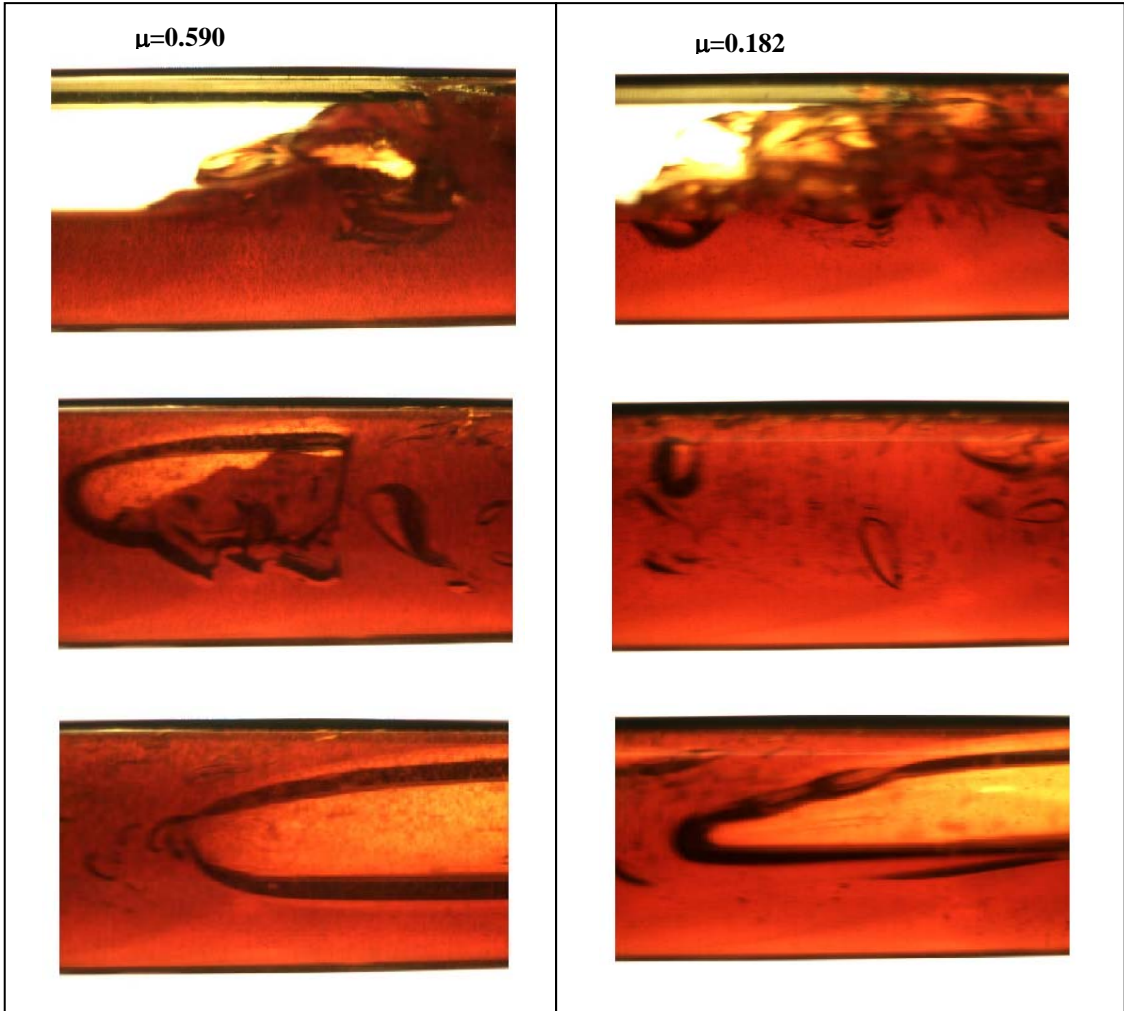


Fig. 1: Comparison of slug front for different viscosities ($v_m=1.51$ m/s)

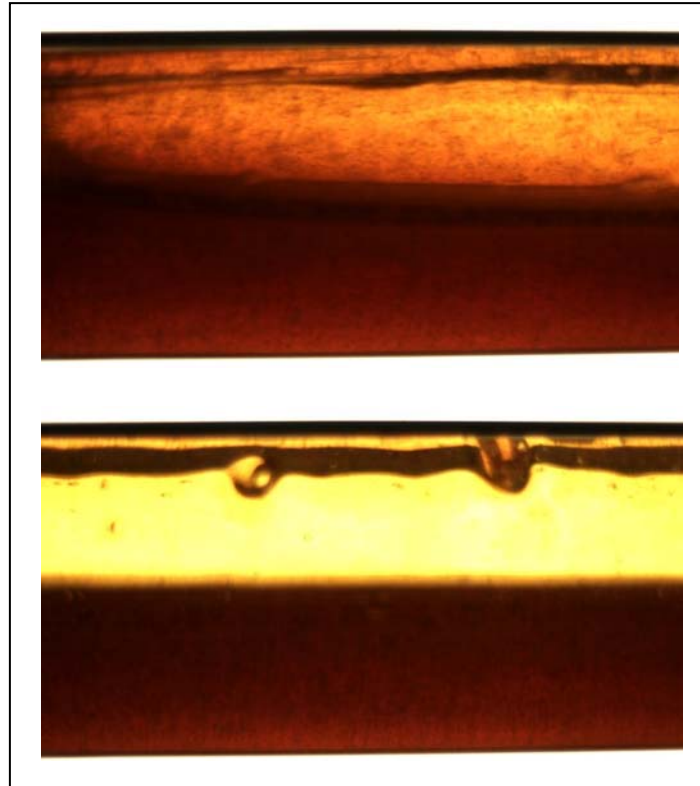


Fig. 2: Developing (top) and developed (bottom) film regions
 ($v_{SL}=0.1$ m/s, $v_{Sg}=2$ m/s, $\mu=0.26$ Pa.s)

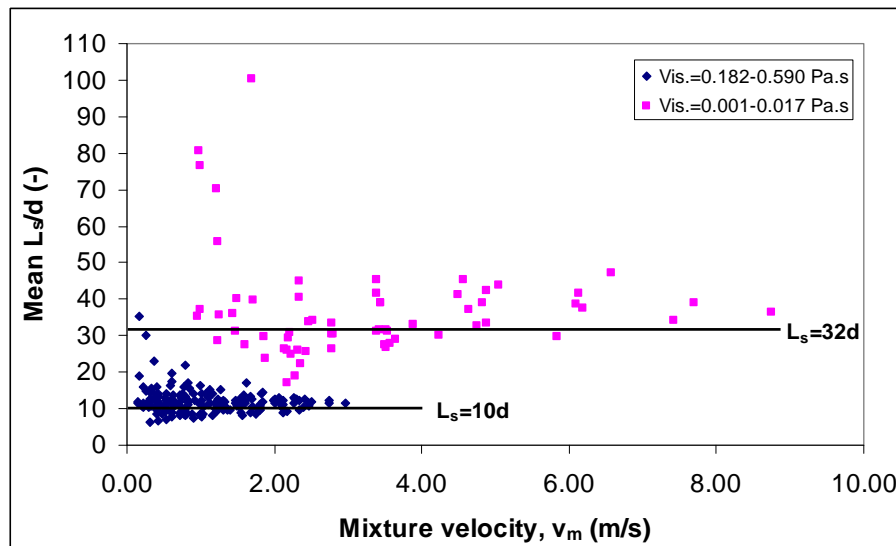


Fig. 3: Evolution of high and low viscosities (Mean slug length vs. Mixture velocity)

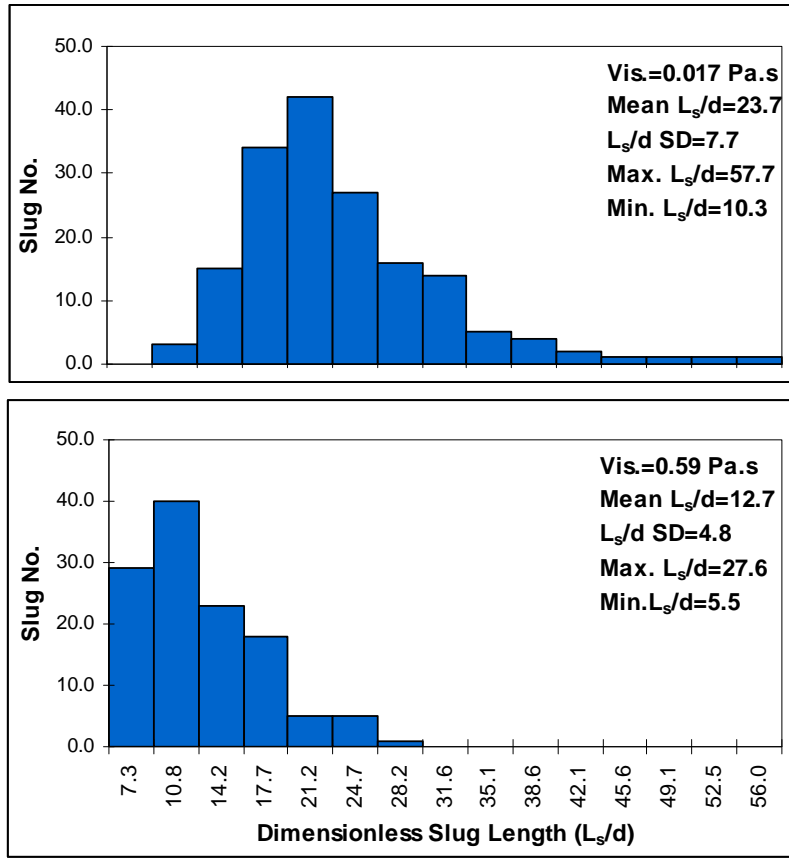


Fig. 4: Slug length distribution comparison of high and low liquid viscosities ($v_{SL}=0.3$ m/s, $v_{Sg}=1.5$ m/s)

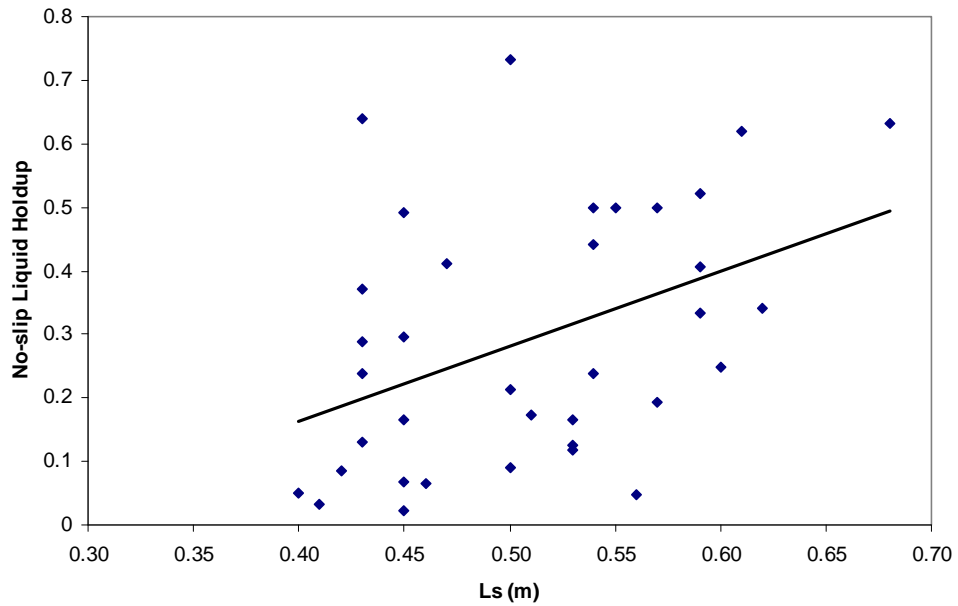


Fig. 5: High viscosity slug length correlation with Lockhart and Martinelli parameter

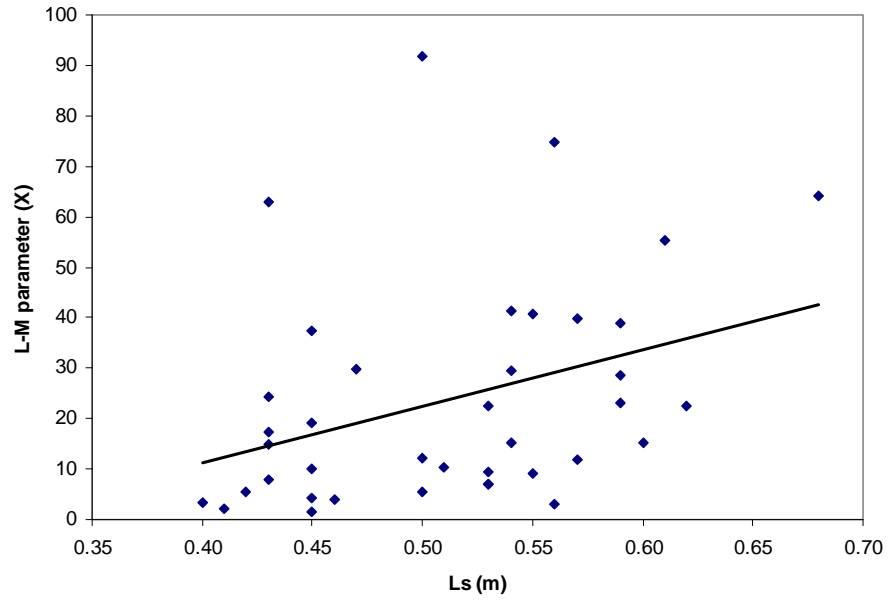


Fig. 6: High viscosity slug length correlation with no-slip liquid holdup

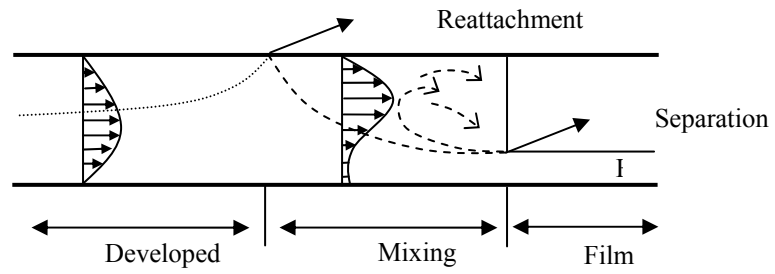


Fig. 7: Light oil minimum slug length physical model (Dukler et al. 1985)

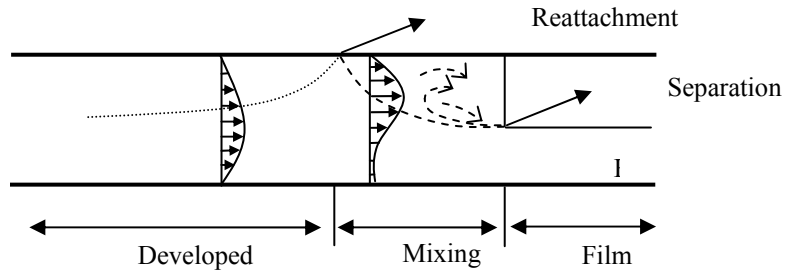


Fig. 8: Proposed high viscosity oil minimum slug length physical model



Fluid Flow Projects

Investigation of Diameter Effect on Drift Velocity

Anoop Kumar Sharma

Advisory Board Meeting, September 30, 2009

Outline

- ◆ Introduction
- ◆ Objectives
- ◆ Literature Review
- ◆ Experimental Setup
- ◆ Experiments
- ◆ Schedule

Introduction

- ◆ Increase in Significance of High Viscosity Oil
- ◆ Current Multiphase Flow Models Developed for Low Viscosity Oils
- ◆ Multiphase Flows Exhibit Significantly Different Behavior for Higher Viscosity Oils

Introduction ...

- ◆ Slug Translational Velocity is Key Closure Relationship for Mechanistic Modeling
- ◆ Gokcal (2008) Conducted Experimental and Theoretical Study
 - Drift Velocity Experiments for Various Inclination and Viscosity

Objectives

- ◆ **To Investigate the Effect of the Diameter on Drift Velocity**
 - **3-in. and 6-in. Pipe**
 - **Various Inclinations and Viscosities**

Literature Review

- ◆ **Nicklin *et al.* (1962)**

$$v_t = C_o v_s + v_d$$

Literature Review ...

◆ Dumitrescu (1943)

- Conducted Theoretical Potential Flow Analysis of Drift Velocity for Vertical Flow
- Constant Value of 0.351 for Froude number , $v_d/(gD)^{1/2}$

Literature Review ...

◆ Davies and Taylor (1950)

- Conducted Experimental Potential Flow Analysis of Drift Velocity for Vertical Flow
- Constant Value of 0.328 for Froude number ($v_d/(gD)^{1/2}$)

Literature Review ...

◆ Benjamin (1968)

- Proposed a Drift Velocity Relationship for Horizontal Flow

$$v_d = 0.542\sqrt{gD}$$

Literature Review ...

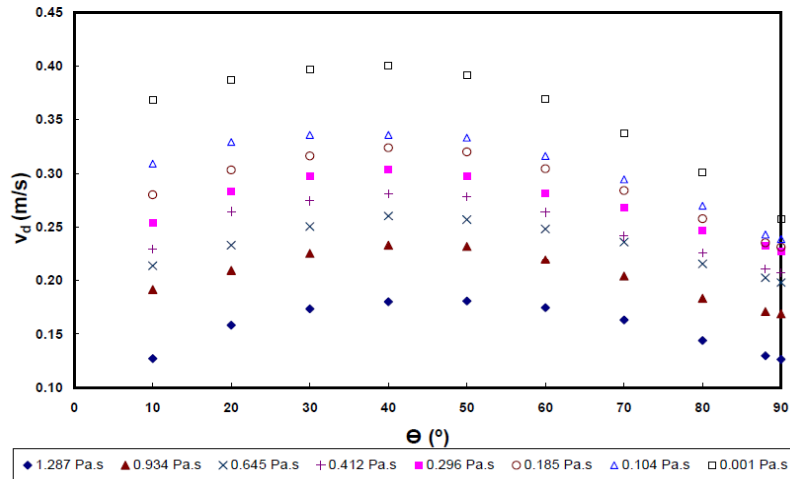
◆ Bendiksen (1984)

- Proposed a Drift Velocity Relationship for Inclined Flow

$$v_d = v_d^h \cos(\theta) + v_d^v \sin(\theta)$$

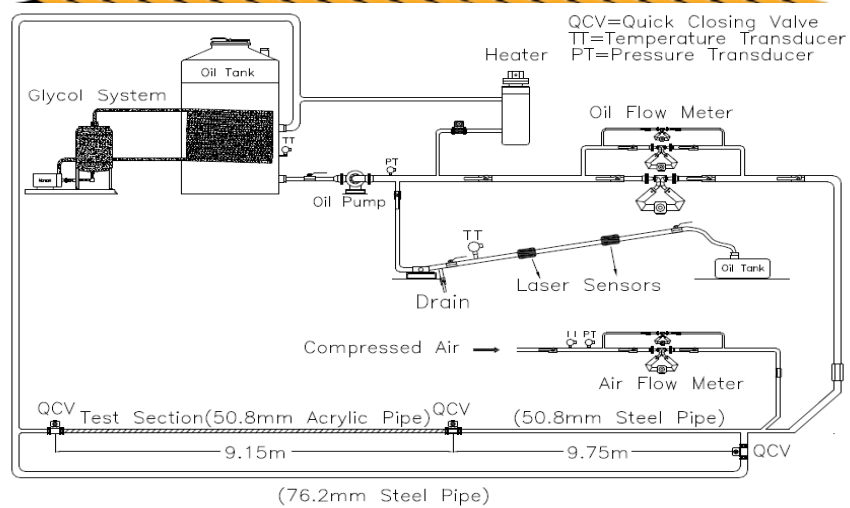
Literature Review ...

🔹 Gokcal (2008) v_d vs. θ for 2-in. pipe



2009

Experimental Setup



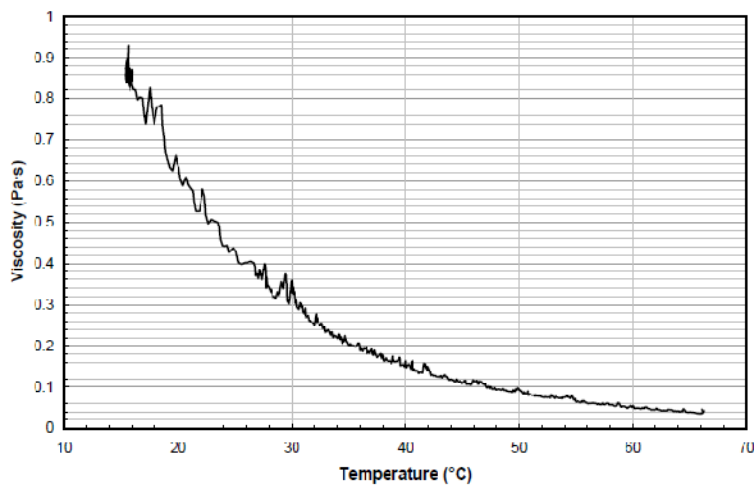
Schematic of Test Facility

Testing Oil

◆ Citgo Sentry 220 Oil

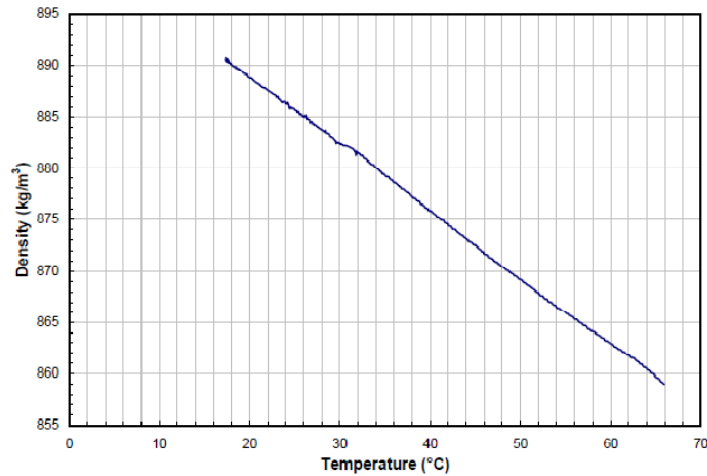
- Gravity: 27.6°API
- Viscosity: 0.220 Pa·s @ 40°C
- Density: 889 kg/m³ @ 15.6°C

Testing Oil ...



Oil Viscosity vs. Temperature for Citgo Sentry 220 Oil

Testing Oil ...

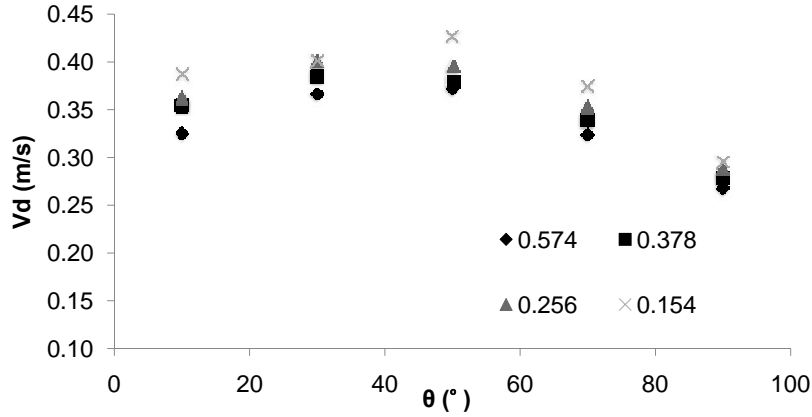


Oil Density vs. Temperature for Citgo Sentry 220 Oil

Experiments

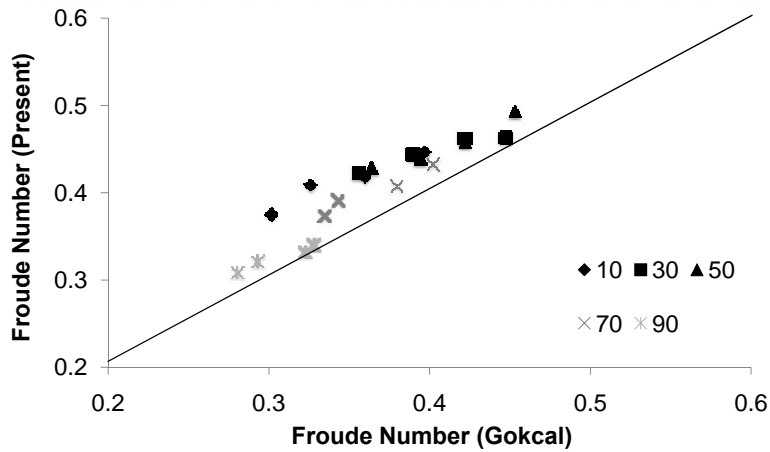
- ◆ **Experimental Matrix**
 - **2-in. Data from Gokcal (2008)**
 - **3-in. and 6-in. Tests**
 - **10° to 90° Inclination**
 - **70°F, 80°F, 90°F, 105°F Temperature**

Experiments...



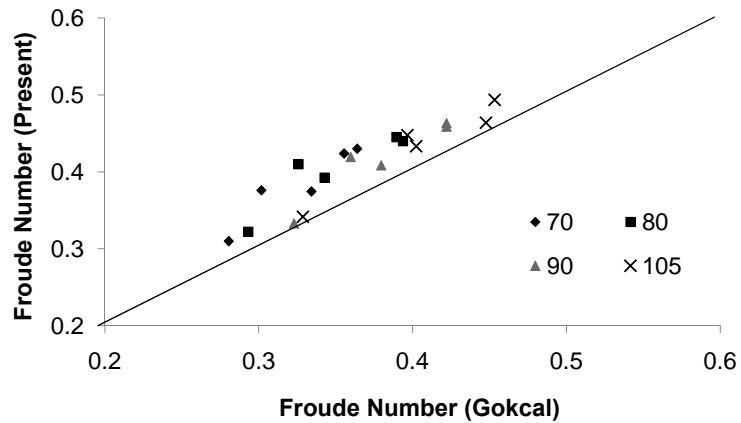
Measured Drift Velocity vs. Inclination Angle for Different Oil Viscosities for 3-in. Pipe

Experiments...



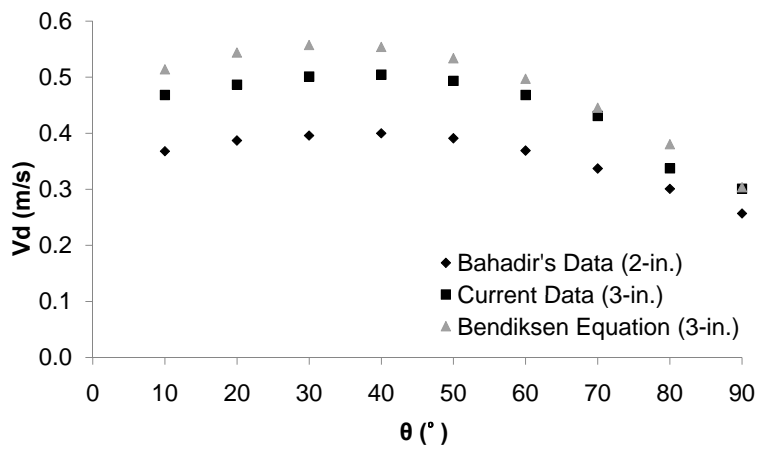
Froude Number Comparison for Different Inclination Angles from Horizontal

Experiments...



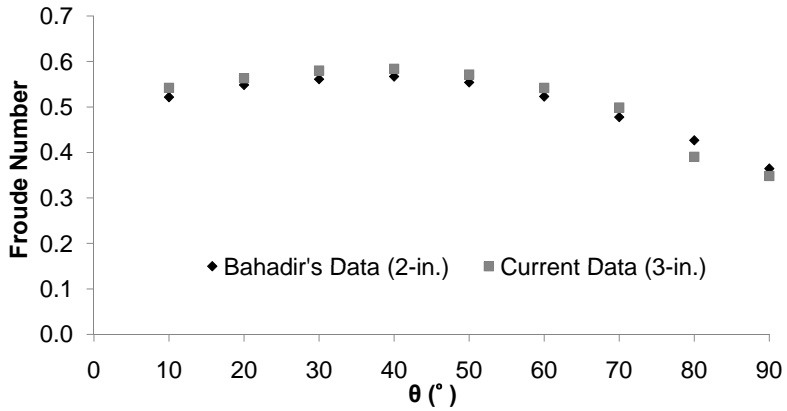
Froude Number Comparison for Different Temperature

Experiments...



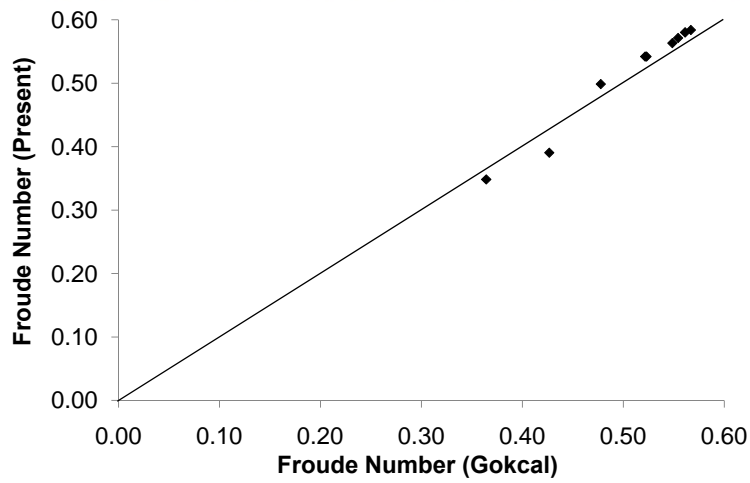
Drift Velocity Comparison for Water

Experiments...



Froude Number Comparison for Water

Experiments...



Froude Number Comparison for Water

Near Future Tasks



- ◆ Experiments on 6-in. Pipe
- ◆ Analysis of All Results
- ◆ Final Report

Project Completion Dates



- ◆ Literature Review.....Completed
- ◆ Experimentation.....October 2009
- ◆ Results Analysis.....October 2009
- ◆ Final Report.....November 2009

Questions & Comments



Investigation of Diameter Effect on Drift Velocity

Anoop Kumar Sharma

PROJECT COMPLETETION DATES:

Literature Review.....	Completed
Experimentation.....	October 2009
Results Analysis.....	October 2009
Final Report	November 2009

Objectives

The objective of this study is:

- to investigate the effect of the diameter on the drift velocity.

Introduction

The world energy demand is increasing and the depletion of conventional oils has put high viscosity or “heavy oil” in the list of one of the most important future hydrocarbon resources. Current multiphase flow models are largely based on experimental data with low viscosity liquids (less than 20 cP). This makes the model predictions more erroneous.

Multiphase flows are expected to exhibit significantly different behavior for higher viscosity oils. Many flow behaviors will be affected by the liquid viscosity, including flow pattern, droplet formation, surface waves, bubble entrainment, slug mixing zones etc.

Gokcal (2008) conducted an experimental and theoretical study to investigate the effects of high oil viscosity on slug flow characteristics, including translational velocity, and slug length and frequency in horizontal pipes. This study is a continuation of Gokcal’s work on translational velocity. Gokcal did drift velocity experiments on 2-in. pipe. In present study same drift velocity experiments will be done

for heavy oil in 3-in. and 6-in. pipes to investigate the effect of diameter on drift velocity.

Literature Review

The slug translational velocity or velocity of slug units is one of the key closure relationships in two-phase flow mechanistic modeling. Translational velocity (v_t) is described as a superposition of bubble velocity in stagnant liquid, i.e. the drift velocity (v_d) and the maximum axial velocity (v_s) in the slug body as proposed by Nicklin *et al.* (1962) in the following equation.

$$v_t = C_o v_s + v_d. \quad (1)$$

The flow coefficient C_o is approximately the ratio of the maximum to the mean velocity of a fully developed velocity profile.

Dumitrescu (1943) and Davies and Taylor (1950) conducted a potential flow analysis to find the drift velocity for vertical flow. Both derived the same dimensionless group Froude number, Fr (v_d/\sqrt{gD}) which has a constant value. Davies and Taylor estimated the constant value as 0.328. Dumitrescu made more accurate calculations and theoretically determined this value as 0.351, which agreed well with the air-water experimental Nicklin *et al.* (1962). Thus,

$$v_d = 0.351\sqrt{gD} . \quad (2)$$

Benjamin (1968) proposed the following drift velocity relationship for horizontal pipes,

$$v_d = 0.542\sqrt{gD}. \quad (3)$$

Benjamin calculated the value of the drift velocity coefficient by using inviscid (potential) flow theory (surface tension and viscosity are neglected). The drift velocity in horizontal slug flow is the same as the velocity of the penetration of a bubble when liquid is drained out of a horizontal pipe. The drift velocity results from hydrostatic pressure difference between top and bottom of the bubble nose. Bendiksen (1984) and Zukoski (1966) verified the study of Benjamin, experimentally.

Bendiksen conducted an experimental study of velocities of single elongated bubbles in flowing liquids at different inclination angles. The measured velocities were plotted against the liquid velocity for each inclination angle. Then, drift velocities were found by the extrapolation of the data to zero liquid velocity. He correlated the drift velocity for inclined flow by using the drift velocities for horizontal and vertical flow:

$$v_d = v_d^h \cos\theta + v_d^v \sin\theta. \quad (4)$$

Gokcal (2008) conducted experimental study on drift velocity of heavy oil at different viscosities corresponding to different temperatures (19.2 °C to 45 °C). The results are shown in Fig. 1.

Experimental Study

Facility

For drift velocity experiments, some modifications were made to the existing heavy oil indoor facility without changing the original structure. A 3.05-m (10-ft) long transparent acrylic pipe with 50.8-mm (3-in.) ID was added to the existing facility temporarily, as shown in Fig. 2. After tests are completed with 3-in. pipe it will be replaced by 6-in. pipe. The acrylic pipe is located close to the oil storage tank. The inclination angle can be changed from 0° to 90°. The oil pump is used to fill up the pipe at various temperatures corresponding to different viscosities. The oil can be captured by valves which are located at the inlet and outlet of the pipe. An air bubble from the bottom of the pipe is released into the stagnant liquid column. The drift velocity of the released air bubble is measured by two laser beams and sensors.

Testing Oil

The Citgo Sentry 220 oil, which is used in the previous study by Gokcal, is used. Following are typical properties of the oil:

- Gravity: 27.6° API
- Viscosity: 0.220 Pa·s @ 40° C
- Density: 889 kg/m³ @ 15.6° C

The oil viscosity and density vs. temperature behavior are shown in Figs. 3 and 4, respectively.

Experiment with 3-in. Pipe

Experiments were conducted on heavy oil for 70°F, 80 °F, 90 °F, 105 °F in 3-in pipe. The corresponding viscosities of oil were 0.574 cP, 0.378 cP, 0.256 cP and 0.154 cP, respectively. For each viscosity, experiments were conducted for inclination angle 10°, 30°, 50°, 70° and 90° from horizontal. The results are shown in Fig. 5. The corresponding data is shown in Table 1. The trend for drift velocity is similar to that of Gokcal (2008) data for 2-in. pipe. Comparison of Froude numbers between current data and Gokcal data for different inclinations from horizontal and temperature are shown in Figs. 6 and 7, respectively. The corresponding data are shown in Table 1.

Few experiments were conducted with water to prove that the system is working properly. In Fig. 8, the results of water drift velocity tests were compared with Gokcal (2008) data and Bendiksen (1984) equation predictions. The corresponding data is given in Table 2. The current results are very close to Bendiksen equation predictions while it follows the same trend as that of Gokcal 2-in. pipe experiments. In Figs. 9 and 10, Froude number from current study and Gokcal (2008) study are compared. The results are almost superimposable which authenticates the results of current study with 3-in. pipe for heavy oil.

Near Future Tasks

The main tasks for the future are:

- Experiments with 6-in. pipe.
- Analyzing the results and writing report.

References

Bendiksen, K. H.: "An Experimental Investigation of the Motion of Long Bubbles in Inclined Tubes," *Int. J. Multiphase Flow* (1984), **10**, 467-483.

Benjamin, T. B., "Gravity Currents and Related Phenomena," *J. Fluid Mech.* (1968), **31** (2), 209-248.

Davies, R. M., and Taylor, G. I., "The Mechanics of Large Bubbles Rising Through Liquids in Tubes," *Proc. Royal Soc. London* (1950), **A 200**, 375-390.

Dumitrescu, D. T., "Strömung an einer Luftblase im senkrechten," *Rohr. Z. Angew. Mat. Mech.*(1943), **23**, 139-149.

Gokcal, B., "An Experimental and Theoretical Investigation of Slug Flow for High Oil Viscosity in Horizontal Pipes," Ph.D. Dissertation, The University of Tulsa (2008).

Nicklin, D. J., Wilkes, J. O., Davidson, J. F., "Two-Phase Flow in Vertical Tubes," *Trans. Inst. Chem. Eng.* (1962), **40**, 61-68.

Table 1: Comparison of Gokcal (2008) and Present Data for Heavy Oil

Temp. (F)	Inclination (°)	Gokcal (2008) (2-in.)		Present Data (3-in.)	
		Vd (m/s)	Froude No.	Vd (m/s)	Froude No.
70	10	0.21	0.302	0.325	0.376
70	30	0.251	0.356	0.366	0.424
70	50	0.257	0.364	0.372	0.430
70	70	0.236	0.334	0.324	0.374
70	90	0.198	0.280	0.268	0.310
80	10	0.23	0.326	0.354	0.410
80	30	0.275	0.390	0.385	0.445
80	50	0.278	0.394	0.380	0.440
80	70	0.242	0.343	0.339	0.392
80	90	0.207	0.293	0.278	0.322
90	10	0.25	0.360	0.362	0.419
90	30	0.298	0.422	0.401	0.463
90	50	0.298	0.422	0.397	0.459
90	70	0.268	0.380	0.353	0.408
90	90	0.228	0.323	0.288	0.333
105	10	0.28	0.397	0.387	0.448
105	30	0.316	0.448	0.401	0.464
105	50	0.32	0.453	0.427	0.494
105	70	0.284	0.402	0.375	0.433
105	90	0.232	0.329	0.295	0.342

Table 2: Comparison of Gokcal (2008), Present Data and Bendiksen (1984) Equation Prediction for Water

Inclination (°)	Gokcal (2008) (2-in.)		Present Data (3-in.)		Bendiksen Eq.
	Vd (m/s)	Froude No.	Vd (m/s)	Froude No.	Vd (m/s)
10	0.368	0.522	0.468	0.54	0.514
20	0.387	0.548	0.487	0.56	0.544
30	0.396	0.561	0.501	0.58	0.558
40	0.400	0.567	0.505	0.58	0.554
50	0.391	0.554	0.494	0.57	0.534
60	0.369	0.523	0.468	0.54	0.497
70	0.337	0.478	0.431	0.50	0.446
80	0.301	0.427	0.337	0.39	0.381
90	0.257	0.364	0.301	0.35	0.304

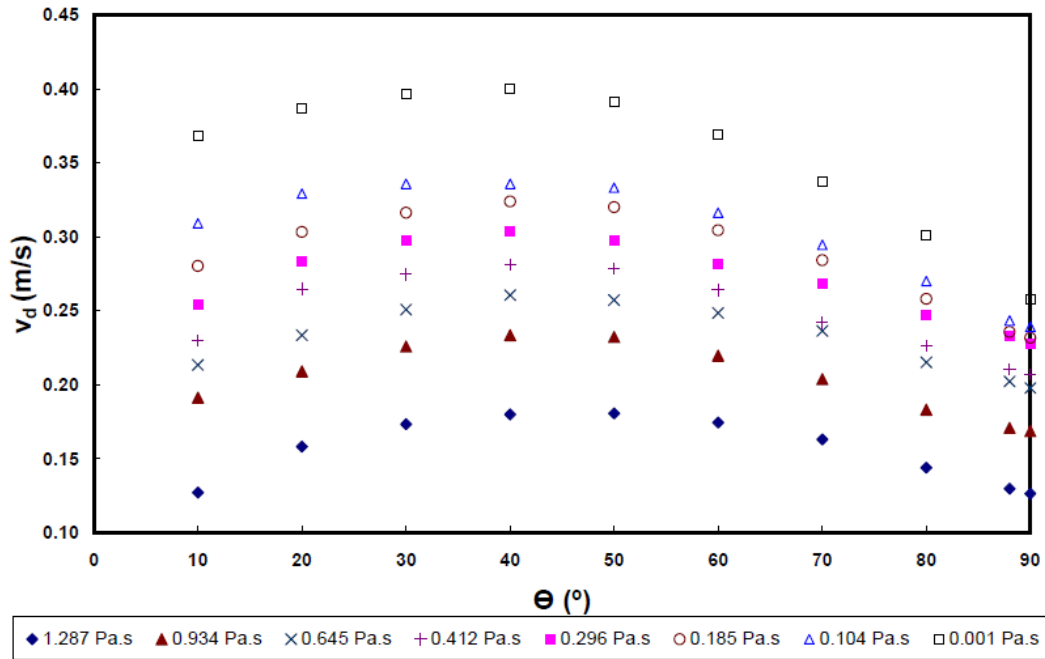


Figure 1: Measured Drift Velocity vs. Inclination Angle for Different Oil Viscosities for 2-in. Pipe (Gokcal, 2008)

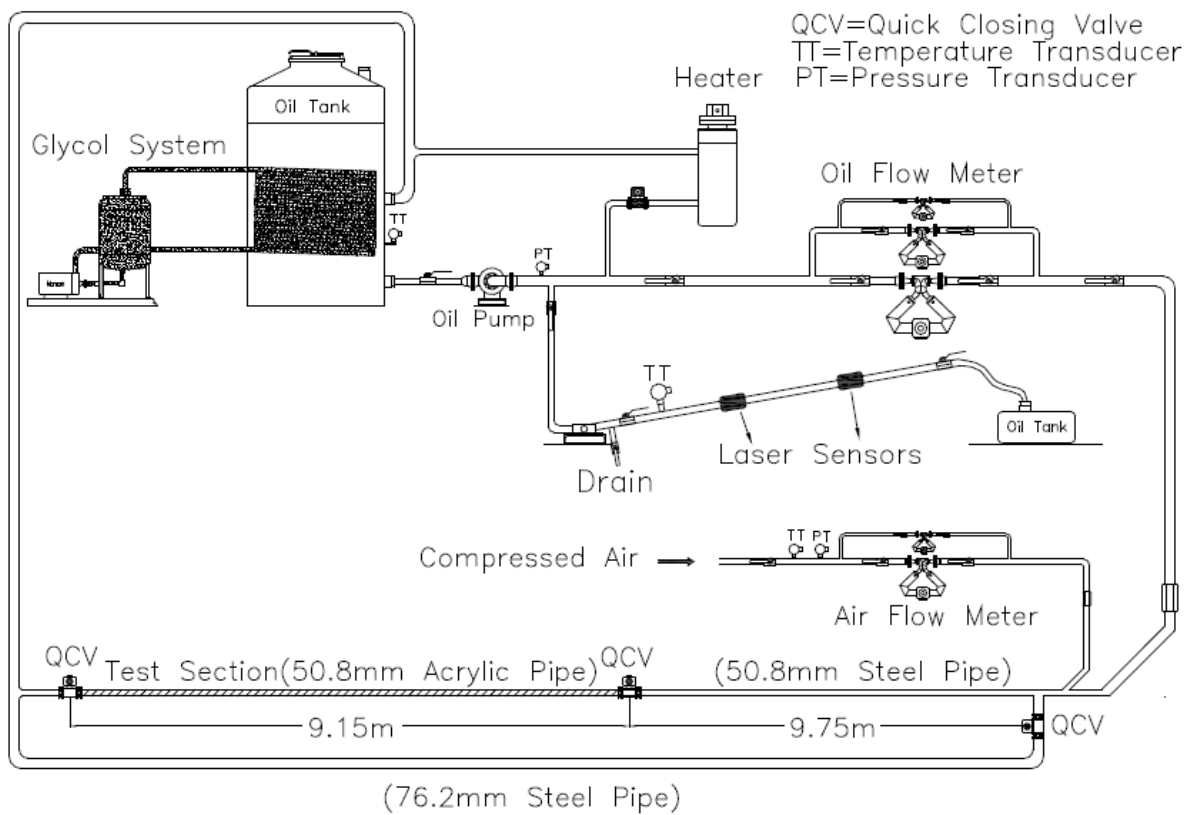


Figure 2: Schematic of Test Facility

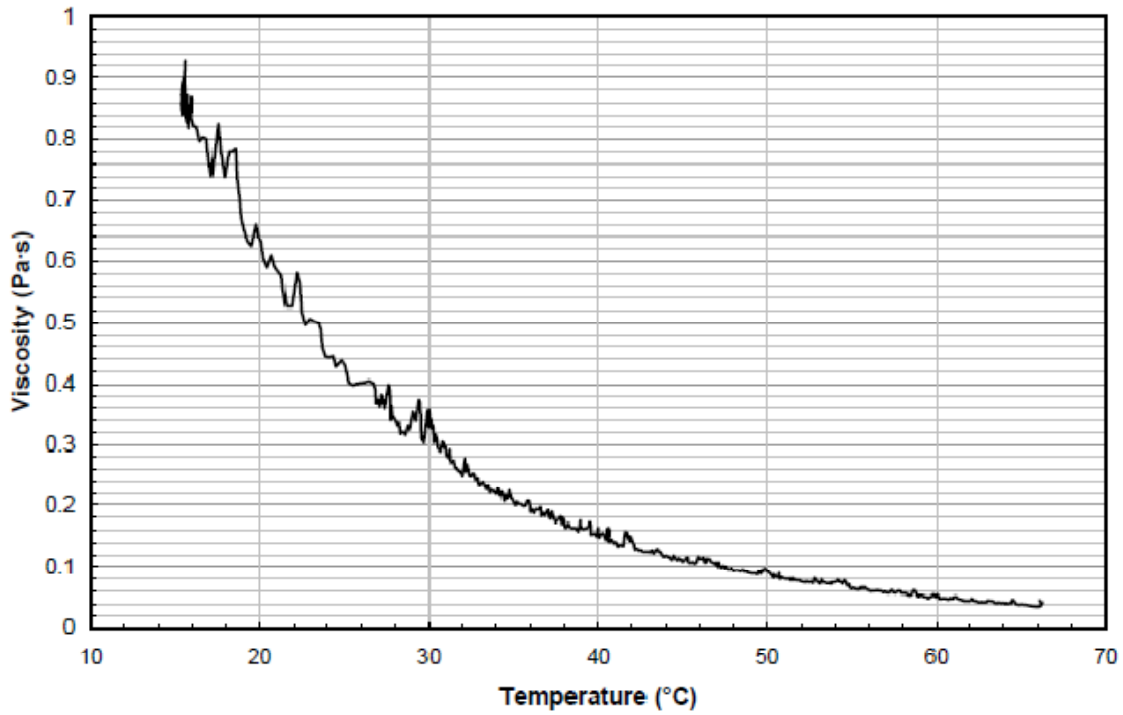


Figure 3: Oil Viscosity vs. Temperature for Citgo Sentry 220 Oil

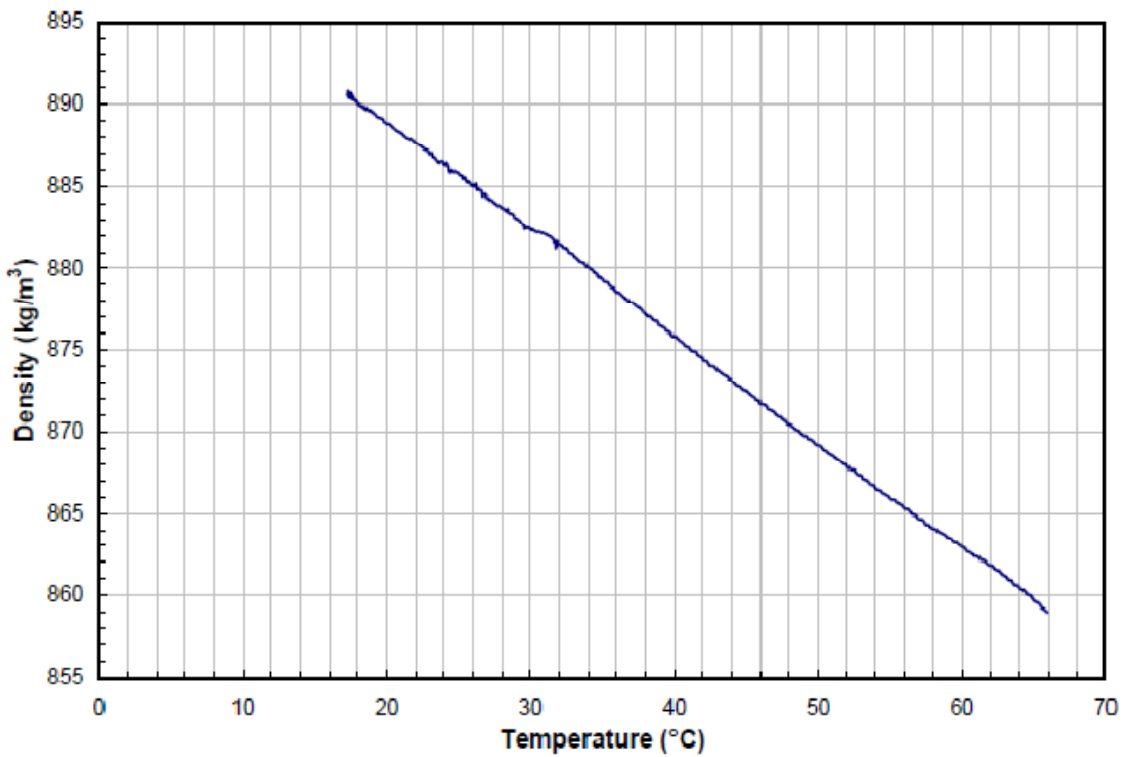


Figure 4: Oil Density vs. Temperature for Citgo Sentry 220 Oil

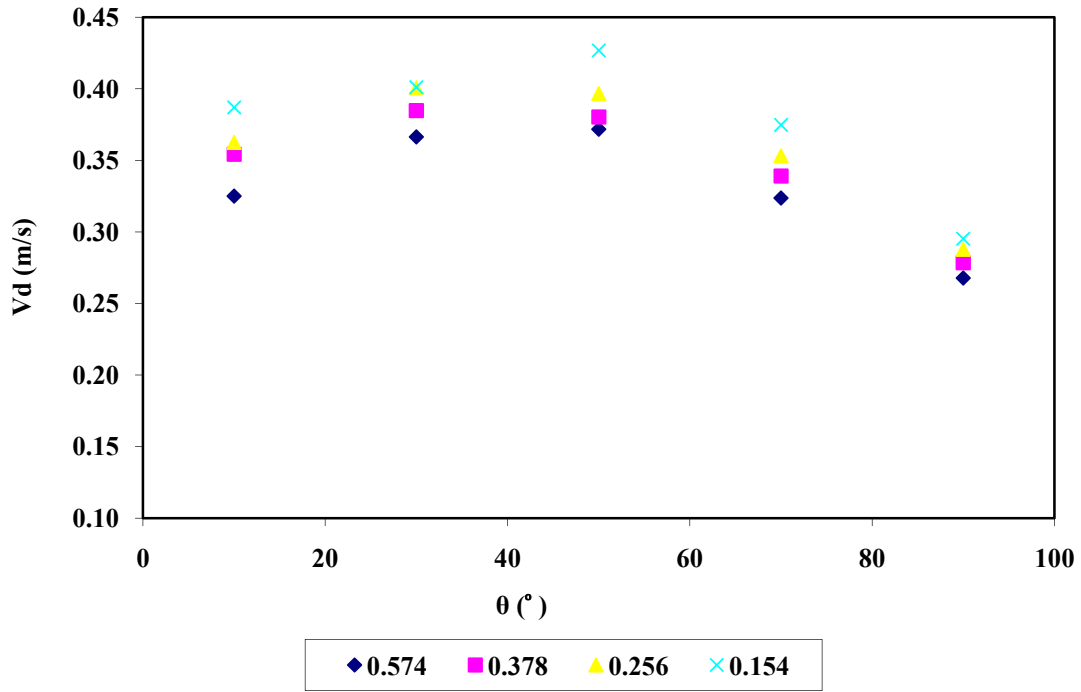


Figure 5: Measured Drift Velocity vs. Inclination Angle for Different Oil Viscosities for 3-in. Pipe (Present Data)

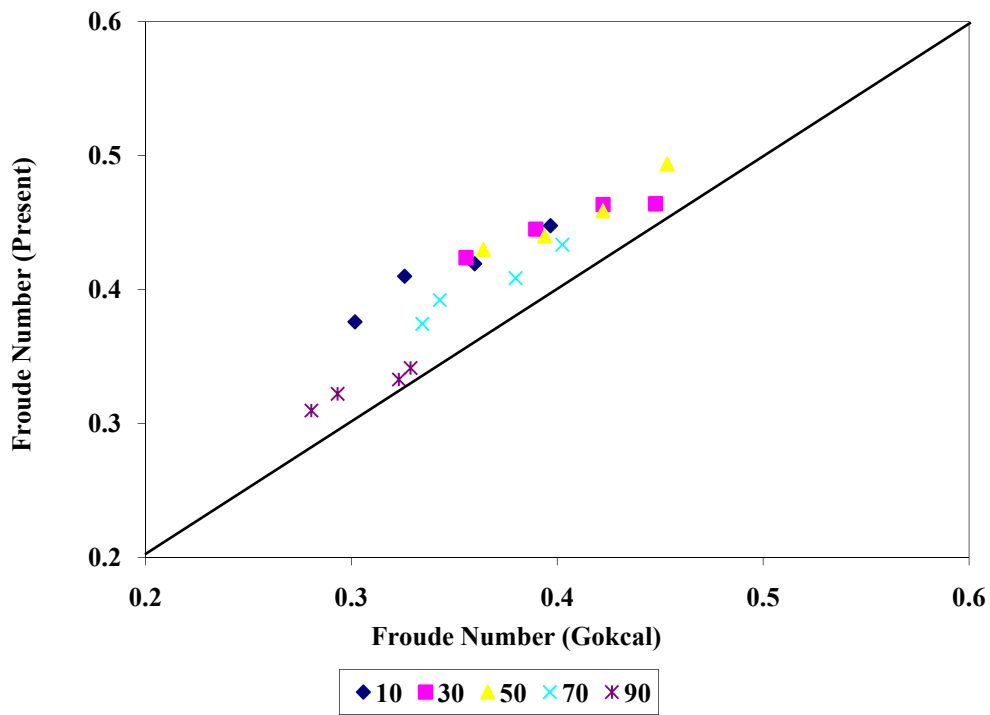


Figure 6: Froude Number Comparison for Different Inclination Angles from Horizontal

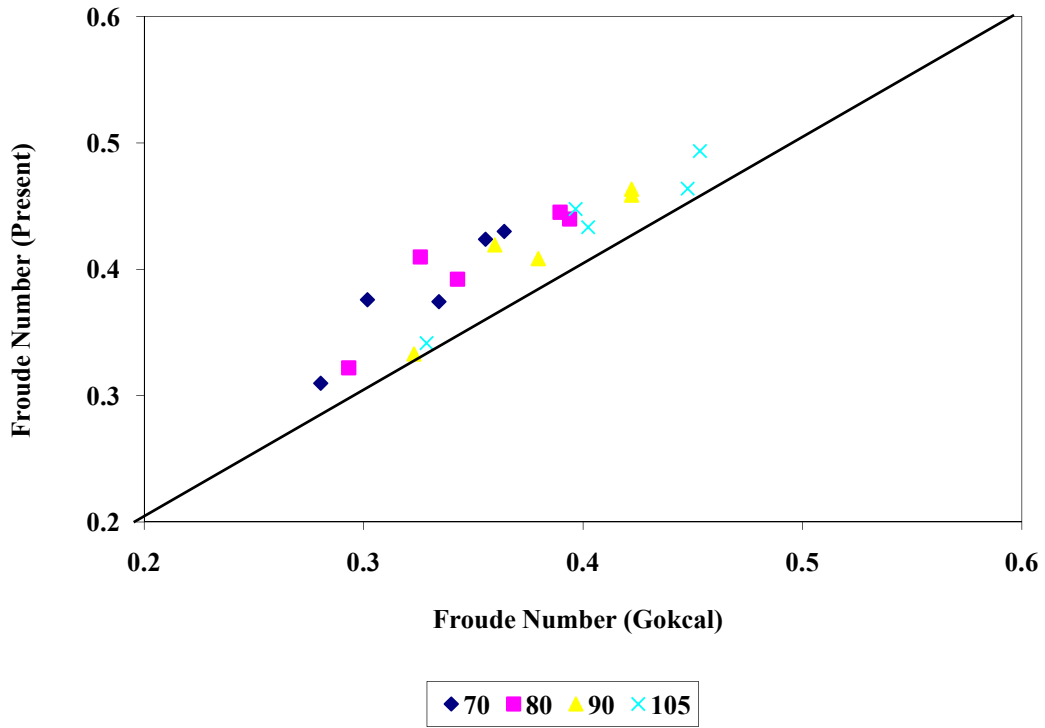


Figure 7: Froude Number Comparison for Different Temperature

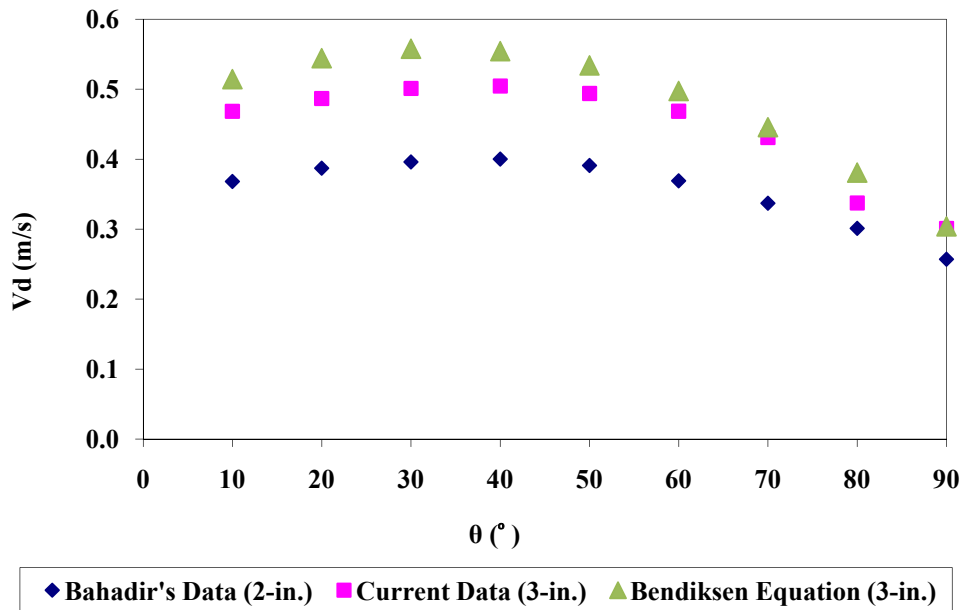


Figure 8: Drift Velocity Comparison for Water

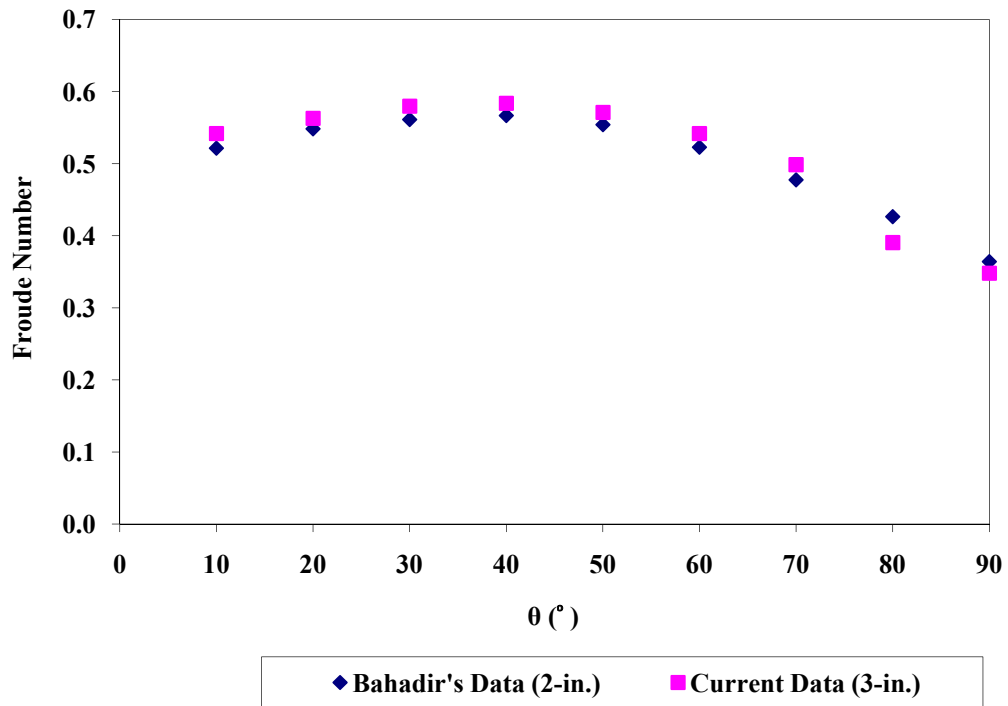


Figure 9: Froude Number Comparison for Water

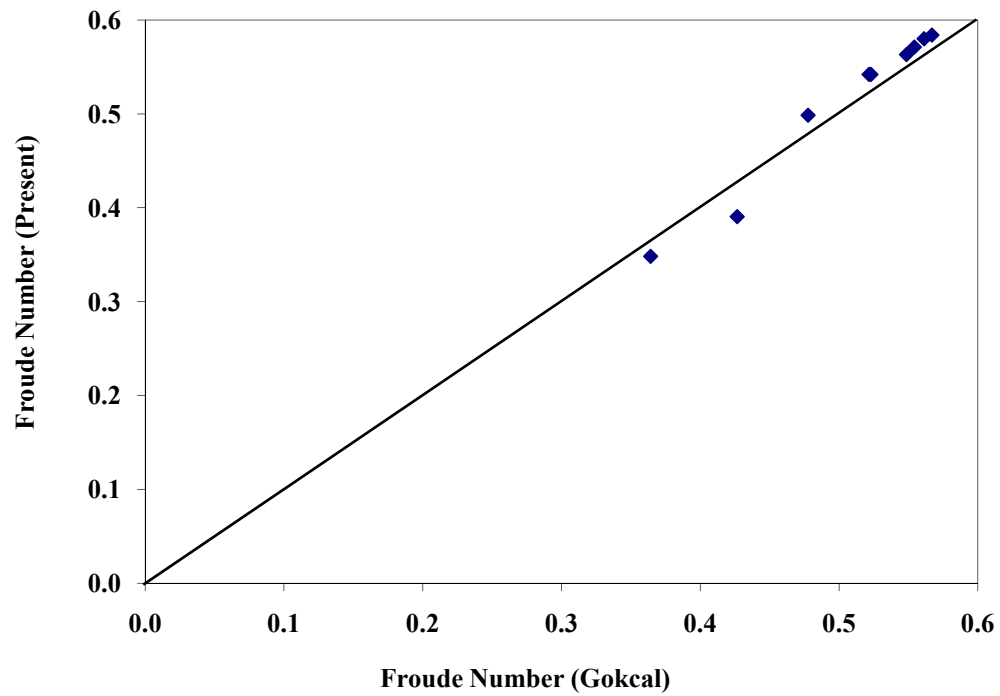


Figure 10: Froude Number Comparison for Water



Fluid Flow Projects

Executive Summary of Research Activities

Cem Sarica

Advisory Board Meeting, September 30, 2009

Low Liquid Loading Flow

◆ Significance

➤ Wet Gas Transportation

- ▲ Holdup and Pressure Drop Prediction
- ▲ Corrosion Inhibitor Delivery (Top of the Line Corrosion)

◆ Objectives

➤ Develop Better Predictive Tools

Low Liquid Loading Flow ...

◆ Past TUFFP Studies

- Two-phase, Small Diameter, Low Pressure
 - ▲ Air-Water and Air-Oil
 - ▲ 2-in. ID Pipe with $\pm 2^\circ$ Inclination Angles from Horizontal
- Two-phase, Large Diameter, Low Pressure
 - ▲ Air-Water
 - ▲ 6-in. ID and $\pm 2^\circ$ Inclination Angles from Horizontal

Low Liquid Loading Flow ...

◆ Past TUFFP Studies ...

- Three-phase, Large Diameter, Low Pressure
 - ▲ Air-Mineral Oil-Water
 - ▲ 6-in. ID, Horizontal Flow
 - ▲ Findings
 - ✦ Observed and Described Flow Patterns and Discovered a New Flow Pattern
 - ✦ Acquired Significant Amount of Data on Various Parameters, Including Entrainment Fraction
 - ▲ Remaining Tasks
 - ✦ Development of Improved Closure Relationships

Low Liquid Loading Flow ...

◆ Current Study

- Three-phase, Large Diameter, Low Pressure Inclined Flow
 - ▲ Air-Mineral Oil-Water
 - ▲ 6-in. ID and $\pm 2^\circ$ Inclination Angles from Horizontal
 - ▲ Objectives
 - ✦ Acquire Similar Data as in Horizontal Flow Study
 - ✦ Develop Improved Closure Relationships

Low Liquid Loading Flow ...

◆ Status

- Re-Started in Spring 2009
 - ▲ New Ph.D. Student
 - ▲ Successful Repeat Tests
 - ▲ Lighter Oil will be Used in Current Study

◆ Future Studies

- Two and Three-phase, Large Diameter, High Pressure Horizontal and Inclined Flow
 - ▲ Requires New High Pressure Facility



Fluid Flow Projects

Low Liquid Loading Gas-Oil-Water Flow

Kiran Gawas

Advisory Board Meeting, September 30, 2009

Outline

- ◆ Objectives
- ◆ Introduction
- ◆ Literature Review
- ◆ Experimental Study
- ◆ Near Future Tasks

Objectives

- ◆ Acquire Experimental Data of Low Liquid Loading Gas-Oil-Water Flow in Horizontal and Near Horizontal Pipes Using Representative Fluids
- ◆ Check Suitability of Available Models for Low Liquid Loading Three Phase Flow and Suggest Improvements If Needed



Introduction

- ◆ Low Liquid Loading Flows Correspond to Liquid to Gas Ratio $\leq 1100 \text{ m}^3/\text{MMsm}^3$
- ◆ Widely Encountered in Wet Gas Pipelines
- ◆ Small Amounts of Liquid Influences Pressure Distribution – Hydrate Formation, Pigging Frequency, Downstream Equipment Design etc.
- ◆ Transport of Additives
- ◆ Limited Research for Low Liquid Loading Three Phase Flow



Literature Review

Two Phase Low Liquid Loading Studies

Author	Experimental Study	Modeling study	Working Fluids	Pipe ID & Inclination Angle
Hart <i>et al.</i> (1989)	Pressure gradient and liquid holdup	ARS model	Air-Water	51 mm & 0°
Grolman and Fortuin (1995)	Pressure gradient and liquid hold up	MARS model	Air-Water	51 mm & 0°, ±1°, ±2°
Chen <i>et al.</i> (1997)	Pressure gradient and liquid holdup	"Double Circle"	Air-Kerosene	77.9 mm
Meng (1999)	Pressure gradient, liquid holdup, wetted wall fraction, liquid entrainment and film thickness	Two-fluid model	Air-Oil	50.1 mm & 0°, ±1°, ±2°
Olive <i>et al.</i> (2003)	Pressure gradient, liquid holdup, wetted wall fraction, liquid entrainment and film thickness	N/A	Air-Water	51 mm & 0°, ±1°, ±2°



Literature Review ...

Author	Experimental Study	Modeling study	Working Fluids	Pipe ID & Inclination Angle
Badie <i>et al.</i> (2000)	Pressure gradient and liquid holdup	N/A	Air-Oil and Air-Water	79 mm & 0°
Badie <i>et al.</i> (2001)	Liquid entrainment	N/A	Air-Water	79 mm & 0°
Fan <i>et al.</i> (2005)	Pressure gradient, liquid holdup, wetted wall fraction, liquid entrainment and film thickness	Two-Fluid Model	Air-Water	51 mm and 149 mm & 0°, ±1°, ±2°



Literature Review ...

Three Phase Flow Studies

Author	Experimental Study	Modeling study	Working Fluids	Pipe ID & Inclination Angle
Taitel <i>et al.</i> (1995)	Pressure gradient and holdup	Three phase stratified flow	Air-Oil-Water	N/A
Khor <i>et al.</i> (1998)	Pressure gradient and holdup	Three phase stratified flow	Air-Oil-Water	N/A
Utvik <i>et al.</i> (2001)	Pressure gradient and flow pattern	N/A	Gas-Oil-Water and Gas-Oil	77.9 mm & 0°
Bonizzi <i>et al.</i> (2003)	N/A	Two fluid model for three phase flow	Gas-Oil-Water	N/A
Zhang and Sarica (2006)	Pressure gradient and holdup	Unified three fluid model	Gas-Oil-Water	N/A

Literature Review ...

♦ Flow Pattern Identification in Three Phase Flow

- Sobocinski (1955),
- Açıkgöz *et al.* (1992)
- Keskin (2005)

Literature Review ...

◆ Low Liquid Loading Gas-Oil-Water Flow

➤ Dong (2007)

- ▲ Air-Oil-Water, 0°, 6-in ID Pipe
- ▲ 156 Tests with up to 17.5-m/s v_{SG} and up to 0.038-m/s v_{SL}
- ▲ Flow Pattern Description
- ▲ Evaluated Fan's Model, Unified Three-phase Model and OLGA



Experimental Study

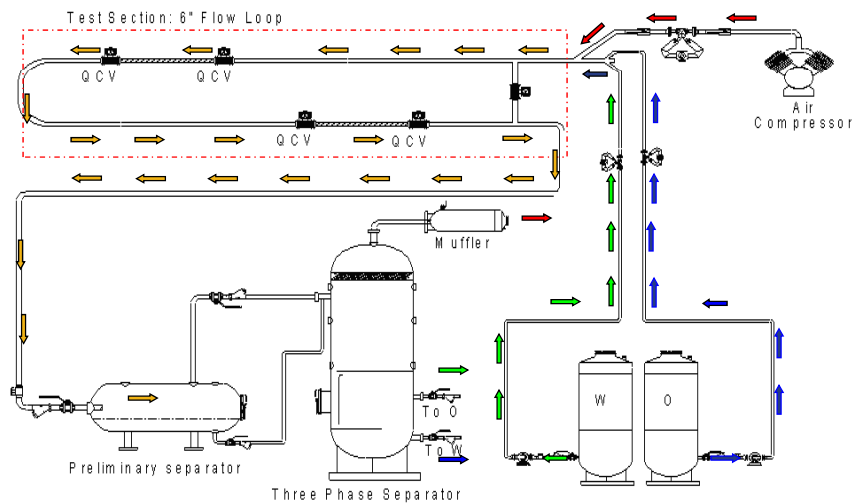
- ◆ Facility
- ◆ Test Section
- ◆ Test Fluids
- ◆ Instrumentation and Data Acquisition
- ◆ Re-commissioning Tests
- ◆ Experimental Program



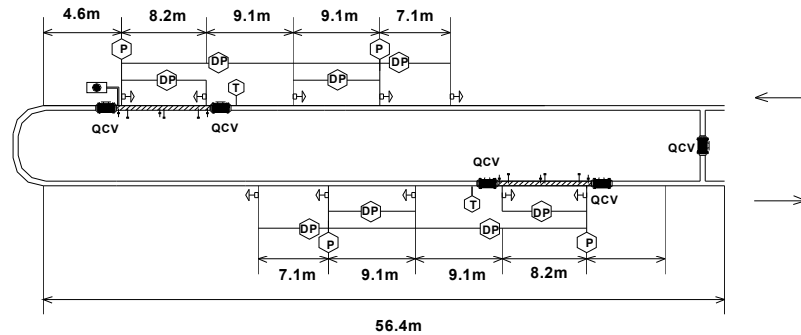
Facility

- ◆ 6-in ID Low Pressure Flow Loop
- ◆ Previously Used by Dong (2007)
- ◆ Re-commissioned During Summer 2009 for the Current Study

Facility ...



Test Section



Test Fluids

- ◆ Test Fluid
 - Gas – Air
 - Water – Tap Water
 - Oil - ??
- ◆ Selection of Test Fluids is Very Important
- ◆ Properties Resembling Those of Wet Gas Condensate
 - Low Viscosity and Specific Gravity

Test Fluids ...

Oil	Specific gravity	Viscosity (cP)	Surface tension (dynes/cm)	Liquid-water interfacial tension (dynes/cm)	Composition
Kerosene	0.775-0.81	2.1-2.2	23-32	47-49	Mainly C9 - C16
Tulco Tech 80 (Dong 2007)	0.86	13.5	29.14	16.38	Contains Mainly C14+
Lubsnap 40 (Meng 1999)	0.877	5.66	30		Hydrotreated Naphthenic Oil
Natural Gas – Sweet	0.62-0.76	Comparable to Water			Mainly C7-C12
Norpar 5s	0.626				C5
Norpar 12	0.749	1.22	25		C12
Isopar G	0.748	1.098	23		Mainly Contains Isoparaffins
Isopar K	0.762	1.14	24		

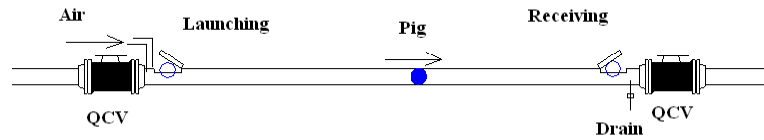


Instrumentation/Data Acquisition

- ◆ Pressure and Temperature : PTs and DPs and TTs
- ◆ Holdup: Quick Closing Valves and Pigging System
- ◆ Wetted Wall Perimeter: Scales on Wall
- ◆ Liquid Film Thickness: Conductivity Probes
- ◆ Liquid Velocity: Cold/Hot Liquid Injection
- ◆ Liquid Entrainment: Iso-kinetic Sampling System
- ◆ Data Acquisition: DeltaV



Holdups: QCVs & Pigging System

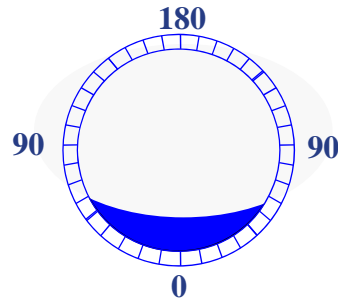


Pigging Efficiency Tests

	Water Test (ml)	Oil Test (ml)	Water + Oil (1:1)	
			Water (ml)	Oil (ml)
1st Pigging	60	70	30	50
2nd Pigging	35	40	10	30
3rd Pigging	15	20	0	15
Percentage Left after Third Pigging	0.5	0.67	0	0.5

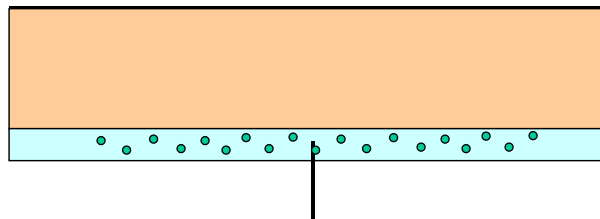
Wetted Perimeter

- Inside Pipe
- Minimize Reading Error



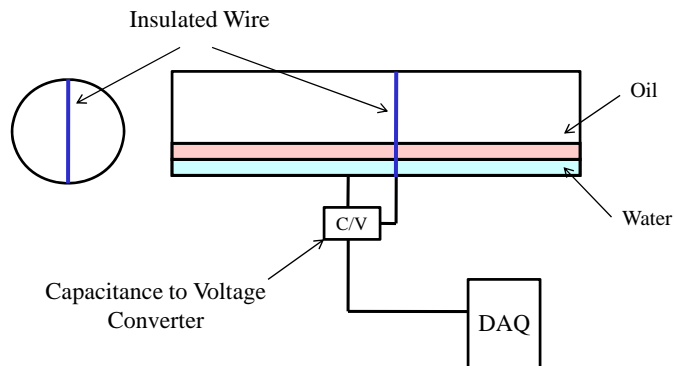
Film Thickness & Phase Continuity: Conductivity Probes

- ◆ Principle: Conductivity Difference
- ◆ Traverse across Pipe

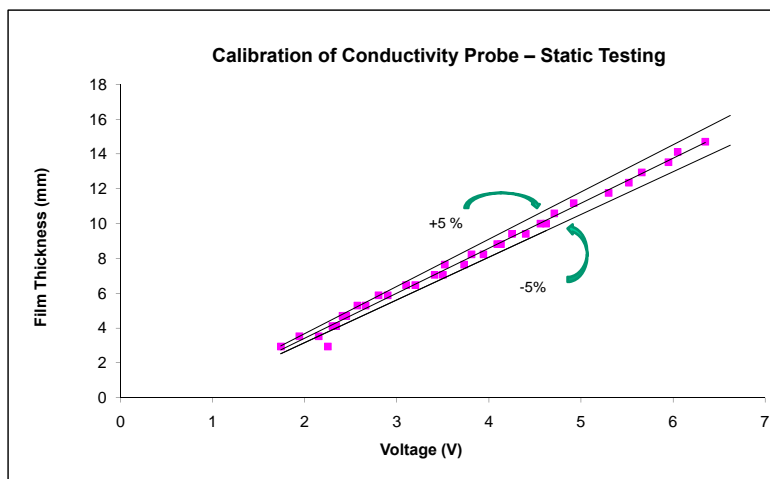


Film Thickness and Phase Continuity: Capacitance Probe

Huang *et al.* 2008



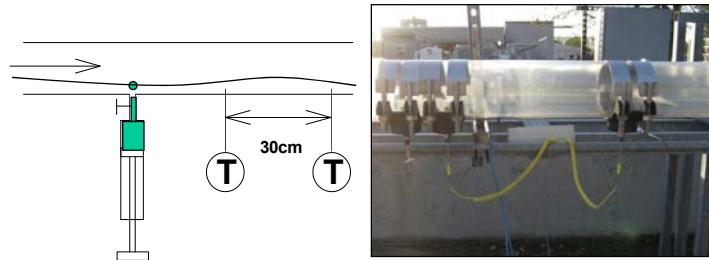
Film Thickness and Phase Continuity: Capacitance Probe ...



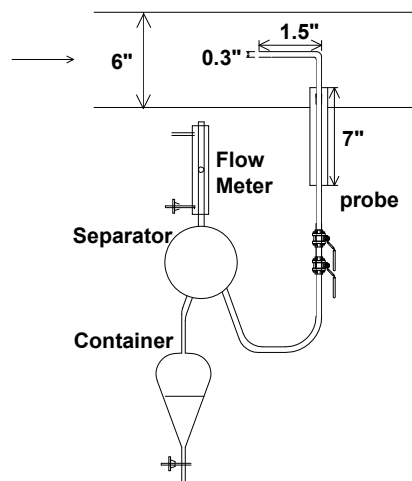
Film Velocity: Cold Liquid Injection

- ◆ Detect Temperature Variation

- ◆ $\text{Velocity} = \frac{\text{Distance}}{\text{Time}}$



Liquid Entrainment: Iso-kinetic Probe



Re-commissioning Tests

- ◆ Repeat of Selected Tests Performed by Dong (2007) - To be Completed after ABM

Gas-Liquid Flow Pattern	Oil/Water Flow Pattern	v_{sg} (m/s)	Liquid Loading (m^3/MSm^3)	Water Cut
Stratified smooth	Oil with discontinuous water strip	5	600	0.1
Stratified wavy	Stratified with channel water and water in oil dispersion	10	600	0.1
Stratified wavy	Stratified wavy with water in oil dispersion	15	300	0.1
Stratified wavy with droplet entrainment	Stratified with channel water and dual dispersion	15	900	0.5

- ◆ Flow Pattern Identification Tests - Completed



Fluid Flow Projects

Advisory Board Meeting, September 30, 2009

Flow Pattern Identification

- ◆ Gas-Liquid-Stratified Smooth/Oil-Water-Oil with Discontinuous Water Strip

Side View



Bottom View



$$v_{SG} = 5 \text{ m/s}, LL = 600 \text{ m}^3/MSm^3, WC = 0.1$$



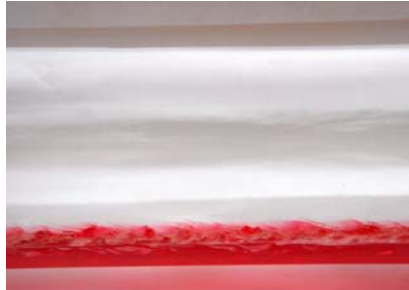
Fluid Flow Projects

Advisory Board Meeting, September 30, 2009

Flow Pattern Identification ...

- ♦ Gas-Liquid-Stratified Wavy/Oil-water-Oil with Channel Water and Dispersion of Water in Oil

Side View



Bottom View



$$v_{SG} = 10 \text{ m/s}, LL = 600 \text{ m}^3/\text{MMsm}^3, WC = 0.1$$



Fluid Flow Projects

Advisory Board Meeting, September 30, 2009

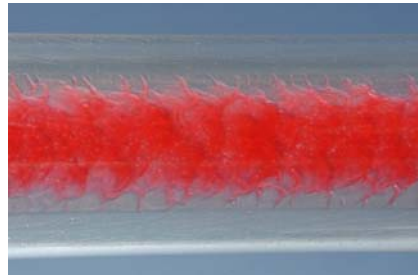
Flow Pattern Identification ...

- ♦ Gas-Liquid-Stratified Wavy/Oil-Water-Water in Oil Dispersion

Side View



Bottom View



$$v_{SG} = 15 \text{ m/s}, LL = 300 \text{ m}^3/\text{MMsm}^3, WC = 0.1$$



Fluid Flow Projects

Advisory Board Meeting, September 30, 2009

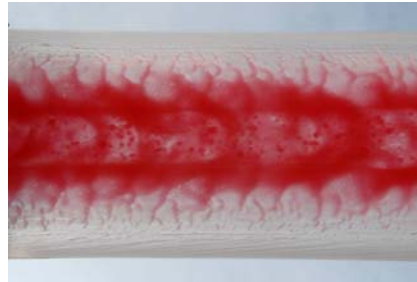
Flow Pattern Identification ...

- ◆ Gas-Liquid-Stratified Wavy/Oil-Water-Channel Water and Dual Dispersion

Side View



Bottom View



$$v_{SG} = 15 \text{ m/s}, LL = 900 \text{ m}^3/\text{MMsm}^3, WC = 0.5$$



Fluid Flow Projects

Advisory Board Meeting, September 30, 2009

Experimental Program

- ◆ Test Ranges
 - Superficial Gas Velocity:
5 to 25 m/s
 - Liquid Loading Level:
50 to 1200 m³/MMsm³
 - Water Cut:
0 to 1
 - Inclination Angles:
0°, +2°, -2°



Fluid Flow Projects

Advisory Board Meeting, September 30, 2009

Experimental Program ...

➤ Test Matrix

v_{Sg} (m/s)	v_{SL} (m/s) Water Cuts : 0, 0.2, 0.4, 0.6, 0.8, 1				
	5	0.00025	0.0015	0.003	0.0045
10	0.0005	0.003	0.006	0.009	0.012
15	0.00075	0.0045	0.009	0.0135	0.018
20	0.001	0.006	0.012	0.018	0.024
25	0.00125	0.0075	0.015	0.0225	0.03

Near Future Tasks

Literature Review	Ongoing
Experimental Testing	October 2009
Data Analysis	February 2010
Model Comparison	April 2010

Questions/Comments



Low Liquid Loading in Gas-Oil-Water Flow

Kiran Gawas

PROJECT COMPLETION DATES:

Literature Review.....	Ongoing
Preliminary Testing.....	September 2009
Testing	October 2009
Data analysis	February 2010
Model comparison	April 2010

Introduction

Low liquid loading gas-oil-water flow is widely encountered in wet gas pipelines. Even though the pipeline is fed with single phase gas, the condensation of the heavier components of the gas along with traces of water results in three phase flow. The presence of these liquids can result in significant changes in pressure distribution. Many issues like hydrate formation, pigging frequency, and downstream facility design dependent on the pressure and holdup are thus also affected. Similarly the transport of contaminants and additives such as corrosion inhibitors is of great significance since most of these additives are observed in the liquid phase. Therefore, understanding of the flow characteristics of low liquid loading gas-oil-water flow is of great importance in transportation of wet gas. However, very few studies have been conducted on low liquid loading especially in three-phase flow.

Several authors have published papers on three-phase flow pattern and modeling of three-phase flow. However most of them do not cover the range of low liquid loading flow. In this study, low liquid loading gas-oil-water flow experiments will be conducted in a 6-in. ID flow loop. The flow pattern, pressure drop, fractions of the three phases, liquid film thickness, wetted wall fractions and entrainment fractions will be observed and measured at different flow rates, liquid loading levels and water cuts.

Literature Review

Although significant research has been conducted in the field of two phase gas-liquid flow much fewer studies have been conducted in the domain of low liquid loading. Hart *et al.* (1989) presented experimental results for air-water system in

horizontal glass pipes. Ethylene glycol was added to study the effect of viscosity while surface active agents were used to study the effect of variation of interfacial tension. Assuming a uniform shape of liquid film they proposed the “Apparent Rough Surface” or ARS model. It was found that the liquid hold-up was not affected by interfacial tension while the pressure drop slightly increased due to lowering of interfacial tension.

Grolman and Fortuin (1995) presented the “Modified Apparent Rough Surface” or MARS model based on the liquid hold-up and pressure gradient data obtained in three different pipe diameters (i.e. 0.015, 0.026 and 0.051 m) with angles of inclination ranging from -3° to 6° . Similar to ARS this model was also derived for low liquid loading case. Liquid entrainment was however not studied in both these models.

Chen *et al.* (1997) proposed the “Double Circle” model based on experimental results for gas liquid two phase flows with low liquid loading for horizontal pipe of diameter 0.0779 m. It was found that four interfacial structures or flow regimes viz. 2-D wave, 3-D wave, roll wave and entrained droplet flow exist for stratified wavy flow pattern. Unlike the ARS model the “Double Circle” model does not assume uniform liquid film thickness. In this model the gas-liquid interface is considered to be a part of circle eccentric to that of the pipe. A new correlation for determining the interfacial friction factor was also obtained based on the results of over 500 experiments.

Meng (1999) investigated low liquid loading flow in horizontal and near horizontal pipes for inclination angles of -2° , -1° , 0° , $+1^\circ$, $+2^\circ$ and pipe inner diameter of 0.0501 m using air and oil as test fluids. Gas and liquid superficial velocities ranged from 5 to

25 m/s and from 0.001 to 0.053 m/s, respectively. Measured parameters included gas and liquid volumetric flow rates, pressure drop, temperature, liquid holdup and droplet deposition rate. Due to increase in liquid entrainment rate it was found that at certain high gas velocities, an increase of liquid loading considerably reduced the pressure gradient and liquid holdup. A new correlation for interfacial friction factor was proposed.

Badie *et al.* (2000) conducted experiments and obtained the pressure gradient and holdup data for low liquid loading air-water and air-oil flows in horizontal pipes with a diameter of 0.079 m. The “apparent rough surface” (ARS) model developed by Hart *et al.* (1989) and the “double circle” model developed by Chen *et al.* (1997) were used to compare the experimental results. These models over predict pressure gradient for air-water flow while under predict pressure gradient for air-oil flows. Double circle model gave better holdup predictions overall while the ARS model performed better at low liquid loading levels.

Badie *et al.* (2001) investigated the behavior of low liquid loading two-phase gas-liquid flow in a 0.079 m ID horizontal pipe using an axial viewing system. The axial images showed that the bulk of the liquid flowed within a liquid layer at the bottom of the pipe, while a significant portion of liquid was entrained as droplets within the gas core and deposited around the pipe at higher gas velocity. Using high speed photography it was found that intermittent waves on the liquid surface are the main reason for liquid entrainment. Thus, it was concluded that droplet deposition is responsible for transport of liquid to the top of the pipe. Although it gave very good qualitative account of liquid entrainment, no data on liquid entrainment fraction was provided.

As a continuation of Meng’s (1999) study, Olive *et al.* (2003) conducted low liquid loading two-phase experiments in a 0.0501 m ID near-horizontal pipe, using water as the liquid phase. A film removal device was developed to measure the liquid droplet entrainment fraction and deposition rate. It was found that at certain superficial gas velocities and relatively high liquid loadings, an increase of superficial gas velocity led to an increase of the liquid holdup. This was due to increase in spreading of liquid film up the wall thus increasing the wall friction which counters the increase in interfacial drag caused by increase in gas velocity. A similar phenomenon was observed at high gas velocities and high liquid loading due to change in flow pattern from stratified wavy to annular flow.

Fan (2005) conducted low liquid loading experiments with air and water on two different flow loops, 0.0501 m ID and 0.1492-m ID pipes. For the 0.0501-m ID facility, the superficial gas velocity ranged from 5 to 25 m/s, and superficial liquid velocity varied from 0.00025 to 0.03 m/s. For the 0.1492 m ID facility, superficial liquid velocity was varied from 0.005 to 0.05 m/s and the superficial gas velocity ranged from 7.5 to 21 m/s. Observed flow patterns from both flow loops were described and compared with model predictions. Several models including the Beggs and Brill (1973) correlation, Zhang *et al.* (2003) model and Hart *et al.* (1989) model were evaluated with the experimental data. It was found that most models could not give satisfactory predictions of pressure drop and liquid holdup, especially when compared with the 0.1492-m ID flow loop results. A mechanistic model for low liquid loading two-phase flow was developed to predict the holdup and pressure drop.

In gas condensate pipelines, a mixture of oil and water can flow with the gas phase. The co-existence of oil and water may cause a significant difference in the flow behavior compared to pure oil or pure water. Hence it is necessary to study three phase gas-oil-water flow. Taitel *et al.* (1995) extended their two phase model for three phase oil-water-gas stratified flow assuming a flat interface and no liquid entrainment. Moreover, the Taitel and Dukler (1976) criterion for transition from stratified to slug flow for two phase flow was applied to the case of three phase flow and was found to agree at low gas flow rates.

Khor *et al.* (1998) developed a computer code (PRESBAL) and studied three-fluid model to estimate three phase stratified flow. The model was essentially similar to Taitel *et al.* (1995) approach. While Taitel *et al.* (1995) eliminated pressure gradient from the momentum equations and solved the resulting simplified expressions for the shear stresses Khor *et al.* (1998) adjusted water and oil levels such that the pressure gradients in different phases were equal. The resulting liquid levels are then used to calculate the corresponding liquid holdups.

Bonizzi *et al.* (2003) developed a mathematical model to simulate three-phase (liquid/liquid/gas) stratified and slug flows. The approach was based on the one dimensional transient two-fluid model in which the two phases consisted of gas and a mixture of the two liquids. The method can predict locally whether the two liquids would form dispersion or stratified flow. It can also predict slugging and reproduce the observed experimental trends for the

major slug properties, such as pressure gradient, slug frequency and total liquid holdup.

Most of the experimental investigations and model predictions are carried out using model fluids. However, Utvik *et al.* (2001) presented an experimental comparison between a light hydrocarbon system from North Sea and model oil system consisting of nitrogen gas, Exxsol D60 and synthetic formation water (similar to that of crude system) in 0.0779 m pipe system. The liquid phase flow patterns studied were oil continuous phase, water continuous phase, separated flow, dispersion of water in oil continuous phase and dispersion of water in oil continuous phase. The gas-liquid flow patterns investigated were slug flow, dispersed flow and stratified flow. The flow patterns and hence the pressure drop observed in the two systems were different for the same flow conditions even though the physical properties of the two fluids were very similar. Thus other physical properties related to oil-water interface significantly influence the flow characteristics.

Applying a similar methodology in the unified modeling of gas-liquid two-phase pipe flow (Zhang *et al.*, 2003), Zhang and Sarica (2006) proposed a unified model for prediction of gas-oil-water flow behavior in wellbores and pipelines. This model describes three-phase flow based on two criteria: gas-liquid flow pattern and oil-water mixing status. The three-phase flow was treated as gas-liquid two-phase flow if the two liquids are fully mixed or as a three-layer stratified flow at low flow rates in horizontal or slightly inclined pipes. Closure relationships describing the distribution between the two liquid phases were proposed. Experimental data for gas-oil-water pipe flow were used to evaluate the model.

Three-phase gas-oil-water flow patterns are a combination of gas-liquid and oil-water flow patterns. Sobocinski (1955), Açıkgöz *et al.* (1992), Oddie *et al.* (2003), Keskin (2005) have carried out extensive experimental work towards determining gas-oil-water three phase flow patterns, pressure drop and holdups. However very little data is available in the range of low liquid loading which is encountered in the wet gas pipelines. Therefore, experimental measurements of the key parameters for low liquid loading three-phase flow in pipes are needed for model development and verification. Models developed for three-phase flow also must be evaluated for their applicability to low liquid loading conditions.

Dong (2007) performed low liquid loading three phase flow experiments on the 0.152 m flow loop at TUFFP and observed several new flow patterns. The flow patterns were classified as follows:

- Stratified-smooth and stratified (SS – ST)
- Stratified-smooth and oil with discontinuous water strip (SS – ODWS)
- Stratified-wavy and stratified (SW – ST)
- Stratified-wavy and water in oil dispersion (SW – DW/O)
- Stratified-wavy and stratified with channel water and water in oil dispersion (SW – STCW & DW/O)
- Stratified-wavy and stratified with channel water and dual dispersion (SW– STCW & DD)
- Stratified-wavy with droplet entrainment and water in oil dispersion (SW & E – DW/O)
- Stratified-wavy with droplet entrainment and stratified with channel water and dual dispersion (SW & E – STCW & DD).

The experimental pressure gradient and liquid holdup values were compared with the predictions of Fan (2005) low liquid loading two-phase flow model, Zhang *et al.*(2003) unified two-phase flow model, Zhang and Sarica (2006) unified three-phase flow model and OLGA simulation.

Thus, the literature review indicates that more experimental data on gas-oil-water three phase flow especially in the case of low liquid loading which is observed in wet gas transportation are needed to better understand the phenomenon and to develop better models. More work related to liquid entrainment, distribution of liquid film and liquid-liquid interface is also required. Closure relationships must be examined based on experimental results so that improvements or new developments can be achieved.

Experimental Study

Experimental Facility and Flow Loop

The experimental facility for this study is the 6-in. flow loop which has been used to conduct research on low liquid loading flow for several years (see Fig. 1). The test section consists of two runs of 6-in ID pipes, each run being 56.4 m in length. Acrylic visualization sections are provided at the end of each run. The inclination angle of the test section can be changed from 0° to 2° in upward and downward direction.

The flow loop is re-commissioned to ensure that it is in working order. This involved checking all the pumps, air compressor, calibration of the instruments, removal of all leaks, and replacement of pipe sections where necessary.

Test Fluids

As shown by Utvik *et al.* (2001) the choice of test fluids play a very important role in the results of the experiments. Since the phenomenon of low liquid loading is observed mainly in case of wet gas pipelines, the test fluid selected should resemble the gas condensates as much as possible. Table 1 represents comparative study of the properties of different oils considered for the selection of test oil. The selected oil should have low viscosity (comparable to that of water), low specific gravity and high interfacial tension with water. On the basis of these criteria the test fluids selected are isopar G, air and water.

Instrumentation and Data Acquisition

The DeltaV™ digital automation system is used as the data acquisition software. Gas flow rate is measured using the micro motion flow meter CMF300 while two micro motion flow meters CMF050 are used to measure oil and water flow rates. The flow meters are calibrated by the manufacturer and have a mass flow rate uncertainty of $\pm 0.1\%$ and density measurement uncertainty of $\pm 0.5\%$.

Pressure, temperature and pressure gradients are measured using Rosemount pressure, temperature transmitters and Rosemount differential pressure transducers respectively.

Liquid holdup is measured by trapping liquid between the two quick-closing valves (QCV) installed on the first run of the test section and then pigging out the entrapped liquid into graduated cylinders. The results of the pigging efficiency tests are as shown in Table 2.

Wetted wall perimeter is measured using grades on pipe circumference. Liquid entrainment fraction is measured using iso-kinetic sampling system. The working principle of which is as shown in Fig. 2.

Liquid film thickness can be measured using conductivity probe. The probe consists of a single wire which traverses across the pipe cross section. The oil water interface is indicated by change in conductance and hence a change in voltage across the probe. This method besides being time consuming

relies on visual observation and manually traversing the probe which can introduce considerable error in the measurement. Hence there is a need to devise a method which can provide real time data on liquid film thickness. Huang *et al.* (2008) used a single wire capacitance probe for measurement of water layer thickness in two phase flow of air-water and water-kerosene in pipes. It was found that the capacitance measurement was relatively unaffected by presence of impurities in water and also by change in shape of the probe. A single wire capacitance probe is being investigated for measurement of water layer thickness in current experimental study. When tested at static conditions the voltage reading varies linearly with the liquid layer thickness as shown in Fig. 3.

Cold liquid injection technique is used to determine liquid velocity. A cold liquid injector is placed at a point in the test section to inject cold oil or water into the test section. Two thermal probes are installed 0.5 ft after the injector with a 1 ft interval between them. The time required for the cold liquid to travel between the two probes is measured which gives the velocity of the liquid.

Preliminary Tests

Preliminary tests were carried out to check the facility and the instruments. This is necessary to ensure that facility works properly and the instruments give reliable measurements. The conditions selected for preliminary tests are as shown in Table 3. The flow patterns indicated in Table 3 were obtained as shown in Fig. 4 to Fig. 7. This confirms the observations made by Dong (2007).

Experimental Program

After the completion of preliminary tests experiments would be performed using Isopar G as the test oil. The proposed test matrix is shown in Table 4. The test results will be compared to the test results of low liquid loading air-oil-water flow experiments in 6- in horizontal pipe (Dong 2007) done on an oil of higher viscosity. The proposed test matrix is designed based on the gas velocities of 5-25 m/s and liquid loading levels of 50-1200 for water cuts of 0.0, 0.2, 0.4, 0.6, 0.8 and 1.0.

Near Future Tasks

1. Acquire experimental data after preliminary tests.
2. Analyze experimental data.
3. Carry out model comparisons and development of a new model if needed.

References

- Açikgöz, M., Franca, F. and Lahey Jr, R. T.: "An Experimental Study of Three-Phase Flow Regimes," *Int. J. Multiphase Flow*, Vol. 18, No. 3, pp. 327-336 (1992).
- Badie, S., Hale C. P., Lawrence, C. J., and Hewitt G. F.: "Pressure Gradient and Holdup in Horizontal Two-Phase Gas-Liquid Flows with Low Liquid Loading," *Int. J. Multiphase Flow*, Vol. 26, No. 9, pp. 1525-1543 (2000).
- Badie, S., Lawrence, C. J., and Hewitt, G. F.: "Axial Viewing Studies of Horizontal Gas-Liquid Flows with Low Liquid Loading," *Int. J. Multiphase Flow*, Vol. 27, pp. 1259-1269 (2001).
- Beggs, H.D. and Brill, J. P.: "A Study of Two-Phase Flow in Inclined Pipes," *J. Pet. Tech*, pp. 607-617 (1973).
- Bonizzi, M., and Issa, R.I.: "On the simulation of three phase slug flow in nearly horizontal pipes using multi-fluid model", *Int. J. Multiphase Flow*, Vol. 29, pp 1719-1747 (2003)
- Chen, X. T., Cai, X. D., and Brill, J. P.: "Gas-Liquid Stratified-Wavy Flow in Horizontal Pipelines," *ASME J. Energy Res. Tech.*, Vol. 119, No. 4, pp. 209-216 (1997).
- Dong, H.-K.: "Low Liquid Loading Gas-Oil-Water Flow in Horizontal Pipes," M.S. Thesis, U. Tulsa. Tulsa, OK. (2007).
- Fan, Y.: "An Investigation of Low Liquid Loading Gas-Liquid Stratified Flow in Near Horizontal Pipes," PhD Dissertation, U. Tulsa, Tulsa, OK (2005).
- Grolman, E. and Fortuin, J.: "Gas-liquid flow in slightly inclined pipes," *Chem. Eng. Sci.*, Vol. 52, No. 24, pp. 4461-4471 (1997).
- Hart, J., Hamersma, P. J., and Fortuin, J. M. H.: "Correlations of Predicting Frictional Pressure Drop and Liquid Holdup during Horizontal Gas-liquid Pipe Flow with a Small Liquid Holdup," *Int. J. Multiphase Flow*, Vol. 15, No. 6, pp. 947-964 (1989).
- Huang, S., Zhang, X., Wang, D., and Lin, Z.: "Equivalent Water Layer Height Measurement by Single Wire Capacitance Probe in Gas-liquid Flows," *Int. J. Multiphase Flow*, Vol.34, pp. 809-818 (2008).
- Keskin, C: "An Experimental and Modeling Study of Gas-Oil-Water Flow in Horizontal and Slightly Inclined Pipes," TUFFP Advisory Board Meeting Report, U. Tulsa, Tulsa, OK (October, 2005).
- Khor, S. H., Mendes-Tatsis, M. A., and Hewitt, G.F.: "One-dimensional Modeling of Phase Holdups in Three Phase Stratified Flow", *Int. J. Multiphase Flow*, Vol. 23, No. 5, pp 885-897, (1997).
- Meng, W.: "Low Liquid Loading Gas-Liquid Two Phase Flow in Near Horizontal Pipes," PhD Dissertation, U. Tulsa, Tulsa, OK (1999).
- Oddie, G., Shi, H., Durlofsky, L. J., Aziz, K., Pfeffer, B., and Holmes, J. A.: "Experimental Study of Two and Three-phase Flows in Large Diameter Inclined Pipes," *Int. J. Multiphase Flow*, Vol. 29, pp. 527-558 (2003).
- Olive, N. R., Zhang, H.-Q., Wang, Q., Redus, C. L., and Brill, J. P.: "Experimental Study of Low Liquid Loading Gas-Liquid Flow in Near Horizontal Pipes," *ASME, J. Energy Res. Tech.*, Vol.125, pp. 294-298 (2003).
- Sobocinski, D. P.: "Horizontal Co-current Flow of Water, Gas-Oil, and Air," M.S. Thesis, U. of Oklahoma, Norman, OK (1955).
- Taitel, Y. and Dukler, A.E.: "A Model for predicting Flow Regime Transition in Horizontal and Near Horizontal Gas-liquid flows", *AIChE J.*, 22, pp 47-55, (1976).
- Taitel, Y., Barnea, D., and Brill, J. P.: "Stratified Three-phase flow in Pipes," *Int. J. Multiphase Flow*, Vol. 21, pp. 53-60 (1995)

Utvik, O. H., Rinde, T., and Valle, A.: “An Experimental Comparison Between a Recombined Hydrocarbon-Water Fluid and a Model Fluid System in Three-Phase Pipe Flow,” *ASME, J. Energy Res. Tech.*, Vol. 123, pp. 253-259 (2001).

Zhang, H.-Q., Wang, Q., Sarica, C., and Brill, J. P.: “Unified Model for Gas-Liquid Pipe Flow via Slug Dynamics – Part I: Model Development,” *ASME J. Energy Res. Tech.*, Vol. 125, No. 12, pp. 266-273 (2003).

Zhang, H.-Q. and Sarica C.: “Unified Modeling for Gas/Oil/Water Pipe Flow-Basic Approaches and Preliminary Validation,” *SPE J. Project, Facilities & Construction*, Vol. 1, No. 2, pp. 1-7 (2006).

Table 1: Physical Properties of Test Oil

Oil	Specific gravity	Viscosity (cP)	Surface tension (dynes/cm)	Liquid-water interfacial tension (dynes/cm)	Composition
Kerosene (Chen <i>et al.</i> , 1997)	0.775-0.81	2.1-2.2	23-32	47-49	Mainly C9 - C16
Tulco Tech 80 (Dong 2007)	0.86	13.5	29.14	16.38	Contains mainly C14+
Lubsnap 40 (Meng 1999)	0.877	5.66	30		Hydro-treated naphthenic oil
Natural gas - sweet	0.62-0.76	Comparable to water			Mainly C7-C12
Norpar 5s	0.626				C5
Norpar 12	0.749	1.22	25		C12
Norpar 13	0.762	2.36	26		C13
Norpar 15	0.772	3.27	27		C15
Exxsol D80	0.8	1.4-1.8			contains C11-C15 - 99%,
Isopar G	0.748	1.098	23		Mainly contains iso-paraffins
Isopar K	0.762	1.14	24		
isopentane	0.62		16	49 at 20 degC	

Table 2: Pigging Efficiency Test Results

	Water Test (ml)	Oil Test (ml)	Water + oil (1:1)	
			Water (ml)	Oil (ml)
1 st pigging	60	70	30	50
2 nd Pigging	35	40	10	30
3 rd Pigging	15	20	0	15
Percentage liquid left at the end of 3 rd pigging	0.5	0.67	0	0.5

Table 3: Conditions for repeat tests

Gas-liquid flow pattern	Oil/Water flow pattern	Vsg (m/s)	Liquid Loading	Water Cut
Stratified smooth	Oil with discontinuous water strip	5	600	0.1
Stratified wavy	Stratified with channel water and water in oil dispersion	10	600	0.1
Stratified wavy	Stratified wavy with water in oil dispersion	15	300	0.1
Stratified wavy with droplet entrainment	Stratified with channel water and dual dispersion	15	900	0.5

Table 4: Test Matrix

Superficial Gas Velocity (m/s)	Superficial Liquid Velocity (m/s) Water cuts : 0,0.2,0.4,0.6,0.8,1				
	5	0.00025	0.0015	0.003	0.0045
10	0.0005	0.003	0.006	0.009	0.012
15	0.00075	0.0045	0.009	0.0135	0.018
20	0.001	0.006	0.012	0.018	0.024
25	0.00125	0.0075	0.015	0.0225	0.03

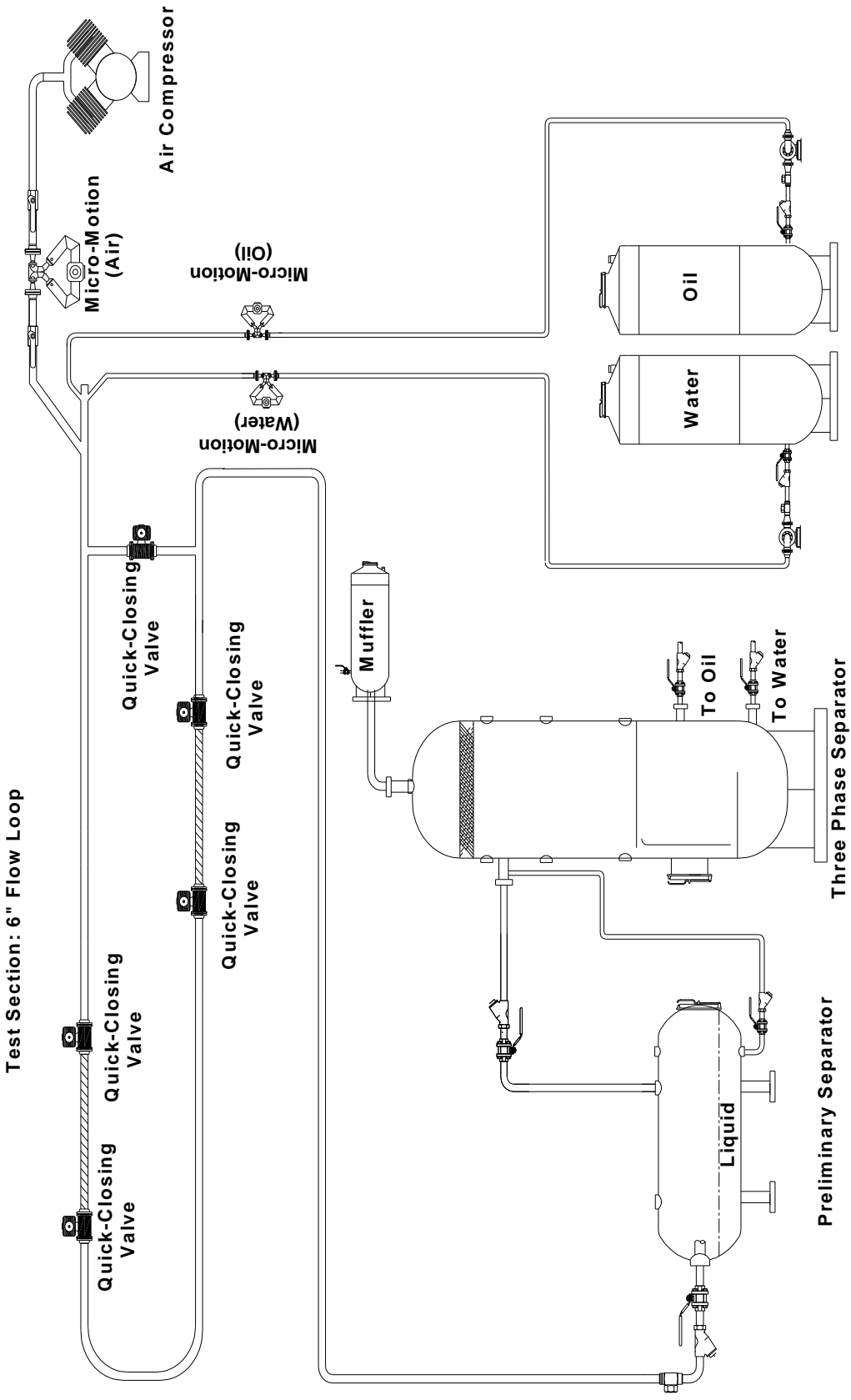


Figure 1: Schematic of Flow Loop.

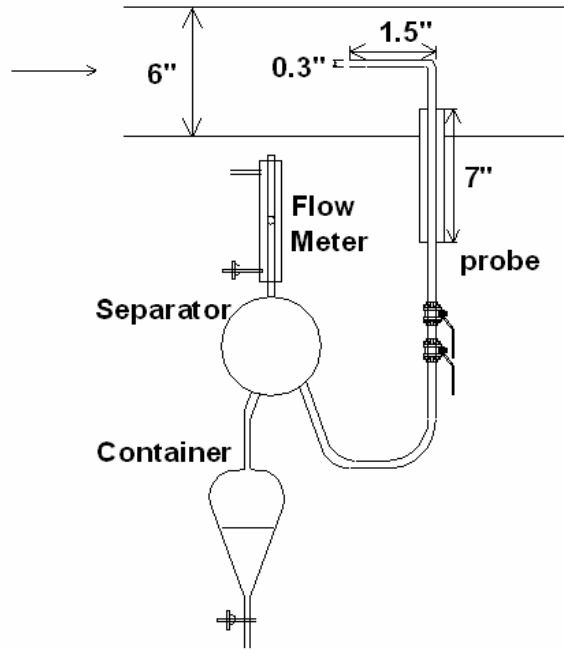


Figure 2: Iso-kinetic sampling probe.

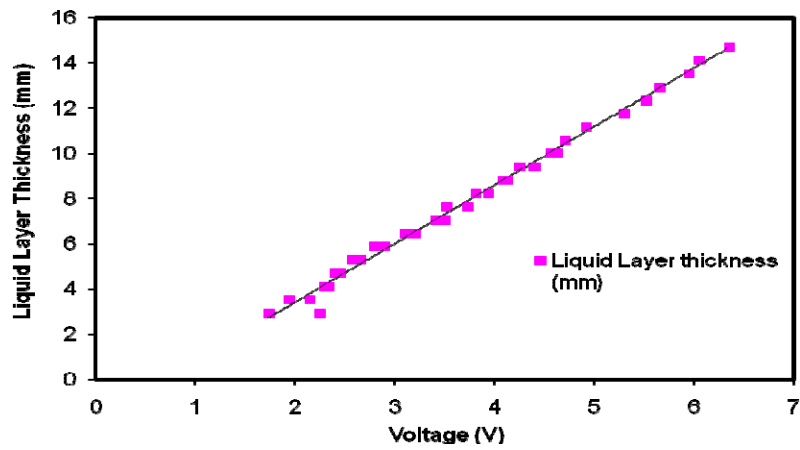


Figure 3: Calibration of capacitance probe.



Figure 4: Gas-Liquid-stratified smooth/Oil-water- oil with discontinuous water strip. (a) Side view. (b) Bottom view

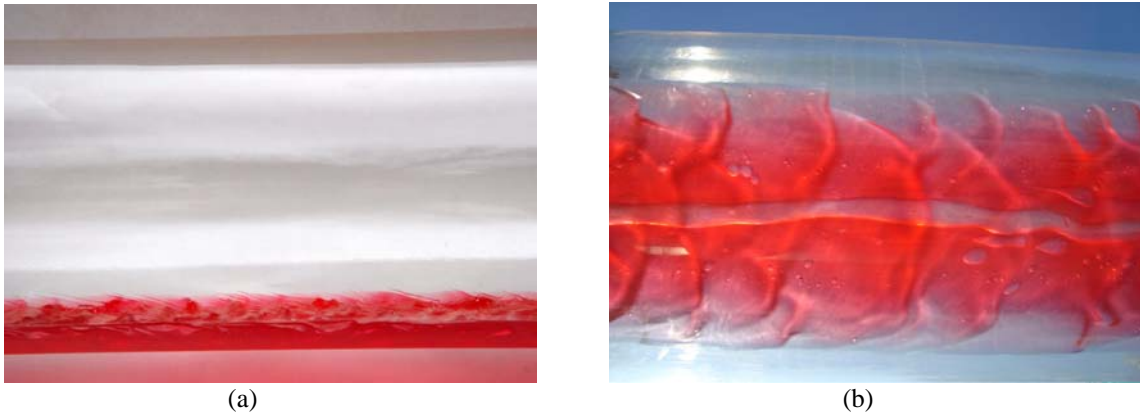


Figure 5: Gas-Liquid-stratified wavy/Oil-water- oil with channel water and dispersion of water in oil. (a) Side view. (b) Bottom view.

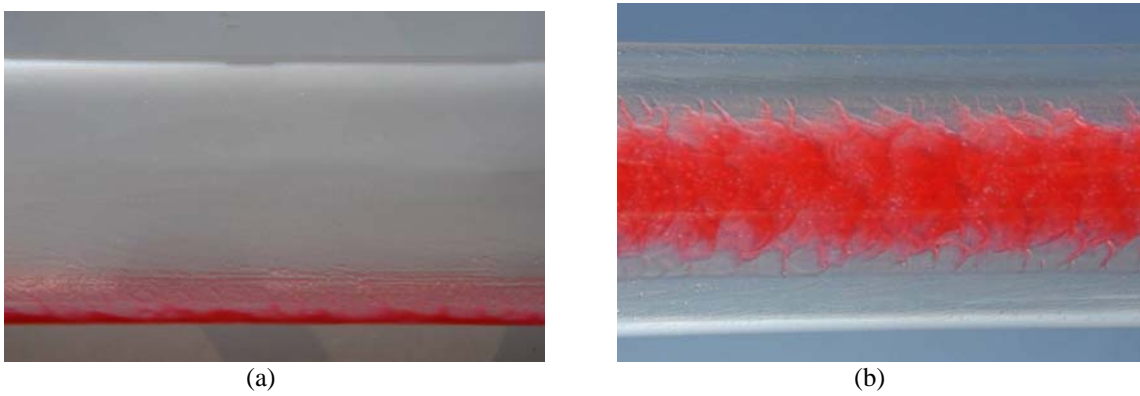


Figure 6: Gas-Liquid-stratified wavy/Oil-water- water in oil dispersion. (a) Side View. (b) Bottom view.



(a)



(b)

Figure 7: Gas-Liquid-stratified wavy/Oil-water-channel water and dual dispersion. (a) Side View. (b) Bottom view.



Fluid Flow Projects

Executive Summary of Research Activities

Cem Sarica

Advisory Board Meeting, September 30, 2009

Up-Scaling Studies

- ◆ **Significance**
 - Better Design and Operation
- ◆ **Objective**
 - Testing and Improvement of Existing Models for Large Diameter and Relatively High Pressures
- ◆ **Past Studies**
 - Low Pressure and 6-in. ID Low Liquid Loading (Fan and Dong)
 - High Pressure 2-in. ID (Manabe, 2002)

Up-Scaling Studies ...



◆ Current Project

- Construction of a New High Pressure, Large Diameter Facility
- Extension of Low Liquid Loading Study to High Pressures is Envisioned as the First Study

Up-Scaling Studies ...



◆ Status

- Design is Complete
- Equipment Purchases
 - ▲ Most of the Equipment are either Purchased or Ordered.
- Construction is Underway

Up-Scaling Studies ...



◆ Near Future Activities

- Completion of Support Structures
- Assembly of All of the Available Components



Fluid Flow Projects

High Pressure – Large Diameter Multiphase Flow Loop

*Polat Abduvayt, Scott Graham
Cem Sarica*

Advisory Board Meeting, September 30, 2009

Outline

- ◆ Introduction
- ◆ Objectives
- ◆ Facility Design and Construction
- ◆ Capital Cost and Time Table?

Introduction

- ◆ **Pressure and Pipe Diameter Affect Flow Behavior in Multiphase Flow Significantly**
- ◆ **Limited Study of Multiphase Flow in Large-Diameter Pipes at Pressure Conditions Higher than 2,000 kpa (290 psi)**
- ◆ **Need**
 - **Investigation of Diameter and Pressure Effects on Multiphase Flow**
 - **Experimental Data**
- ◆ **Requires a Proper Facility**

Objectives

- ◆ **Design and Construct a 6 in. ID High Pressure Multiphase Facility**
- ◆ **Conduct Research Projects to Better Understand Multiphase Flow**
- ◆ **Upscale Available Predictive Tools**

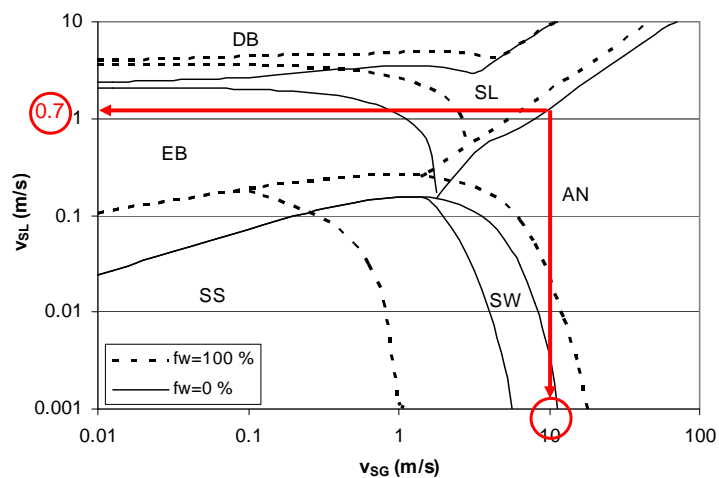
Facility Design and Construction

- ◆ **Design**
 - Fluids
 - Operating Range
 - Facility Layout
 - Instrumentation
- ◆ **Construction Activities**

Fluids

- ◆ **Gas Phase**
 - Nitrogen
 - Natural gas
- ◆ **Oil Phase**
 - Tulco Tech-80 Mineral Oil

Operating Range (Flow Pattern Map)



 Fluid Flow Projects

Advisory Board Meeting, September 30, 2009

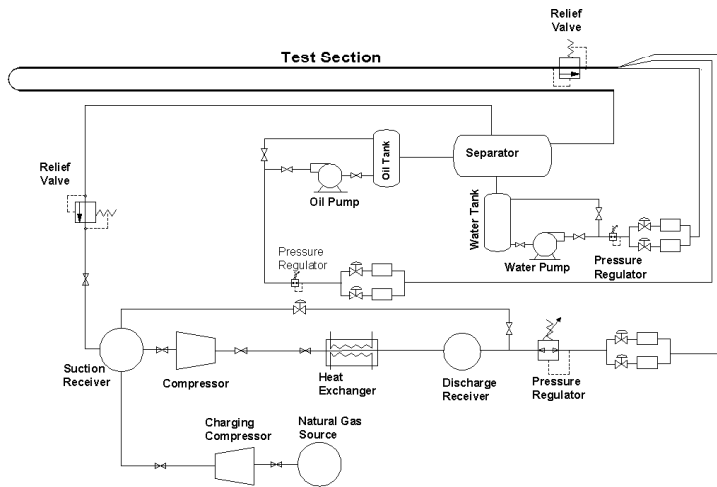
Operating Range ...

- ◆ Operating Pressure = 500 psig
- ◆ $v_{SL, \max} = 0.7$ m/s; $v_{SG, \max} = 10$ m/s
- ◆ f_w Between 0 and 100 %
- ◆ $q_{G, \max} = 18$ MMSCFD
- ◆ $q_{L, \max} = 200$ GPM
- ◆ Separator 54" x 10' @ 600 psig

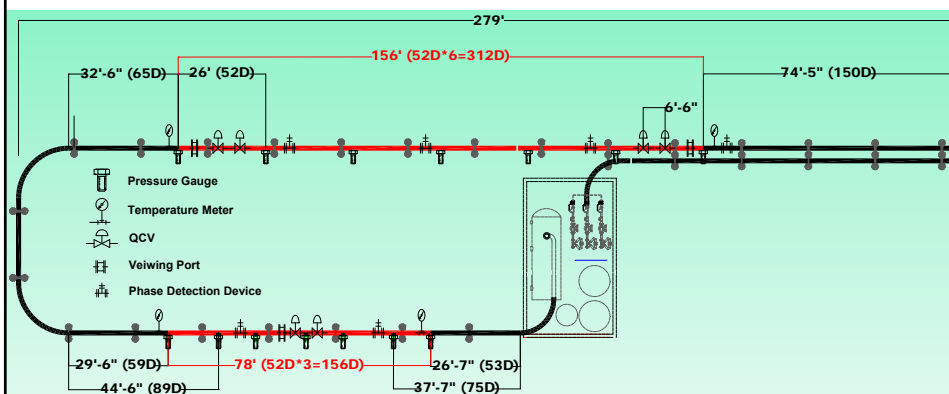
 Fluid Flow Projects

Advisory Board Meeting, September 30, 2009

Facility Diagram



Facility Layout



Facility Layout ...



- ◆ **6 in. ID Stainless Steel Pipe**
- ◆ **Test Section-1**
 - **156 ft (312D) Long and $-3^\circ < \theta < +3^\circ$**
- ◆ **Test Section-2**
 - **78 ft (156D) Long and Horizontal**
- ◆ **Flow Development Sections with Sufficient Lengths**

Facility Layout ...



- ◆ **Test Section-1**
 - **Six 26 ft (52D) Long Pressure Drop Sections**
 - **Two 6.5 ft Long Trap Sections**
 - **Two Viewing Ports**
 - **Two Temperature Transducers**
 - **Four Phase Detection Devices (TBD)**
- ◆ **Test Section-2**
 - **Six Pressure Drop Sections**
 - **One 6.5 ft Trap Section**
 - **One Viewing Port**
 - **Two Phase Detection Devices (TBD)**
 - **Two Temperature Transducers**

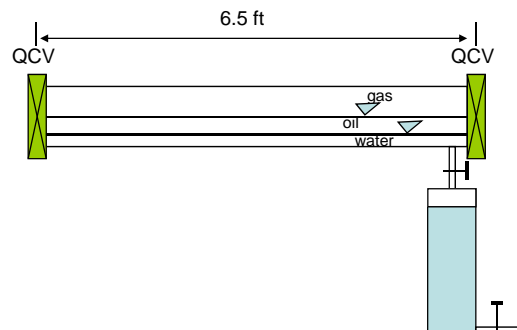
Basic Instrumentation

	Pressure (psig)	Capacity
Gas Flow Rate	600	18 MMSCFD
Water Flow Rate	600	200 GPM
Oil Flow Rate	600	200 GPM
Differential Pressure	500	0 – 50 in H ₂ O
Pressure	600	0 – 800 psi
Temperature	500	0-100 °C
Quick Closing Valves	600	6 in. ID

Specific Instrumentation

◆ Trap Sections

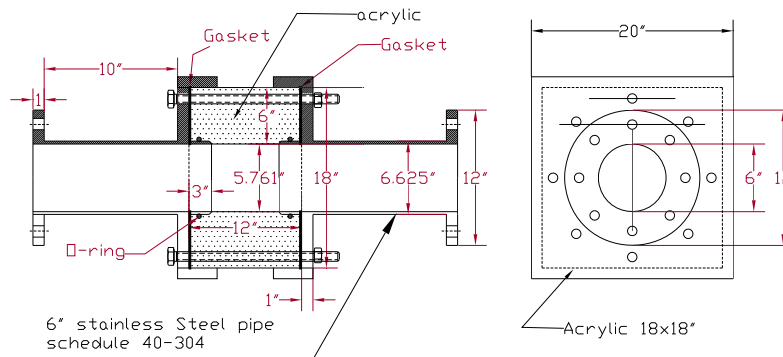
- Test Section-1
 - ▲ Located at Upstream and Downstream
- Test Section-2
 - ▲ Located at Center



Special Instrumentation ..

◆ Whole Perimeter Viewing Section

➤ Visual Flow Observation

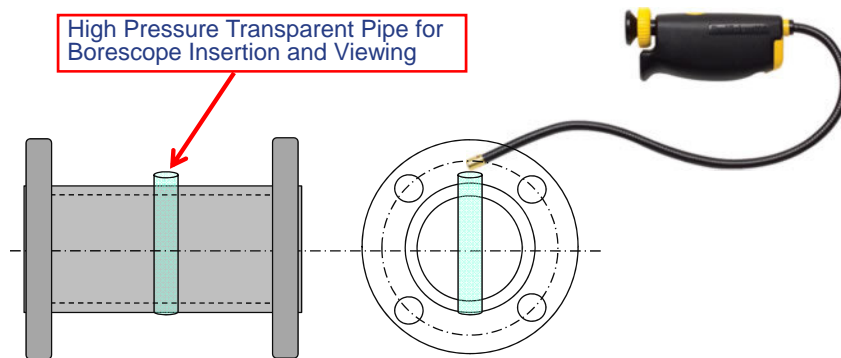


Special Instrumentation ...

◆ Boroscope

➤ Visual Flow Observation

High Pressure Transparent Pipe for
Boroscope Insertion and Viewing



Construction Activities

- ◆ Equipment Pad
- ◆ Piers
- ◆ Structure

Equipment Pad

Rebar Detail



Equipment Pad ...



Rebar Detail ...



Equipment Pad ...



Rebar Detail ...



Equipment Pad ...



Monolithic Pour



 Fluid Flow Projects

Advisory Board Meeting, September 30, 2009

Equipment Pad ...



Monolithic Pour ...



 Fluid Flow Projects

Advisory Board Meeting, September 30, 2009

Piers



Rebar



Piers ...

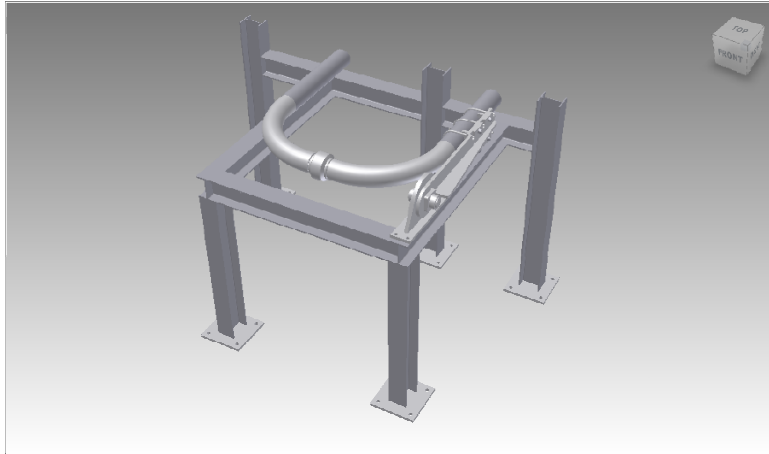


Pouring



Structure

🔹 Mechanical Pivot

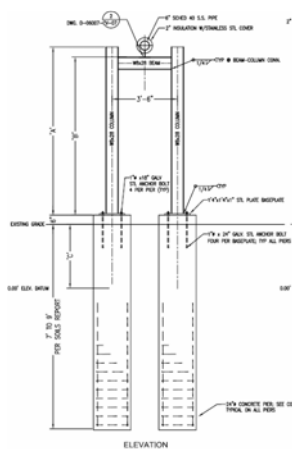


 Fluid Flow Projects

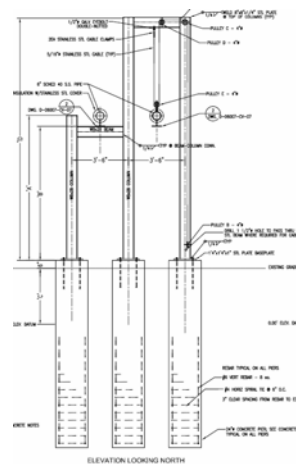
Advisory Board Meeting, September 30, 2009

Structure ...

🔹 Support Detail



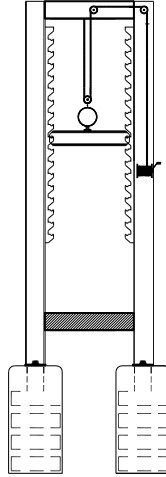
 Fluid Flow Projects



Advisory Board Meeting, September 30, 2009

Structure ...

💧 Lifting Mechanism



Capital Cost Analysis

Equipment	Purchased	To Be Purchased by Dec. 2009	To Be Purchased at a Later Date
Oil Tank	35,000.00		
Air Exchanger	70,000.00		
Moyno Pump	23,500.00		
2phase Separator	39,000.00		
3phase Separators	30,000.00		
Transmitters	33,000.00		
Instrumentation	39,075.00		
Compressor	243,980.00		
P&ID, Permit Review, Civil/Structural Design	84,888.62		
Generator	64,965.00		
Concrete		92,000.00	
Steel Structure		77,000.00	
Commercial Steel			50,000.00
Quick Closing Valves		25,000.00	
Surge Control Package		56,000.00	
Valves			30,000.00
Instrumentation			17,000.00
Suction Control Valve			10,000.00
DAQ			12,000.00
Misc. (switches, motors)			50,000.00
Fittings			10,000.00
Welding Process Area			40,000.00
Speciality Instrumentation			75,000.00
Water Phase			
Tank			35,000.00
Meters			33,000.00
Subtotals	663,408.62	250,000.00	362,000.00

Capital Cost Analysis ...



Total Estimated Cost	\$ 1,275,408.62
Total Expended (Dec. 2009)	\$ 913,408.62
Amount Needed for Completion	\$ 362,000.00
Amount Allocated in 2010 Budget	\$ 175,000.00
Projected Shortfall	\$ (187,000.00)



Fluid Flow Projects

Executive Summary of Research Activities

Cem Sarica

Advisory Board Meeting, September 30, 2009

Unified Model

- ◆ **Objective**
 - **Develop and Maintain an Accurate and Reliable Steady State Multiphase Simulator**
- ◆ **Past Studies**
 - **Zhang et al. Developed “Unified Model” in 2002 for Two-phase Flow**
 - ▲ **Became TUFFP’s Flagship Steady State Simulator**
 - ▲ **Applicable for All Inclination Angles**
 - **“Unified Model was Extended to Three-phase in 2006**

Unified Model ...

◆ Current Activities

- Code and Software Improvement Efforts

Unified Model ...

◆ Future Activities

- Continue Improvements in Both Modeling and Software Development



Fluid Flow Projects



Unified Model Updates

Holden Zhang

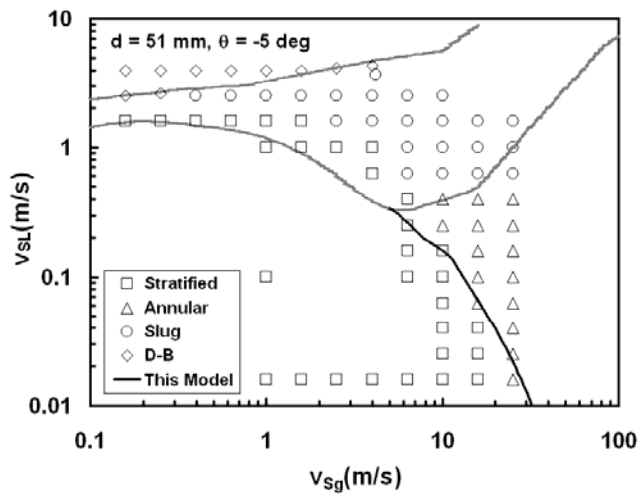
Advisory Board Meeting, September 30th, 2009

Wetted Wall Fraction Model

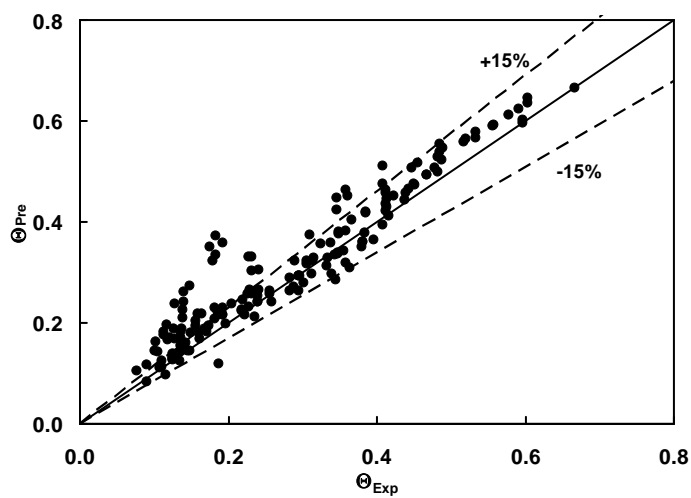


- ◆ **Grolman Correlation Replaced with Our Generalized Model**
- ◆ **Model Based on Gas Liquid Stratified Flow Froude Number**
 - **Unifies Predictions of Wetted Wall Fraction, Liquid Film Gravity Center and Transition to Annular Flow**
 - **Applicable for Stratified/Annular Flow, Slug Film Region, All Inclination Angles**

Wetted Wall Fraction Model ...



Wetted Wall Fraction Model ...



Other Improvements

- ◆ Added Range Checks for Inputs
- ◆ Fixed Bugs
- ◆ Improved Convergence from 98% to 99.98%
 - Unconverged Cases Mainly Intermittent
 - Will Study Case by Case to Eliminate Them

Documentation

- ◆ Documented Models Reflected in Computer Programs
 - Listed in Tables Unknowns and Corresponding Equations
 - Completed Gas-Liquid and Oil-Water Models
 - Completing Oil-Water-Gas and Heat Transfer Models



Fluid Flow Projects

Executive Summary of Research Activities

Cem Sarica

Advisory Board Meeting, September 30, 2009

Transient Modeling

◆ Significance

- Industry has Capable All Purpose Transient Software
 - ▲ OLGA, PLAC, TACITE
- Efforts are Well Underway to Develop Next Generation All Purpose Transient Simulators
 - ▲ Horizon, LEDA
- Need for a Simple Transient Flow Simulator

Transient Modeling ...

- ◆ **Objective**
 - **Development and Testing of a Simple and Fast Transient Flow Simulator That Can Be Used as a Screening Tool**
- ◆ **Project Proposal Rated High in Recent TUFFP Questionnaire**
- ◆ **Past Studies**
 - **TUFFP has Conducted Many Transient Multiphase Studies**
 - ▲ **Scoggins, Sharma, Dutta-Roy, Taitel, Vierkandt, Sarica, Vigneron, Minami, Gokdemir, Zhang, Tengesdal, and Beltran**

Transient Modeling ...

- ◆ **Status**
 - **Researcher is Identified**
 - **Delayed due to Maternity Leave of the Researcher**
 - **Will Resume After Advisory Board meeting**



Fluid Flow Projects



2009 Questionnaire

Holden Zhang

Advisory Board Meeting, September 30, 2009

2009 Questionnaire Results

#	Research Title	Stams	Baker Atlas	BP	Chevron	ConocoPhillips	ExxonMobil	JOGMEC	Kuwait Oil Co.	STP Group	Marathon	MMS	Penex	Petrobras	Rosneft	Schlumberger	Shell	Total	Total Scores	Priority Ranking	Ranking(2008)
5	Effect of High Viscosity on Multiphase Flow Behavior	O	3	5	4	5	5	4	4	5	4	3		5		4	5	4	60	1	1
1	Gas-Oil-Water Flow in Pipes	O	5	5	3	5	2	3	4	4	5	4		5		4	4	5	58	2	4
9	Up-scaling Studies in Multiphase Flow	O	4	5	5	5	5	3	4	4	4	2		5		3	3	5	57	3	2
2	Oil-Water Flow	O	4	4	3	5	2	2	4	3	5	4		5		4	4	5	54	4	7
3	Unified Modeling of Multiphase Pipe Flows (Including Gas-Liquid, Oil-Water and Gas-Oil-Water)	O	5	4	3	4	2	4	4	2	5	2		5		5	3	4	52	5	3
17	Investigation of High Viscosity Two-Phase Flow Pattern in Vertical Wells	P	3	4	3	4	2	5	4	4	3	2		4		5	5	4	52	5	8
7	Three-Phase Flow in Near-Horizontal Pipelines with Low Oil-Water Loadings	O	3	4	3	5	5	4	4	3	3	4		3		2	2	5	50	7	6
10	Low-Liquid-Loading Flow in Vertical Configuration	P	5	3	3	4	5	4	2	2	5	3		3		5	1	4	49	8	11
4	Multiphase Flow in Hilly Terrain Pipelines	O	4	4	3	3	4	4	4	3	3	3		4		2	2	5	48	9	11

#	Research Title	Status	Baker Atlas	BP	Chevron	ConocoPhillips	ExxonMobil	IOGMEC	Kuwait Oil Co.	STP Group	Marathon	MMS	Pemex	Petrobras	Rosneft	Schlumberger	Shell	Total	Total Scores	Priority Ranking	Ranking(2008)
12	Investigation of Four-Phase Solid, Water, Oil and Gas Flow	P	4	5	1	4	5	4	3	2	2	2	4			2	4	5	47	10	11
6	Closure Laws for Droplet-Homophase Interaction	O	3	4	4	4	3	4	3	3	5	2	3			3	1	4	46	11	8
18	Multiphase Flow Metering	P	4	4	1	2	2	5	5	1	2	5	4			2	4	4	45	12	18
8	Simplified Transient Multiphase Flow Model	O	4	2	2	4	2	4	3	1	3	3	5			5	1	4	43	13	5
14	Investigation of Inversion Point in Oil-Water Flow	P	4	3	2	2	2	3	4	3	2	2	4			5	3	4	43	13	16
16	Two-Phase Downward Flow and Gas Carryunder	P	2	3	2	4	2	4	2	4	5	2	3			2	3	5	43	13	8
19	Integration of Multiphase Flows Modeling from Reservoir, Wellbore and Pipelines to Surface Facilities	P	3	3	1	2	2	2	5	1	2	5	5			5	2	4	42	16	15
11	Effect of Drug Reducing Agents on Single Phase and Two-Phase Flow in Pipes	P	2	3	2	5	5	4	3	2	2	2	2			1	3	3	39	17	18
15	Modeling of Foam Flow in Wells	P	3	4	3	2	4	4	2	1	5	2	2			2	2	3	39	17	14
13	Gas-Liquid Flow in Undulating Horizontal Wells	P	4	3	2	3	2	1	4	2	3	4	4			2	1	3	38	19	16



Fluid Flow Projects

Business Report

Cem Sarica

Advisory Board Meeting, September 30, 2009

Membership Status

◆ Current Status

- **Membership Stands at 16**
 - ▲ 15 Industrial and MMS
- **Efforts Continue to Increase Membership**
 - ▲ CNOOC Expected to Join

Personnel Changes

- ◆ **Computer Manager Position Eliminated**
- ◆ **Mr. Benin Chelinsky Jeyachandra and Mr. Ge Yuan Join TUFFP Team as Research Assistant to Pursue MS Degree in Petroleum Engineering**

Papers and Publications

- ◆ **Gokcal, B., Alsarkhi, A. and Sarica, C.: “Effects of High Viscosity on Drift Velocity for Inclined Pipes,” *SPE Projects, Facilities & Construction Journal*, June 2009**
- ◆ **Atmaca, S., Alsarkhi, A., Zhang, H. Q. and Sarica, C.: “Characterization of Oil Water Flows in Inclined Pipes,” *SPE Projects, Facilities & Construction Journal*, June 2009**
- ◆ **Dong, H., Zhang, H. Q., and Sarica, C. “An Experimental Study of Low Liquid Loading Gas-Oil-Water Flow in Horizontal Pipes,” Proceedings of 14th International Conference Multiphase Production 09, Cannes, France, June 17-19, 2009.**
- ◆ **Alsarkhi, A. and Sarica, C. “New Dimensionless Parameters and a Power Law Correlation for Pressure Drop of Gas-Liquid Flows in Horizontal Pipelines,” Proceedings of 14th International Conference Multiphase Production 09, Cannes, France, June 17-19, 2009**
- ◆ **Sarica, C., Zhang, H. Q., and Wilkens, J. R.: “Sensitivity of Slug Flow Mechanistic Models on Slug Length,” To Be Presented at ASME’s Annual OMAE 2009 Meeting, Honolulu, Hawaii, May 31-June 5, 2009**

Next Advisory Board Meetings

◆ Tentative Schedule

➤ May 11, 2010

- ▲ TUHOP Meeting
- ▲ TUFFP Workshop
- ▲ Facility Tour
- ▲ TUHOP/TUFFP Reception

➤ May 12, 2010

- ▲ TUFFP Meeting
- ▲ TUPDP Dinner

➤ May 13, 2010

- ▲ TUPDP Meeting

◆ Venue is The University of Tulsa

Financial Report

◆ Year 2009 Update

- TUFFP Industrial Account
- TUFFP MMS Account

◆ Year 2010 Proposal

- TUFFP Industrial Account
- TUFFP MMS Account

2009 Industrial Account Summary

(Prepared September 11, 2009)

Anticipated Reserve Fund Balance on January 1, 2009		\$ 452,358.43		
Income for 2009				
2009 Membership Fees (15 @ \$48,000 - excludes MMS)		\$ 720,000.00		
Total Budget		\$ 1,172,358.43		
 Projected Budget/Expenditures for 2009				
	Budget	Revised Budget 2/11/09	Expenses September 09	Anticipated 2009 Expenses
90101-90103 Faculty Salaries	29,251.82	29,074.14	19,562.62	19,562.62
90600-90609 Professional Salaries	106,676.24	109,752.00	72,190.97	96,410.24
90700-90703 Staff Salaries	45,866.45	45,279.00	33,693.46	42,509.11
90800 Salaries - Part-time	-	-	-	-
91000 Graduate Students - Monthly	58,100.00	54,650.00	53,525.00	62,825.00
91100 Students - Hourly	15,000.00	15,000.00	9,899.97	10,800.00
91800 Fringe Benefits (33% - July 1st - 34%)	59,992.19	58,805.74	41,819.16	53,051.04
93100 General Supplies	3,000.00	3,000.00	2,784.20	5,323.24
93101 Research Supplies	100,000.00	100,000.00	48,213.70	80,000.00
93102 Copier/Printer Supplies	500.00	500.00	-	500.00
93103 Component Parts	-	-	1,585.90	1,585.90
93104 Computer Software	4,000.00	4,000.00	218.39	400.00
93106 Office Supplies	2,000.00	2,000.00	1,153.14	1,425.00
93200 Postage/Shipping	500.00	500.00	3,195.41	7,100.00
93300 Printing/Duplicating	2,000.00	2,000.00	2,101.43	4,000.00
93400 Telecommunications	3,000.00	3,000.00	1,237.05	2,200.00
93500 Membership/Subscriptions	1,000.00	1,000.00	50.00	400.00
93600 Travel	-	-	-	-
93601 Travel - Domestic	10,000.00	10,000.00	4,021.74	7,000.00
93602 Travel - Foreign	10,000.00	10,000.00	2,203.96	2,203.96
93606 Visa	-	-	-	-
93700 Entertainment (Advisory Board Meetings)	10,000.00	10,000.00	7,636.28	12,500.00
94803 Consultants	16,000.00	18,500.00	20,780.33	20,780.33
94813 Outside Services	20,000.00	20,000.00	22,769.07	22,769.07
95103 Equipment Rental	-	-	2,752.24	2,752.24
95200 F&A (55.6%)	141,721.35	141,867.93	105,012.84	128,551.06
98901 Employee Recruiting	3,000.00	3,000.00	3,923.05	3,923.05
99001 Equipment	600,000.00	400,000.00	158,819.40	513,000.00
99002 Computers	8,000.00	8,000.00	1,604.61	1,604.61
99300 Bank Charges	40.00	40.00	30.00	30.00
81801 Tuition/Fees	30,665.00	30,067.00	23,375.00	23,375.00
81806 Graduate Fellowship	-	-	2,608.03	2,608.03
Total Expenditures	1,280,313.05	1,080,035.81	646,766.96	1,129,189.50
Anticipated Reserve Fund Balance as of 12/31/09				\$ 43,168.93

2009 MMS Account Summary

(Prepared September 15, 2009)

Reserve Balance as of 12/31/08		\$ 5,769.94
2009 Budget		\$ 48,000.00
Total Budget		\$ 53,769.94
 Projected Budget/Expenditures for 2009		
	Budget	2009 Anticipated Expenditures
91000 Students - Monthly	27,900.00	23,925.00
95200 F&A	15,512.40	13,302.30
81801 Tuition/Fees	-	-
Total Anticipated Expenditures as of 12/31/09	43,412.40	37,227.30
Total Anticipated Reserve Fund Balance as of 12/31/09		\$ 16,542.64

2010 Industrial Account Projections

(Prepared September 15 2009)

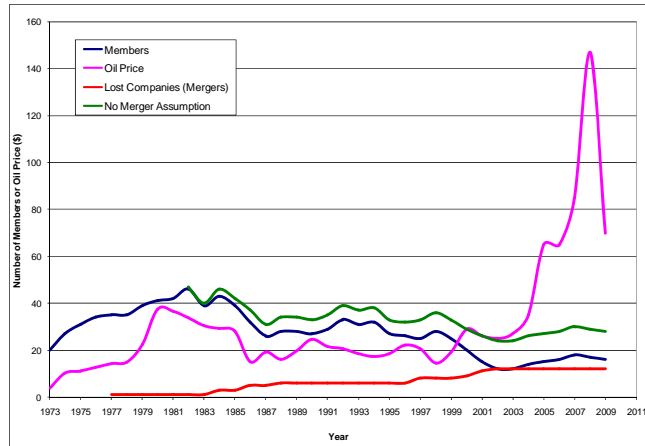
Anticipated Reserve Fund Balance on January 1, 2009	\$43,168.93
Income for 2010	
2010 Anticipated Membership Fees (15 @ \$48,000 - excludes MMS)	\$720,000.00
Total Income	\$763,168.93
2009 Anticipated Expenditures	Projected Budget
90101-90103 Faculty Salaries	29,074.14
90600-90609 Professional Salaries	47,628.54
90700-90703 Staff Salaries	35,262.50
91000 Graduate Students	41,550.00
91100 Undergraduate Students	15,000.00
91800 Fringe Benefits (34%)	38,068.16
93100 General Supplies	3,000.00
93101 Research Supplies	50,000.00
93102 Copier/Printer Supplies	500.00
93104 Computer Software	4,000.00
93106 Office Supplies	2,000.00
93200 Postage/Shipping	500.00
93300 Printing/Duplicating	2,000.00
93400 Telecommunications	3,000.00
93500 Memberships/Subscriptions	1,000.00
93601 Travel - Domestic	10,000.00
93602 Travel - Foreign	10,000.00
93700 Entertainment (Advisory Board Meetings)	10,000.00
81801 Tuition/Student Fees	17,898.00
94803 Consultants	0.00
94813 Outside Services	20,000.00
95200 Indirect Costs (55.6%)	93,694.44
98901 Employee Recruiting	3,000.00
99001 Equipment	200,000.00
99002 Computers	8,000.00
99300 Bank Charges	40.00
Total Expenditures	\$645,215.78
Anticipated Reserve Fund Balance on December 31, 2010	\$117,953.15

2010 MMS Account Projections

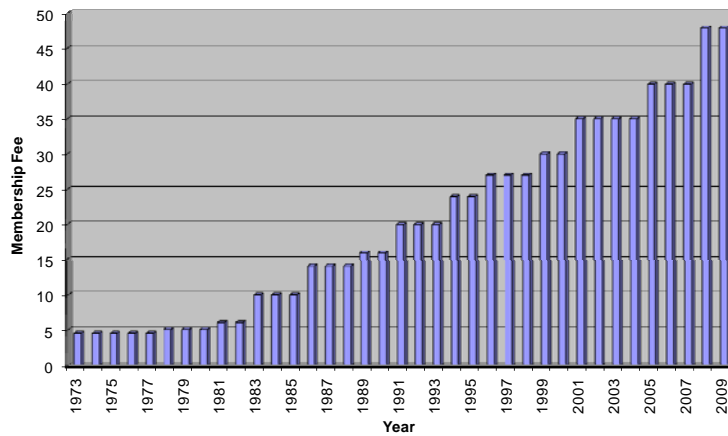
(Prepared September 15, 2009)

Account Balance - January 1, 2010	\$16,542.64
Income for 2009	
2009 Membership Fee	\$48,000.00
Remaining Balance	\$64,542.64
2009 Anticipated Expenditures	Projected Budget
90101-90103 Faculty Salaries	-
90600-90609 Professional Salaries	8,624
90700-90703 Staff Salaries	-
91000 Graduate Students	29,000.00
91800 Fringe Benefits (34%)	2,931.99
95200 Indirect Costs (55.6%)	20,918.67
Total Expenditures	\$61,474.16
Anticipated Reserve Fund Balance on December 31, 2010	\$3,068.48

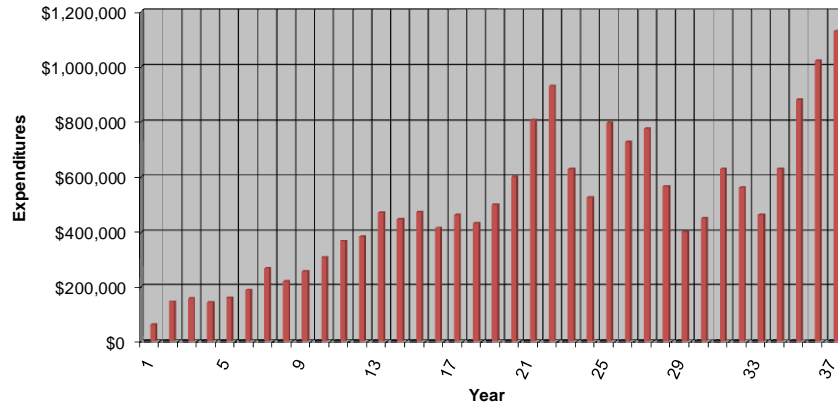
History – Membership



History – Membership Fees



History - Expenditures



Membership Fees

- ◆ 2009 Membership Dues
 - 3 Unpaid
 - Need Prompt Payments

Introduction

This semi-annual report is submitted to Tulsa University Fluid Flow Projects (TUFFP) members to summarize activities since the March 25, 2009 Advisory Board meeting and to assist in planning for the next six months. It also serves as a basis for reporting progress and generating discussion at the 73rd semi-annual Advisory Board meeting to be held in Gallery Room of Allen Chapman Activity Center (ACAC) of the University of Tulsa Main Campus, ACAC 440 South Gary, Tulsa, Oklahoma on Wednesday, September 30, 2009.

The activities will start with Tulsa University High Viscosity Projects (TUHOP) Advisory Board meeting on September 29, 2009 between 8:00 a.m. and noon in Gallery at ACAC. Between 1:00 and 3:00 p.m. on September 29, 2009, there will be TUFFP workshop in the same room. There will be presentations made by TUFFP member companies. Concurrently, Tulsa University Hydrate Flow Performance (TUHFP) JIP Advisory Board meeting will be held in Chateau at ACAC between 8:30 a.m. and 4:00 p.m. A facility tour will be held on September 29, 2009 between 3:30 and 5:30 p.m. Following the tour, there will be a TUHFP/TUHOP/TUFFP reception between 6:30 and

9:30 p.m. at Oklahoma Aquarium, 300 Aquarium Drive Jenks, OK, 74037.

TUFFP Advisory Board meeting will convene at 8:00 a.m. on September 30th and will adjourn at approximately 5:00 p.m. Following the meeting, there will be a joint TUFFP and TUPDP dinner between 5:30 and 9:00 p.m. in Alcove at ACAC.

The Tulsa University Paraffin Deposition Projects (TUPDP) Advisory Board meeting will be held on October 1st in Gallery Room of Allen Chapman Activity Center (ACAC) of the University of Tulsa Main Campus, between 8:30 a.m. and 1:00 p.m.

The reception and the dinner will provide an opportunity for informal discussions among members, guests, and TU staff and students.

Several TUFFP/TUPDP/TUHOP facilities will be operating during the tour. An opportunity will also be available to view the hydrate flow loop.

The following dates have tentatively been established for spring 2010 Advisory Board meetings. The venue for spring 2010 Advisory Board meetings is tentatively set to be the University of Tulsa Main Campus.

2010 Spring Meetings

May 11, 2010	Tulsa University High Viscosity Oil Projects (TUHOP) JIP Meeting Tulsa University Fluid Flow Projects (TUFFP) Workshop Facility Tour TUHOP – TUFFP Reception
May 12, 2010	Tulsa University Fluid Flow Projects (TUFFP) Advisory Board Meeting TUFFP – TUPDP Reception
May 13, 2010	Tulsa University Paraffin Deposition Projects (TUPDP) Advisory Board Meeting

Personnel

Dr. Cem Sarica, Professor of Petroleum Engineering, continues as Director of TUFFP and TUPDP, and as Co-Principal Investigator of TUHFP and TUHOP.

Dr. Holden Zhang, Assistant Professor of Petroleum Engineering, serves as Principal Investigator of TUHOP and Associate Director of TUFFP.

Dr. Brill continues to be involved as the director emeritus on a voluntary basis.

Dr. Polat Abduvayt continues as TUFFP Post Doctoral Research Associate.

Dr. Mingxiu (Michelle) Li continues to serve as a Research Associate for TUHOP and TUFFP.

Mr. Scott Graham continues to serve as Project Engineer. Scott oversees all of the facility operations and continues to be the senior electronics technician for TUFFP, TUPDP, and TUHOP.

Mr. Craig Waldron continues as Research Technician, addressing our needs in mechanical areas. He also serves as a flow loop operator for TUPDP and Health, Safety, and Environment (HSE) officer for TUFFP, TUPDP and TUHOP.

Mr. Brandon Kelsey serves as an electro-mechanical technician serving TUFFP, TUPDP, and TUHOP projects.

Ms. Linda Jones continues as Project Coordinator of TUFFP, TUPDP and TUHOP projects. She keeps the project accounts in addition to other responsibilities such as external communications, providing computer support for graduate students, publishing and distributing all research reports and deliverables, managing the computer network and web sites, and supervision of part-time office help.

Computer manager position and web administrator position is eliminated effective August 31, 2009 as part of our cost cutting efforts. Mr. James Miller started Oklahoma State University to pursue BS degree in Computer Science. TUFFP web site will now be managed by Ms. Lori Watts of Petroleum Engineering. The computer related support will be provided by the IT support staff of College of Engineering and Natural Sciences.

Table 1 updates the current status of all graduate students conducting research on TUFFP projects for the last six months.

Mrs. Gizem Ersoy Gokcal is studying slug flow evolution in three-phase gas-oil-water flow in hilly terrain pipelines. Gizem has recently accepted a position with Technip in Houston, TX, USA, effective September 2009. She plans to complete her Ph.D. study while working for Technip.

Mr. Kyle Magrini successfully defended his master thesis on the study titled "*Liquid Entrainment in Annular Two-phase in Inclined Pipes*" in August 2009 as part of his MS degree requirements. Immediately after, he has accepted a position with South West Energy in Houston, TX, an independent operator in lower 48 states.

Mr. Anoop Sharma successfully defended his master thesis on the study titled "*A Modeling of Hydrodynamics of Oil-Water Pipe Flow Using Energy Minimization Concept*" in June 2009 as part of his MS degree requirements. Anoop started working for Schlumberger effective September 15, 2009.

Ms. Tingting Yu successfully defended her master thesis on the study titled "*Modeling of Gas-Liquid Flow in Upward Vertical Annuli*" in May 2009 as part of his MS degree requirements. Ms. Tingting Yu started working for SPT in Houston Office in May 2009.

Ms. Ceyda Kora, from Turkey, is pursuing her MS degree in Petroleum Engineering. Ceyda has received a BS degree in Petroleum and Natural Gas Engineering from Middle East Technical University in 2008. She is studying the effects of high viscosity oil on liquid slug holdup.

Mr. Kiran Gawas, from India, is pursuing his Ph.D. degree in Petroleum Engineering. Kiran has a BS degree in Chemical Engineering from University of Mumbai, Institute of Chemical Technology and a Master of Technology degree from Indian Institute of Technology (IITB). He is studying Low Liquid Loading Three-phase Flow.

Mr. Benin (Ben) Chelinsky Jeyachandra, from India, and Mr. Ge Yuan, from Peoples Republic of China, have recently joined the TUFFP to pursue his MS degree in Petroleum Engineering. Ben has received a BS degree in Chemical Engineering from Birla Institute of Technology and Science University in 2008. Ge has received a BS degree in Chemical Engineering and Technology from Dalian University of Technology in 2009. Both Ben and Ge will be assigned their research projects after the Advisory Board meeting.

A list of all telephone numbers and e-mail addresses for TUFFP personnel are given in Appendix D.

Table 1***2009 Fall Research Assistant Status***

<i>Name</i>	<i>Origin</i>	<i>Stipend</i>	<i>Tuition</i>	<i>Degree Pursued</i>	<i>TUFFP Project</i>	<i>Completion Date</i>
Gizem Ersoy Gokcal	Turkey	Yes – TUFFP	Yes – TUFFP	Ph.D. – PE	Slug Flow Evolution in Three-Phase Gas-Oil-Water Flow in Hilly Terrain Pipelines	Fall 2009
Kiran Gawas	India	Yes – TUFFP	Waived (TU)	Ph.D. – PE	Three-phase Gas-Oil-Water Low Liquid Loading	Fall 2012
Ceyda Kora	Turkey	Yes – TUFFP	Waived (MMS)	MS. – PE	Effects of High Viscosity Oil on Liquid Slug Holdup	Fall 2010
Benin (Ben) Chelinsky Jeyachandra	India	Yes – TUFFP	Waived (MMS)	MS – PE	To Be Assigned After Advisory Board meeting	Fall 2011
Ge Yuan	PRC	Yes – TUFFP	Yes – TUFFP	MS – PE	To Be Assigned After Advisory Board meeting	Fall 2011

Membership

The current membership of TUFFP stands at 15 industrial members and Mineral Management Services of Department of Interior (MMS).

Our efforts to increase the TUFFP membership level continues. It is expected that in near future CNOOC will be a member.

Table 2 lists all the current 2009 TUFFP members. A list of all Advisory Board representatives for these members with pertinent contact information appears in Appendix B. A detailed history of TUFFP membership is given in Appendix C.

Table 2

2009 Fluid Flow Projects Membership

Baker Atlas	Minerals Management Service
BP Exploration	PEMEX
Chevron	Petrobras
ConocoPhillips	Rosneft
Exxon Mobil	Schlumberger
JOGMEG	Shell Global Solutions
KOC	SPT
Marathon Oil Company	Total

Equipment and Facilities Status

Test Facilities

The construction of a high pressure (500 psi operating pressures) and large diameter (6 in. ID) facility is currently underway. Concrete work has been completed. Steel structures have been fabricated and expected to be mounted on the concrete structure during October 2009. As reported before The Sundyne Gas compressor is on location as well as the 500KVA diesel generator that will be providing the electricity for the compressor and liquid pumps. The separator has been received. The other equipment such as liquid pumps, liquid tanks,

the surge tank for gas, flow meters, and instrumentation have been ordered and expected to be received this fall. Process equipment assembly is expected to be completed this fall. Due to budgetary limitations, we will defer the purchase of stainless steel pipes to 2010.

High Viscosity Multiphase Flow facility is modified by replacing the steel pipe sections with transparent PVC pipe to better assess the inlet and outlet effects. Moreover, a new holdup measurement device is designed, constructed, and commissioned.

Detailed descriptions of these modification efforts appear in a progress presentation given in this brochure. A site plan showing the location of the various TUFFP and TUPDP test facilities on the North Campus is given in Fig. 1.

Financial Status

TUFFP maintains separate accounts for industrial and U.S. government members. Thus, separate accounts are maintained for the MMS funds.

As of September 28, 2009, 13 of the 16 TUFFP members had paid their 2009 membership fees. We really appreciate your prompt payment of the membership dues if your company has not yet paid the membership fee.

Table 3 presents a financial analysis of income and expenditures for the 2009 Industrial member account as of September 15, 2009. Also shown are previous 2009 budgets that have been reported to the members. The total industry expenditures for 2009 are projected to be \$1,129,189.50. The industry reserve account is expected to be \$43,168.93 at the end of 2009 assuming that all the unpaid membership fees are collected.

Table 4 presents a financial analysis of expenditures and income for the MMS Account for 2009. This account is used primarily for graduate student

stipends. A balance of \$16,542.64 will be carried over to 2010.

The University of Tulsa waives up to 19 hours of tuition for each graduate student that is paid a stipend from the United States government, MMS funds. Moreover, The University of Tulsa has granted tuition waiver for one Ph.D. student. A total of 47 hours of tuition (equivalent of \$42,000) were waived for 2009.

Tables 5-6 present the projected budgets and income for the Industrial, and MMS accounts for 2010. The 2010 TUFFP industrial membership is assumed to stay at 15 in this analysis. This will provide \$720,000.00 of industrial membership income for 2010. The sum of the 2010 income and the reserve account is projected to be \$763,168.93. The expenses for the industrial member account are estimated to be \$645,215.78 leaving a balance of \$117,953.15. The MMS account is expected to have a carryover of \$3,068.48.

Table 3: TUFFP 2009 Industrial Budget Summary

(Prepared September 11, 2009)

Anticipated Reserve Fund Balance on January 1, 2009	\$ 452,358.43
Income for 2009	
2009 Membership Fees (15 @ \$48,000 - excludes MMS)	\$ 720,000.00
Total Budget	\$ 1,172,358.43

Projected Budget/Expenditures for 2009

	Budget	Revised Budget 2/11/09	Expenses September 09	Anticipated 2009 Expenses
90101-90103 Faculty Salaries	29,251.82	29,074.14	19,562.62	19,562.62
90600-90609 Professional Salaries	106,676.24	109,752.00	72,190.97	96,410.24
90700-90703 Staff Salaries	45,866.45	45,279.00	33,693.46	42,509.11
90800 Salaries - Part-time	-		-	
91000 Graduate Students - Monthly	58,100.00	54,650.00	53,525.00	62,825.00
91100 Students - Hourly	15,000.00	15,000.00	9,899.97	10,800.00
91800 Fringe Benefits (33% - July 1st - 34%)	59,992.19	58,805.74	41,819.16	53,051.04
93100 General Supplies	3,000.00	3,000.00	2,784.20	5,323.24
93101 Research Supplies	100,000.00	100,000.00	48,213.70	80,000.00
93102 Copier/Printer Supplies	500.00	500.00	-	500.00
93103 Component Parts			1,585.90	1,585.90
93104 Computer Software	4,000.00	4,000.00	218.39	400.00
93106 Office Supplies	2,000.00	2,000.00	1,153.14	1,425.00
93200 Postage/Shipping	500.00	500.00	3,195.41	7,100.00
93300 Printing/Duplicating	2,000.00	2,000.00	2,101.43	4,000.00
93400 Telecommunications	3,000.00	3,000.00	1,237.05	2,200.00
93500 Membership/Subscriptions	1,000.00	1,000.00	50.00	400.00
93600 Travel			-	
93601 Travel - Domestic	10,000.00	10,000.00	4,021.74	7,000.00
93602 Travel - Foreign	10,000.00	10,000.00	2,203.96	2,203.96
93606 Visa			-	
93700 Entertainment (Advisory Board Meetings)	10,000.00	10,000.00	7,636.28	12,500.00
94803 Consultants	16,000.00	18,500.00	20,780.33	20,780.33
94813 Outside Services	20,000.00	20,000.00	22,769.07	22,769.07
95103 Equipment Rental			2,752.24	2,752.24
95200 F&A (55.6%)	141,721.35	141,867.93	105,012.84	128,551.06
98901 Employee Recruiting	3,000.00	3,000.00	3,923.05	3,923.05
99001 Equipment	600,000.00	400,000.00	158,819.40	513,000.00
99002 Computers	8,000.00	8,000.00	1,604.61	1,604.61
99300 Bank Charges	40.00	40.00	30.00	30.00
81801 Tuition/Fees	30,665.00	30,067.00	23,375.00	23,375.00
81806 Graduate Fellowship			2,608.03	2,608.03
Total Expenditures	1,280,313.05	1,080,035.81	646,766.96	1,129,189.50

Anticipated Reserve Fund Balance as of 12/31/09	\$ 43,168.93
---	--------------

Table 4: TUFFP 2009 MMS Budget Summary

(Prepared September 15, 2009)

Reserve Balance as of 12/31/08		\$ 5,769.94
2009 Budget		\$ 48,000.00
Total Budget		\$ 53,769.94
 Projected Budget/Expenditures for 2009		
	Budget	2009 Anticipated Expenditures
91000 Students - Monthly	27,900.00	23,925.00
95200 F&A	15,512.40	13,302.30
81801 Tuition/Fees		
Total Anticipated Expenditures as of 12/31/09	43,412.40	37,227.30
 Total Anticipated Reserve Fund Balance as of 12/31/09		 \$ 16,542.64

Table 5: 2010 Projected TUFFP Industrial Budget

(Prepared September 15 2009)

Anticipated Reserve Fund Balance on January 1, 2009	\$43,168.93
Income for 2010	
2010 Anticipated Membership Fees (15 @ \$48,000 - excludes MMS)	\$720,000.00
Total Income	\$763,168.93
2009 Anticipated Expenditures	Projected Budget
90101-90103 Faculty Salaries	29,074.14
90600-90609 Professional Salaries	47,628.54
90700-90703 Staff Salaries	35,262.50
91000 Graduate Students	41,550.00
91100 Undergraduate Students	15,000.00
91800 Fringe Benefits (34%)	38,068.16
93100 General Supplies	3,000.00
93101 Research Supplies	50,000.00
93102 Copier/Printer Supplies	500.00
93104 Computer Software	4,000.00
93106 Office Supplies	2,000.00
93200 Postage/Shipping	500.00
93300 Printing/Duplicating	2,000.00
93400 Telecommunications	3,000.00
93500 Memberships/Subscriptions	1,000.00
93601 Travel - Domestic	10,000.00
93602 Travel - Foreign	10,000.00
93700 Entertainment (Advisory Board Meetings)	10,000.00
81801 Tuition/Student Fees	17,898.00
94803 Consultants	0.00
94813 Outside Services	20,000.00
95200 Indirect Costs (55.6%)	93,694.44
98901 Employee Recruiting	3,000.00
99001 Equipment	200,000.00
99002 Computers	8,000.00
99300 Bank Charges	40.00
Total Expenditures	\$645,215.78
Anticipated Reserve Fund Balance on December 31, 2010	\$117,953.15

Table 6: TUFFP Projected 2010 MMS Budget

(Prepared September 15, 2009)

Account Balance - January 1, 2010	\$16,542.64
Income for 2009	
2009 Membership Fee	\$48,000.00
Remaining Balance	\$64,542.64
2009 Anticipated Expenditures	Projected Budget
90101-90103 Faculty Salaries	-
90600-90609 Professional Salaries	8,624
90700-90703 Staff Salaries	-
91000 Graduate Students	29,000.00
91800 Fringe Benefits (34%)	2,931.99
95200 Indirect Costs (55.6%)	20,918.67
Total Expenditures	\$61,474.16
Anticipated Reserve Fund Balance on December 31, 2010	\$3,068.48

Miscellaneous Information

Fluid Flow Projects Short Course

The 34th TUFFP “Two-Phase Flow in Pipes” short course offering is scheduled for May 17-21, 2010. For this short course to be self sustaining, at least 10 enrollees are needed. We urge our members to let us know soon if they plan to enroll people in the short course.

James P. Brill to Receive Two Prestigious SPE Awards

We are proud and happy to announce that Dr. James P. Brill received the honorary member award as well as Legends of Production recognition. Honorary member award is the highest SPE award. The award presentation will be made at the upcoming 2009 SPE ATCE. Please join us in congratulating Jim.

Dr. Eissa Al-Safran Continues His Sabbatical in TUFFP

Dr. Eissa Al-Safran of Kuwait University is working on the investigation of the slug length for high viscosity oil and gas two-phase flow as part of his sabbatical assignment with TUFFP.

BHR Group Conference on Multiphase Technology

Since 1991, TUFFP has participated as a co-sponsor of BHR Group Conferences on Multiphase Production. TUFFP personnel participate in reviewing papers, serving as session chairs, and advertising the conference to our members. This conference is one of the premier international event providing delegates with opportunities to discuss new research and developments, to consider innovative solutions in multiphase production area.

14th International Conference on Multiphase Technology, supported by IFP, Technology Initiatives and TUFFP, was held 17-19 of June 2009 in Cannes, France. Over 120 delegates participated in the conference. Alex Hunt of Total E&P UK served as the technical chair of the conference. Dr. Cem Sarica made two technical paper presentations based on TUFFP research.

7th North American Conference on Multiphase Technology, sponsored and supported by Neotechnology Consultants of Calgary, Canada, sponsored by Bornemann Pumps and SPT Group and supported by TUFFP, is scheduled to be held 2-4 of June 2010 in Banff, Canada. The conference will

benefit anyone engaged in the application, development and research of multiphase technology for the oil and gas industry. Applications in the oil and gas industry will also be of interest to engineers from other industries for which multiphase technology offers a novel solution to their problems. The conference will also be of particular value to designers, facility and operations engineers, consultants and researchers from operating, contracting, consultancy and technology companies. The conference brings together experts from across the American Continents and Worldwide.

The scope of the conference includes variety of subjects pertinent to Multiphase Production in both technology development and applications of the existing technologies. The detailed information about the conference can be found in BHRg's (www.brhgroup.com).

Publications & Presentations

Since the last Advisory Board meeting, the following publications and presentations are made.

- 1) Gokcal, B., Alsarkhi, A. and Sarica, C.: “Effects of High Viscosity on Drift Velocity for Inclined Pipes,” *SPE Projects, Facilities & Construction Journal*, June 2009
- 2) Atmaca, S., Alsarkhi, A., Zhang, H. Q. and Sarica, C.: “Characterization of Oil Water Flows in Inclined Pipes,” *SPE Projects, Facilities & Construction Journal*, June 2009
- 3) Dong, H., Zhang, H. Q., and Sarica, C. “An Experimental Study of Low Liquid Loading Gas-Oil-Water Flow in Horizontal Pipes,” Proceedings of 14th International Conference Multiphase Production 09, Cannes, France, June 17-19, 2009.
- 4) Alsarkhi, A. and Sarica, C. “New Dimensionless Parameters and a Power Law Correlation for Pressure Drop of Gas-Liquid Flows in Horizontal Pipelines,” Proceedings of 14th International Conference Multiphase Production 09, Cannes, France, June 17-19, 2009
- 5) Sarica, C., Zhang, H. Q., and Wilkens, J. R.: “Sensitivity of Slug Flow Mechanistic Models on Slug Length,” To Be Presented at ASME’s Annual OMAE 2009 Meeting, Honolulu, Hawaii, May 31-June 5, 2009.

Tulsa University Paraffin Deposition Projects (TUPDP) Activities

The third three year phase of TUPDP continues. The studies concentrate on the paraffin deposition characterization of single-phase turbulent flow, oil-water paraffin deposition, gas-oil-water paraffin deposition. Phase-IV proposal discussions will be made at Fall Advisory Board meeting of TUPDP

Tulsa University Heavy Oil Projects (TUHOP) Activities

The Center of Research Excellence (TUCoRE) initiated by Chevron at The University of Tulsa funds

several research projects on flow assurance topics. TUFFP researchers are involved in various TUCoRE activities. One such activity is on High Viscosity Multiphase Flow (TUHOP). Up to this date, Chevron has provided TU to \$680,000 for improvement of an existing high pressure multiphase flow facility. Moreover, this research is leveraged by forming a Joint Industry Project. Current members of the JIP are BP, Chevron and Petrobras.

Two-Phase Flow Calendar

Several technical meetings, seminars, and short courses involving two-phase flow in pipes are scheduled for 2009 and 2010. Table 9 lists meetings that would be of interest to TUFFP members.

Table 9

Meeting and Conference Calendar**2009**

October 4 - 7	SPE Annual Technical Conference and Exhibition, New Orleans, Louisiana
December 7 - 9	International Petroleum Technology Conference, Doha, Qatar

2010

May 3 - 6	Offshore Technology Conference, Houston, Texas
May 11	TUHOP Advisory Board Meeting, Tulsa, Oklahoma
	TUFFP Spring Workshop, Tulsa, Oklahoma
May 12	TUFFP Spring Advisory Board Meeting, Tulsa, Oklahoma
May 13	TUPDP Spring Advisory Board Meeting, Tulsa, Oklahoma
May 17 - 21	TUFFP Short Course, Tulsa, Oklahoma
May 30 – June 4	International Conference on Multiphase Flow, Tampa, Florida
June 2 - 4	BHRg's 7 th North American Conference on Multiphase Technology, Banff, Canada
September 20 - 22	SPE Annual Technical Conference and Exhibition, Florence, Italy
November 9	TUHOP Advisory Board Meeting, Tulsa, Oklahoma
	TUFFP Fall Workshop, Tulsa, Oklahoma
November 10	TUFFP Advisory Board Meeting, Tulsa, Oklahoma
November 11	TUPDP Advisory Board Meeting, Tulsa, Oklahoma

Appendix A

Fluid Flow Projects Deliverables¹

1. "An Experimental Study of Oil-Water Flowing Mixtures in Horizontal Pipes," by M. S. Malinowsky (1975).
2. "Evaluation of Inclined Pipe Two-Phase Liquid Holdup Correlations Using Experimental Data," by C. M. Palmer (1975).
3. "Experimental Evaluation of Two-Phase Pressure Loss Correlations for Inclined Pipe," by G. A. Payne (1975).
4. "Experimental Study of Gas-Liquid Flow in a Pipeline-Riser Pipe System," by Z. Schmidt (1976).
5. "Two-Phase Flow in an Inclined Pipeline-Riser Pipe System," by S. Juprasert (1976).
6. "Orifice Coefficients for Two-Phase Flow Through Velocity Controlled Subsurface Safety Valves," by J. P. Brill, H. D. Beggs, and N. D. Sylvester (Final Report to American Petroleum Institute Offshore Safety and Anti-Pollution Research Committee, OASPR Project No. 1; September, 1976).
7. "Correlations for Fluid Physical Property Prediction," by M. E. Vasquez A. (1976).
8. "An Empirical Method of Predicting Temperatures in Flowing Wells," by K. J. Shiu (1976).
9. "An Experimental Study on the Effects of Flow Rate, Water Fraction and Gas-Liquid Ratio on Air-Oil-Water Flow in Horizontal Pipes," by G. C. Laflin and K. D. Oglesby (1976).
10. "Study of Pressure Drop and Closure Forces in Velocity- Type Subsurface Safety Valves," by H. D. Beggs and J. P. Brill (Final Report to American Petroleum Institute Offshore Safety and Anti-Pollution Research Committee, OSAPR Project No. 5; July, 1977).
11. "An Experimental Study of Two-Phase Oil-Water Flow in Inclined Pipes," by H. Mukhopadhyay (September 1, 1977).
12. "A Numerical Simulation Model for Transient Two-Phase Flow in a Pipeline," by M. W. Scoggins, Jr. (October 3, 1977).
13. "Experimental Study of Two-Phase Slug Flow in a Pipeline-Riser Pipe System," by Z. Schmidt (1977).
14. "Drag Reduction in Two-Phase Gas-Liquid Flow," (Final Report to American Gas Association Pipeline Research Committee; 1977).
15. "Comparison and Evaluation of Instrumentation for Measuring Multiphase Flow Variables in Pipelines," Final Report to Atlantic Richfield Co. by J. P. Brill and Z. Schmidt (January, 1978).
16. "An Experimental Study of Inclined Two-Phase Flow," by H. Mukherjee (December 30, 1979).

¹ Completed TUFFP Projects – each project consists of three deliverables – report, data and software. Please see the TUFFP website

17. "An Experimental Study on the Effects of Oil Viscosity, Mixture Velocity and Water Fraction on Horizontal Oil-Water Flow," by K. D. Oglesby (1979).
18. "Experimental Study of Gas-Liquid Flow in a Pipe Tee," by S. E. Johansen (1979).
19. "Two Phase Flow in Piping Components," by P. Sookprasong (1980).
20. "Evaluation of Orifice Meter Recorder Measurement Errors in Lower and Upper Capacity Ranges," by J. Fujita (1980).
21. "Two-Phase Metering," by I. B. Akpan (1980).
22. "Development of Methods to Predict Pressure Drop and Closure Conditions for Velocity-Type Subsurface Safety Valves," by H. D. Beggs and J. P. Brill (Final Report to American Petroleum Institute Offshore Safety and Anti-Pollution Research Committee, OSAPR Project No. 10; February, 1980).
23. "Experimental Study of Subcritical Two-Phase Flow Through Wellhead Chokes," by A. A. Pilehvari (April 20, 1981).
24. "Investigation of the Performance of Pressure Loss Correlations for High Capacity Wells," by L. Rosslund (1981).
25. "Design Manual: Mukherjee and Brill Inclined Two-Phase Flow Correlations," (April, 1981).
26. "Experimental Study of Critical Two-Phase Flow through Wellhead Chokes," by A. A. Pilehvari (June, 1981).
27. "Experimental Study of Pressure Wave Propagation in Two-Phase Mixtures," by S. Vongvuthipornchai (March 16, 1982).
28. "Determination of Optimum Combination of Pressure Loss and PVT Property Correlations for Predicting Pressure Gradients in Upward Two-Phase Flow," by L. G. Thompson (April 16, 1982).
29. "Hydrodynamic Model for Intermittent Gas Lifting of Viscous Oils," by O. E. Fernandez (April 16, 1982).
30. "A Study of Compositional Two-Phase Flow in Pipelines," by H. Furukawa (May 26, 1982).
31. "Supplementary Data, Calculated Results, and Calculation Programs for TUFFP Well Data Bank," by L. G. Thompson (May 25, 1982).
32. "Measurement of Local Void Fraction and Velocity Profiles for Horizontal Slug Flow," by P. B. Lukong (May 26, 1982).
33. "An Experimental Verification and Modification of the McDonald-Baker Pigging Model for Horizontal Flow," by S. Barua (June 2, 1982).
34. "An Investigation of Transient Phenomena in Two-Phase Flow," by K. Dutta-Roy (October 29, 1982).
35. "A Study of the Heading Phenomenon in Flowing Oil Wells," by A. J. Torre (March 18, 1983).
36. "Liquid Holdup in Wet-Gas Pipelines," by K. Minami (March 15, 1983).
37. "An Experimental Study of Two-Phase Oil-Water Flow in Horizontal Pipes," by S. Arirachakaran (March 31, 1983).

38. "Simulation of Gas-Oil Separator Behavior Under Slug Flow Conditions," by W. F. Giozza (March 31, 1983).
39. "Modeling Transient Two-Phase Flow in Stratified Flow Pattern," by Y. Sharma (July, 1983).
40. "Performance and Calibration of a Constant Temperature Anemometer," by F. Sadeghzadeh (August 25, 1983).
41. "A Study of Plunger Lift Dynamics," by L. Rosina (October 7, 1983).
42. "Evaluation of Two-Phase Flow Pressure Gradient Correlations Using the A.G.A. Gas-Liquid Pipeline Data Bank," by E. Caetano F. (February 1, 1984).
43. "Two-Phase Flow Splitting in a Horizontal Pipe Tee," by O. Shoham (May 2, 1984).
44. "Transient Phenomena in Two-Phase Horizontal Flowlines for the Homogeneous, Stratified and Annular Flow Patterns," by K. Dutta-Roy (May 31, 1984).
45. "Two-Phase Flow in a Vertical Annulus," by E. Caetano F. (July 31, 1984).
46. "Two-Phase Flow in Chokes," by R. Sachdeva (March 15, 1985).
47. "Analysis of Computational Procedures for Multi-Component Flow in Pipelines," by J. Goyon (June 18, 1985).
48. "An Investigation of Two-Phase Flow Through Willis MOV Wellhead Chokes," by D. W. Surbey (August 6, 1985).
49. "Dynamic Simulation of Slug Catcher Behavior," by H. Genceli (November 6, 1985).
50. "Modeling Transient Two-Phase Slug Flow," by Y. Sharma (December 10, 1985).
51. "The Flow of Oil-Water Mixtures in Horizontal Pipes," by A. E. Martinez (April 11, 1986).
52. "Upward Vertical Two-Phase Flow Through An Annulus," by E. Caetano F. (April 28, 1986).
53. "Two-Phase Flow Splitting in a Horizontal Reduced Pipe Tee," by O. Shoham (July 17, 1986).
54. "Horizontal Slug Flow Modeling and Metering," by G. E. Kouba (September 11, 1986).
55. "Modeling Slug Growth in Pipelines," by S. L. Scott (October 30, 1987).
56. "RECENT PUBLICATIONS" - A collection of articles based on previous TUFFP research reports that have been published or are under review for various technical journals (October 31, 1986).
57. "TUFFP CORE Software Users Manual, Version 2.0," by Lorri Jefferson, Florence Kung and Arthur L. Corcoran III (March 1989)
58. "Simplified Modeling and Simulation of Transient Two Phase Flow in Pipelines," by Y. Taitel (April 29, 1988).
59. "RECENT PUBLICATIONS" - A collection of articles based on previous TUFFP research reports that have been published or are under review for various technical journals (April 19, 1988).

60. "Severe Slugging in a Pipeline-Riser System, Experiments and Modeling," by S. J. Vierkandt (November 1988).
61. "A Comprehensive Mechanistic Model for Upward Two-Phase Flow," by A. Ansari (December 1988).
62. "Modeling Slug Growth in Pipelines" Software Users Manual, by S. L. Scott (June 1989).
63. "Prudhoe Bay Large Diameter Slug Flow Experiments and Data Base System" Users Manual, by S. L. Scott (July 1989).
64. "Two-Phase Slug Flow in Upward Inclined Pipes", by G. Zheng (Dec. 1989).
65. "Elimination of Severe Slugging in a Pipeline-Riser System," by F. E. Jansen (May 1990).
66. "A Mechanistic Model for Predicting Annulus Bottomhole Pressures for Zero Net Liquid Flow in Pumping Wells," by D. Papadimitriou (May 1990).
67. "Evaluation of Slug Flow Models in Horizontal Pipes," by C. A. Daza (May 1990).
68. "A Comprehensive Mechanistic Model for Two-Phase Flow in Pipelines," by J. J. Xiao (Aug. 1990).
69. "Two-Phase Flow in Low Velocity Hilly Terrain Pipelines," by C. Sarica (Aug. 1990).
70. "Two-Phase Slug Flow Splitting Phenomenon at a Regular Horizontal Side-Arm Tee," by S. Arirachakaran (Dec. 1990)
71. "RECENT PUBLICATIONS" - A collection of articles based on previous TUFFP research reports that have been published or are under review for various technical journals (May 1991).
72. "Two-Phase Flow in Horizontal Wells," by M. Ihara (October 1991).
73. "Two-Phase Slug Flow in Hilly Terrain Pipelines," by G. Zheng (October 1991).
74. "Slug Flow Phenomena in Inclined Pipes," by I. Alves (October 1991).
75. "Transient Flow and Pigging Dynamics in Two-Phase Pipelines," by K. Minami (October 1991).
76. "Transient Drift Flux Model for Wellbores," by O. Metin Gokdemir (November 1992).
77. "Slug Flow in Extended Reach Directional Wells," by Héctor Felizola (November 1992).
78. "Two-Phase Flow Splitting at a Tee Junction with an Upward Inclined Side Arm," by Peter Ashton (November 1992).
79. "Two-Phase Flow Splitting at a Tee Junction with a Downward Inclined Branch Arm," by Viswanatha Raju Penmatcha (November 1992).
80. "Annular Flow in Extended Reach Directional Wells," by Rafael Jose Paz Gonzalez (May 1994).
81. "An Experimental Study of Downward Slug Flow in Inclined Pipes," by Philippe Roumazelles (November 1994).
82. "An Analysis of Imposed Two-Phase Flow Transients in Horizontal Pipelines Part-1 Experimental Results," by Fabrice Vigneron (March 1995).

83. "Investigation of Single Phase Liquid Flow Behavior in a Single Perforation Horizontal Well," by Hong Yuan (March 1995).
84. "1995 Data Documentation User's Manual", (October 1995).
85. "Recent Publications" A collection of articles based on previous TUFFP research reports that have been published or are under review for various technical journals (February 1996).
86. "1995 Final Report - Transportation of Liquids in Multiphase Pipelines Under Low Liquid Loading Conditions", Final report submitted to Penn State University for subcontract on GRI Project.
87. "A Unified Model for Stratified-Wavy Two-Phase Flow Splitting at a Reduced Tee Junction with an Inclined Branch Arm", by Srinagesh K. Marti (February 1996).
88. "Oil-Water Flow Patterns in Horizontal Pipes", by José Luis Trallero (February 1996).
89. "A Study of Intermittent Flow in Downward Inclined Pipes" by Jiede Yang (June 1996).
90. "Slug Characteristics for Two-Phase Horizontal Flow", by Robert Marcano (November 1996).
91. "Oil-Water Flow in Vertical and Deviated Wells", by José Gonzalo Flores (October 1997).
92. "1997 Data Documentation and Software User's Manual", by Avni S. Kaya, Gerad Gibson and Cem Sarica (November 1997).
93. "Investigation of Single Phase Liquid Flow Behavior in Horizontal Wells", by Hong Yuan (March 1998).
94. "Comprehensive Mechanistic Modeling of Two-Phase Flow in Deviated Wells" by Avni Serdar Kaya (December 1998).
95. "Low Liquid Loading Gas-Liquid Two-Phase Flow in Near-Horizontal Pipes" by Weihong Meng (August 1999).
96. "An Experimental Study of Two-Phase Flow in a Hilly-Terrain Pipeline" by Eissa Mohammed Al-Safran (August 1999).
97. "Oil-Water Flow Patterns and Pressure Gradients in Slightly Inclined Pipes" by Banu Alkaya (May 2000).
98. "Slug Dissipation in Downward Flow – Final Report" by Hong-Quan Zhang, Jasmine Yuan and James P. Brill (October 2000).
99. "Unified Model for Gas-Liquid Pipe Flow – Model Development and Validation" by Hong-Quan Zhang (January 2002).
100. "A Comprehensive Mechanistic Heat Transfer Model for Two-Phase Flow with High-Pressure Flow Pattern Validation" Ph.D. Dissertation by Ryo Manabe (December 2001).
101. "Revised Heat Transfer Model for Two-Phase Flow" Final Report by Qian Wang (March 2003).
102. "An Experimental and Theoretical Investigation of Slug Flow Characteristics in the Valley of a Hilly-Terrain Pipeline" Ph.D. Dissertation by Eissa Mohammed Al-safran (May 2003).
103. "An Investigation of Low Liquid Loading Gas-Liquid Stratified Flow in Near-Horizontal Pipes" Ph.D. Dissertation by Yongqian Fan.

104. "Severe Slugging Prediction for Gas-Oil-Water Flow in Pipeline-Riser Systems," M.S. Thesis by Carlos Andrés Beltrán Romero (2005)
105. "Droplet-Homophase Interaction Study (Development of an Entrainment Fraction Model) – Final Report," Xianghui Chen (2005)
106. "Effects of High Oil Viscosity on Two-Phase Oil-Gas Flow Behavior in Horizontal Pipes" M.S. Thesis by Bahadir Gokcal (2005)
107. "Characterization of Oil-Water Flows in Horizontal Pipes" M.S. Thesis by Maria Andreina Vielma Paredes (2006)
108. "Characterization of Oil-Water Flows in Inclined Pipes" M.S. Thesis by Serdar Atmaca (2007).
109. "An Experimental Study of Low Liquid Loading Gas-Oil-Water Flow in Horizontal Pipes" M.S. Thesis by Hongkun Dong (2007).
110. "An Experimental and Theoretical Investigation of Slug Flow for High Oil Viscosity in Horizontal Pipes" Ph.D. Dissertation by Bahadir Gokcal (2008).
111. "Modeling of Gas-Liquid Flow in Upward Vertical Annuli" M.S. Thesis by Tingting Yu (2009).
112. "Modeling of Hydrodynamics of Oil-Water Pipe Flow using Energy Minimization Concept" M.S. Thesis by Anoop Kumar Sharma (2009).

Appendix B

2009 Fluid Flow Projects Advisory Board Representatives

Baker Atlas

Dan Georgi
Baker Atlas
2001 Rankin Road
Houston, Texas 77073
Phone: (713) 625-5841
Fax: (713) 625-6795
Email: dan.georgi@bakeratlas.com

Datong Sun
Baker Atlas
2001 Rankin Road
Houston, Texas 77073
Phone: (713) 625-5791
Fax: (713) 625-6795
Email: datong.sun@bakeratlas.com

BP

Official Representative & UK Contact

Paul Fairhurst
BP
Flow Assurance Engineering – UTG
Building H
Chertsey Road
Sunbury on Thames, Middlesex TW16 7LN
England
Phone: (44 1 932) 774818
Fax: (44 7 787) 105183
Email: fairhucp@bp.com

Alternate UK Contact

Andrew Hall
BP
Pipeline Transportation Team, EPT
1H-54 Dyce
Aberdeen, AB21 7PB
United Kingdom
Phone: (44 1224) 8335807
Fax:
Email: halla9@bp.com

Alternate UK Contact

Trevor Hill
BP
E&P Engineering Technical Authority – Flow Assurance
Chertsey Road
Sunbury on Thames, Middlesex TW16 7BP
United Kingdom
Phone: (44) 7879 486974
Fax:
Email: trevor.hill@uk.bp.com

US Contact

Taras Makogon
BP
501 Westlake Park Blvd.
Houston, Texas 77079
Phone: (281) 366-8638
Fax:
Email: taras.makogon@bp.com

US Contact

George Shoup
BP
501 Westlake Park Blvd.
Houston, Texas 77079
Phone: (281) 366-7238
Fax:
Email: shoupgj@bp.com

US Contact

Oris Hernandez
Flow Assurance Engineer
BP
501 Westlake Park Blvd.
Houston, Texas 77079
Phone: (281) 366-5649
Fax:
Email: oris.hernandez@bp.com

Chevron

Lee Rhyne
Chevron
Flow Assurance Team
1400 Smith Street, Room 23188
Houston, Texas 77002
Phone: (713) 372-2674
Fax: (713) 372-5991
Email: lee.rhyne@chevron.com

Sam Kashou
Chevron
1500 Louisiana Street
Houston, Texas 77002
Phone: (832) 854-3917
Fax: (832) 854-6425
Email: samkashou@chevron.com

Jeff Creek
Chevron
Flow Assurance Team
1600 Smith Street
Houston, Texas 77002
Phone: (713) 754-7347
Fax: (713) 754-7300
Email: lcrc@chevron.com

Hariprasad Subramani
Chevron
Flow Assurance
1400 Smith Street, Room 23192
Phone: (713) 372-2657
Fax: (713) 372-5991
Email: hjsubramani@chevron.com

ConocoPhillips, Inc.

Tom Danielson
ConocoPhillips, Inc.
600 N. Dairy Ashford
1036 Offshore Building
Houston, Texas 77079
Phone: (281) 293-6120
Fax: (281) 293-6504
Email: tom.j.danielson@conocophillips.com

Kris Bansal
ConocoPhillips, Inc.
1034 Offshore Building
600 N. Dairy Ashford
Houston, Texas 77079
Phone: (281) 293-1223
Fax: (281) 293-3424
Email: kris.m.bansal@conocophillips.com

Yongqian Fan
ConocoPhillips, Inc.
600 N. Dairy Ashford
1052 Offshore Building
Houston, Texas 77079
Phone: (281) 293-4730
Fax: (281) 293-6504
Email: yongqian.fan@conocophillips.com

ExxonMobil

Don Shatto
ExxonMobil
P. O. Box 2189
Houston, Texas 77252-2189
Phone: (713) 431-6911
Fax: (713) 431-6387
Email: don.p.shatto@exxonmobil.com

Jiyong Cai
ExxonMobil
P. O. Box 2189
Houston, Texas 77252-2189
Phone: (713) 431-7608
Fax: (713) 431-6387
Email: jiyong.cai@exxonmobil.com

Nader Berchane
ExxonMobil Upstream Research Company
Gas & Facilities Division
P. O. Box 2189
Houston, Texas 77252-2189
Phone: (713) 431-6059
Fax: (713) 431-6322
Email: nader.berchane@exxonmobil.com

JOGMEC

Tomoko Watanabe
JOGMEC
1-2-2, Hamada, Mihama-ku
Chiba, 261-0025 Japan
Phone: (81 43) 2769281
Fax: (81 43) 2764063
Email: watanabe-tomoko@jogmec.go.jp

Masaru Nakamizu
JOGMEC
One Riverway, Suite 450
Houston, Texas 77056
Phone: (713) 622-0204
Fax: (713) 622-1330
Email: nakamizu-masaru@jogmec.go.jp

Kuwait Oil Company

Eissa Alsafran
Kuwait University
College of Engineering and Petroleum
Petroleum Engineering Department
P. O. Box 5969
Safat – 13060 – Kuwait
Phone: (965) 4987699
Fax: (965) 4849558
Email: eisa@kuniv.edu.kw
dr_ealsafran@yahoo.com

Adel Al-Abbasi
Manager, Research and Technology
Kuwait Oil Company (K.S.C.)
P. O. Box 9758
Ahmadi – Kuwait 61008
Phone: (965) 398-8158
Fax: (965) 398-2557
Email: aabbasi@kockw.com

Ahmad K. Al-Jasmi
Team Leader R & T (Surface)
Research and Technology Group
Industrial Area
Kuwait Oil Company
P. O. Box 9758
Ahmadi – Kuwait 61008
Phone: (965) 3984126
(965) 3866771
Fax: (965) 3989414
Email: ajasmi@kockw.com

Bader S. Al-Matar
Snr. Reservoir Engineer
R & T Subsurface Team
Kuwait Oil Company
P. O. Box 9758
Ahmadi – Kuwait 61008
Phone: (965) 398-9111 ext. 67708
Email: bmatar@kockw.com

Marathon Oil Company

Rob Sutton
Marathon Oil Company
P. O. Box 3128
Room 3343
Houston, Texas 77253
Phone: (713) 296-3360
Fax: (713) 296-4259
Email: rpsutton@marathonoil.com

Minerals Management Services

Sharon Buffington
Minerals Management Services
Technology Research Assessment Branch
381 Elden Street
Mail Stop 2500
Herndon, VA 20170-4817
Phone: (703) 787-1147
Fax: (703) 787-1555
Email: sharon.buffington@mms.gov

Kurt Stein
Program Analyst
Minerals Management Services
Engineering and Research Branch
Mail Stop 4021
381 Eldon Street
Herndon, VA 20170-4817
Phone: (703) 787-1687
Fax: (703) 767-1549
Email: Kurt.Stein@mms.gov

Pemex

Miguel Hernandez
Pemex
1er Piso Edificio Piramide
Blvd. Adolfo Ruiz Cortines No. 1202
Fracc. Oropeza CP
86030 Villahermosa, Tabasco,
Mexico
Phone:
Fax:
Email: mhernandezga@pep.pemex.com

Jose Francisco Martinez
Pemex
Phone:
Fax:
Email: fmartinezm@pep.pemex.com

Dr. Heber Cinco Ley
Pemex Exploracion y Produccion
Subdireccion de la Coordinacion Tecnica de Explotacion
Gerencia de Sistemas de Produccion
Av. Marina Nacional Num 329
Torre Ejecutiva Piso 41
Colonia Huasteca C. P. 11311
Mexico D.F.

Petrobras

Rafael Mendes
Petrobras
Cidade Universitaria – Quadra 7 – Ilha do Fundao
CENPES/PDEP/TEEA
Rio de Janeiro 21949-900
Brazil
Phone: (5521) 38652008
Fax:
Email: rafael.mendes@petrobras.com.br

Marcelo Goncalves
Petrobras
Cidade Universitaria – Quadra 7 – Ilha do Fundao
CENPES/PDEP/TEEA
Rio de Janeiro 21949-900
Brazil
Phone: (5521) 38656712
Fax: (5521) 38656796
Email: marcelog@petrobras.com.br

Kazuishi Minami
Petrobras
Av. Republica do Chile
65 – 17° Andar – Sala 1703
Rio de Janeiro 20035-900
Brazil
Phone: (55 21) 5346020
Fax: (55 21) 5341128
Email: minami@petrobras.com.br

Ibere Alves
Petrobras
Phone: (55 21) 5343720
Email: ibere@petrobras.com.br

Rosneft

Vitaly Krasnov
Rosneft Oil Company
Sofiyskaya embankment 26/1
115998 Moscow
Russia
Phone:
Fax:
Email: v_krasnov@rosneft.ru

Vitaly Yelitcheff
Rosneft Oil Company
450092 ufa
Revolutionnaya Str, 96/2
Russia
Phone: (73472) 289900
Fax: (73472) 289900
Email: vityal@ufanipi.ru
vyelitcheff@gmail.com

Schlumberger

Mack Shippen
Schlumberger
5599 San Felipe
Suite 1700
Houston, Texas 77056
Phone: (713) 513-2532
Fax: (713) 513-2042
Email: mshippen@slb.com

William Bailey
Principal
Schlumberger – Doll Research
1 Hampshire Street, MD-B213
Cambridge, MA 02139
Phone: (617) 768-2075
Fax:
Email: wbailey@slb.com

Sammy Haddad
GFM Reservoir Domain Champion & Res. Eng. Advisor
Schlumberger Middle East S.A.
Mussafah
P. O. Box 21
Abu Dhabi, UAE
Phone: (971 2) 5025212
Fax:
Email: shaddad@abu-dhabi.oilfield.slb.com

Shell Global Solutions

Rusty Lacy
Fluid Flow (OGUF)
Shell Global Solutions (US) Inc.
Westhollow Technology Center
3333 Hwy 6 South
Houston, Texas 77082-3101
Phone: (281) 544-7309
Fax: (281) 544-8427
Email: rusty.lacy@shell.com

Ulf Andresen
Fluid Flow Engineer
Shell Global Solutions (US) Inc.
Westhollow Technology Center
3333 Hwy 6 South
Houston, Texas 77082
Phone: (281) 544-6424
Fax:
Email: ulf.andresen@shell.com

SPT

Richard Shea
SPT
11490 Westheimer, Suite 720
Houston, Texas 77077
Phone: (281) 496-9898 ext. 11
Fax: (281) 496-9950
Email: richard.shea@sptgroup.com

Yordanka Gomez-Markovich
SPT
Flow Assurance
DEV-GP6-1438
Phone: (281) 654-7549
Fax: (281) 654-6202
Email: yordanka.e.gomez@exxonmobil.com

Lee Norris
SPT
11490 Westheimer, Suite 720
Houston, Texas 77077
Phone: (281) 496-9898 ext. 14
Fax: (281) 496-9950
Email: hln@sptgroup.com

TOTAL

Benjamin Brocart
Research Engineer
Rheology and Disperse Systems
TOTAL Petrochemicals France
Research & Development Centre Mont/Lacq
B. P. 47 – F – 64170
Lacq, France
Phone: (33 559) 926611
Fax: (33 559) 926765
Email: Benjamin.brocart@total.com

Emmanuel Duret
TOTAL Exploration & Production
DGEP/SCR/ED/ECP
2, place Jean Millier – La Defense 6
92078 Paris la Defense Cedex - France
Phone: (33) 1 47 44 35 03
Fax:
Email: emmanuel-denis.duret@total.com

Appendix C

History of Fluid Flow Projects Membership

1973			
1.	TRW Reda Pump	12 Jun. '72	T: 21 Oct. '77
2.	Pemex	15 Jun. '72	T: 30 Sept. '96 R: Dec '97 Current
3.	Getty Oil Co.	19 Jun. '72	T: 11 Oct. '84 with sale to Texaco
4.	Union Oil Co. of California	7 Jul. '72	T: for 2001
5.	Intevep	3 Aug. '72	TR: from CVP in '77; T: 21 Jan '05 for 2006
6.	Marathon Oil Co.	3 Aug. '72	T: 17 May '85 R: 25 June '90 T: 14 Sept. '94 R: 3 June '97 Current
7.	Arco Oil and Gas Co.	7 Aug. '72	T: 08 Dec. '97
8.	AGIP	6 Sep. '72	T: 18 Dec. '74
9.	Otis Engineering Corp.	4 Oct. '72	T: 15 Oct. '82
10.	ConocoPhillips, Inc.	5 Oct. '72	T: Aug. '85 R: 5 Dec. '86 Current
11.	Mobil Research and Development Corp.	13 Oct. '72	T: 27 Sep. 2000
12.	Camco, Inc.	23 Oct. '72	T: 15 Jan. '76 R: 14 Mar. '79 T: 5 Jan. '84
13.	Crest Engineering, Inc.	27 Oct. '72	T: 14 Nov. '78 R: 19 Nov. '79 T: 1 Jun. '84
14.	Chevron	3 Nov. '72	Current
15.	Aminoil	9 Nov. '72	T: 1 Feb. '77

16.	Compagnie Francaise des Petroles (TOTAL)	6 Dec. '72	T: 22 Mar. '85 R: 23 Oct. '90 T: 18 Sep. '01 for 2002 R: 18 Nov. '02 Current
17.	Oil Service Co. of Iran	19 Dec. '72	T: 20 Dec. '79
18.	Sun Exploration and Production Co.	4 Jan. '73	T: 25 Oct. '79 R: 13 Apr. '82 T: 6 Sep. '85
19.	Amoco Production Co. (now as BP Amoco)	18 May '73	
20.	Williams Brothers Engrg. Co.	25 May '73	T: 24 Jan. '83

1974

21.	Gulf Research and Development Co.	20 Nov. '73	T: Nov. '84 with sale to Chevron
22.	El Paso Natural Gas Co.	17 Dec. '73	T: 28 Oct. '77
23.	Arabian Gulf Exploration Co.	27 Mar. '74	T: 24 Oct. '82
24.	ExxonMobil Upstream Research	27 Mar. '74	T: 16 Sep. '86 R: 1 Jan. '88 T: 27 Sep. 2000 R: 2007 Current
25.	Bechtel, Inc.	29 May '74	T: 14 Dec. '76 R: 7 Dec. '78 T: 17 Dec. '84
26.	Saudi Arabian Oil Co.	11 Jun. '74	T: for 1999
27.	Petrobras	6 Aug. '74	T: for 2000 R: for 2005 Current

1975

28.	ELF Exploration Production (now as TotalFina Elf)	24 Jul. '74	T: 24 Feb. '76 Tr. from Aquitaine Co. of Canada 19 Mar. '81 T: 29 Jan. '87 R: 17 Dec. '91
29.	Cities Service Oil and Gas Corp.	21 Oct. '74	T: 25 Oct. '82 R: 27 Jun. '84 T: 22 Sep. '86

30.	Texas Eastern Transmission Corp.	19 Nov. '74	T: 23 Aug. '82
31.	Aquitaine Co. of Canada, Ltd.	12 Dec. '74	T: 6 Nov. '80
32.	Texas Gas Transmission Corp.	4 Mar. '75	T: 7 Dec. '89

1976

33.	Panhandle Eastern Pipe Line Co.	15 Oct. '75	T: 7 Aug. '85
34.	Phillips Petroleum Co.	10 May '76	T: Aug. 94 R: Mar 98 T: 2002

1977

35.	N. V. Nederlandse Gasunie	11 Aug. '76	T: 26 Aug. '85
36.	Columbia Gas System Service Corp.	6 Oct. '76	T: 15 Oct. '85
37.	Consumers Power Co.	11 Apr. '77	T: 14 Dec. '83
38.	ANR Pipeline Co.	13 Apr. '77	TR: from Michigan- Wisconsin Pipeline Co. in 1984 T: 26 Sep. '84
39.	Scientific Software-Intercomp	28 Apr. '77	TR: to Kaneb from Intercomp 16 Nov. '77 TR: to SSI in June '83 T: 23 Sep. '86
40.	Flopetrol/Johnston-Schlumberger	5 May '77	T: 8 Aug. '86

1978

41.	Norsk Hydro a.s	13 Dec. '77	T: 5 Nov. '82 R: 1 Aug. '84 T: 8 May '96
42.	Dresser Industries Inc.	7 Jun. '78	T: 5 Nov. '82

1979

43.	Sohio Petroleum Co.	17 Nov. '78	T: 1 Oct. '86
44.	Esso Standard Libya	27 Nov. '78	T: 2 Jun. '82
45.	Shell Internationale Petroleum MIJ B.V. (SIPM)	30 Jan. '79	T: Sept. 98 for 1999

1980

46.	Fluor Ocean Services, Inc.	23 Oct. '79	T: 16 Sep. '82
47.	Texaco	30 Apr. '80	T: 20 Sep. '01 for 2002
48.	BG Technology (Advantica)	15 Sep. '80	T: 2003

1981		
-------------	--	--

49.	Det Norske Veritas	15 Aug. '80	T: 16 Nov. '82
-----	--------------------	-------------	----------------

1982		
-------------	--	--

50.	Arabian Oil Co. Ltd.	11 May '82	T: Oct.'01 for 2002
-----	----------------------	------------	---------------------

51.	Petro Canada	25 May '82	T:28 Oct. '86
-----	--------------	------------	---------------

52.	Chiyoda	3 Jun. '82	T: 4 Apr '94
-----	---------	------------	--------------

53.	BP	7 Oct. '81	Current
-----	----	------------	----------------

1983		
-------------	--	--

54.	Pertamina	10 Jan. '83	T: for 2000 R: March 2006
-----	-----------	-------------	------------------------------

1984		
-------------	--	--

55.	Nippon Kokan K. K.	28 Jun. '83	T: 5 Sept. '94
-----	--------------------	-------------	----------------

56.	Britoil	20 Sep. '83	T: 1 Oct. '88
-----	---------	-------------	---------------

57.	TransCanada Pipelines	17 Nov. '83	T:30 Sep. '85
-----	-----------------------	-------------	---------------

58.	Natural Gas Pipeline Co. of America (Midcon Corp.)	13 Feb. '84	T:16 Sep. '87
-----	---	-------------	---------------

59.	JGC Corp.	12 Mar. '84	T: 22 Aug. '94
-----	-----------	-------------	----------------

1985		
-------------	--	--

60.	STATOIL	23 Oct. '85	T:16 Mar. '89
-----	---------	-------------	---------------

1986		
-------------	--	--

61.	JOGMEC (formerly Japan National Oil Corp.)	3 Oct. '86	T: 2003 R: 2007 Current
-----	--	------------	--------------------------------------

1988		
-------------	--	--

62.	China National Oil and Gas Exploration and Development Corporation	29 Aug. '87	T:17 Jul. '89
-----	--	-------------	---------------

63.	Kerr McGee Corp.	8 Jul. '88	T:17 Sept. '92
-----	------------------	------------	----------------

1989		
-------------	--	--

64.	Simulation Sciences, Inc.	19 Dec. '88	T: for 2001
-----	---------------------------	-------------	-------------

1991		
-------------	--	--

65.	Advanced Multiphase Technology	7 Nov. '90	T:28 Dec. '92
-----	--------------------------------	------------	---------------

66.	Petronas	1 Apr. '91	T: 02 Mar. 98 R: 1 Jan 2001 T: Nov. 2008 for 2009
-----	----------	------------	---

1992

67.	Instituto Colombiano Del Petroleo	19 July '91	T: 3 Sep. '01 for 2002
68.	Institut Francais Du Petroleo	16 July. '91	T: 8 June 2000
69.	Oil & Natural Gas Commission of India	27 Feb. '92	T: Sept. 97 for 1998

1994

70.	Baker Jardine & Associates	Dec. '93	T: 22 Sept. '95 for 1996
-----	----------------------------	----------	--------------------------

1998

71.	Baker Atlas	Dec. 97	Current
72.	Minerals Management Service (Department of Interior's)	May. 98	Current

2002

73.	Schlumberger Overseas S.A.	Aug. 02	Current
74.	Saudi Aramco	Mar. 03	T: for 2007

2004

75.	YUKOS	Dec. '03	T: 2005
76.	Landmark Graphics	Oct. '04	T: 2008

2005

77.	Rosneft	July '05	Current
-----	---------	----------	----------------

2006

78.	Tenaris		T: Sept 2008 – for 2009
79.	Shell Global		Current
80.	Kuwait Oil Company		Current

2009

81.	SPT		Current
-----	-----	--	----------------

Note: T = Terminated; R = Rejoined; and TR = Transferred

Appendix D

Contact Information

Director

Cem Sarica

(918) 631-5154
cem-sarica@utulsa.edu

Associate Director

Holden Zhang

(918) 631-5142
hong-quan-zhang@utulsa.edu

Director Emeritus

James P. Brill

(918) 631-5114
brill@utulsa.edu

Project Coordinator

Linda M. Jones

(918) 631-5110
jones@utulsa.edu

Project Engineer

Scott Graham

(918) 631-5147
sdgraham@utulsa.edu

Research Associates

Polat Abduvayt

(918) 631-5138
polat-abduvayt@utulsa.edu

Mingxiu (Michelle) Li

(918) 631-5107
michelle-li@utulsa.edu

Research Technicians

Brandon Kelsey

(918) 631-5133
brandon-kelsey@utulsa.edu

Craig Waldron

(918) 631-5131
craig-waldron@utulsa.edu

Research Assistants

Gizem Ersoy

(918) 631-5119
gizem-ersoy@utulsa.edu

Kiran Gawas

(918) 631-5117
kiran-gawas@utulsa.edu

Benin Jeyachandra

(918) 631-5119
bjeyachandra@utulsa.edu

Ceyda Kora

(918) 631-5117
ceyda-kora@utulsa.edu

Kyle Magrini

(918) 631-5119
kyle-magrini@utulsa.edu

Anoop Sharma

(918) 631-5124
anoop-sharma@utulsa.edu

Ge Yuan

(918) 631-5124
ge-yuan@utulsa.edu

Web Administrator
Lori Watts

(918) 631-2979
lori-watts@utulsa.edu

Fax Number:
Web Sites:

(918) 631-5112
www.tuffp.utulsa.edu